Characteristics of Upper Troposphere and Lower Stratosphere in Relation to Asian Summer Monsoon

Thesis submitted to the

Cochin University of Science and Technology
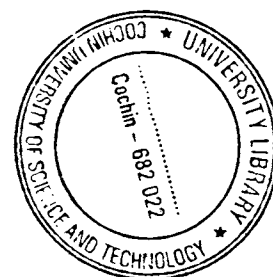
in partial fulfillment of the requirement for the Degree of
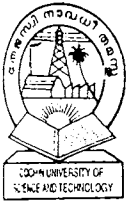
DOCTOR OF PHILOSOPHY

in

ATMOSPHERIC SCIENCE

BY

V. MADHU

Department of Atmospheric Sciences
Cochin University of Science and Technology
Lake Side Campus, Cochin - 682 016

October 2004
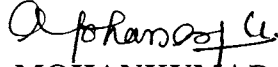
CERTIFICATE

This is to certify that the thesis entitled **Characteristics of Upper Troposphere and Lower Stratosphere in Relation to Asian Summer Monsoon** is a bonafide record of research work done by **Mr. V. MADHU** in the Department of Atmospheric Sciences, Cochin University of Science and Technology. He carried out the study reported in this thesis, independently under my supervision. I also certify that the subject matter of the thesis has not formed the basis for the award of any Degree or Diploma of any University or Institution.

Certified that **Mr. V. MADHU** has passed the Ph.D qualifying examination conducted by the Cochin University of Science and Technology in September 2001.

K. MOHANKUMAR
(Supervising Teacher)

Cochin
October 7 ,2004

Preface

The lower stratosphere is very much linked dynamically, chemically and radiatively with the upper troposphere, even though the characteristics of these regions are different. We cannot limit our studies in the troposphere, in order to understand monsoon and other weather phenomenon take place in the troposphere. So lower stratosphere should also consider for the proper understanding of monsoon variability and its predictability. The region of Upper Troposphere and Lower Stratosphere (UT/LS) is getting more attention in the current research of global climate and its variability. It has been noticed that there is a lot of variability in the Indian Summer Monsoon Rainfall (ISMR) for the past several decades. This is mainly because of the influence of the weather systems, which occur globally and regionally contribute to the variability in the monsoon rainfall. Country like India depends on its national income on agriculture; hence the summer monsoon rainfall is very important as far the agriculture sector is concerned. The accurate prediction of monsoon will help us to have safer way of doing agriculture and thereby proper planning in the agricultural sector of the country to minimize the loss due to the monsoon rainfall variability. The present study mainly concentrated on the interannual variability of zonal wind, temperature and ozone in association with Asian summer monsoon with special reference to the Indian context and are presented in this thesis

Chapter 1 describes about the introductory topics based on the Upper Troposphere and Lower Stratosphere. In this chapter a brief description about the middle atmospheric phenomenon and its effect on the variability in Asian summer monsoon are mentioned. *Chapter 2* presented with the interannual variability in zonal wind (QBO) and how the easterly and westerly phases linked with the DRY and WET seasons of Indian summer monsoon. Also analyzed the variations in the QBO periodicity and onset of easterly/westerly

phases in connection with monsoon. Monthly mean values of zonal wind obtained from NCEP/NCAR reanalysis and Indian summer monsoon rainfall data for the period 1960 to 2002, have been used for the study. *Chapter 3* describes advanced statistical tools such as Morlet Wavelet analysis and Empirical Orthogonal Functions (EOF) used for analysing the zonal wind over the Asian summer monsoon region for the upper troposphere and lower stratospheric levels.

Chapter 4 describes an interesting phenomenon of the tropical easterly zonal wind in the UT/LS during the southwest monsoon period (June to September) having opposite relation with ISMR (Dipole). In the DRY years upper troposphere winds (Tropical Easterly Jet over South Asia) have westerly anomalies and lower stratosphere has easterly anomalies. In WET years the anomalies are opposite. Also noted that the easterly wind and tropical easterly jet stream have a decreasing trend for the period 1960 to 1998.

Chapter 5 describes the temperature characteristics in the UT/LS region, mainly the interannual variability. It is also found a quasi-biennial periodicity in temperature even at the upper tropospheric level, which is significant at 95% above the confidence level. Here also we applied the EOF and Wavelet transform to understand the major periodicities in the temperature variation in the upper troposphere and lower stratosphere. The role of solar activity and how it modulates the temperature variation in the upper troposphere and lower stratosphere has also been studied. We have computed the decadal trend of temperature at different stratospheric and tropospheric levels. The cooling trend in the stratospheric temperature over the Asian monsoon region is due to the depletion in the stratospheric ozone and increase in the production of CFCs due to the anthropogenic activities.

The total ozone variability over 12 Indian stations from the southern latitude (Bangalore) to northern high latitude (Srinagar), obtained from the Total Ozone

Mapping Spectrometer TOMS during the period 1979 to 1992 have been studied and presented in *Chapter 6*. Two predominant oscillations in total ozone are noted with periodicities of 16-18 months and a qausi-beinnial periodicity (26-32 months) for all the stations. QBO periodicity is less significant for the northern latitude stations. During the DRY years the total ozone is higher compared to WET years for all the stations. This kind of variation in the total ozone is linked with the phases of the QBO mode of oscillation and found more ozone in the easterly phases of the QBO. Another notable feature is that the total ozone is higher when the tropopause height is less during the DRY monsoon years. *Chapter 7* summarises the major outcome of the doctoral thesis work and the future scope of the study. References and appendix are listed at the end of the thesis.

CONTENTS

Chapter 1

Introduction

1.1 Relevance of the study

Traditionally, the Upper Troposphere and Lower Stratosphere (UT and LS) have been treated as separate region, with the tropopause acting as a transport barrier between the lowermost layers of the atmosphere. The stratosphere is a region of high stability, rich in ozone, poor in water vapour and temperature increases with altitude. The lower stratospheric ozone absorbs the harmful ultra violet (UV) radiation from the sun and protects the life on the Earth. On the other hand, the troposphere has high concentrations of water vapour, low ozone and temperature decrease with altitude. The convective activity is more in the troposphere than in the stratosphere. Early atmospheric scientists believed that the weather occurs mainly in the lowermost layer (troposphere) of the atmosphere.

Even though stratosphere and troposphere are distinctly opposite in characteristics, the changes which occur in these layers contribute to the climate variability. Increase in the ozone content in the upper troposphere leads to many breathing problems, and decrease in the stratospheric ozone leads to disturbance of the radiative balance of the earth-atmosphere system. Therefore more ultraviolet radiation from the sun to fall on the earth surface and thereby diseases, like skin cancer and other breathing problem to the human kind. So there must be equilibrium in the characteristics of wind, temperature and ozone content of these layers of the atmosphere for the better weather and safety life on the earth.

The stratosphere is the transition region, which interacts with the weather systems in the lower atmosphere and the richly ionized upper atmosphere. Therefore, this part of the atmosphere provides a long list of challenging scientific problems of basic nature involving its thermal structure, energetic, composition, dynamics, chemistry and modeling. The lower stratosphere is very much linked dynamically, radiatively and chemically with the upper

troposphere, even though the temperature characteristics of these regions are different. Hence we cannot limit our studies in the troposphere alone for the better understanding of the tropospheric weather sytems, such as monsoon variability and predictability. Hence the Upper Troposphere and Lower Stratosphere (UT/LS) region in the atmosphere is getting more attention in the current research of global climate variability.

1.2 Justification of the study

The aim of the present study is to identify some important characteristics of the winds, temperature and ozone in the Upper Troposphere and Lower Stratosphere over the Asian summer monsoon region, more specifically over the Indian subcontinent, which play significant role in monsoon variability. It has been noticed that there is considerable variability in the Indian summer monsoon rainfall (ISMR) for the past decades. To understand this variability in the monsoon rainfall we have to undergo a detailed study of the interannual and intraseasonal variability of the winds, temperature, ozone etc. The weather systems, which occur globally and regionally, contribute some variability in the monsoon rainfall. It has been established that the El Nino, which occurs in the Pacific Ocean, has some influence on the Indian summer monsoon rainfall. Normally during the El Nino years Indian monsoon will be weaker compared to other years.

Awareness of the need to understand and predict the monsoon over India has recently generated much interest in the possible relationship between the amount and distribution of Indian monsoon rainfall and antecedent regional and global features. The most important need in monsoon forecasting is to predict with a reasonable degree of success, the years of excess and deficient rainfall. It was shown that the variations in the monsoon have some link with the upper tropospheric thermal and circulation anomalies (*Murakami, 1974; Krishnamuti et al., 1975; Kanamitsu et al., 1978*). The stratospheric quasi-biennial oscillation (QBO) is a dominant mode of interannual variation of the equatorial lower

stratospheric zonal wind and there is some relation with the phases of the QBO (zonal wind direction changes from easterly to westerly, in the tropical stratosphere with periodicity of about 26 months) and Indian summer monsoon. The strong easterly phase of the QBO was associated with weak (DRY) Indian monsoon and weak easterly/westerly phase with strong (WET) monsoon (*Mukherjee et al., 1985*). If a relation between QBO and Indian monsoon rainfall could be established, it would be of immense use for making long-range prediction of the monsoon variability, which will be highly beneficial for agriculture and thus, the economy of the country.

The decrease in stratospheric ozone and increase in the tropospheric ozone is a major concern in climate change and variability. The stratospheric ozone is transported to upper troposphere through Stratosphere-Troposphere Exchange processes (STE). The ozone absorbs UV radiation in the lower stratosphere and keeps radiative balance (thermal structure) of the earth–atmosphere system. Hence the study of ozone variability is important to understand the climate variability. Stratospheric changes can affect the climate in a quite complex way through radiative and dynamical interactions with the troposphere. The climate could be changed as a result of alterations in the incoming and outgoing radiative fluxes. There is also the possibility that ozone changes in the stratosphere could lead to changes in the stratospheric distribution of wind and temperature and thus affect the dynamical interactions between the troposphere and stratosphere.

The stratosphere is coupled dynamically and radiatively with the upper troposphere in different aspects of exchange processes such as trace gases, water vapour, mass and vertical transport of momentum flux etc. Water vapour is the most important greenhouse gas, although it has not received the attention paid to the anthropogenic greenhouse gases. It has long been recognised as crucial in determining the radiative balance of the Earth. Recently it has been re-emphasized that the far infrared component of the water vapour emission plays a

significant role in the water vapour greenhouse effect (*Clough et al., 1992; Sinha et al., 1995*). Sinha and Harries (1995) clearly demonstrate that most of the greenhouse trapping due to water vapour absorption occurs in the middle and upper troposphere. They also show that in the tropical troposphere a relatively small change of the water vapour abundance (17%) will produce the same greenhouse forcing as doubling the CO_2 concentrations

1.3 Temperature structure of the atmosphere

The gaseous area surrounding the earth is divided into mainly four concentric spherical strata separated by narrow transition zones based on the vertical changes in temperature with altitude. These concentric spherical strata are named as Troposphere, Stratosphere, Mesosphere and Thermosphere above the Mesopause (Figure 1.1). Atmospheric layers are charecterised by differences in chemical composition that produce variations in temperature.

The *troposphere* is the atmospheric layer closest to the earth' surface and contains the largest percentage of the mass of the total atmosphere. It is characterised by the density of the air and the average vertical temperature change of the region is $6°$ K per kilometer. Temperature and water vapor content in the troposphere decrease rapidly with altitude. Water vapor plays a major role in regulating air temperature because it absorbs solar energy and thermal radiation from the planet's surface. The troposphere contains 99% of the water vapor in the atmosphere. Water vapor concentrations vary with latitude. They are higher above the tropics, where they may be as high as 3%, and decrease toward the polar regions. All weather phenomena occur within the troposphere, although turbulence and convection may extend into the lower portion of the stratosphere. Troposphere means "region of mixing" or "turning" and is so named because of vigorous convective air currents within the layer. A narrow zone called the tropopause separates the troposphere. This ranges in height from 8 km in high latitudes, to 18 km above the equator and also varies with the

4
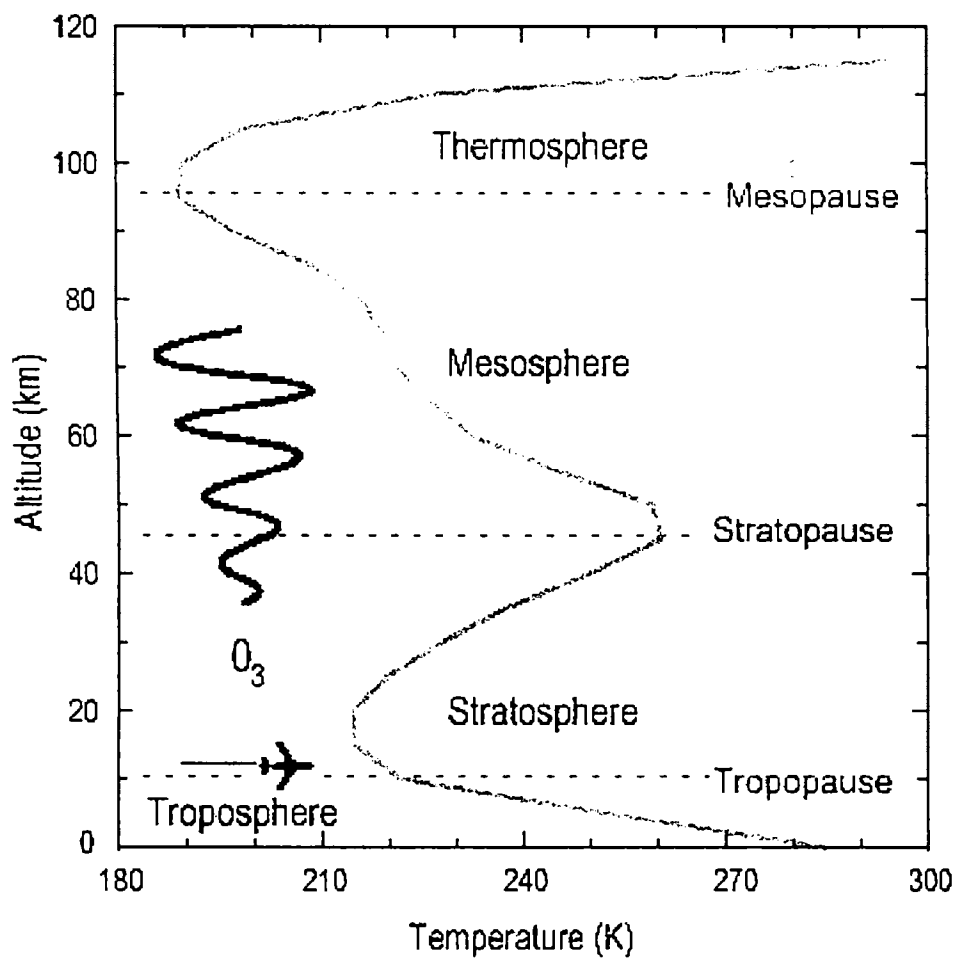
Figure 1.1: The thermal structure of the atmosphere

seasons; highest in summer and lowest in winter. Air temperature within the tropopause remains constant with increasing altitude.

The *stratosphere* is the second major strata of the atmosphere. It resides between 10-18 and 50 km above the planet's surface. The air temperature in the stratosphere increases up to the stratopause region (~50 km). Because the air temperature in the stratosphere increases with altitude, it does not cause convection and has a stabilizing effect on atmospheric conditions in the region. Ozone plays the major role in regulating the thermal regime of the stratosphere. Solar energy is converted to kinetic energy when ozone molecules absorb ultraviolet radiation, resulting in heating of the stratosphere. The ozone layer is located at an altitude between 20-30 km. Approximately 90% of the ozone in the atmosphere resides in the stratosphere. Major part of the tropospheric ozone is stratospheric origin as consequences of the stratospheric intrusion associated with tropopause folding in cyclogenetic processes. Ozone absorbs the bulk of solar ultraviolet radiation in wavelengths from 290-320 nm. These wavelengths are harmful to life because they can be absorbed by the nucleic acid in cells. Meteorological conditions strongly affect the distribution of ozone. Most ozone production and destruction occurs in the tropical upper stratosphere, where the largest amounts of ultraviolet radiation are present. Dissociation takes place in lower regions of the stratosphere and occurs at higher latitudes than does production.

The *mesosphere* a layer extending from approximately 50 km to 80 km is characterized by decreasing temperatures, which reach 190-180° K at an altitude of 80 km. In this region, concentrations of ozone and water vapour are negligible. Hence the temperature is lower than that of the troposphere or stratosphere. With increasing distance from Earth's surface the chemical composition of air becomes strongly dependent on altitude and the atmosphere becomes enriched with lighter gases. At very high altitudes, the residual gases

begin to stratify according to molecular mass, because of gravitational separation.

The *thermosphere* is located above the mesosphere and is separated from it by the mesopause transition layer. The temperature in the thermosphere generally increases with altitude up to $1000-1500°$ K. This increase in temperature is due to the absorption of intense solar radiation by the limited amount of molecular oxygen. At an altitude of 100-200 km, the major atmospheric components are still nitrogen and oxygen. At this extreme altitude gas molecules are widely separated.

1.4 The tropopause

The tropopause is an important meteorological concept. It separates the troposphere from the stratosphere, i.e., two volumes of air with significantly different properties (*Holton et al., 1995*). The tropopause height varies from 7-10 km in polar regions to 16-18 km in the tropics. Large-scale meteorological processes (low and high pressure systems) cause day-to-day variations. The systematic seasonal variations of the tropopause height at mid-latitudes vary from about 8 km in winter to about 12 km in summer.

Traditionally, the tropopause has been defined as the lowest level at which the vertical temperature gradient, $\partial T/\partial Z$, exceeds the value $2°$ K/km, provided the average $\partial T/\partial Z$ between the level and all higher levels within 2 km does not fall below this value (*WMO, 1957*). This so defined "*thermal tropopasuse*" and can be obtained from single temperature profiles and can be applied in both the tropics and the extra-tropics. The tropical tropopause layer (TTL), that region of the tropical atmosphere extending from the zero net radiative heating level (355° K, 150 hPa, 14 km) to the highest level that convection reaches (420-450° K, 70 hPa, 18-20 km). The TTL can be thought of as a transition layer between the troposphere and stratosphere and its structure and climatological aspects are very important for understanding the various

coupling processes (*Atticks et al., 1983; Seidel et al., 2001; George et al., 2002*). The influence of the quasi-bienniel oscillation (QBO) and the El Nino southern oscillation (ENSO) on the tropical cold point tropopause have been separated using bivariate regression. The stratospheric zonal wind shear at 50 hPa leads to the variation in the tropical cold point tropopause (CPT) temperature by about 6 months (*Zhou et al., 2001*). Various tropopause acronyms are illustrated below in Table 1.1(*SPARC News letter 17, 2001*).

TROPOPAUSE ACRONYMS	
LRT	*Lapse-rate tropopause: the conventional meteorological definition of the tropopause, in both tropics and extratropics, as the base of a layer at least 2km thick, in which the rate of decrease of temperature with height is less than 2K/km.*
CPT	*Cold-point tropopause: the level of minimum temperature. This is useful, and also significant, in the tropics.*
TTT	*Tropical thermal tropopause: since in the tropics the LRT and the CPT are usually less than 0.5km apart (with the LRT the lower) we ignore the distinction between them and refer to the TTT. The TTT is typically at 16-17km.*
STT	*Secondary tropical tropopause: the level of maximum convective outflow, above which the lapse rate departs from the moist adiabat. The STT is typically at 11-12km.*
TTL	*Tropical tropopause layer: the region between the STT and the TTT*
CSRT	*Clear-sky radiative tropopause: the level at which the clear-sky heating is zero. Below the CSRT there is descent on average (outside convective clouds). Above the CSRT there is ascent on average. The CSRT is typically at 14-16km.*

Table 1.1: Tropopause acronyms (*SPARC, News letter17, 2001*)

More recently the so-called "*dynamical tropopause*" has become popular (*Danielsen, 1968; Hoskins et al., 1985*). It is defined through a specific value of Potential Vorticity (*PV*) and can be used throughout the extra-tropics. For conservative flow, the dynamical tropopause (unlike the thermal tropopause) is a materiel surface, this is an advantage for instance when considering the

exchange of mass across the tropopause (*Wirth, 1995; 2001; Wirth et al., 1999*). Despite over all similarities between the thermal and dynamical tropopause, they are certainly not identical and in specific situations, there may be significant differences. For an atmosphere at rest PV is essentially a measure of static stability, and one can basically enforce both tropopause to be at the same altitude through a suitable choice of the PV value for the dynamical tropopause.

Apart from *thermal* and *dynamical* tropopause, there is another category for the definition of the tropopause based on the ozone content (*Bethen et al., 1996*) called "*ozone tropopause*". In most seasons, ozone-mixing ratio similar to PV features a sharp positive vertical gradient at a particular altitude somewhere in the tropopause region. It can be used to be defining an "ozone tropopause" from a single ozone sounding. In addition, ozone-mixing ratio like PV is approximately materially conserved on synoptic time scales. Therefore one may expect that the ozone tropopause behave similarly to the dynamical tropopause.

Tropopause region is critical region for climate. This region exhibits a complex interplay between dynamics, transport, radiation, chemistry, and microphysics. This is particularly highlighted in the case of ozone and water vapour, which provide much of the climate sensitivity in this region.

1.5 Static stability of the stratospheric air

The stratospheric temperature increases with height due to the absorption of UV radiation by the stratospheric ozone. As the air parcel displaced above becomes cooler than the surrounding, convection rarely occurs in the stratosphere. Potential temperature (θ) is a measure of static stability of the atmosphere.

$$\theta = T(p/p_s)^\kappa \qquad \qquad ...(1.1)$$

where T is the temperature P_s is 1000 hPa and K = R/C$_p$. The potential temperature (θ) is defined as the temperature of the air parcel would have if

compressed adiabatically from its existing pressure levels to 1000 hPa level. If the potential temperature increases with height the air is stably stratified. If it decreases with the height, the air is said be unstable. In the stratosphere, the potential temperature increases with height (Figure 1.2). At 30 hPa stratospheric level the potential temperature is about $560°$ K or even more. As the potential temperature becomes very high at the higher levels in the stratosphere, it is extremely difficult for the air parcels in that level to move up or down. The air will tend to remain in an isentropic surface (equal potential temperature surface) for several days. So the potential temperature is widely used as vertical co-ordinates in stratospheric studies. But in the upper troposphere potential temperature from $380°$ K and reaches a value of $320°$ K in the lower troposphere. Hence the troposphere air is convective unstable and have a tendency to rise up from the equatorial region.

1.6 Characteristics of upper troposphere and lower stratosphere

The upper troposphere and lower stratosphere (UT/LS) is a complex region and the interface between the troposphere and stratosphere through exchange process take places. Radiative and chemical time scales are relatively long, so transport is very important. The radiative properties and phase changes of atmospheric moisture link the hydrological and energy cycles of the earth system. Since the average residence time of water vapor in the atmosphere is around ten days, the atmospheric branch is a relatively fast component of the global hydrological cycle. Rainfall in the deep tropics is particularly important as forcing mechanism for the atmospheric large-scale circulation and climate.

Many climate and environmental quality issues involve in the interface between the stratosphere and the troposphere, known as the Upper Troposphere /Lower Stratosphere (UT/LS). The UT/LS has some distinct characteristics, which will influence its role in Earth's climate. The UT/LS contain the coldest parts of the lower atmosphere, to the extent that highly reactive particles can be produced. The upper troposphere and lower stratosphere are inseparably
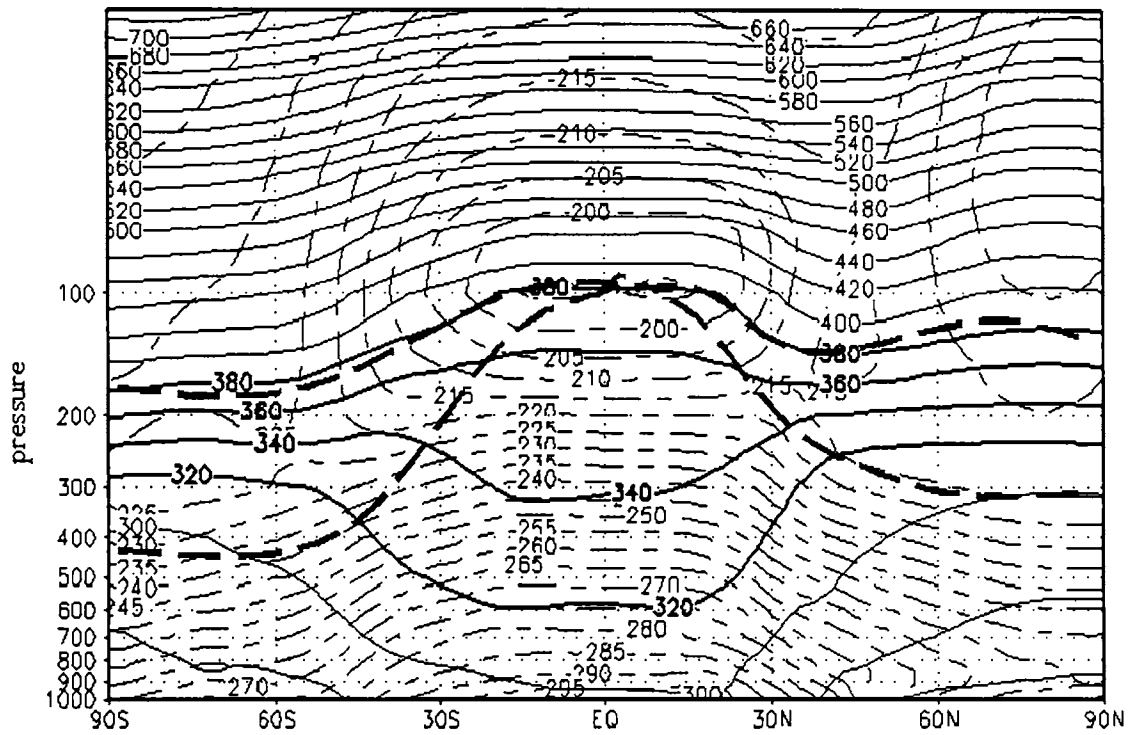
Figure 1.2: Latitude–altitude cross-section for January climatology (1960-98) showing longitudinally averaged potential temperature (solid contours) and temperature (dashed contour). The heavy dashed contour (cut off the 380° K isentropic line) denotes the 2 PVU potential vorticity contour, which approximate the tropopause outside the tropics.

connected *via* transport of chemicals; their effect on each other is very large and significant. What happens in the UT/LS is determined to some extent by the processes occur in the lower troposphere. For example, the source of all the ingredients for photochemical production of ozone in the UT and destruction in the LS originate from the lower atmosphere and has to pass through the UT to reach the LS. Similarly, the contents of the LS are passed through the UT to be removed, and affects this area.

However, models of this part of the atmosphere do not perform well, and our understanding of trends in radiatively important trace species, such as ozone and water vapour, is not adequate. Understanding the role of the stratosphere in climate requires the proper treatment of transport and mixing in the upper troposphere and lower stratosphere (a very difficult problem involving theoretical understanding, global observations, and modeling), radiative processes, and the chemistry and microphysics of stratospheric ozone depletion, all of which are coupled since their time scales are similar. Atmospheric measurements in this region are difficult and incomplete. This is a particularly difficult region to observe globally with useful resolution using satellite instruments.

1.7 Stratosphere-troposphere exchange (STE)

The stratosphere and troposphere are inseparable in a dynamical sense (Hoskins *et al.,* 1985) they are very different, with respect to their vertical transport time scales and chemical sense. The tropopause separates the troposphere from the stratosphere (typically at 17-20 km) in the tropics and at 12 km at mid-latitudes). In the tropics, the tropopause more or less coincides with temperature minimum, the so-called cold points at 100 hPa (Figure 1.2). Above the tropopause the temperature (and thus the static stability) increases again in the stratosphere. This is due to absorption of solar radiation by ozone (O_3) molecules in the ozone layer centered at approximately 25 km. Source of this

natural ozone layer in the photolysis of oxygen molecules by solar radiation (*Chapman, 1930*).

The increase of temperature with height in the stratosphere corresponds to a stable stratification, i.e., vertical motions are hampered. The time scale for vertical transport will therefore be large. The troposphere where the temperature decreases with height, on the other hand, is prone to instabilities. Once convection is triggered warm bubbles of air can ascend to the upper troposphere in less than an hour. As soon as the temperature minimum at the tropospause is reached the bubbles are no longer buoyant and further upward motion prohibites by the stable lapse rate of the stratosphere. Thus the tropopause forms a transport barrier between these atmospheric layers. The transport barrier corresponds to a steep gradient in the potential vorticity (*PV*) from the troposphere to the stratosphere. The vertical component of the potential vorticity (*PV*) is defined as

$$PV = -g(f + \zeta)\frac{\partial \theta}{\partial P} \qquad \qquad ...(1.2)$$

where 'g' denotes the acceleration of gravity , $f = 2\Omega\sin\phi$, the coriolis parameter, ζ the relative vorticity, θ the potential temperature and P the pressure. The strong gradient of the *PV* at the tropopause can (partly) be understood as due to the difference in lapse rate $\partial\theta/\partial P$ between tropopause and stratopause.

The extra-tropical tropopause is often defined in terms of specific *PV* contour (often 1-2 *PVU* = 2 x 10^{-6} m^2s^{-1} kg^{-1}), the so-called "dynamical tropopause" instead of the "thermal" World Meteorological Organization (WMO) definition. The heavy dashed contour in the Figure 1.2, represent the 2 *PVU* contour drawn schematically). The potential vorticity is conserved in adiabatic frictionless flow. This is a powerful tool to analyse the large-scale motions of the atmosphere. The *PV* therefore serves as a dynamical tracer of the stratospheric air (*Haynes et al., 1986*). Over the equator the term $(f + \zeta)$

11

changes the sign and *PV* become less useful and hence in the tropics 380° K contour of θ can be used. Figure 1.2 shows that the tropopause height is highest in the tropics and crosses isentropic surface towards the poles. Strong *PV* gradient prevail at the stratosphere-troposphere interactions. Stratosphere-troposphere exchange can influence the radiative balance in the troposphere and lower stratosphere (*Ramaswami et al., 1992; Toumi et al., 1994*) and therefore plays a significant role in the global climate system.

1.8 Dynamical aspects of stratosphere –troposphere exchange

The coupling between stratosphere and troposphere form an essential part of the synthesis of middle atmospheric process. The dynamical connection between the stratosphere and the troposphere has two quite distinct aspects. The first aspect is the transport and mixing of mass and chemical species between the stratosphere and troposphere traditionally referred to as stratosphere-troposphere exchange (STE). This aspect affects climate in numerous ways. Example, the impact of aircraft emission on the ozone layer, the vertical structure of greenhouse gas distribution in the upper troposphere and lower stratosphere and mid-latitude ozone depletion. A simple model that describe STE as exchange between two well-mixed boxes has only limited applicability due to the stratified nature of the stratosphere and the associated vertical transport time (*Holton, et al., 1995*). Rather STE must be placed in the framework of the general circulation.

Figure 1.3 gives a conceptual model of the global-scale circulation in the upper troposphere and lower stratosphere (i.e. the dynamical aspects of STE). From the figure three regions are identified: the troposphere, the *'lowermost' extra-tropical stratosphere* (the region between the thick dashed contours) and the rest is stratosphere. The isentropic surface in the lowermost stratosphere also lies partly in the troposphere. This facilitate the quasi-horizontal or isentropic STE (shown double headed arrow), as air masses can move freely on isentropic surfaces without the need for additional energy source. Hence this is called the

12

Large-Scale Subsidence

Wave- driven extra
tropical Pump

Large Scale
Ascent

Middle Stratosphere

Cumilo
nimbus
clouds

Two way Exchange

Cut-off Cyclone

Tropopause folds

Lower Stratosphere

2-PVU

Troposphere

Cumulus
convection

500

'00

200

300

400
500
600
700
800
900
1000

380

360

340

320

-300-

-280-

340

320

90S   80S   70S   60S   50S   40S   30S   20S   10S   EQ

Pole

Equator
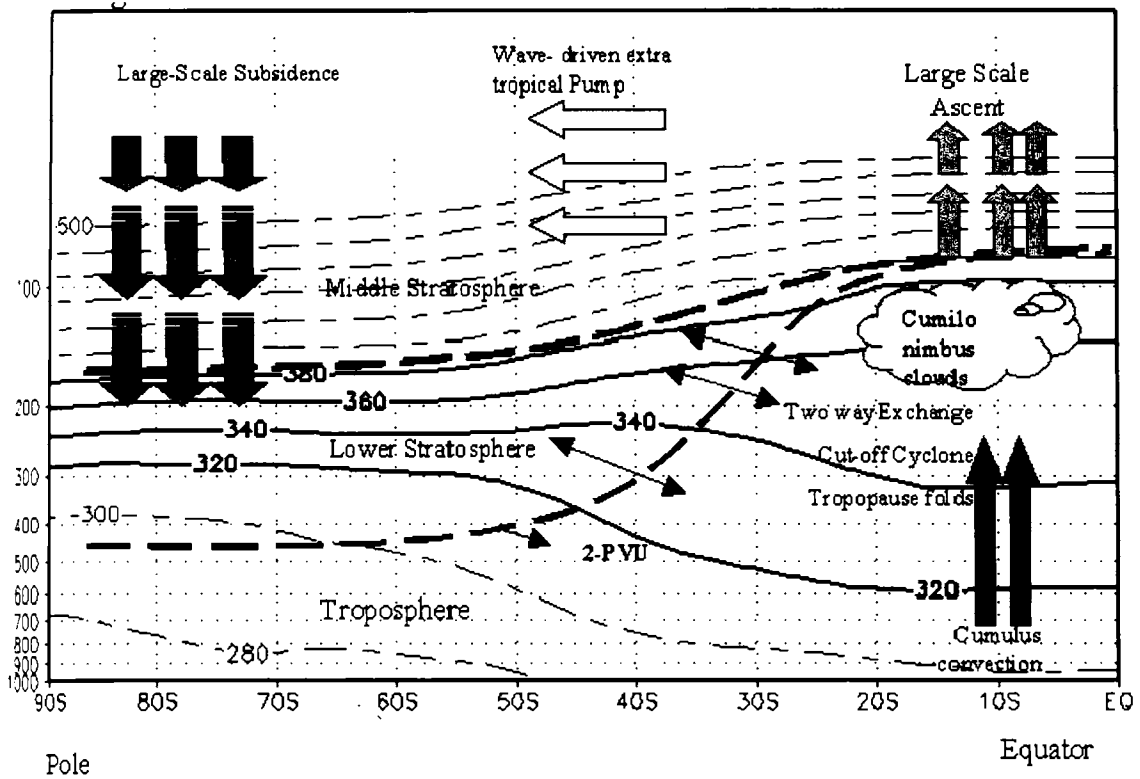
Figure 1.3: Dynamical aspects of stratosphere-troposphere exchange.The tropopause is shown by the thick dashed line. The lines of isentropic surface labeled in Kelevin's. The region between the heavily dashed line are called the lower most stratosphere. The region above 380° K surface is the overworld.

adiabatic transport. Quasi-horizontal STE can be significantly faster than STE across isentropic surfaces, which does require an energy source such as radiational heating (diabatic transport).

The cross-isentropic diabatic large-scale meridional overturning circulation is depicted by the thick arrows in Figure 1.3 and is known as the *Brewer-Dobson Circulation*, large–scale stratospheric circulation cell characterized by rising motion in the tropics and descending motion at mid and high latitudes (Brewer, 1949). Recent observational studies based on long-lived gases with known troposphere trend such as CO_2 (*Schmidt et al., 1991; Boering et al., 1996*) to show that the time scale for the overturning of the "Brewer-Dobson" circulation cell in ~ 5years. The dynamics in the stratosphere are known to be driven by the planetary waves entering the stratosphere through the lower boundary (the upper troposphere). These tropospheric waves propagate into the stratosphere and interact with the mean flow, while the stratospheric circulation also influence on the large-scale flow in the troposphere. The stationary planetary waves are generated by zonal asymmetries in the orography and in the land sea distribution, while transient planetary waves are generated to synoptic scale weather systems. In the northern hemisphere winter, the stationary and transient component are of comparable strength at the tropopause level, interannual variation in the tropospheric state might thus be a natural sources of the interannual variability in the stratosphere, and correlation do exists between stratospheric variability.

The Brewer Dobson (BD) circulation is thought to be controlled by the non-local response to breaking of Gravity and Rossby waves in the extra-tropical stratosphere (*Haynes et al., 1991*). The wave driven forces indicate a pumping action where air is sucked up from the tropical lowermost stratosphere transported meriodionally towards the poles, where it is pushed downward again. The BD circulation is strongest in the northern hemispheric winter because of the extra-tropical wave activities are strongest at that time and thus implying

13

stronger extra-tropical pumping. Upward transport in the uppermost tropical troposphere is also controlled by local process such as radiational heating and incidental overshooting convection. The redistribution of green house gases, especially water vapour, convection considerably changes the radiative properties of the upper troposphere and lower stratosphere. The deepest convection sometimes reaches and even lifts the tropopause, thereby triggering stratosphere-troposphere exchange (STE). If the convection reaches its uppermost boundary, the tropopause, turrets may overshoots into the stable stratified stratosphere (Danielsen, 1982).

The second aspect is the structure of the tropopause principally its height and its latitudinal structure (*Reid et al., 1981; 1985*). This aspect controls for example, the temperature minimum at the tropical tropopause (which strongly affects stratospheric water vapour and thereby many aspects of stratospheric chemistry). Reiter *et al.* (1969) studied the role of the tropopause in stratosphere-troposphere exchange process. Apart form this global scale STE, finer details in STE are provided by small-scale processes. The strong increase in height of the tropopause in the subtropics coincides with the axis of an upper troposphere Subtropical Jet Stream (STJ). This jet stream is strongest in winter hemisphere. Isentropic exchange due to tropopause deformations at the tropopause break can lead to thin filaments or 'streamers in the strong shear zones near the STJ (*Appenzeller et al., 1997*). Deformation of tropopause associated with the STJ can also cause more vertically oriented filamentary structure, the so called " tropopause folds".

Browell *et al.* (1987) determined the structure of such tropopause fold from airborne lidar and in situ measurements. The STE mechanism cause high ozone rich air to penetrate into the lowermost stratosphere to the troposphere is believed to be associated with such folds (*Lamarque et al., 1994; Danielsen, 1968; Ancellet et al., 1991*). Finally, at even smaller scales, clear- air turbulence (CAT) is another mechanisms of STE when the Richardson number in the strong

shear zones near the STJ reaches a critical value (*Shapiro, 1978; Pepler et al., 1998*). Andrews *et al.* (1987) and Shapiro *et al.* (1980) described the various processes by which the stratosphere-troposphere exchange takes place.

1.9 Quasi-biennial oscillation (QBO)

This is an oscillation of 26 to 28 months prevails over seasonal variations in zonal wind at heights of 15 to 30 km known as quasi-biennial oscillation (QBO). This variation is seen to descend with time in alternating series of easterlies and westerly that attain speeds 20 to 30 ms^{-1}. At higher levels, the QBO gives way to the semi-annual oscillation, which is a harmonic of the seasonal cycle. The QBO is symmetric about the equator and is confined to latitudes of less than about 15 degree. Even though it is nearly periodic, the QBO is not a harmonic of the seasonal cycle.

Stratospheric quasi-biennial oscillation (QBO) is a dominant mode of interannual variation of the equatorial stratosphere and its role in coupling the tropical and extra-tropical stratosphere as well as the stratosphere and troposphere. Although the QBO is a major tropical phenomenon and affect the stratospheric flow from pole to pole modulating the effects of extra-tropical waves. Indeed, study of the QBO is inseparate from the study of the atmospheric wave motion that drive it and are modulated by it (*Baldwin et al., 2001*). The QBO is not confined to atmospheric dynamics. Chemical constituents, such as ozone, water vapour and methane are affected by circulation changes induced by the QBO.

There are substantial QBO signals in many of the short-lived chemical constituents. QBO periodicity is observed not only in zonal winds but other atmospheric parameters such as ozone, temperature, geo-potential height etc. The discovery of the quasi-biennial oscillation and subsequent development in observation and theory we have to refer the study of Maruyama (1997) and Labitzke *et al.* (1999). The discovery of the QBO must be credited to the

15

independent work of Reed et al. (1961). Veryard and Ebden (1961) extended this study to found a dominant period of 26 months and observed similar perturbation in temperature. With the observation of large period cycle starting in 1963, Angell and Korshover (1964) coined the term " quasi-biennial oscillation" which gained acceptance and was abbreviated as QBO.

The QBO is definitely not a biennial oscillation, there is a tendency for seasonal preference in the phase reversal (*Dunkerton, 1990*) so that, for example, the onset of both easterly and westerly wind regime occurs mainly during northern hemisphere late spring at the 50 hPa level. Wallace and Holton (1968) tried to derive the QBO in a numerical model through heat sources or through extra-tropical planetary scale waves propagating towards the equator. They showed that lateral momentum transfer by planetary waves could not explain the downward propagation of the QBO without loss of amplitude. And they made the crucial realization that the only way to reproduce the observations was to have a driving force (a momentum source) which actually propagates downward with the mean equatorial winds.

It was believed that the forcing of the QBO to eastward and westward propagating equatorial gravity waves. The theory of equatorial waves was first developed during the late 1960's in parallel with the theory of the QBO. Wallace and Kousky (1968) first showed that observations of equatorial Kelvin waves in the lower stratosphere and noted that the wave produced an upward flux of westerly momentum, which could account for the westerly acceleration associated with QBO. A net easterly acceleration is contributed by Rossby-gravity waves (*Bretherton, 1969*). Holton and Lindzen (1972) refined the work of Lindzen and Holton (1968) by simulating, in a 1-D model, a QBO driven by vertically propagating Kelvin waves, which contribute a westerly force, and Rossby-gravity waves, contribute an easterly force. The Holton and Lindzen mechanism continued to be the accepted paradigm for the QBO for more than two decades.

16

The QBO is a tropical phenomenon; it influences the global stratosphere, and major winter stratospheric warming preferentially occurs during the easterly phase of the QBO (*Holton et al., 1980*). The QBO along with sea surface temperatures and El Niño Southern Oscillation (ENSO) are thought to affect the monsoon. Tropical cyclone frequency in the northwest Pacific increases during the westerly phase of the QBO (Chan, 1995). Gray, (1984) has shown a linkage of the zonal wind with the frequency of the hurricanes forming in the Atlantic basin and El Nino episodes. Activity in the southwest Indian basin, however, increases with the easterly phase of the QBO. The decay of aerosol loading following volcanic eruptions such as El Chichon and Pinatubo depends on the phase of the QBO. Through the modulation of winds, temperature, extra tropical waves and the circulation and transport of trace constituents and may be a factor in stratospheric ozone depletion. Thus an understanding of the QBO and its global effects necessary for studies of long-term variability or trends in trace gases and aerosols. Detailed discussion of QBO in zonal wind and its relation to Asian summer monsoon is presented in Chapter two of the thesis.

1.10 Sudden stratospheric warming (SSW)

The first observation of stratospheric sudden warming (SSW) was reported by Scherhag, in 1952 and first theoretical explanation proposed by Matsuno (1971). It is a peculiar type of phenomenon observed in the polar lower stratosphere in the northern hemisphere during winter. A heating of the polar region and reversal of the temperature gradient characterise a major warming and the zonal wind has a typical lifetime of a few weeks. Such warming is observed in average every second year but with irregular intervals between one and five years (*Andrews et al., 1987*).

Occasionally during northern winter, the circulation becomes highly disturbed, accompanied by a marked amplification of planetary waves; the disturbed motion is characterized by marked deceleration of zonal-mean westerlies or even a reversal into zonal mean easterlies. At the same time,

temperature over the polar cap increases sharply by as much as 50° K, so the dark winter pole actually becomes warmer than the illuminated tropics. This dramatic sequence of events takes place in just a few days and is known as a sudden stratospheric warming (SSW). During major SSW, the north pole warms dramatically with reversal of meridional temperature gradient and breakdown of polar vortex occurs. The polar vortex is replaced by high over this region. The westerlies in the Arctic at 10 hPa are replaced by easterlies so that the center of the vortex moves south of 60° N - 65° N during the breakdown of polar vortex. The vortex is either displaced entirely or split into two. This type of warming has not been observed in the Antarctic. Minor warming can indeed be intense and sometimes also reverse the temperature gradient, but they do not results in a reversal of the circulation at 10 hPa level. They are found in the Antarctic as well as Arctic regions.

In some case of warming as much as 40° C to 60° C in a few days have occurred at the 10 hPa level (*Andrews et al., 1987*). Numerous studies of the energetics of sudden warming confirm that enhanced propagation of energy from the troposphere by planetary scale waves, primarily zonal wave numbers 1 and 2 is essentially for the development of the warming. Since the sudden warming is observed only in the northern hemisphere, it is logical to calculate that topographically forced wave are responsible for the vertical energy propagation. The southern hemisphere with its relatively small landmasses at middle latitudes has much smaller amplitude stationary planetary waves. There are different theories emerged to explain the stratospheric warming phenomena (*Matsuno, 1971; Charney et al., 1961; Dunkerton et al., 1981; Mc Intyre, 1982; O'Neill, 1982; Schoeberl, 1978*). The number of warming is such that it agree reasonably well with the number of quasi-biennial oscillation (QBO) cycles in the equatorial lowermost stratosphere; a possible relationship with the equatorial QBO has been noted by several authors (*Holton et al., 1980; Dunkerton et al., 1988*).

1.11 Solar activities

For many years between 1826 and 1843, a German amateur astronomer called Schwabe observed the sun and counted the number of sunspots and he could found that about every 11 years, the number of sunspots goes from small to large and back to small again. Times of peak activity are called solar maxima, and times of minimal or no activity is called solar minima. This is the solar cycle. Because the magnetic polarities of the sun flip at the end of every such cycle, may refer to the length of the entire solar cycle as 22 years. Nevertheless, the cycle of activity (sunspot cycle) is complete over only 11 years, and the polarity itself doesn't appear to influence the level of activity. Thus we can talk about a general solar activity cycle and not just the sunspot cycle. The solar cycle is not just about sunspots. It turns out that all kinds of things on the sun (e.g. flares, prominences, and coronal mass ejection) go through the same cycle and are most common when sunspots are maximum. All of these phenomenon appear in he sun's atmosphere (photosphere, chromospheres, and corona/solar wind), and all are connected by the same root causes.

The production of sunspots, prominences, and flares results from the interaction of the sun's magnetic filed, its differential rotation, and its convection. A newly discovered phenomenon, the Coronal Mass Ejection (CME), is frequently with flares and sunspots, as well. Sunspot is small area on the sun that appears darker because they are $1500\text{-}2000°$ K cooler than the average $5800°$ K surface temperatures of the sun. There is no doubt that the sun's cycle of activity affects the climate of the earth. Eleven-year cycles in the thickness of tree rings, in the varying thickness of annual sediments laid down in river deltas, in the thickness of annual sediment layers at the bottom of lakes--all attest to some kind of connection.

Even more dramatic is the period between 1645 and 1715, sometimes called the Little Ice Age, when the global temperature dropped measurably and overall climate chilled. During the same 70-year period, almost no sunspot

appeared. Those years comprise what is often called the Maunder Minimum. The connection between the sunspot cycle and climate cycles on the earth can be understood by a simple mechanism. The more heat is in the earth's atmosphere, the more energy there is available for storms and precipitation. It makes intuitive sense that the energy released while the sun is near solar maximum, in the form of flares and CMEs and a more powerful solar wind, ought to be able to provide extra heat to earth's surface to provide direct heating there. So the solar activity is very much influencing the climate variability in the upper troposphere and lower stratosphere.

1.12 Atmospheric ozone and its environmental impacts

It should be noted that the Ozone (O_3) is an essential atmospheric component is indeed a trace substance and even at the peak of the ozone layer the ozone-mixing ratio is only about 10 ppm (parts per million) by volume. If the entire atmospheric ozone content were brought to standard temperature and pressure ($0°$ C, 1013.25 hPa) the thickness of the column would only be about 3 mm (i.e. 300 Dobson Units). Stratospheric ozone protects life from the harmful UV–B (λ= 280-320 nm) and UV-C (λ= 220 nm) radiation by absorbing it and preventing them from reaching the earth surface. As a result there is a strong radiative heat input into the stratosphere, which cause the observed temperature inversion between the tropopause and the stratosphere.

The concentration of ozone is highly variable both in space and time. The ozone levels may range from less than 100 DU to over 500 DU globally. This variability depends not only on the distribution of ozone source and sinks, but also importantly on transport of ozone by all scales of atmospheric motions. Ozone is produced in the lower stratosphere, maximum value of ozone found in the spring season in the northern hemisphere, it occurs at high latitudes, where as in the southern hemisphere it occurs at middle latitude. The absorption of solar radiation by the ozone not only determines the thermal structure (*Andrews et al., 1987*) but also the ecological framework for life on the earth's surface.

20

Decreased ozone results in increased UV transmission, which can affect the health of human, animals and planets (*Leun et al., 1995*). Also the absorption of solar UV radiation by O_3 protects the biosphere from biologically harmful UV radiation. The existence of the ozone layer is crucial not only to the general circulation of the atmosphere, but also to the very existence of life itself.

Therefore the ozone trends, in the UT/LS region will be major topics in the next decades because of the emission of tropospheric ozone precursor are expected to increase largely due to the growth of the population and industrial development. The concentration of ozone is greatly influenced by the processes, which take place in the tropics such as photochemistry, rapid convective mixing, widespread biomass burning and growing industrial emission. The photochemical production of ozone is greatest in the tropical lower stratosphere, but this will be transported in to the polar region by wind motion.

1.12.1 Ozone hole

A severe depletion of stratospheric ozone over Antarctica that occurs every northern hemisphere spring. The possibility exists that ozone hole could form over the arctic as well. The depletion is caused by a chemical reaction involving ozone and chlorine, primarily from human produced sources, cloud particle and low temperatures. The ozone holes defined as the area with total ozone below 220 DU, with largest areas were observations in the late 1990's. The area affected by the ozone hole is increased by more than a factor of 10 since the early 1980s, and has been 20-25 x 10^6 km^2 in the 1990's (*Uchino et al., 1999*). Figure 1.4 it is very clearly seen that the decreasing trend of ozone (below 220 DU) from the total ozone measured by Television Infrared Observation Satellite (TIROS) Operational Vertical Sounder (TOVS), averaged from 70° S to 90° S from 1979 to 1996 (*Neuendorfer, 1996*). Systematic measurements of ozone revealed that the ozone abundance over many regions of the globe have decreased markedly since about 1980's. Figure 1.5 shows the
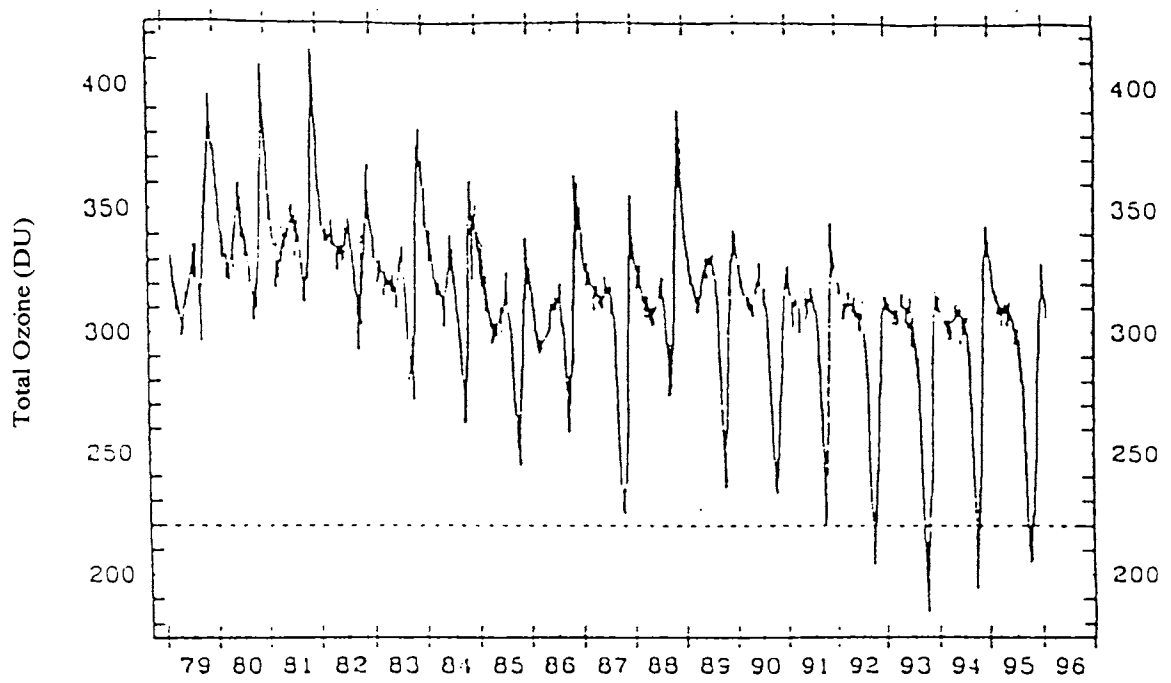
Figure 1.4: Total ozone measured by TIROS Operational Sounder (TOVS), averaged from 70° to 90° S from 1979 to 1996 (Neuendorfer, 1996)
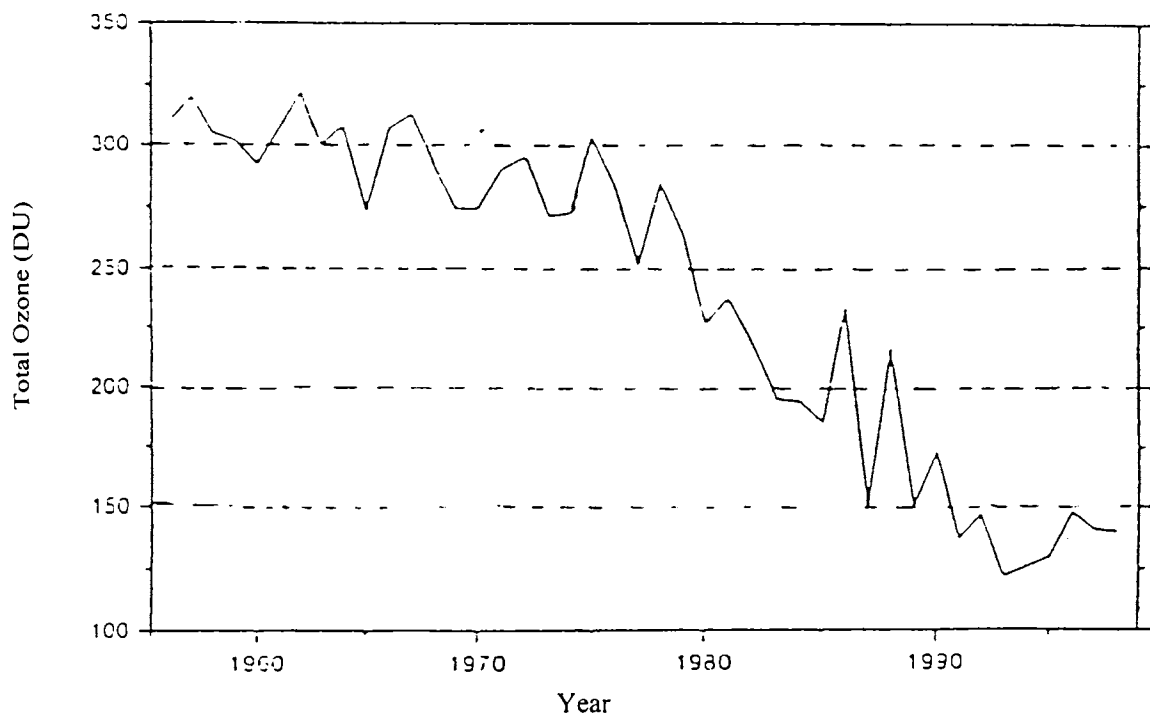
Figure 1.5: Total ozone measurements in October at Halley Bay (75° 31 'S, 26° 40' W) Antarctica from 1956 to 1998 (Farman et al., 1985; Jones and Shanklin, 1995)

total ozone measurements in October at Halley Bay (75°31' S, 26° 40' W) in Antarctica from 1956 to 1998 (*Farman et al., 1985; Jones et al., 1995*)

Observations during the past few decades have shown that decreasing trends of ozone in the lower stratosphere and increasing trends in the upper troposphere both have important climate effects and are mostly due to human perturbations. Most ozone depletion has been observed in the lower stratosphere (LS). There is also concern about possible ozone changes in the upper troposphere (UT). Because earth's climate will be sensitive to the vertical distribution of a greenhouse gas, the combination of ozone loss in the LS and increases in the UT is of concern. Ozone depletion is largest in the lower stratosphere with year-round reduction in mid-and high latitudes in both hemispheres.

Long- term observations indicate that stratospheric ozone depletion in the southern winter spring season over Antarctica started in the late 1970s, leading to a strong decrease in October total ozone means. Present values are only approximately half of those observed prior to 1970 (*Staechelin et al., 2001*). In the Arctic, large ozone depletion was observed in winter and spring in some recent years. Satellite and ground based measurements show no significant trends in the tropics but significant long term decreasing trends in the northern and southern middle latitudes (of the order of 2- 4 % per decade in the period from 1970 to 1996). Ozone at northern mid-latitudes decreased by −7.4 ± 2 % per decade at 40 km above mean sea level, while ozone loss was small at 30 km. Large trends were found in the lower stratosphere, -5.1±1.8 % at 20 km and − 7.3 ± 4.6% at 15 km, where the bulk of the ozone resides (*Staehelin et al., 2001*).

Possible destruction of the stratospheric ozone layer has been widely discussed both publicly and scientifically. The depletion of stratospheric ozone is occurring by various means, by the eruption of volcanoes, loading of aerosols, chlorofluorocarbon (CFC) etc, and thereby the climate change. Marko *et al.* (1993) showed that there is a decrease of 6% of ozone from the climatology in

the equatorial region using the Total Ozone Mapping Spectrometer (TOMS) data after the eruption Mt. Pinatubo (15.14° N, 120.35° E) on June 15, 1991 in Philippines. Since the beginning of the 1970s, Johnston (1971) first discussed stratospheric ozone depletion caused by chain reaction of nitrogen oxides emitted from a fleet of supersonic transport planes operate in the lower stratosphere. In recent years the consequences of emission from flying in the stratosphere were evaluated (*Brasseur et al., 1998, Penner et al., 1999*). There are some ongoing projects, which evaluate the state of the stratospheric ozone problem (*WMO, 1999; Stolarski et al., 1992; Harris et al., 1997*). Harris *et al.,* (1998) and Randel *et al.,* (1999) presented the trend in the vertical distribution of ozone.

1.12.2 Protection of ozone layer

The Montreal protocol on substances that deplete the ozone layer is a landmark of international agreement designed to protect the stratospheric ozone layer. The treaty was originally signed in 1987 and substantially amended in 1990 and 1992. The Montreal protocol stipulates that the production and consumption of compounds that deplete ozone in the stratosphere-chlorofluorocarbons (CFCs), halogens, carbon tetrachloride, and methyl chloroform are to be phased out by 2000 (2005 for methyl chloroform). Scientific theory and evidence suggest that, once emitted to the atmosphere, these compounds could significantly deplete the stratospheric ozone layer that shields the planet from damaging UV-B radiation. Changes in atmospheric ozone are also important for climate change (*Houghton et al., 1995*). Due to the decreasing trend in the stratospheric ozone a small negative radiative forcing (a tendency to cool), and an increase in tropospheric ozone results in a positive radiative forcing. The decrease of stratospheric ozone lead to enhanced UV-B radiation in the troposphere, which turn accelerates certain important photolysis rates (*Tang et al., 1998*).

1.13 International activities connected with UT and LS

The strong interactions between stratospheric scientists and their counterparts in the troposphere are essential to understand more about the upper troposphere and lower stratospheric processes and its impacts on the troposphere weather changes. This realization has led to a co-operation between the International Global Atmospheric Chemistry (IGAC) project of the IGBP and the Stratospheric Process And their Role in Climate (SPARC) activity of World Climate Research Program (WCRP). Some of the activities of the UT/LS initiative are the first of these joint ventures between International Geosphere-Biopshere Program (IGBP) and SPARC. Several other projects are started worldwide to study more about the dynamical, radiative and thermal aspects of the upper troposphere and lower stratosphere (UT/LS).

1.13.1 Stratospheric process and their role in climate (SPARC)

This is an ongoing project of the World Climate Research Programme (WCRP), which focus on understanding stratospheric changes and their relation to troposphere climate mainly on the research of upper troposphere and lower stratosphere (UT/LS) region of the atmosphere. SPARC efforts are underway to document and interpret indicators of stratospheric change such as trends in temperature, ozone, water vapour, and dynamics. They have identified three major areas of research and the major requirement needed for the future study.

A.   Stratospheric indicators of climate change

   a)   Continued measurement with an emphasis on high quality, validated data sets with global coverage.

   b)   Continued data quality control and quality assurance.

   c)   On going assessment of trends of ozone, water vapour etc.

24

d) Understanding of past change in ozone, temperature and water vapour can be used to provide forcing for General Circulation Model (GCM) studies of past changes in climate.

B. *Stratospheric processes and their relation to climate.*

a) Interdisciplinary studies need to promote on the complex region around the tropopause.

b) Support for a balanced programe of processes studies are important to maintain a balanced programe of laboratory investigations, field measurements and theoretical and modeling work for the future development in the field.

c) Planned field campaigns are needed to improve our understanding of particular processes.

C *Modeling of stratospheric effects on climate*

a) Improved and enlarged climatology of many stratospheric constituents and its properties being prepared for the better modeling.

b) Improved understanding of interannual variability such as quasi-biennial oscillation (QBO) and solar cycle and its causes and mechanism linking them to climate are required.

c) Improved representation of the stratosphere in General Circulation Models (GCMs).

1.13.2 Stratospheric tracers of atmospheric transport (STRAT)

Beginning in May 1995, the NASA ER-2 flight has flown with instruments to investigate the movement of long-lived trace gases in the lower stratosphere and upper troposphere. By increasing our understanding of such

motions, the Stratospheric TRacers of Atmospheric Transport (STRAT) experiment should increase our ability to determine whether certain gases in aircraft exhaust get in the prime ozone production region in the tropics. STRAT deployments have been successfully staged in May 1995, October-November 1995, January-February 1996, July-August 1996, and September 1996.

1.13.3 The stratospheric photochemistry aerosols and dynamic experiment (SPADE)

In November 1992 and April-May 1993, the NASA ER-2 aircraft mission to examine photochemical reactions affecting ozone loss. SPADE was a part of the Atmospheric Effects of Stratospheric Aircraft (AESA) program under the NASA High Speed Research Program (HSRP), and was staged to deal especially with possible effects of a projected fleet of supersonic aircraft, quantifying some of the key chemical reactions rates affecting ozone production and loss.

1.13.4 Photochemistry of ozone loss in the arctic region in summer (POLARIS)

The Photochemistry of Ozone Loss in the Arctic Region In Summer (POLARIS) is the latest in a series of high-altitude airborne investigations of atmospheric ozone spanning more than a decade. The objective of POLARIS is to understand the behaviour of polar stratospheric ozone as it changes from very high concentrations in spring down to very low concentrations in autumn.

1.13.5 The solar stellar irradiance comparison experiment (SOLSTICE)

Its NASA's project provides the scientific community with long term, accurate measurement of ultra violet radiation (UV) and Far Ultra Violet (FUV) radiation. SOLSTICE is operated from the Laboratory for Atmospheric and Space Physics (LASP) at the University of Colorado, Boulder.

1.13.6 Upper atmosphere research satellite (UARS)

As the first major element in NASA's Earth Science Enterprises (formerly Mission to Planet Earth), the Upper Atmosphere Research Satellite (UARS) have carried out the first systematic, comprehensive study of the stratosphere and furnish important new data on the mesosphere and thermosphere. UARS chemistry and dynamics sensors took measurements of temperature, pressure, wind velocity, and gas species concentrations in the altitude ranges from surface to 100 km.

1.13.7 Troposphere emission spectrometer (TES)

TES is a satellite instrument designed to measure the state of the earth's troposphere. This infrared fourier transform spectrometer will provide key data for studying tropospheric chemistry, troposphere-biosphere interaction, and troposphere-stratosphere exchanges. TES built for NASA by the Jet Propulsion Laboratory, California Institute of Technology. It is scheduled for launch into polar orbit aboard NASA's third Earth Observing Systems spacecraft (EOS-Aura) in July 2004.

Global Ozone Monitoring Experiment (GOME), Measurement of Ozone and Water vapour by Airbus In-service Aircraft (MOZAIC), Shuttle Ozone Limb Sounding Experiment/Limb Ozone Retrieval Experiment (SOLSE/LORE), and Total Ozone Mapping Spectrometer (TOMS) are some of the international projects deals with different problems in the lower and middle atmosphere.

1.14 Asian summer monsoon

Like any other troposphere circulations, solar heating essentially drives the monsoon. Summer monsoon of Southeast Asia is the largest anomaly of the general circulation. A planetary scale seasonally reversing monsoon circulation is found in the low level of the atmosphere over north Indian Ocean and south Asia. During northern summer the land gets heated and low-pressure area

centered over Pakistan gets established over the Asian continent. The surrounding sea area warm only slightly. Low level winds from the ocean across the equator and to the east flow into planetary scale low. This is the summer monsoon. Winds are southwesterly over north-Indian Ocean. A typical month is July. Figure 1.6(a) represents the climatology (1960-1998) of the July wind and relative humidity (RH) for the 925 hPa level. We can see the high relative humidity region over the Indian region.

During the northern winter (typical month January) Asian continents gets very little solar radiation, as sun is overhead in the southern hemisphere. But the Asian continent loses heat through infrared radiation. As consequences the land cools fast and a high-pressure area on planetary scale centered over Siberia covers the Asian continent. The outflow from these high moves over the north Indian Ocean as northeasterly winds and crosses the equator to the South Indian Ocean. Figure 1.6 (b) represents January month climatology (1960-1998) of wind and relative humidity at 925 hPa levels. Thus for six months of the year (May to October), south Asia and north Indian ocean has south-westerlies and for the other six months (November to April) north easterlies. The reversing wind system is shallow (in the lowest 1 km only). Two important conditions given by Ramage (1971) for planetary monsoon are as follows:

a)   The prevailing wind direction should shift by at lest 120° between January and July.

b)   The mean resultant winds in at least one of the months should exceed 3 ms^{-1}

The dominant monsoon systems are the Asian-Australian, the African and the American monsoon (*Trenberth et al., 2000*). Although the recurrence of the summer monsoon over India is markedly regular, its activity often varies from year to year. One extremity may result in severe drought, a single sufficient factor to disrupt the economy of the country. Therefore, it is vital to study the

b) JULY
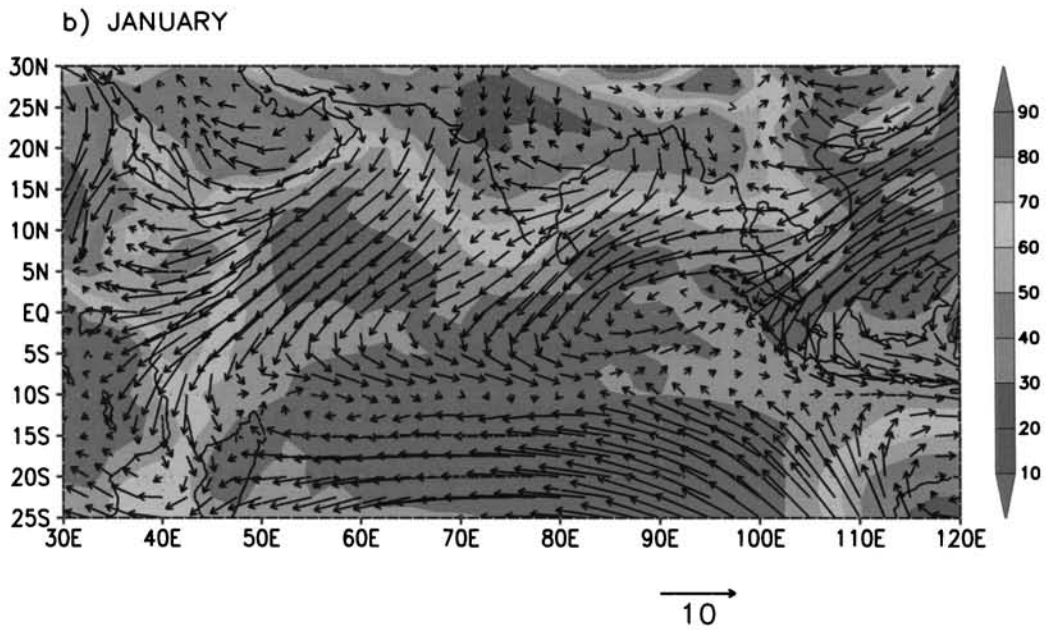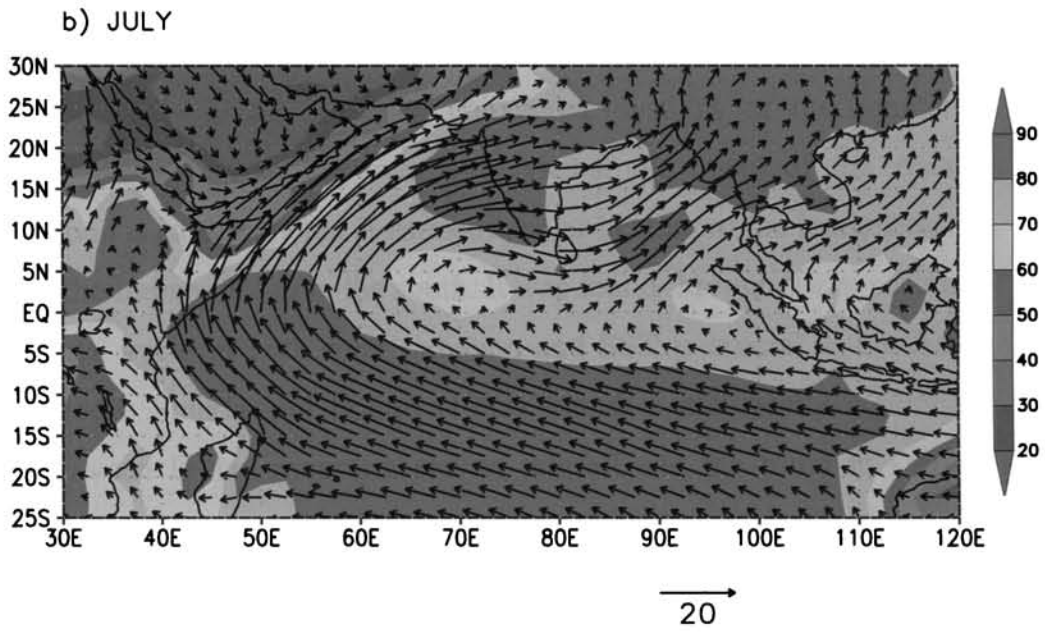
b) JANUARY

Figure 1.6: Climatology of Wind and Relative humidity (R.H%) at 925 hPa
from 1960-1998.a) JULY and b) JANUARY

dynamics of the monsoon that are responsible for these variations, and that occur before the monsoon season, to improve the long-range prediction of monsoon activity. Asian monsoon accounts for nearly 80% of the rainfall over the Indian region, and the associated large-scale heat source due to intense convection within deep clouds plays a major role in the global climate system. According to estimates of Jagar (1983) over 40% of the global precipitation falls within $15°$ of the equator, primarily in the towering convective systems of the equatorial trough region. According to the traditional views, the onset of the Asiatic summer monsoon is caused by the asymmetric solar heating of the landmasses in the north and the Indian Ocean in the south. It was found through the experiment that the seasonal cycle in both solar radiation and SST is crucial to the Asian summer monsoon. Shukla and Polino (1983) found a statistically significant correlation between Indian monsoon season rainfall and the trend in Darwin pressure anomalies from the preceding December- February to March-May.

Indian region being the most convectively active on the planet, is known for the occurrence of many convective phenomena of varying time and spatial scales like thunderstorm, cyclones winter and summer monsoons. They are interannual with strong biennial component, intraseasoanl (30-50 days), biweekly, super synoptic (active and break cycles) and synoptic (3-5 days). The summer monsoon of India has been viewed as a manifestation of the deep clouds embedded within the tropical convergence zone (TCZ). The major heat source triggered by the intense convection within deep clouds of the Asian summer monsoon plays a major role in the global climate system and its variability (*Yasunari, 1990, 1991; Lau et al., 1988*). Intra-seasonal oscillation play a crucial role in explaining the monsoon variability on both interannual and synoptic time scales, different time scales are interconnected and influence each other (*Goswami et al., 1998; Ferrenti et al., 1997*). The variability associated with the active and break spells cycles of monsoon (*Ramage, 1971*) explains differences in the seasonal rainfall between good and bad monsoon years (*Sikka, 1980; Krishnamurti et al., 1976*).

1.14. 1 Monsoon experiments

World Climate Research Program (WCRP) implemented Global Energy and Water Cycle Experiment (GEWEX) to understand the basic physical processes, particularly energy transfer and hydrological cycle. As part of GEWEX, the GEWEX Asian monsoon experiment known as (GAME) is proposed to understand the full energy transfer and water cycle process both at regional and continental scales associated with the full seasonal march of the Asian monsoon. One of the specific objectives of GAME is to resolve the diurnal cycles of cumulus convection and they conducted special experiments. "Convection in Asian Monsoon System during 1998 known as CAMS –98 from April to September during 1998 and was continued during the July-August 1999. GARP Atlantic Tropical Experiments (GATE), Global Energy and Water Cycle Experiment (GEWEX) Cloud System Studies (GCSS) and Tropical Ocean Global Atmospheric Experiment /Coupled Ocean Atmosphere Response Experiment (TOGA/COARE) are some of the field programs to understand the tropical convergence zone and moist convection associated with monsoon.

First attempt to study monsoon boundary layer over ocean region was made during the International Indian Ocean Experiment (IIOE) in 1963-65. Indo-Soviet Monsoon Experiment (ISMEX) in 1973 and 1977, Global Atlantic Tropical Experiment (GATE) in 1974, Monsoon Experiment (MONEX-77) and MONEX-79 etc followed it. Monsoon Trough Boundary Layer Experiment known as MONTBLEX- 90 was carried out during 1987-1990 over the Indian region (*Narasimha et al., 1997*). MONTBLEX-90 was carried out over monsoon trough region, the chief seat of monsoon convection, and is the boundary layer components of the Indian Ocean Experiment (INDOEX).

1.15 Significance of the present study

Despite several international efforts such as GATE. ISMEX, MONEX and national experiments such as BOBMEX, ARMEX, MONTBLEX, and

INDOEX, the nature of variability and predictability of the Asian Summer monsoon is still a debating issues among the scientific community all over the globe. The Asian monsoon is an important climate system that affects the lives of billions of people in the world. Undoubtedly, an improved knowledge of the mechanisms for the interannual variability of the monsoon is important for improving our skill of seasonal-to-interannual predictions for the monsoon. A detailed investigation of the link between the upper troposphere and lower stratosphere region of the Asian summer monsoon and how the variability in the upper troposphere and lower stratosphere contributes to the total variability of the Asian summer monsoon will be interesting. By understanding the dynamic, thermal and radiative characteristics of the upper troposphere and lower stratosphere will expected to improve the accuracy in the long-term predictions of the Asian summer monsoon. Hence the present topic is quite relevant for the economical and agricultural developments of our country.

Chapter 2

*Zonal Wind Characteristics and its
Interannual Variability in relation to Asian
Summer Monsoon*

2.1 Introduction

The quasi-biennial oscillation dominates the variability of the equatorial stratosphere (~16-50 km) and is easily seen as downward propagating easterly and westerly wind regimes, with a periodicity of approximately 26 months. This periodicity in zonal wind discovered by Reed et al. (1961) and Veryard and Ebdon (1961). This quasi-biennial oscillation (QBO) is the major interannual variability in the equatorial stratospheric zonal wind and it contributes to the stratospheric dynamics and the Stratosphere-Troposphere Exchange (STE) processes. Observational studies of Wallace and Kausky (1968a) and modeling study by Lindzen and Holton (1968) suggest that planetary scale vertically propagating internal gravity waves are the momentum source for the oscillation. Absorption of westerly (easterly) momentum in the westerly (easterly) shear zones result in the general downward propagation of two shear zones, giving an alteration in zonally symmetric east and west wind regimes. The quasi-biennial oscillation is considered to be the tropical lower stratospheric phenomena but it influences the stratospheric flow from pole to pole by modulating the effects of extra tropical waves.

The search for an explanation for the qausi-beinnial oscillation initially involved a variety of other causes like some internal feed back mechanisms, natural period of atmospheric oscillations, an external process, or some combinations of these mechanisms. All these attempts failed to explain the features such as the downward propagation and maintenances of the amplitude of the QBO and hence increase in energy density as it descends. Apparently, forcing by zonally asymmetric waves required to explain the equatorial westerly wind maximum. Wallace and Holton (1968) showed that lateral momentum transfer by planetary waves could not explain the downward propagation of the QBO without loss of amplitude. And they concluded that the only way to reproduce the observations was to have a driving force (a momentum source) with the mean equatorial winds.

Booker and Bretherton (1967) studied the role of gravity wave absorption and QBO propagation. Lindzen (1987) realized that vertically propagating gravity waves would provide the necessary wave forcing for the QBO. Number of attempts were made to explain the origin of the upward propagating equatorial waves. Holton (1972) showed that the pulsation of the major regions of the tropical rainfall would lead to the generation of both westerly and easterly waves of roughly the right characteristics. Pawson *et al.* (1993) showed faster and more regular downward propagation of the westerly phase and the stronger intensity and longer duration of the easterly phase. The latitudinal structure of the QBO in zonal wind derived from long time series of wind observation at many tropical stations (*Dunkerton et al., 1985*). The amplitude of the QBO is latitudinally symmetric and the maximum is centered over the equator with a meridional half width of approximately 12 degree. Holton *et al.* (1972) and Lindzen (1987) described the theory of QBO and associated developments of the equatorial waves (*Yanai et al.,1966; Maruyama, 1967; Hayashi, 1974*) both are inseparable.

A study of Rao *et al.* (1978) using the rocket wind data over the tropical station Thumba (08° 29'N, 76° 56'E) revealed that the quasi-biennial oscillation in the lower and middle stratosphere are out of phase by six months. The dominant features in the upper troposphere and lower stratosphere are the appearance of tropical easterly jet during the period June to September. The *westerlies or easterlies in the lower stratosphere over the equator extend to about* $10°N$ in the period of November to May. In the middle stratosphere (~ 32 km) the qausi-beinnial oscillation follows a regular alteration of easterly and westerly *with a downward phase propagation of one km per month, while the quasi-*biennial oscillation in the lower stratosphere interacts with monsoon circulation. There is a substantial evidence for the influence of the QBO on chemical constituents such as ozone and other trace elements. The first simulation of the ozone QBO was carried out by Reed (1964) using a simplified linear model.

The four possible wind phases are W, W/E, E and E/W during March to May in the equatorial lower stratosphere are linked with the onset of southwest monsoon near the normal date and normal rains over India. Appearance of the easterlies in the lower stratosphere over Gan Island (00° 41 S, 73° 09 E) in May is an indication of the onset of monsoon over Kerala a month later and they suggested an out of phase relation between QBO and monsoon circulation. The phases of the QBO over the equator appears to give a prior indication of the onset of southwest monsoon over Kerala and also the rainfall in the central parts of the country. Rao *et al.* (1978) showed that the zonal wind and rainfall over India and westerly phase of zonal wind at 50 hPa are favourable for normal monsoon. In this chapter the interannual variability of zonal wind in the lower stratosphere (QBO), its periodicity and phase variation have been studied in relation to Asian summer monsoon.

2.1.1 Dynamical overview of quasi-biennial oscillation

Figure. 2.1 shows an overview of the quasi-biennial oscillation during the northern winter. The diagram spans the troposphere, stratosphere and mesosphere from pole to pole and shows schematically the differences in zonal wind between 40 hPa easterly and westerly phases of the QBO (black contours). The easterly anomalies are light blue and westerly anomalies are pink. Convection in the tropical troposphere ranging from the scale of mesoscale convective complexes (spanning more than 100 km) to planetary scale phenomena, produces a broad spectrum of waves (wavy arrows) including gravity wave, inertia-gravity, Kelvin and Rossby gravity waves. The propagation of planetary scale waves (purple arrows) are shown at middle to high latitudes. These waves with a variety of vertical and horizontal wavelengths and phase speeds propagate into the stratosphere transporting easterly and westerly zonal momentum at stratospheric levels, during the zonal wind anomalies of the QBO (Dunkerton, 1997). Table 2.1 shows the details of the waves responsible for the development QBO and its propagation. Waves with very short horizontal

34

Figure labels:

.001 / 100

.01 / 80

.1 / km 60

hPa

Stratopause

Tropical Waves:
• gravity
• inertia gravity
• Kelvin
• Rossby-gravity

MQBO

Planetary
Scale
Waves

W

E

1

10

100

1000

Tropopause

Convection

SP   60°S   30°S   EQ   30°N   60°N   NP

40

20

0
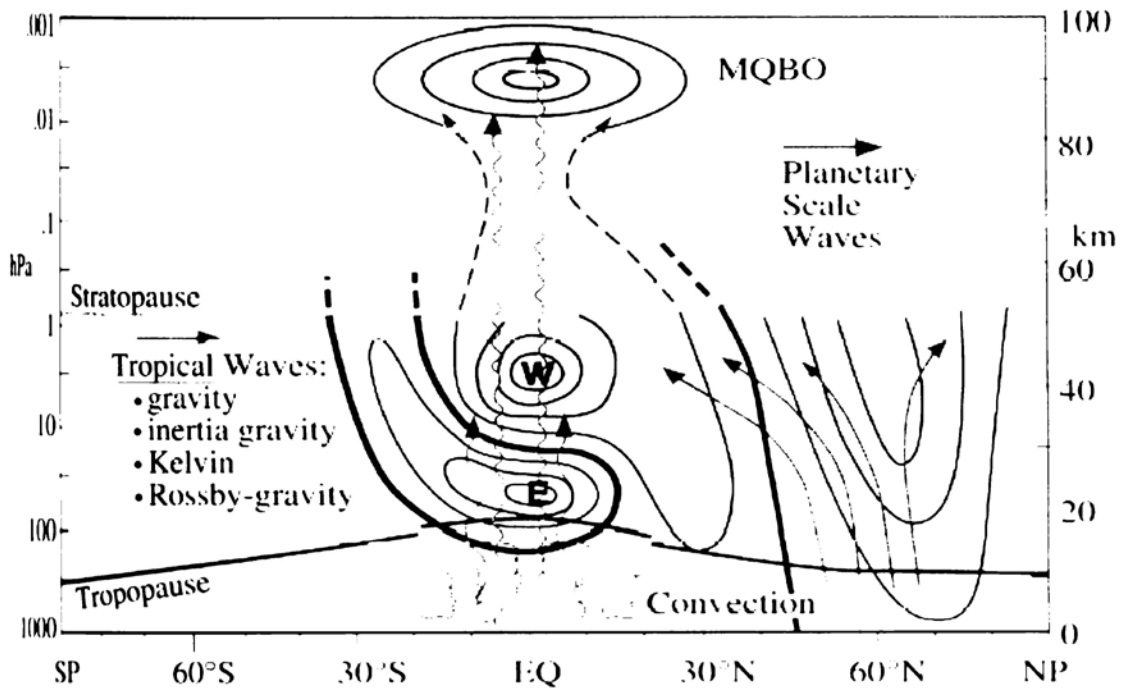
Figure 2.1: Dynamical overview of the QBO during northern winter (Baldwin *et al.*, 2001)

Type of Waves	Period (days)	Wave number	Zonal Wavelength (km)
Kelvin andRossby-gravity *waves* (*Equatorially trapped waves*)	≥ 3 days	**1-4**	≥ 10,000 km
Inertiagravity waves (*May or not equatorially trapped*)	~ 1-3 days	~ 4-40	~1000-10, 000 km
Gravity waves (*Propagating rapidly in the vertical*)	≤ 1day	**> 40**	~ 10-1000 km

Table 2.1: Atmospheric waves relevant to the QBO

wavelengths ≤10 km tend to be trapped vertically at tropospheric levels near the altitude where they are forced and are not believed to play a significant role in middle atmospheric dynamics.

All these waves originate in the tropical troposphere and propagate vertically to interact with the QBO. Equatorward propagating waves originating outside the tropics, such as planetary Rossby waves from the winter hemisphere, may have some influence on the upper levels of the QBO (*Ortland, 1997*). The lower region of the QBO (~20- 23 km) near the equator is relatively shielded from the intrusion of extra-tropical planetary wave (*O' Sullivan, 1997*). For each wave the vertical profile of the zonal wind determines the critical level at or below which the momentum is deposited. The critical level for these waves developed in part on the shear zones of the QBO. Some gravity waves propagate through the entire stratosphere and produce a QBO near the mesosphere known as the mesospheric quasi-biennial oscillation or MQBO.

In the tropical lower stratosphere the time averaged wind speeds are small, so the easterly minus westerly composite in the figure (2.1) is similar in appearance to the actual winds during the easterly phase of the QBO. At high latitudes, there is a pronounced annual cycle, with strong westerly winds during the winter season. To the north of the equator in the lower stratosphere, tropical winds alter the effective wave-guide for upward and equatorward propagating planetary scale waves (curved purple arrows). The effect of the zonal wind structure in the easterly phase of the QBO is to focus more wave activity towards the pole, where the waves converge and slow the zonal–mean flow. Thus the polar vortex north of ~ 45° N shows weaker westerly winds (or easterly shown in light blue). The high-latitude wind anomalies penetrate the troposphere and provide a mechanism for the QBO to have small influences on troposphere weather patterns.

The climatological circulation is characterized by large -scale ascent in the tropics, broad poleward transport in the stratosphere, and compensating

35

sinking through the extra-tropical tropopause (*Holton et al., 1995*). The transport of trace chemical species into or out of the stratosphere is the result of both large-scale circulation and mixing process associated with waves. Chemical process, like ozone depletion, not only depends on the concentrations of trace species, but may also depend on temperature. Since the QBO modulates the global stratospheric circulation including the polar region an understanding of the effects of the QBO not only on dynamics and temperature but also on the distribution of trace species is essential in order to understand global climate variability and change.

2.1.2 Modeling of quasi-biennial oscillation

Modeling studies were made by scientist all over the world to understand more about the quasi-biennial oscillation and its impacts on world climate. So climate scientist looked this problem using the different angles with one-dimensional model to the three-dimensional General Circulation Models (GCM) to simulate the QBO like pattern. But unfortunately many models failed to explain the different characteristic of the QBO properties due to various reasons. Modeling studies (*Gray et al., 1989; Dunkerton, 1997*) showed that Kelvin and Rossby Gravity waves are insufficient to account QBO. Many people modeled QBO incorporating the different aspects of QBO propagation. There are lot of modeling studies have been made to understand the QBO development and its alternating periodicity in phase propagation (*Tanaka et al., 1985; Coy, 1983; Dunkerton et al., 1984; Hamilton, 1981; Geller et al., 1997; Dunkerton, 1997*).

Ling and London (1986) included the QBO variation of zonal wind in a 1-D Radiative –Dynamical –Photochemical model of the stratosphere. This was followed by a 2-D simulation (*Gray et al., 1989*) including the latitudinal structure and interaction with the annual cycle and subsequently by 3--D simulation (*Hess et al., 1995*), which included a better representation of wave driven transport. The first realistic simulation of the QBO in a GCM was made by Takahashi (1996). The simulation of a QBO in a GCM requires fine vertical

36

resolution in the stratosphere, small diffusion coefficients and moderate to high horizontal resolution and a convection scheme that generate sufficient waves to drive QBO. The vertical grid spacing in the stratosphere must be sufficient to resolve the waves and their interaction with the men flow. The value used in simulations of the QBO range from 500 m (*Takahashi, 1996*) to 1500 m (*Untch, 1998*). High horizontal resolution is not always required for the simulation of QBO in GCM. But Hamilton *et al.* (1999) found that a horizontal resolution of 2.0° X 2.4° was needed. As in the real atmosphere, it appears that a broad spectrum of waves supplies the necessary forcing in these simulations.

2.1.3 Quasi-biennial oscillation and its relation to Indian summer monsoon

Some studies have already been made to understand the link between the equatorial lower stratosphere QBO and upper troposphere circulation. In the late 1970s some evidence for a link between the Indian Monsoon Rainfall (IMR) and stratospheric zonal winds was produced (*Rao et al., 1978; Mukherjee et al., 1979, Mohankumar, 1996*). Mukherjee *et al.* (1985) found a significant (at the 5% level) simultaneous correlation of +0.39 between the monsoon rainfall and mean zonal wind for June-August at 30 hPa level using the wind data for Balboa (9° N, 80° W) for the period 1951-1982. Bhalme *et al.* (1987) correlated the January 10 hPa zonal wind anomalies at Balboa with Indian Monsoon Rainfall (IMR) and found a correlation of 0.52 during the period 1958-1985. They found that the IMR tends to be less (more) than normal during an easterly (westerly) anomaly. By the beginning of 1990's, additional evidence has been found on the links between stratospheric winds and ISMR. The India Meteorological Department (*Gowarikaer et al., 1991*) uses 16 predictors is an operational long range-forecasting model. Two of these predictors are related to the stratosphere, namely the 50 hPa wind pattern in winter and the 10 hPa zonal wind pattern in January.

Using the rocketsonde data over Thumba (8° 30' N & 76° 54' E) George *et al.* (1975) found QBO in the middle stratosphere over the Indian region. Sasi

and Sengupta (1980) and Appu *et al.* (1980) studied the variation of amplitudes and phases of annual and semi-annual oscillations of zonal wind and temperature with height over the Indian equatorial station (Thumba). They have examined the middle atmospheric oscillations (annual and semi-annual) and the southwest monsoon over India.

2.2 Data and methodology

Monthly zonal wind data from the National Center for Environmental Prediction/ National Center for Atmospheric Research (NCEP/NCAR) reanalysis (*Kalnay et al., 1996*) used for the study of interannual variability (QBO) and its phase variation in relation to Asian summer monsoon. This is a gridded binary data, which has 144 longitude grids and 73 latitude grids with resolution of 2.5° longitude X 2.5° latitude. Also we used the monthly anomaly data of zonal wind for the period 1948-2002.

2.2.1 NCEP/NCAR reanalysis data

Reanalysis data contrast the traditional data sets in two fundamental ways: (a) an atmospheric general circulation model (AGCM) is an integral component of the analysis system and (2) a wide range of observations. This data set gives very useful dynamical quantities that cannot be determined by* subjective analysis but may be more accurate than the traditional analysis *particularly* in the data spars regions of the atmosphere. However, the difference in the AGCMs and the analysis methods will lead to differences in reanalysis. Several inter comparison studies have been made to understand the magnitude and nature of this uncertainity in NCEP/NCAR reanalysis.

The NCEP assimilation system used observations from the rawinsonde network, satellite sounding (Tiros Operational Vertical Sounder, TOVS data), aircraft, satellite (GMS, GOES, and METEOSAT) cloud drift winds. These data were subjected to stringent quality control (*Kalnay et al., 1996*). Three dimensional variation techniques (spectral statistical interpolation) were used to

interpolate the data into model grid. A T62 global spectral model, corresponding to approximate grid point spacing of 208 km was used in NCEP reanalysis. This model used σ- levels as vertical co –ordinate.

The reanalyzed gridded fields have been classified into four classes, depending upon the relative influence of the observational data and model on the gridded variable (Table 2.2). Reanalysis outputs are available in 17 standard pressure levels (1000, 925, 850, 700, 600, 500, 400, 300, 250, 200, 150, 100, 70, 50, 30, 20, and 10 hPa), 11 isentropic surfaces (650, 550, 450, 400, 350, 330, 315, 300, 290, 280, and 270° K) and 28 sigma levels (0.9950, 0.9821, 0.9644, 0.9425, 0.9159, 0.8838, 0.8458, 0.8014, 0.7508, 0.6943, 0.6329, 0.5681, 0.5017, 0.4357, 0.3720, 0.3125, 0.2582, 0.2101, 0.1682, 0.1326, 0.0782, 0.0580, 0.0418, 0.0288, 0.0183, 0.0101, and 0.0027). NCEP/NCAR data have good vertical coverage up to the middle stratosphere (10 hPa) level. There are 7 pressure levels and 4 isentropic surfaces present above the tropical tropopause. NCEP/NCAR data set has been validated with observational data sets

Class	Relative influence of Observational Data and Model on Reanalysis Variable
A	Strongly influenced by observational data (most reliable) *[e.g. upper air temperature and wind]*
B	Model has very strong influence than observational data *[e.g. humidity and surface temperature]*
C	Derived solely from model fields forced by data assimilation to remain close to the atmosphere. *[e.g. clouds, precipitation, and surface fluxes]*
D	Obtained from climatological values and does not depend on model *[e. g. plant resistance, land-sea mask]*

Table 2.2   Classification of NCEP/NCAR reanalysis fields (Kalnay et al., 1996).

39

In a series of studies (*Pawson et al., 1998a; 1998b; 1999*) validated the tropical stratosphere (thermal structure, annual cycle, QBO etc) in NCEP data. They found good agreement between observed values and reanalysis values. At the uppermost level (10 hPa), the reanalysis system found to perform poor due to the proximity of the upper boundary.

2.2.2   All India summer monsoon rainfall series

Several Indian summer monsoon rainfall series have been prepared with the number of rainguage varying from 300 to 3000 spreads all over India for the different lengths of period starting from the year 1841 onwards. The most systematic rainfall series was prepared by Parthasarathy *et al.* (1994) based on fixed network of rainguages. This series is available for the period 1871 to 1993, based on 306 well distributed rainguage stations over India, one from each of the districts in the plain region (29 subdivisions) of India and updated the ISMR value up to 2000 from the India Meteorological Department (IMD). The monthly rainfall data at these 306 stations were taken from the records of the India Meteorological Department. The mean value of all Indian summer monsoon rainfall (June to September) is 852.4 mm with a standard deviation of 84.69 mm for the above period.

2.3 Results and discussion

2.3.1 Interannual variability of zonal wind

Figure 2.2 shows the latitudinal variation of zonal wind averaged over the Indian longitude belt (65° E - 90° E) for 30 hPa level. We have taken the latitudes from 0 to 25° N. The easterly and westerly phases of the QBO is separated with zero values (thick contour) of the zonal wind. The easterly and westerly phases of QBO are downward propagating type at 30 hPa level. Easterly and westerly periodicity of QBO has greater variation during the period of study. The westerly phases are stronger in 1980, 1983 and 1999 and the easterly phases are stronger in 1984, 1994 and 1996 during the period of study. The DRY years
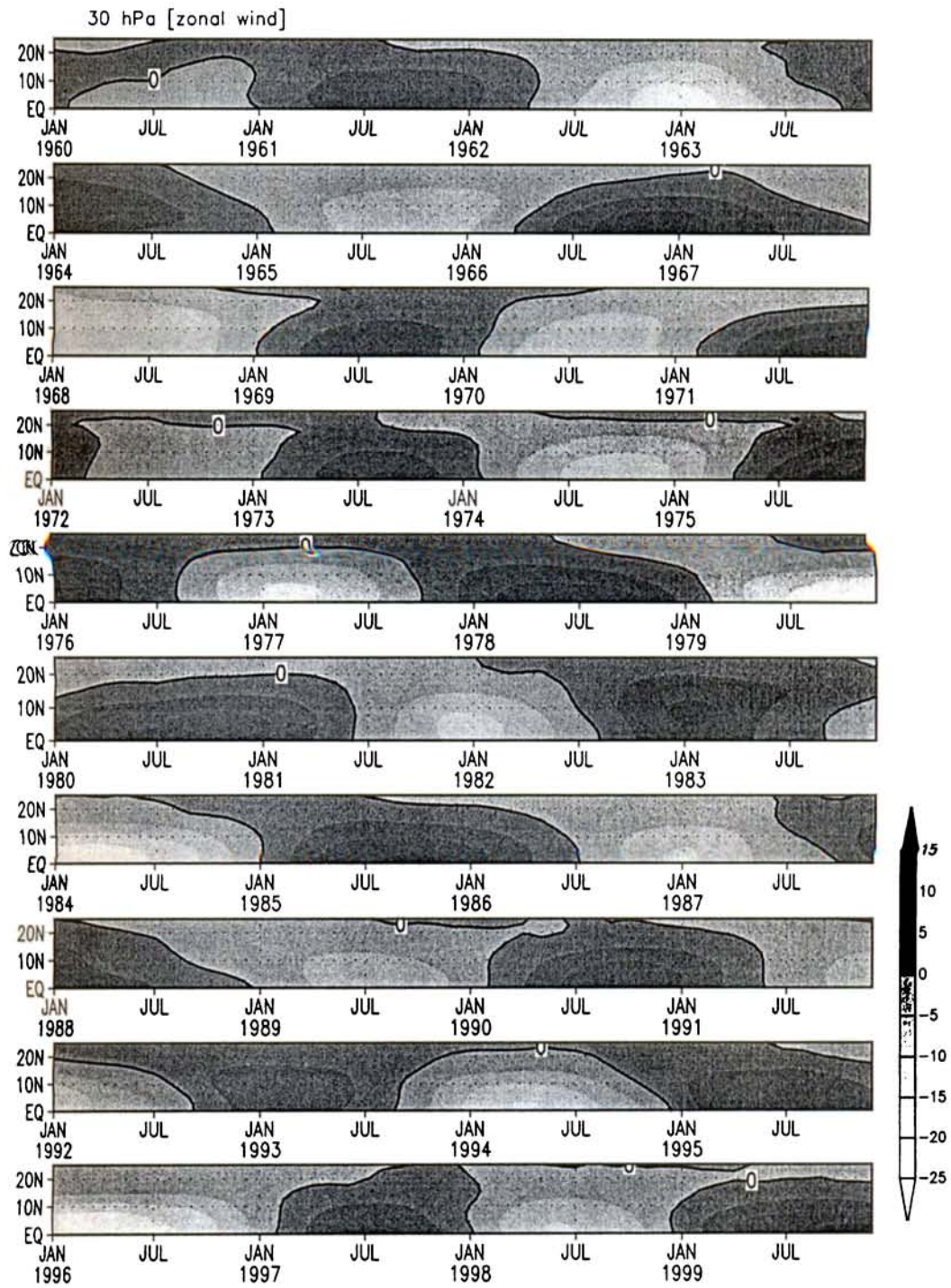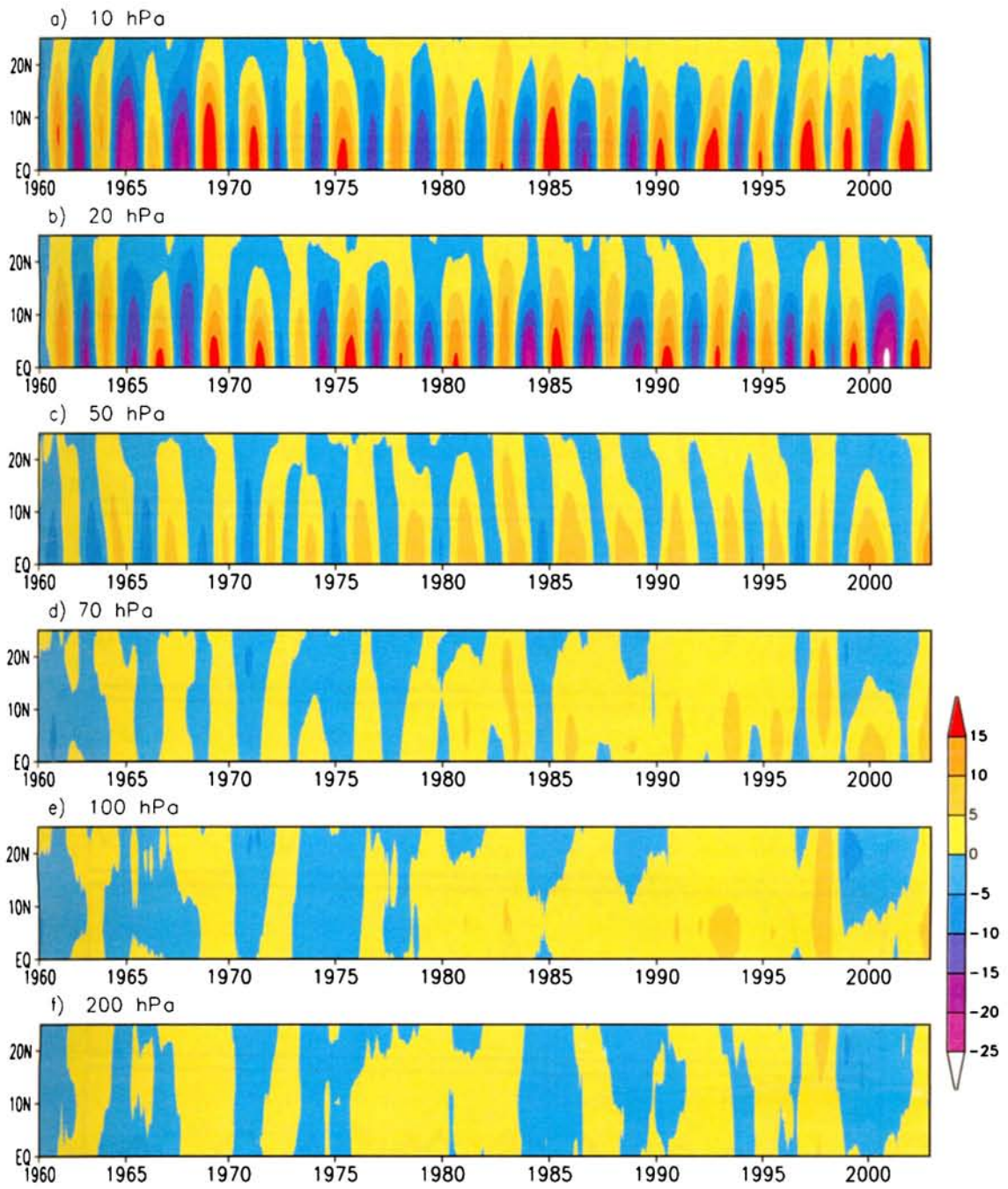
30 hPa [zonal wind]

Figure 2.2: Phase variation of QBO with time over the Indian longitude belt (65° E – 90° E) at 30 hPa level .

(1965, 1972, 1979, 1982 and 1987) and WET years (1961, 1975 1983 and 1988) fall in the easterly and westerly wind phases of QBO in the lower stratosphere (figure 2.2). It seems that the easterly and westerly phases of the QBO have *some* association with the Indian summer monsoon rainfall.

Figure 2.3 (a to f) represent the latitudinal variation of zonal wind *anomaly* with time for the period 1960 to 2002. We have considered the UT/LS pressure levels 10 hPa , 20 hPa , 50 hPa , 70 hPa , 100 hPa and 200 hPa respectively to understand the latitudinal variation of the QBO. The QBO periodicity and amplitudes are stronger at 10 hpa and 20 hPa levels. And the periodicity of QBO seen up to 50 hPa and the periodicity get affected for the *lower levels of the atmosphere (upper troposphere). The easterly and westerly* change of zonal wind is significant for the stratospheric circulation and the *weather* changes, which take place in the upper troposphere. The easterly and westerly wind periodicity are dissipated at the upper tropospheric levels .The quasi-biennial oscillation is global phenomenon so it can contribute much in the global climate change. Therefore we need a detailed study of phase and periodicity variation of quasi-biennial oscillation and its role in monsoon rainfall and its variability. This kind of periodicity variation in the QBO can contribute to the weather changes in the troposphere globally and regionally.

2.3.2 Quasi -biennial oscillation and its periodicity variation

Figure 2.4 (a to g) show the zonal wind averaged over Indian region (0°-25°N & 65° E-90° E) for the UT/LS pressure levels (10 hPa, 20 hPa, 30 hPa, 50 hPa , 70 hPa, 100 hPa and 200 hPa) during the period 1960 to 2002. During the period of study a clear easterly and westerly phase change over of zonal wind (QBO) with a periodicity of approximately of 26 months is seen in the stratospheric levels. The QBO periodicity in zonal wind seen up to 50 hPa level. The amplitude of the QBO is decreasing when it descends to the lower levels of the stratosphere. At 10 hPa level the amplitude of QBO varies between –15 to 15 ms^{-1} and 20 hPa level amplitude vary between –10 to 10 ms^{-1}. At 50 hPa the

41

Figure 2.3: Latitudinal variation of zonal wind averaged over the Indian longitude belt (65°E-90°E) for the UT/LS pressure levels (a) 10 hPa, (b) 20 hPa, (c) 50 hPa (d)70 hPa, (e)100 hPa and (f) 200 hPa
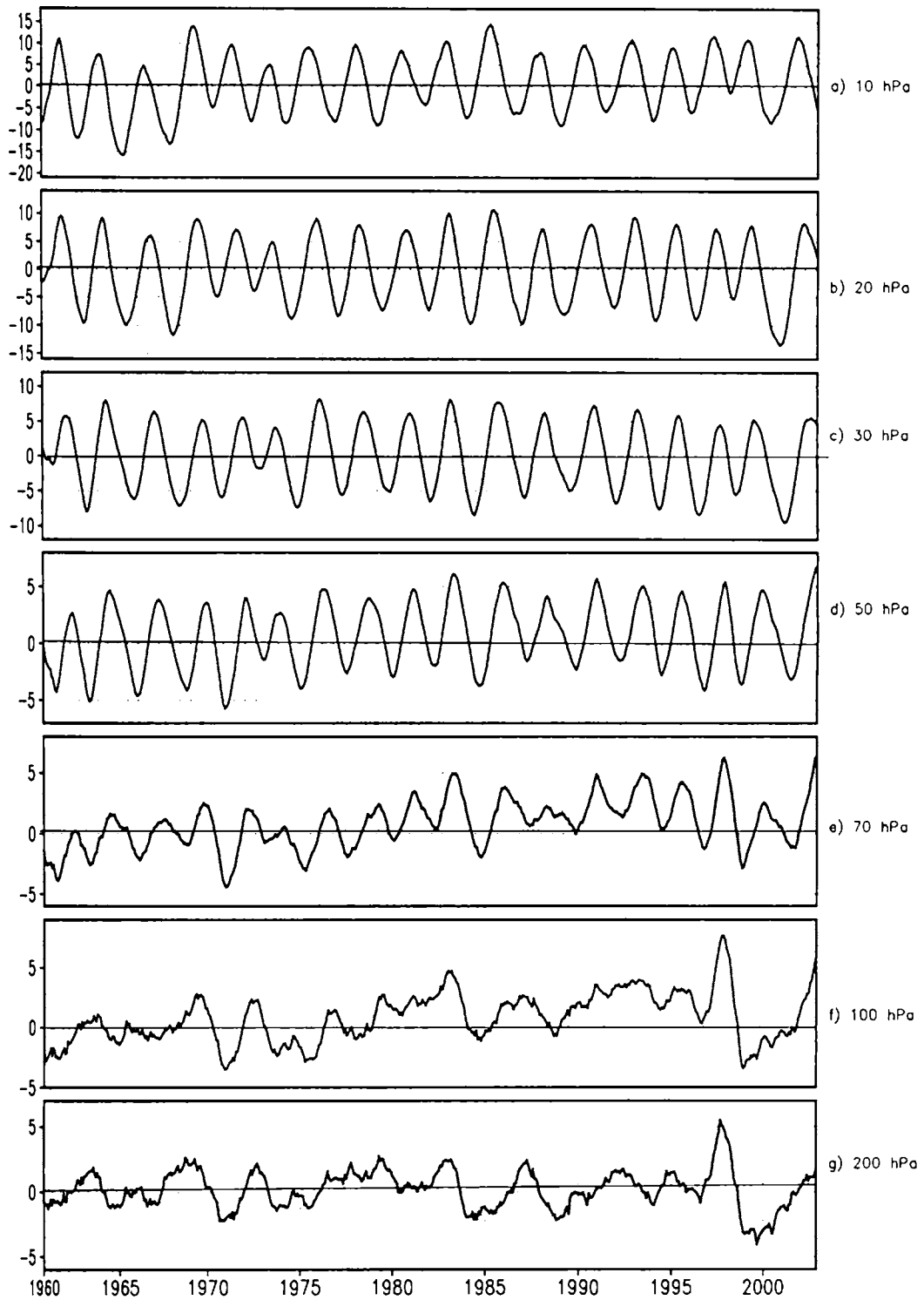
Figure 2.4 : Zonal wind anomaly averaged over the region (0° - 25° N &
65° E-90° E) for the UT/LS pressure levels. a) 10 hPa, b) 20 hPa , c) 30 hPa,
d) 50 hPa , e) 70 hPa , f) 100 hPa and g) 200 hPa

amplitude is almost reduced and the value vary between -5 to 5 ms⁻¹. Zonal wind anomaly shows a similar pattern of variation at the 100 hPa and 200 hPa level with a sudden variation of westerly to easterly during 1998. Table 2.3 shows the average duration of easterly and westerly phases of QBO for the levels 10 hPa, 20 hPa and 30 hPa over the Indian summer monsoon region. It is noticed that the average easterly periodicity is higher than the average westerly periodicity for the above levels over the Asian monsoon region. The approximate value obtained for the mean easterly and westerly periodicities of QBO are 14 and 13 months respectively over the Asian monsoon region for the different stratospheric levels.

The phases of QBO	Periods in (Months)		
	10 hPa	20 hPa	30 hPa
Easterly phase	14.59	14.10	14.19
Westerly phase	12.9	13.0	13.0
Easterly and westerly phase (QBO)	27.49	27.10	27.19

Table 2.3: Average duration of easterly and westerly phases of QBO in summer monsoon region.

Figure 2.5(a to f) represents the duration of individual easterly (gray bar) and westerly phases (dark bar) of QBO for the stratospheric levels (10 hPa, 20 hPa and 30 hPa) over the Indian summer monsoon region (65° E - 90° E & 0°- 25° N). The average QBO periodicity is ~27 months for all the levels, but some individual years there is a greater variation in the periodicity and amplitude of QBO over the summer monsoon region. The mean value of the periodicity of easterly phases and westerly phases are 14 and 13 months respectively at 10 hPa level and there is no larger variation from its mean value during the period of study. The possibility of reaching easterly wind maximum is during May (figure
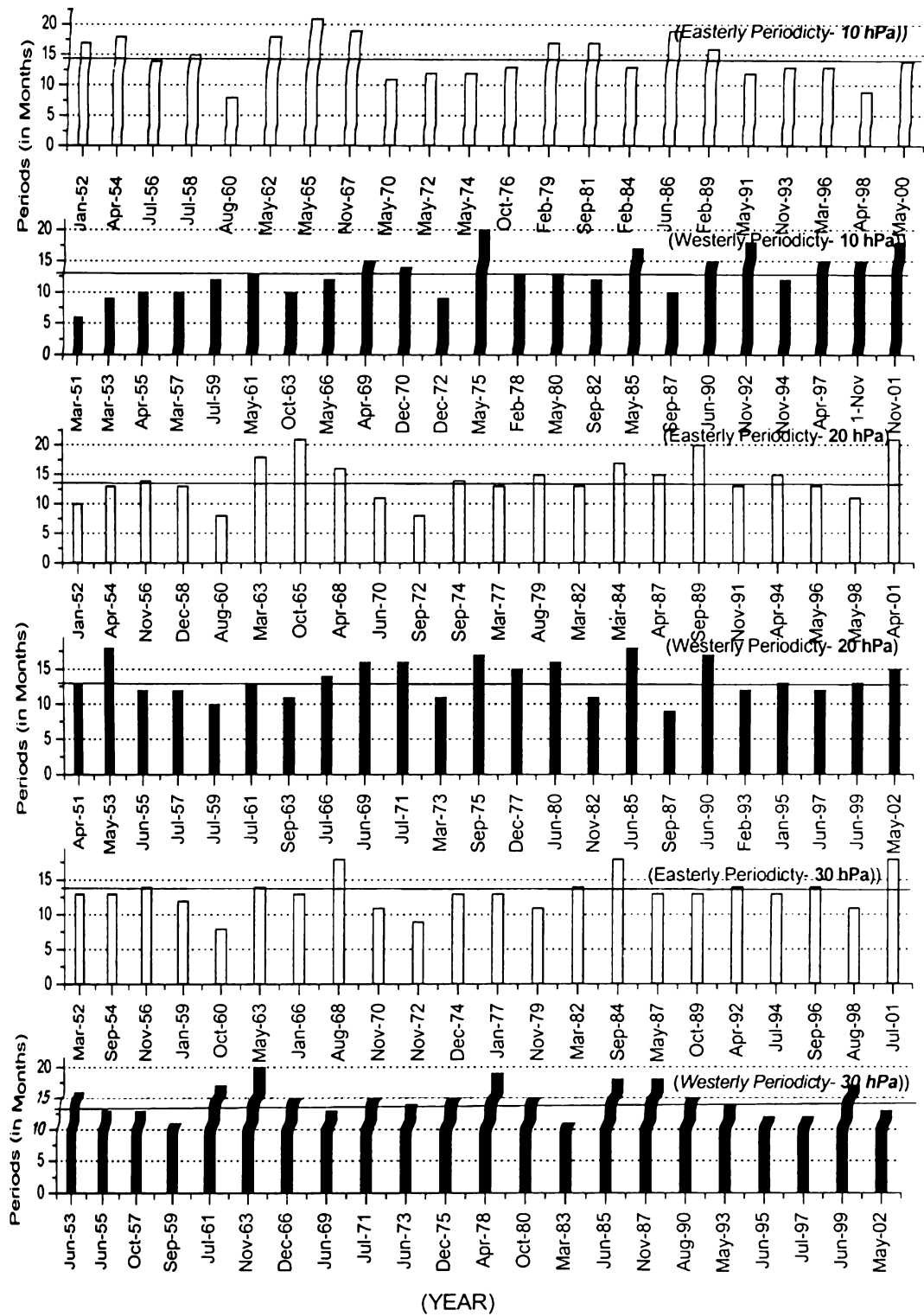
Figure 2.5: Duration of Easterly phases (Gray Bar) and Westerly periodicity (Dark Bar) over the Asian monsoon region for the levels 10 hPa , 20 hPa and 30 hPa (65° E - 90° E & 0°-25° N).

2.5(a) and westerly during March to May at 10 hPa level. For the westerly phase reaching its maximum periodicity during June to July for the levels 20 hPa and 30 hPa (fig.2.5 (d) & (f)) during the monsoon season.

Figure 2.6 (a to f) shows the zonal wind maximum plotted with the respective month during the easterly and westerly phases of QBO. The horizontal line parallel to the x-axis represents the mean value of zonal wind maximum. There is larger fluctuation in both easterly wind and westerly wind maximum seen during the period March 1951 to November 2001 at 10 hPa level (figure 2.6 (a) & (b)). For other levels (20 hPa and 30 hPa) the easterly and westerly wind maximum does not show greater variations from the mean value. Also noted that the possibility of reaching easterly wind maximum is in May at 10 hPa level, as in the case periodicity variation. The westerly wind maxima also seen during June to July similar to the periodicity variations at 20 hPa and 30 hPa level. The westerly periodicity and westerly wind reaches its maximum value during the monsoon period (June to July). This can influence the Indian summer monsoon activity. So we need further study to understand the periodicity variation and the Indian summer monsoon rainfall.

2.3.3 Phase transition of quasi-biennial oscillation

Tables 2. 4(a) to (f) shows the transition month of westerly to easterly phase and easterly to westerly for the stratospheric levels (10 hPa, 20 hPa and 30 hPa). Here the zonal wind anomaly is averaged over the region (65° E - 90° E & 0° - 25° N) for the period of study. Each column of the table representing the year with respect to the transition month of QBO phase (easterly to westerly and westerly to easterly) over the Asian summer monsoon region. The westerly to easterly transition of QBO take place for the period April to June and October to November with maximum transition occur during November at 10 hPa level (Table 2.4 (a)). During January to March the transition of westerly to easterly wind regime rarely occur at 10 hPa level and easterly to westerly transition take
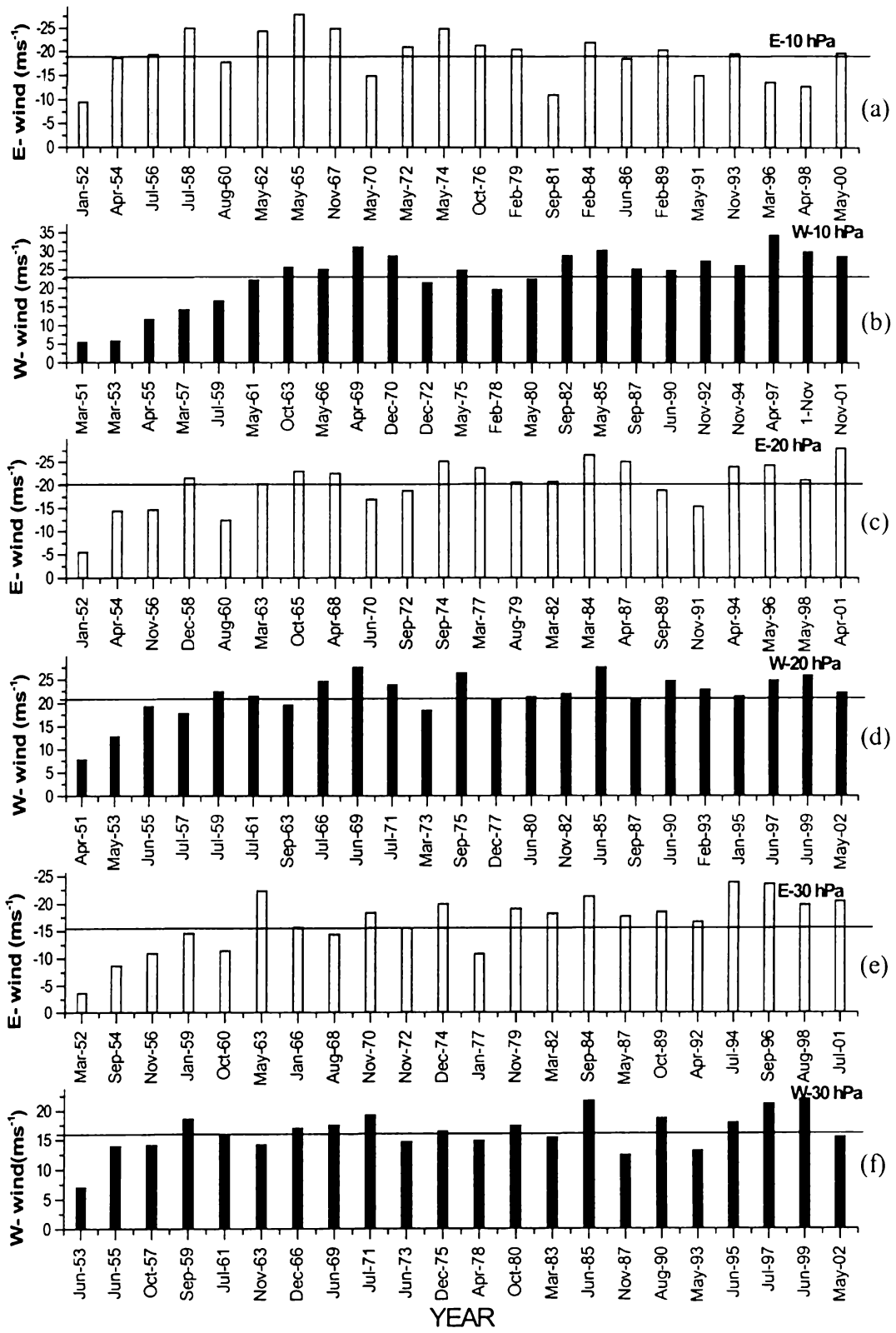
43

Figure 2.6: Wind maximum during the Easterly (Gray Bar) and Westerly (Dark bar) phases of QBO over the region (65° E-90° E & 0°-25° N)

Table 2.4 (a)   Westerly to Easterly (W → E) Transition Months at **10 hPa** .

No.of Transition	JAN	FEB	MAR	APR	MAY	JUN	JUL	AUG	SEP	OCT	NOV	DEC
6											1990	
5											1985	
4											1971	
3				1993	1965					1999	1961	
2			1988		1983	1978				1997	1957	1980
1		1969	1964	1976	1951	1957	1953	1973		1969	1955	1966

Table 2.4 (b)   Easterly to Westerly (E → W) Transition Months at **10 hPa**

No.of Transition	JAN	FEB	MAR	APR	MAY	JUN	JUL	AUG	SEP	OCT	NOV	DEC
3	1987				1982		1998				1991	
2	1957				1977	1994	1996	1989		1960	1979	2000
1	1955	1959			1963	1984	1968	1974	1970	1952	1972	1965

Table 2.4(c)- Westerly to Easterly (W → E) Transition Months at **20 hPa** .

No.of Transition	JAN	FEB	MAR	APR	MAY	JUN	JUL	AUG	SEP	OCT	NOV	DEC
4				1988	1991							
3	1970			1986	1983						1999	
2	1962			1972	1981					1985	1997	
1	1956		1958	1960	1967			1951		1978	1973	1953

Table 2.4(d)- Easterly to Westerly (E→ W) Transition Months at **20 hPa**

No.of Transition	JAN	FEB	MAR	APR	MAY	JUN	JUL	AUG	SEP	OCT	NOV	DEC
3	1980					1992	1987					1989
2	1975		1966			1982	1977		1994	1998	1996	1972
1	1955		1957	1959		1952	1963	2001	1968	1984	1970	1960

Table 2.4(e)- Westerly to Easterly (W → E) Transition Months at **30 hPa** .

No.of Transition	JAN	FEB	MAR	APR	MAY	JUN	JUL	AUG	SEP	OCT	NOV	DEC
4						1991						
3				1979	2000	1981						
2	1998		1970	1974	1972	1962	1986	1976				
1	1954	1989	1956	1965	1960	1958	1983	1967		1993	1995	

Table 2.4(f)- Easterly to Westerly (E → W) Transition Months at **30 hPa**

No.of Transition	JAN	FEB	MAR	APR	MAY	JUN	JUL	AUG	SEP	OCT	NOV	DEC
4		1973							1992			
3	1997	1971			1975				1987			
2	1985	1969	1990		1966			1982	1977		2001	
1	1961	1955	1980		1957	1959		1963	1952		1994	1998

Table 2.4 (a to f): shows the phase transition of zonal wind (QBO) for the stratospheric levels with respect to the months over the Indian region (65°E –90°E & 0°-25°N)

place during May to December at this level. During the equinoctial period (March, April, and September) both transitions (W → E and E → W) rarely occur. At 20 hPa level (Table 2.4(c) and Table 2.4(d)) the majority of W → E transition take place during the pre-monsoon period (April to May) and post-monsoon period (October to November). There are no transitions from W → E take place during monsoon periods at 20 hPa level. But in many cases the E → W transition takes place during the months January to June. During the month of May there is no transition from easterly to westerly compared to westerly to easterly transition at 20 hPa level.

From the above tables, maximum possibility of westerly to easterly transition of QBO generally falls in the month of May and easterly to westerly transition occur on January. At 30 hPa level (table 2.4(e) and (f)), the transition of westerly to easterly phase occur during the month of April to May, the respective monsoon will be below Normal or DRY years and if the transition of easterly to westerly phase occur during January to February the respective monsoon will be above normal or WET monsoon years. This kind of phase transition at 30 hPa level will help us for the advanced prediction of the monsoon. From the above discussions the WET and above Normal condition can be predicted *in well advance compared to the DRY and below Normal conditions of Indian summer monsoon.*

Figure 2.7 represent the composites of westerly phases and easterly phases of QBO over the Indian summer monsoon region for the lower stratospheric levels (10 hpa, 30 hPa and 50 hPa). The composite are prepared by selecting 19 westerly and 17 easterly phases of QBO at 10 hPa, 18 westerly phases and 17 easterly phases of QBO at 30 hPa and 19 westerly and 18 easterly phases of QBO at 50 hPa levels, respectively during the period of study 1960 to 2002. The gradient of the easterly and westerly phases of the QBO are in the north-south direction over the Indian region. When the QBO is descending to the
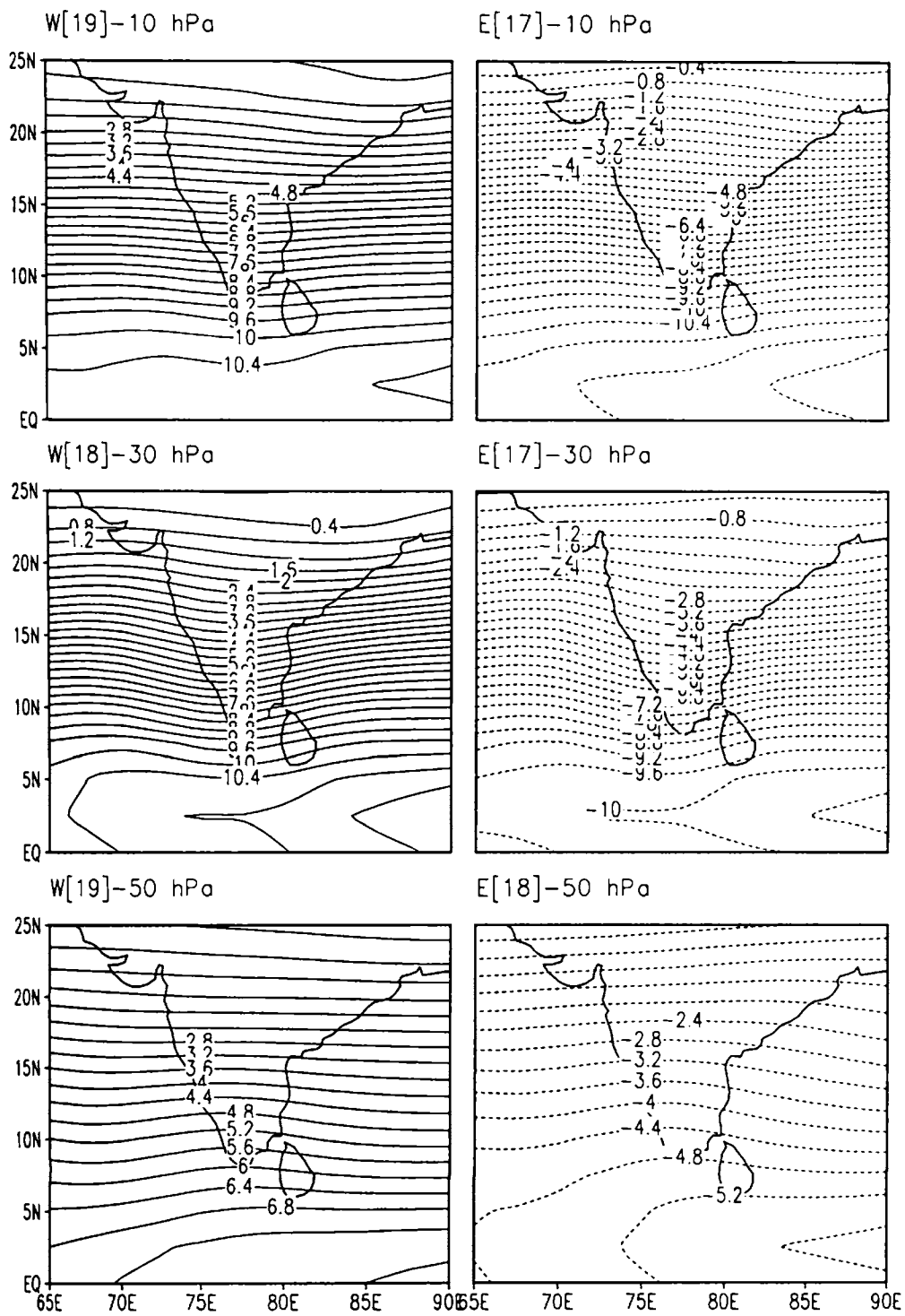
Figure 2.7: Composites of Westerly (solid contour) and Easterly phases (dotted contour) of QBO in zonal wind (ms⁻¹) for the period 1960 to 2002.

lower levels of the stratosphere, there is decrease in the north-south gradient of easterly and westerly phases of the QBO.
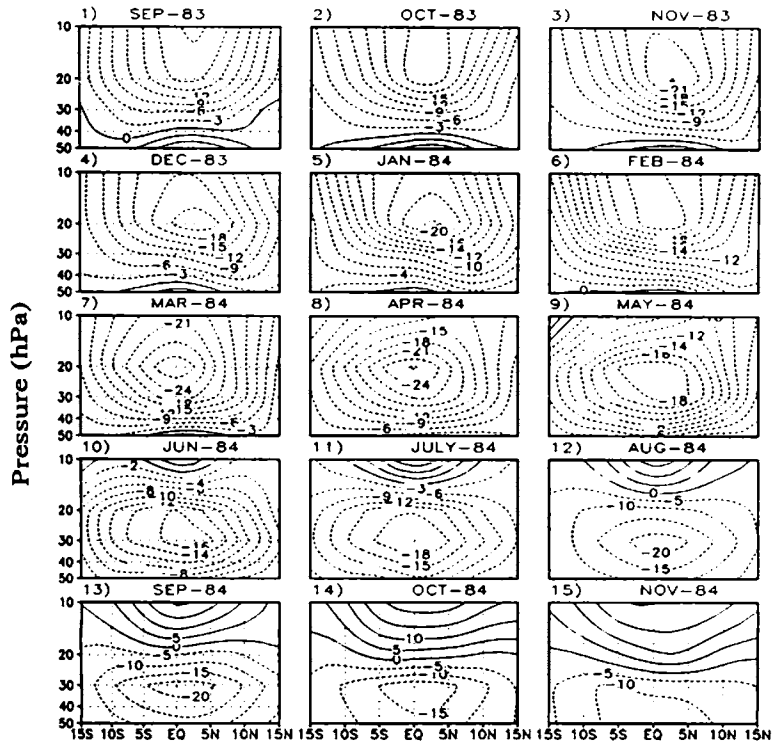
The easterly to westerly phase transition of QBO for the period September 1983 to February 1986 over the Indian longitude belt (65° E to 90° E) is shown in the Figure 2.8. The doted contour and solid contour represent the easterly and westerly wind phases. The onset of easterly and westerly wind phases starts at 32 km (10 hPa level) and descending to the lower stratospheric levels (50 hPa).

Figure 2.9, represent the vertical structure of zonal wind anomaly averaged over the region (0°-25° N & 65°E- 90° E) for the period 1961-1998. The altitude is marked in pressure levels starts from 70 hPa to 10 hPa (i.e from the lower stratosphere to the middle stratosphere). The figure shows the descending pattern of easterly to westerly phases of QBO from altitude 32 km (10 hPa) to the lower level 18 km (70 hPa). The light and dark shaded regions represent the easterly and westerly phases of QBO respectively. All the drought years (1965, 1972, 1979 and 1987) fall in the easterly phases of the QBO. It is also noted that the WET years (1961, 1975, 1983 and 1994) fall in the weak easterly/westerly phases of the QBO at 10 hPa level. Therefore the easterly /westerly phase change at the lower stratosphere play a major role in the long term prediction of the Indian summer monsoon rainfall whether it is a deficient or excess years. The easterly phases are stronger than the westerly phases and the periodicity of easterly and westerly varies in some years.

2.3.4 QBO phases and Indian summer monsoon rainfall

The phases of stratospheric QBO during the Indian summer monsoon period (June- September) are shown in table 2.5. From the table 2.5, wind pattern of the levels 10 hPa, 20 hPa, 30 hPa and 50 hPa are shown with the Indian monsoon rainfall (IMR) for the period 1960-2000. This wind structure is over the Indian region (65° E - 90° E & 0° -25° N). During monsoon season there
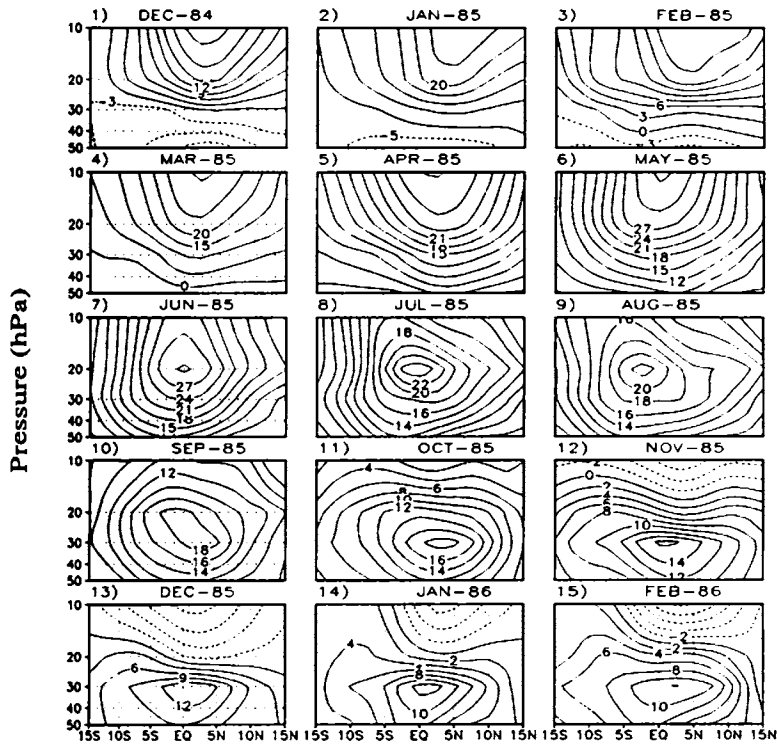
45

Figure 2.8: The easterly to westerly phase transition of QBO over the Indian longitude belt averaged (65°E - 90°E) from September 1983 to February 1986
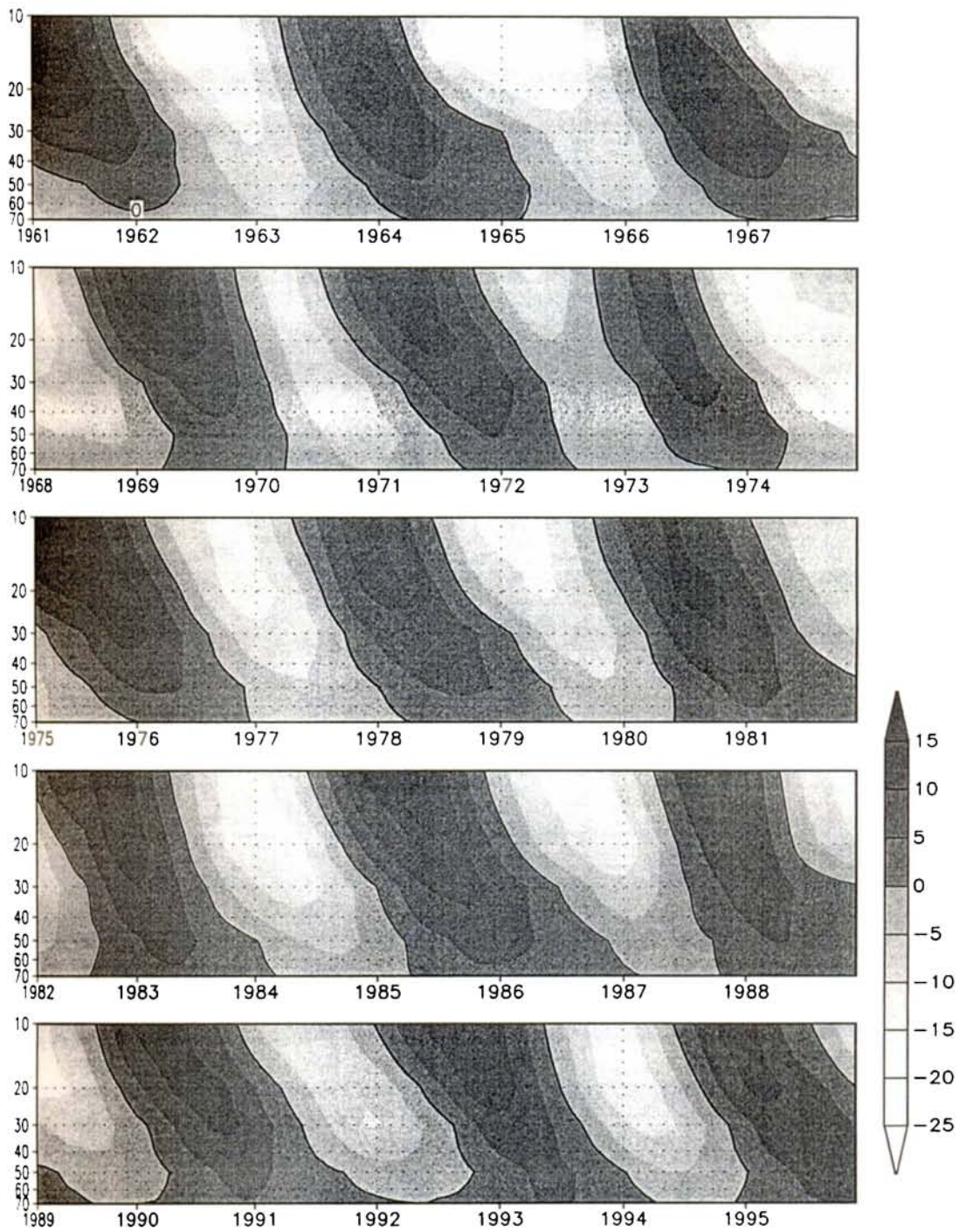
Figure 2. 9:   The vertical structure (from 70 hPa to 10 hPa) of QBO in zonal wind averaged over the region (0°-25° N & 65°-90°E). Dark and light shaded region represent the westerly and easterly phases of QBO.

YEAR	10 hpa	20hpa	30 hpa	50 hpa	IMR(mm)	TYPE
1960	E	E	E	E	839.8	BN
1961	W	W	W	W/E	1020.3	WET
1962	E	E	E	E	809.8	BN
1963	W	W	E/W	E/W	857.9	AN
1964	E	W/E	W	W	922.6	AN
1965	E	E	E	E	709.4	DRY
1966	W	W	W	E/W	739.9	AN
1967	E	E	W/E	W	860.1	AN
1968	E/W	E/W	E	E	754.6	AN
1969	W	W	W	W	831	BN
1970	E/W	E	E	E	938.8	AN
1971	W/E	W	W	W	886.8	AN
1972	E	E	E	E	652.9	DRY
1973	W/E	W	W	W	913.4	AN
1974	E	E	E	E	748.1	AN
1975	W	W	W	W	962.9	WET
1976	E	E	W/E	W	856.8	AN
1977	W	E/W	E	E	883.2	AN
1978	W/E	W/E	W	W	909.3	AN
1979	E	E	E	E	707.8	DRY
1980	W	W	W	W	882.8	AN
1981	E	E	E	W	852.2	AN
1982	W	W	E/W	E/W	735.4	DRY
1983	E	W/E	W/E	W	955.7	WET
1984	E/W	E	E	E	836.7	BN
1985	W	W	W	W	759.8	AN
1986	E	E	W/E	W	743	AN
1987	W	E/W	E/W	E	697.3	DRY
1988	E	W/E	W	W	961.5	WET
1989	E/W	E	E	W/E	866.7	AN
1990	W	W	W	W	908.7	AN
1991	E	E	E	W/E	784.6	BN
1992	W	E/W	E/W	W	784.9	BN
1993	E	W/E	W	W	896.7	AN
1994	E/W	E/W	E	E	953	WET
1995	E	W/E	W/E	W	827	BN
1996	E/W	E	E	E	853	AN
1997	W	W	W	W	872	AN
1998	E/W	E	E	E	874	AN
1999	W/E	W	W	W	827	BN
2000	E	E	E	W	770.2	BN

Table 2.5: QBO phases during the monsoon period (JJAS) over the Indian region (0°-25°N & 65°E-90°E). AN- above normal, BN- below normal, DRY- dry year, WET –wet years of monsoon. Easterly and Westerly winds are represented with the letters E and W respectively..

are four types of wind prevailed over the stratospheric region namely Easterly (E), Westerly (W), Easterly to westerly (E/W) and Westerly to Easterly (W/E). From the table the DRY years (1965, 1972, 1979 and 1987) fall in the easterly phases and WET years (1959, 1961, 1975 and 1983) occur in the westerly phases of QBO. If the phases of QBO in the lower stratosphere are strong westerly/weak easterly *(strong easterly/weak westerly phases) the respective* Indian summer monsoon will be WET/above Normal (DRY/below Normal). Thus there is a strong relation in the rainfall that we received during the Indian summer monsoon period and the phases of the qausi-beinnial oscillation prevailed in the lower stratosphere.

2.3.5 Correlation between zonal wind and ISMR

Figure 2.10 (a to f) shows the zonal wind anomaly averaged during monsoon periods (June to September) at different pressure levels with ISMR from 1948 to 1998. The Indian summer monsoon rainfall during June to September also collected for the period 1960 to 1993 *(Parthasarathy et al.,* *1994)* and updated the ISMR value up to 1998 from the Indian Meteorological Department (IMD). The zonal wind anomalies averaged over the Indian region $(65^{\circ} E - 90^{\circ} E$ & $0^{\circ} - 25^{\circ}$ N) from June to September for the UT/LS levels (10 hPa, 30 hPa, 70 hPa, 100 hPa and 200 hPa) are correlated with the Indian *summer monsoon rainfall. For the stratospheric levels 10 hPa and 30 hPa the* zonal wind anomaly show an in phase relation with Indian summer monsoon rainfall (ISMR) and keep a positive correlation values 0.039 and 0.162 respectively. *The upper troposphere keeps an out of phase relation with the zonal* wind anomaly and Indian summer monsoon rainfall. The correlations obtained for zonal wind anomaly and rainfall values are –0.196, -0.302 and –0.587 for the pressure levels 70 hpa, 100 hPa and 200hPa respectively. Hence the lower stratospheric zonal wind anomaly keep an in phase relation and upper troposphere zonal wind anomaly keep an out of phase relation with the Indian

U-10 hPa

zonal wind (m/s)

11
6
1
-4
-9
-14

(a)

U-30 hPa

8
5
2
-1
-4
-7

(b)

U-70 hPa

6
3
0
-3
-6
-9

(c)

U-100 hPa

4
0
-4
-8

zonal wind (m/s)

(d)

U-200 hPa

4
2
0
-2

zonal wind (m/s)

(e)

ISMR(mm)

ISMR (mm)

20
10
0
-10
-20
-30

(f)

1948   1954   1960   1966   1972   1978   1984   1990   1996
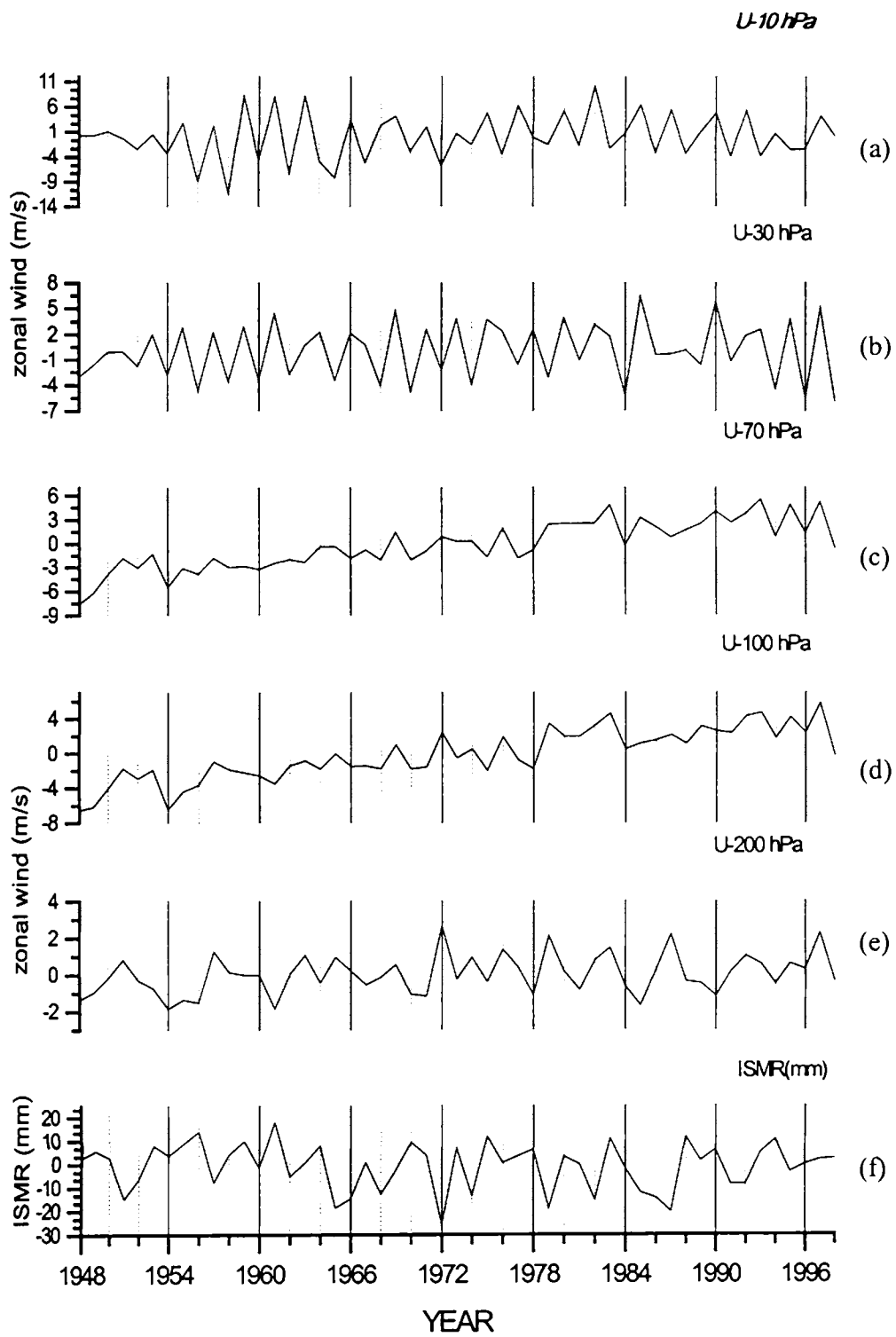
YEAR

Figure 2.10 : Zonal wind anomaly averaged over the region (65° E-90°E & 0°-25°N) for the pressure levels a) 10 hPa, b)30 hPa, c) 70 hPa, d) 100 hPa , e) 200 hPa and (f)the Indian summer monsoon rainfall anomaly.

summer monsoon rainfall. The above correlations are significant at above 95% confidence level using Student's 't' test.

2.4 Summary

The structures of QBO in zonal wind, its phase variation, and periodicity variation over the Asian summer monsoon region have been studied. During the period of study the periodicity and amplitude have greater variations over the region. This variation in the periodicity and amplitude of QBO may affect the monsoon rainfall variability. Also we studied the phase transition of QBO and found that the majority of the cases the westerly to easterly transition occur during May and easterly to westerly transition occur during January. The phases QBO in the lower stratosphere is strong easterly or weak westerly then the respective Indian summer monsoon will be DRY or below Normal and phases with strong westerly or weak easterly the resulting Indian summer monsoon will be WET or above Normal year.

Chapter 3

Analysis of Zonal Wind pattern in the UT/LS of Asian Summer Monsoon Region using Wavelet Transform and Empirical Orthogonal Function

3.1 Introduction

The need for exploratory methods of data analysis in climate comes from the need to separate the climate 'signals' from the background of climate variability or 'noise'. This decomposition of the data is done with the hope of identifying the physical process responsible for the generation of the climate signal. A climate signal is, in general terms, the result of interactions among physical processes within the Atmosphere- Ocean- Cryosphere system, which operate on a wide range of physical and temporal scales. The range of process involved extends over spatial scales of a few meters to thousands of kilometers and temporal scales of hours to millions of years. The interactions within the components of the climate system usually include positive and negative feedbacks that act on different scales. When these feedbacks combine properly and balance each other, they give rise to irregular but approximately cyclic climate variations.

The complicated behaviour and the nonlinear character of the climate system make exploratory data analysis methods difficult. The choice of the appropriate methods of analysis is of extreme importance when the objective is to search for specific signals in time and space, within large multivariate data sets. A fundamental characteristic of the climate data is the high dimensions of the variable representing the state of the system at any given time. Due to the features, it is often advantageous to split the full phase into two subspaces, i.e., the signal and the noise subspaces, in space or in time, or in space and time, which is determined by the system dynamics. Noise can be physical or instrumental and comprises all those features and details that are considered irrelevant for the signal. Generally, the signal has longer scales in space and time than the noise. The signal has also fewer degrees of freedom than the noise.

In this study two advanced statistical techniques such as Wavelet Transform (WT) and Empirical Orthogonal Function (EOF) have been used to

48

understand the spatial and temporal variability of zonal wind in the UT/LS of Asiatic monsoon region. Theory and methods of analysis of zonal wind with Wavelet Transform and EOF techniques have been presented in this chapter.

3.2 Data and analysis techniques

Monthly values of zonal wind anomaly for the period May 1960 to December 2002 (512 data points) and zonal wind for the period January 1960 to April 1981(256 data points) averaged over a region (0°-15° N & 65° E – 90° E) are subjected to Morlet Wavelet Technique, a continuous wavelet transform for the analysis of zonal wind over the Asian summer monsoon region.

Second approach we adopted to study the zonal wind is the Empirical Orthogonal Function (Singular Value Decomposition (SVD) method) which provide us the spatial and temporal patterns of the zonal wind variation over the Asian summer monsoon region (20° S - 30° N & 40° E - 120° E). We used the monthly values of zonal wind from the NCEP/NCAR reanalysis (*Kalnay et al., 1996*) data to do the Wavelet analysis and EOF analysis of zonal wind over the Asian summer monsoon region.

3.2.1 Wavelet analysis

Wavelet analysis is a powerful technique for signal processing that is extensively used recently. Since its introduction by Morlet (1983), Wavelet Transform (WT) has found wide application in diverse fields of science, such as seismic signal detection, Atmospheric Sciences, Image processing, Optics, Turbulence, Quantum mechanics, Chaos, Medical research etc. Wavelet transform (WT) is an analysis tool well suited to the study of multi-scale, non-stationary process occurring over finite spatial and temporal domains. It can be used to analyze the localized variation of power within a time series. By decomposing a time series into time-frequency space, one is able to determine both the dominant modes of variability and how those modes vary in time. Its uniqueness is its capability of simultaneously localizing the variability of the

49

signal in both time and frequency domains. By localization in time and frequency of the fluctuations in a signal we mean a quantitative representation of their spectral makeup as a function of time itself. As such it adds a new dimension to the time-honored Fourier analysis. Wavelet analysis is therefore particularly suitable for diagnosing fluctuations that tend to have an episodic character and consist of multi-scale components.

Recently, wavelet analysis is beginning to make inroads into the traditional Atmospheric and Oceanographic studies. Wavelet technique is used to analyses the multi-time scale oscillations present in the atmospheric and oceanic parameters .The wavelet transform has been used for numerous studies in Geophysics and various applications including the El-Nino Southern Oscillation (*Gu et al., 1995*); central England temperature (*Baliunas et al., 1997*); the dispersion and ocean waves (*Mayer et al., 1993*) and coherent structure in turbulent flows (*Farge, 1992*). Continuous wavelets are particularly effective for event finding such wavelets have been used in a variety of recent atmospheric and oceanographic applications for depicting the characteristics of fronts (*Gamage et al., 1993*), atmospheric turbulence (*Hudgins et al., 1993; Collineau et al., 1993*), breaking of wind waves (Liu, 1994) and biennial oscillation in tropospheric temperature and Monsoon activity (*Mohankuamr et al., 2000*) and temporal structure of the southern oscillation (*Wang et al., 1996*).The occurrence of climate event is represented, in parts, by a set of local parameters characterizing its frequency, intensity, time position and duration. The time-integrated characteristics of these localized signals provide the global information, which describes the temporal mean states over some averaged period, but to define a true climate signal, both local and global information need to be preserved. However, because of the uncertainity principles, it is impossible to achieve increased frequency resolution without suffering reduced precision in time localization and vice-versa. Traditional analysis tools such as Fourier transform or time filter do not provide much flexibility in the choice of an optimal combination in the simultaneous representation of both local and global

50

signals. As we discussed in the previous section, the wavelet transform is a tool that is ideally suitable for to achieve both.

3.2.1.1 Wavelet transforms

A WT uses generalized local base function (Wavelets) that can be stretched and translated with a flexible resolution in both frequency and time. Wavelet transform converts one dimensional time series into two-dimensional frequency- time domain. The flexible windows are adaptive to the entire time-frequency domain, known as the Wavelet Domain (WD), which narrows while focusing on high–frequency signals and widens while searching the low-frequency background. Because of the "uncertainty principle" (*Chui, 1992*), the width and the height of a time-frequency window cannot be arbitrary. As a result, high precision in time localization in the high-frequency band can be achieved at the expense of reduced frequency resolution and vice versa for low-frequency components. In this way a WT allow the wavelets to be scaled to match most of the high-and low-frequency signals so as to achieve the optimal resolution with the least number of base function. The detailed description of the wavelet technique is given as Appendix I.

3.2.2 Empirical orthogonal function analysis (EOF)

There are several statistical methods used for the detection of climate signals. The method of Principal Component Analysis (PCA), often referred to as Empirical Orthogonal Function (EOF) analysis, can be utilized effectively to link the spatial and temporal pattern of the data field. This method attempts to exploit the information available in spatially distributed data set and involve Eigenvalue decompositions. It is used in climate studies to be presented with a large climate data set consisting of time series over grids of stations, which we wish to compress into a smaller number of independent pieces of information. Usually data is in the form of simultaneous time series records from a grid on a horizontal plane $x_i(t)$, $y_i(t)$. The grid points may be regularly spaced (such as

51

locations of meteorological and oceanographic stations). The data also may be in the form of time series on a cross-section on a vertical plane, $x_i(t)$, $z_i(t)$.

Analysis of the data sets with the described characteristics, that is, consisting of a number of spatially distributed time series, are known on multivariate analyses. The Empirical Orthogonal Functions (EOF) approach was first introduced in fluid dynamics by Lorenz (1956) representing pressure and temperature fields over the United States in a way that reduced the number of predictors necessary for a statistical forecasting scheme. The EOF approach has been widely applied in meteorology and oceanography, because it has many desirable properties, such as the fact that the resulting features are based on the characteristics of the data themselves, they are linearly independent of one another, and a measure of their relative importance is provided. The theory and methodology for doing the empirical orthogonal functions (EOF) has been described by many peoples (*Hardy, 1977; Horel 1981, 1984; Kutzbach, 1967; Ludwig et al., 1980; Lumley, 1981; von Storch et al., 1999; Wilks, 1995*).

There are two approaches for computing EOFs for a number of time series. First constructs the covariance matrix of the data series and then decomposes it into eigenvalues and eigenvectors. The second uses the Singular Value Decomposition (SVD) of the data matrix to obtain eigenvalues, eigenvectors and time varying amplitude (Principal Components) *without* computing a covariance matrix. The EOFs obtained from the two methods are identical. The main difference between the two is given by the greater degree of sophistication, computational speed and stability of the singular value decomposition approach. In this study we have used the singular value decomposition method for analyzing the zonal wind over the Asian monsoon region.

Legler (1983) used the EOF analysis to study wind stress vectors over the tropical Pacific Ocean from 1961 to 1978. Rasmusson *et al.* (1981) studied the biennial variations in surface temperature over the United States using the SVD

method of EOF analysis. Wallace *et al.* (1992) used the SVD approach to study the wintertime sea surface temperature and 500 mb height anomalies. In the past, Empirical Orthogonal Function have been utilized to analyse a variety of scalar fields. Kutzbach (1967) analyzed monthly mean sea surface pressure, surface temperature, and precipitation over some 23 points in North America. Kundu and Allan (1976) used a vector EOF analysis on current meter data in the Oregon Coast upwelling region. An empirical orthogonal function analysis has been performed on temperature, salinity, oxygen and nutrient distributions of the Mediterranean Sea (*Fusco et al., 2003*). Horel (1984) discusses the application of complex principal component analysis to the study of traveling atmospheric waves. A detailed description of the EOF method is given as Appendix II.

3.3 Results and discussion

3.3.1 Wavelet spectrum of zonal wind over the UT/LS of Asian summer monsoon region

Figure 3.1 (a to c) represent the wavelet spectrum of zonal wind (anomaly) for the lower stratospheric levels 10 hPa, 30 hPa and 50 hpa averaged over the region ($0°-15°$ N & $65°$ E - $90°$ E) for the period May 1960 to December 2002 (512 data points). We studied the interannual variability of the zonal wind anomaly over the tropical lower stratospheric region. The figure represents the wavelet spectrum with x-axis as the time and y–axis as the period in months. The maximum period displayed in the figure is 72 months; eventhough periods upto 204 months is computed. The dominant oscillations in the wavelet spectrum of zonal wind for the lower stratosphere is QBO mode with a periodicity of approximately 26 to 30 months and is stronger at 10 hPa level (figure 3.1(a)). Annual oscillation is not seen in the wavelet spectrum of zonal wind anomaly of the lower stratosphere. Also noted that there is a greater variation in the period and intensity of easterly and westerly phases of QBO during the period 1960 to 1978. During this period there was perturbations in the periodicity of 11-year solar cycle and there is very small values of solar flux variation during the solar
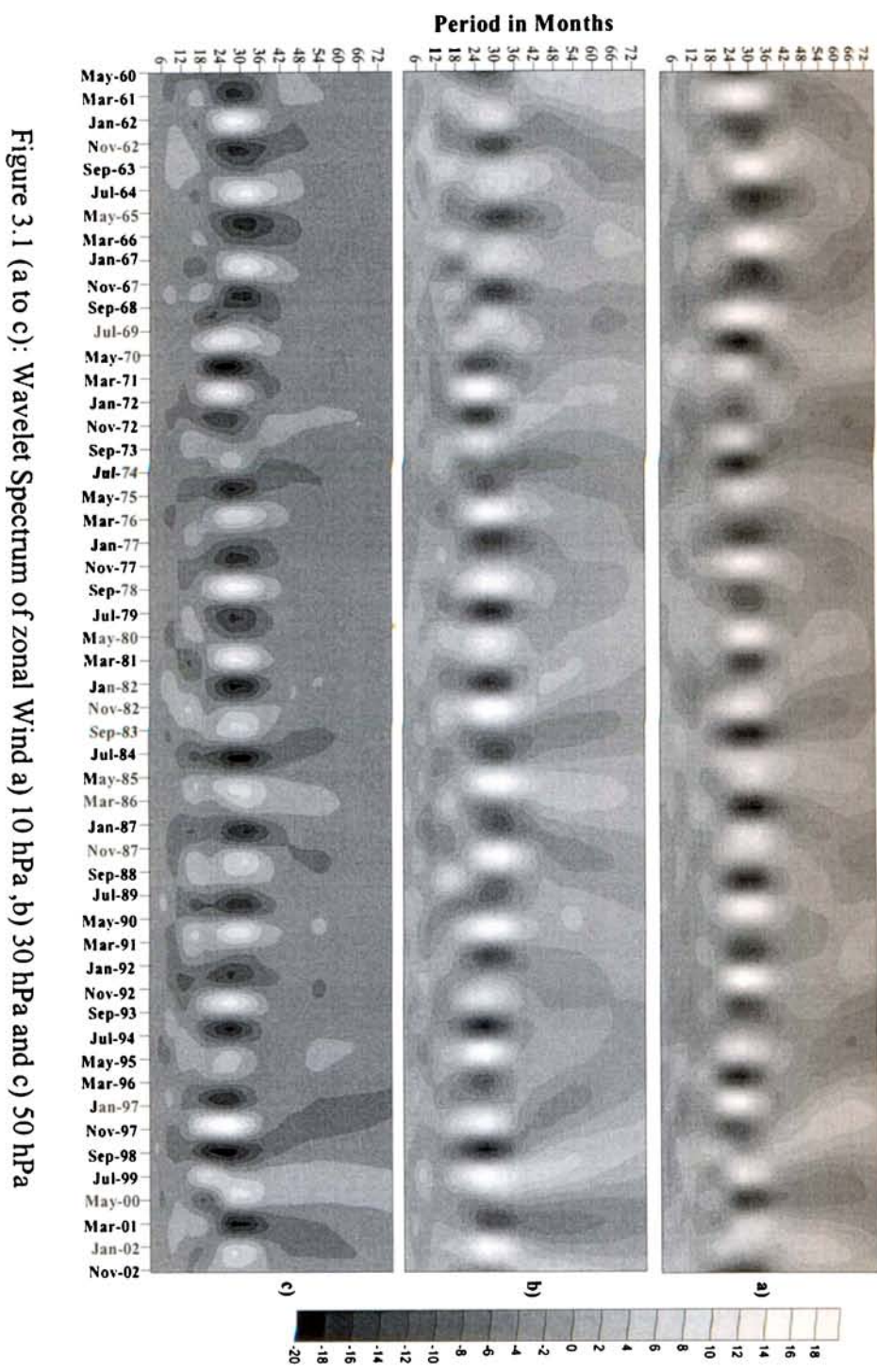
Figure 3.1 (a to c): Wavelet Spectrum of zonal Wind a) 10 hPa ,b) 30 hPa and c) 50 hPa

maximum periods, compared to other solar maxima during the solar cycle from 1960 to 2002. These variations in the solar cycle may affect the stratospheric QBO periodicity and its intensity. Thus, there must be a link between the QBO cycle and 11-year solar cycle in the tropical lower stratospheric and zonal wind variation. So it needs further detailed study to establish the relation connecting the QBO periodicity and 11-year solar cycle.

Figure 3.2(a to c) shows the wavelet spectrum of zonal wind anomaly at levels 70 hPa, 100 hPa and 200 hPa levels respectively. In the upper troposphere (200 hPa & 100 hPa) there is no indication of any signal (either QBO or annual oscillation) in the zonal wind. The QBO oscillations are significant only at 70 hPa levels. Figure 3.3 (a to f) represents the power spectrum of the zonal wind anomaly for the UT/LS region with the period in months in the x-axis and normalized power in the y–axis. The 95% confidence level is also plotted as a dotted line in the figure along with the spectrum). In this figure, time period versus power is represented graphically along the x -axis and y-axis respectively. The peaks are representing the dominant oscillations in the zonal wind variation. The figure illustrates that the QBO (with a periodicity of 26 to 30 months) is the only major oscillation present in the time series and is above the 95% confidence level.

Figure 3.4 (a to h) represents the wavelet spectrum for the zonal wind, data over the Indian region ($0^{\circ} -15^{\circ}$ N & 60° E - 90° E) for the period January 1960 to April 1981 (256 data points) with all the periods displayed in the spectrum. The QBO signal in the lower stratosphere gradually diminishes as it reaches to the lower levels of the atmosphere. At the same time there is an appearance of annual signals in the (100 hPa, 200 hPa, 850 hPa levels) lower levels of the atmosphere. At 70 hPa level, both the annual periodicity and QBO periodicity is co-exist which can be considered as the transition level of QBO mode to annual mode of variability in the UT/LS region. The 11- year solar cycle is also present in zonal wind but not significant compared to the QBO
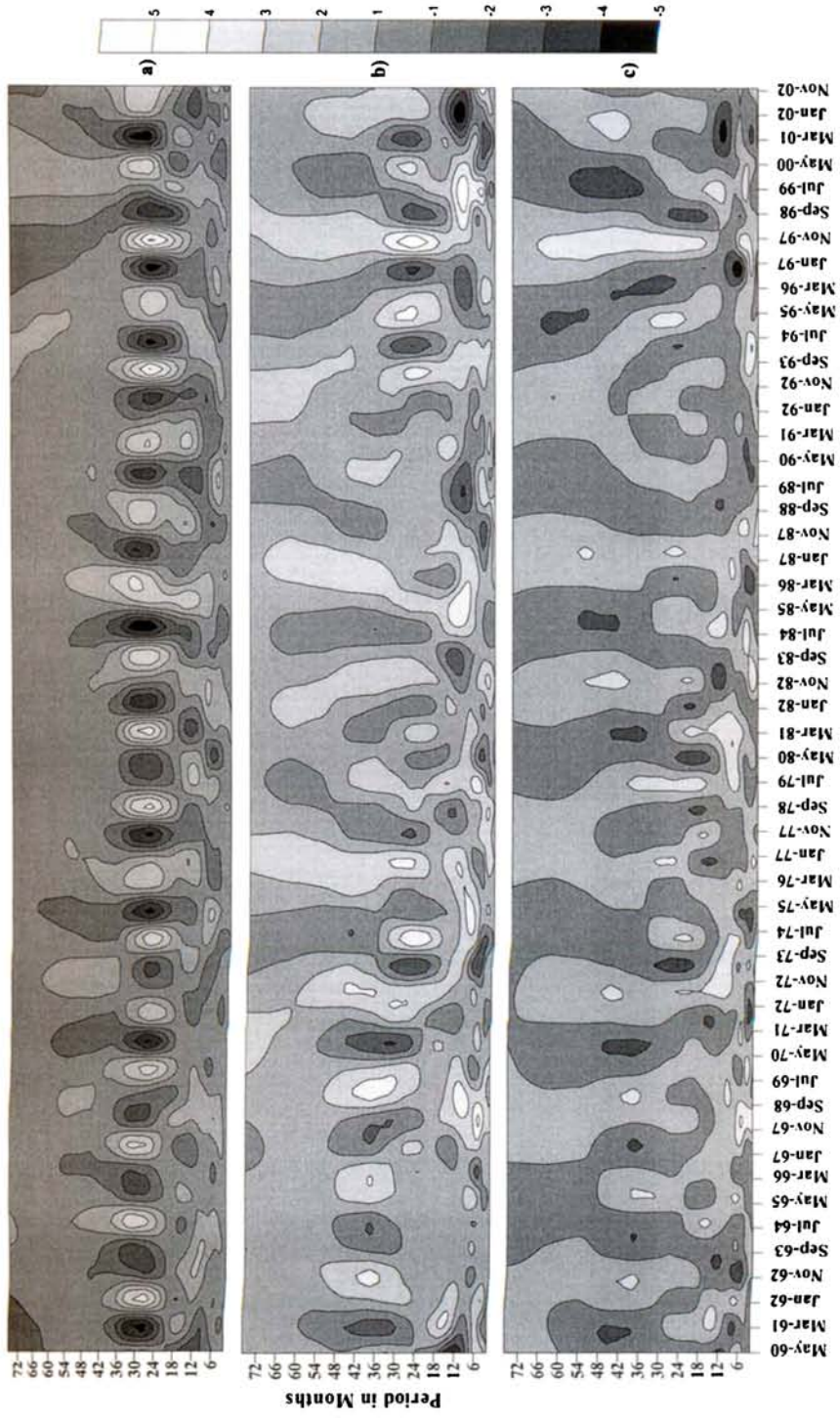
54

Figure 3.2 (a to c) : Wavelet Spectrum of zonal Wind a) 70 hPa , b) 100 hPa and c) 200 hPa
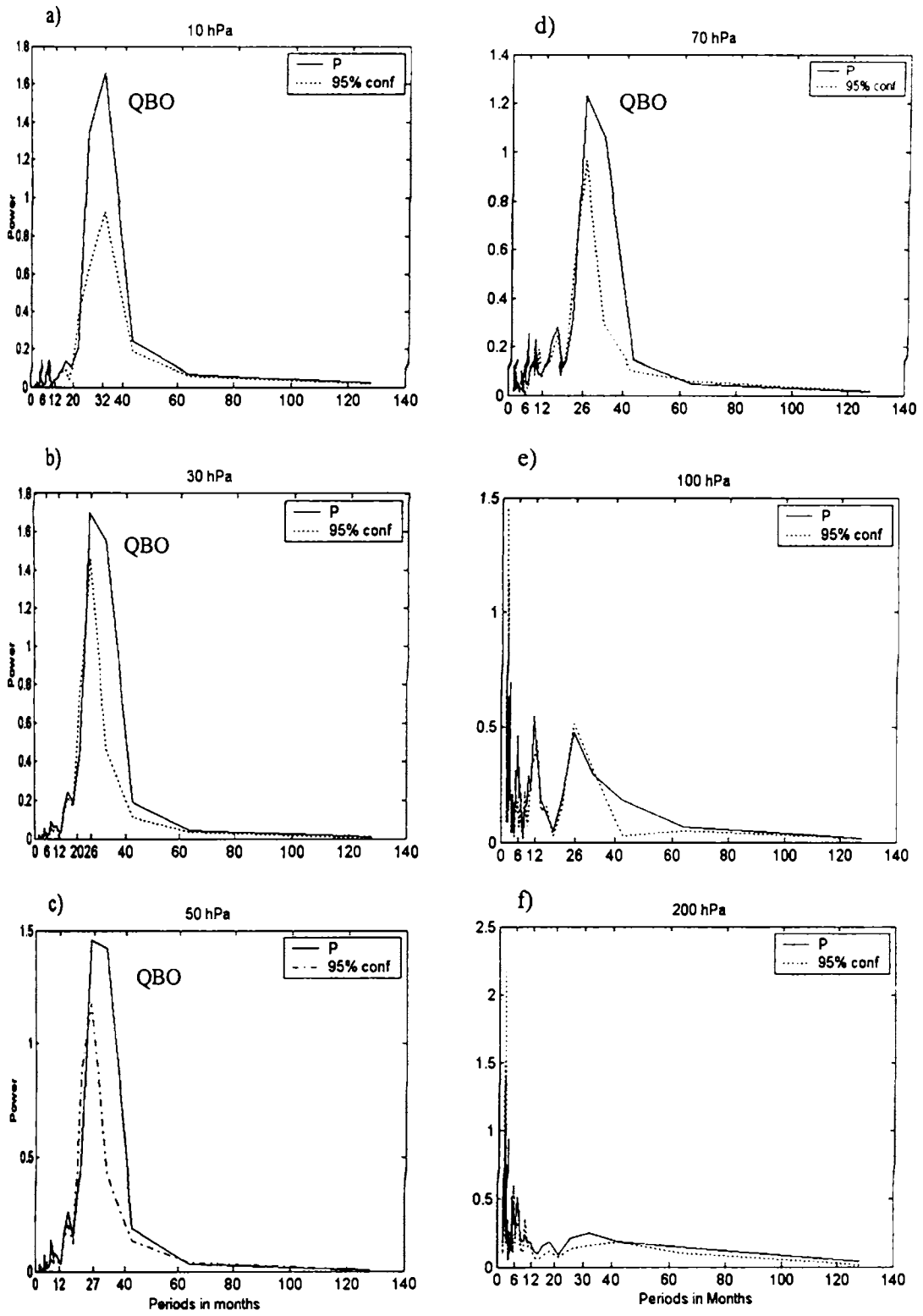
Figure 3.3 (a – f) Power spectrum of zonal wind anomaly for the UT/LS levels

LOWER STRATOSPHERE [ZONAL WIND]
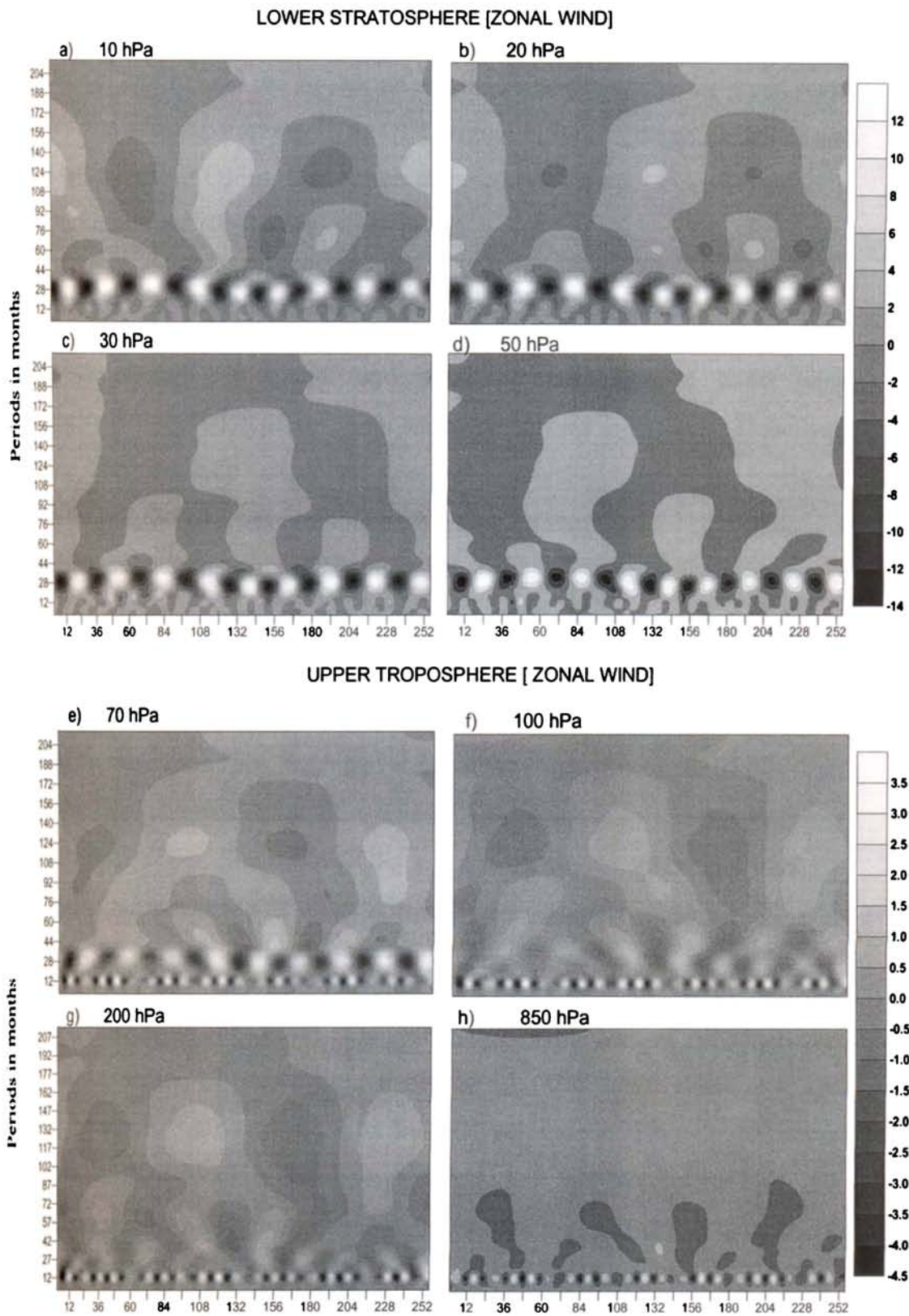
UPPER TROPOSPHERE [ZONAL WIND]

Figure 3.4 (a to h) Wavelet spectrum of zonal wind for the UT/LS pressure levels

mode. Figure 3.5 (a to h) represents the corresponding power spectrum of zonal wind, which is used for the wavelet transform. The power spectrum method is a good statistical tool to find the variations (oscillations) present in the given set of time series data of any parameter. The QBO signal in the stratospheric levels and annual oscillations (AO) in the upper tropospheric levels in zonal wind is statistically significant (95% confidence level).

3.3.2 EOF analysis of zonal wind over the Asian summer monsoon region

To understand the spatial and temporal variability of zonal wind characteristics in the UT/LS of Asian monsoon region we used the SVD analysis techniques. The first EOF expresses the maximum function of the variance present in the original data set possible with a single functional form. The second explains the maximum amount of the variance remaining with a function that is orthogonal to the first, and so on. Since the EOFs are an orthogonal and complete function set within the data set, we can project the data on these functions like they were Sines and Cosines. The resulting amplitudes as a function of the corresponding $A_n(t)$ and $B_n(t)$ of the Fourier analysis, but we call them the Principal Component or PCs. The PCs show the amplitude versus time of the individual EOFs. Since the EOFs are orthogonal in space and PCs are orthogonal in time makes the EOFs an optimal representation of the data.

The EOF pattern shows the spatial variation of eigenvector and the Principle Components represent the temporal variation of eigenvectors represented in terms of expansion coefficients. The contribution of the percentage variance of the each EOF to the total variance is also calculated and presented in the EOFs pattern. We have multiplied each EOFs pattern with the corresponding standard deviation of the Principal Component (PCs) in order to normalise EOF pattern suitable for the interpretation of results. We have done the EOF analysis of zonal wind with the help of a Fortran Program written for the SVD method suitable to the grided binary data set.
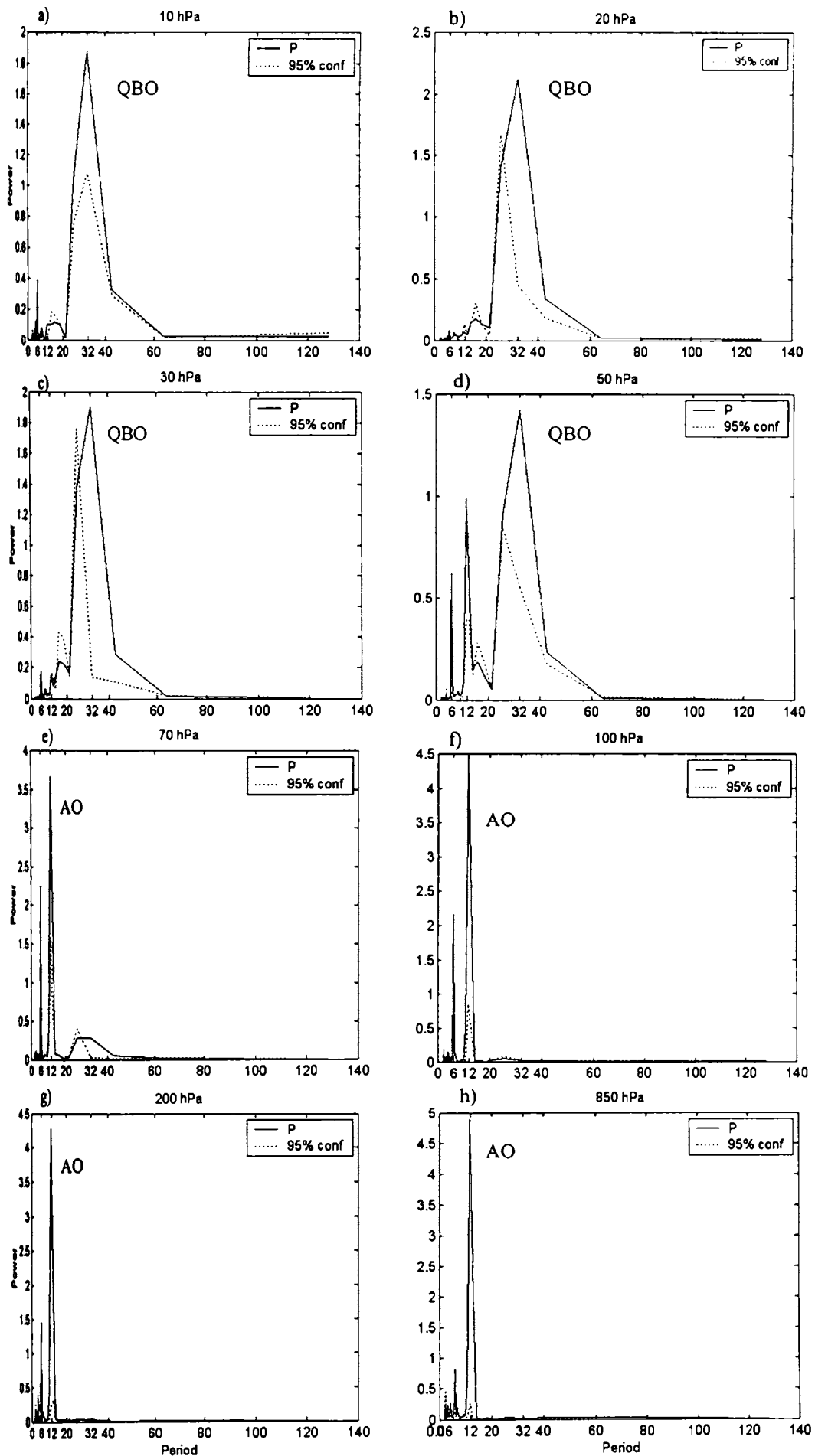
55

Figure 3.5 (a –h): Power spectrum of zonal wind for the UT/LS levels

Figure 3.6 represents the EOF patterns and the corresponding Principal Components (PC) for the stratospheric level 10 hPa (32 km). The first spatial pattern (EOF-1) over the region shows a unipole type and is the dominant percentage of variability (78.93%) in the zonal wind data representing the QBO mode. The maximum values of EOF coefficients are present in the equatorial region (10° S - 15° N) and decreases towards the poles. It is well known that the QBO periodicity in zonal wind is most prominent in the equatorial region. The temporal variability of the eigenvector is represented as PC1 in terms of expansion coefficients. This PC1 represents the highest eigenvalues and the expansion coefficients vary temporally with a periodicity of 28 months same as the QBO periodicity. Hence at 10hPa level the dominant signal in the zonal wind is the quasi-biennial oscillation. The first Principal Component (PC) of the zonal wind at 10 hPa shows that, the magnitude of westerly phase of QBO are stronger and tend to easterly phases with a QBO periodicity.

The second spatial pattern (EOF-2) and PC-2 show the next dominant variability in the data. At 10 hPa level the second most prominent oscillation is the annual mode in the data with percentage variation of 14.44% to the total variability. Here the spatial pattern is of dipole type (north-south) with the positive coefficients increasing from the equatorial region to the north and negative coefficients increasing towards the south from the equatorial region. PC (2) at this level shows that the zonal wind oscillates between the negative and positive phases with an annual periodicity, which is in accordance to the zonal wind climatalogy at 10 hPa; with almost regular oscillation throughout the study period. Third spatial pattern (EOF-3) shows the next percentage of variability in the data set and the value is 4.05 % and is of tri-pole type with north south direction with the positive coefficients concentrated in the equatorial region. The temporal variability in the PC-3 shows the combination of both qausi-beinnial mode and semiannual mode signal in the data series. The Fourth EOF pattern and corresponding and PC 4 can be treated as the noise present in the total variability in the zonal wind.

56
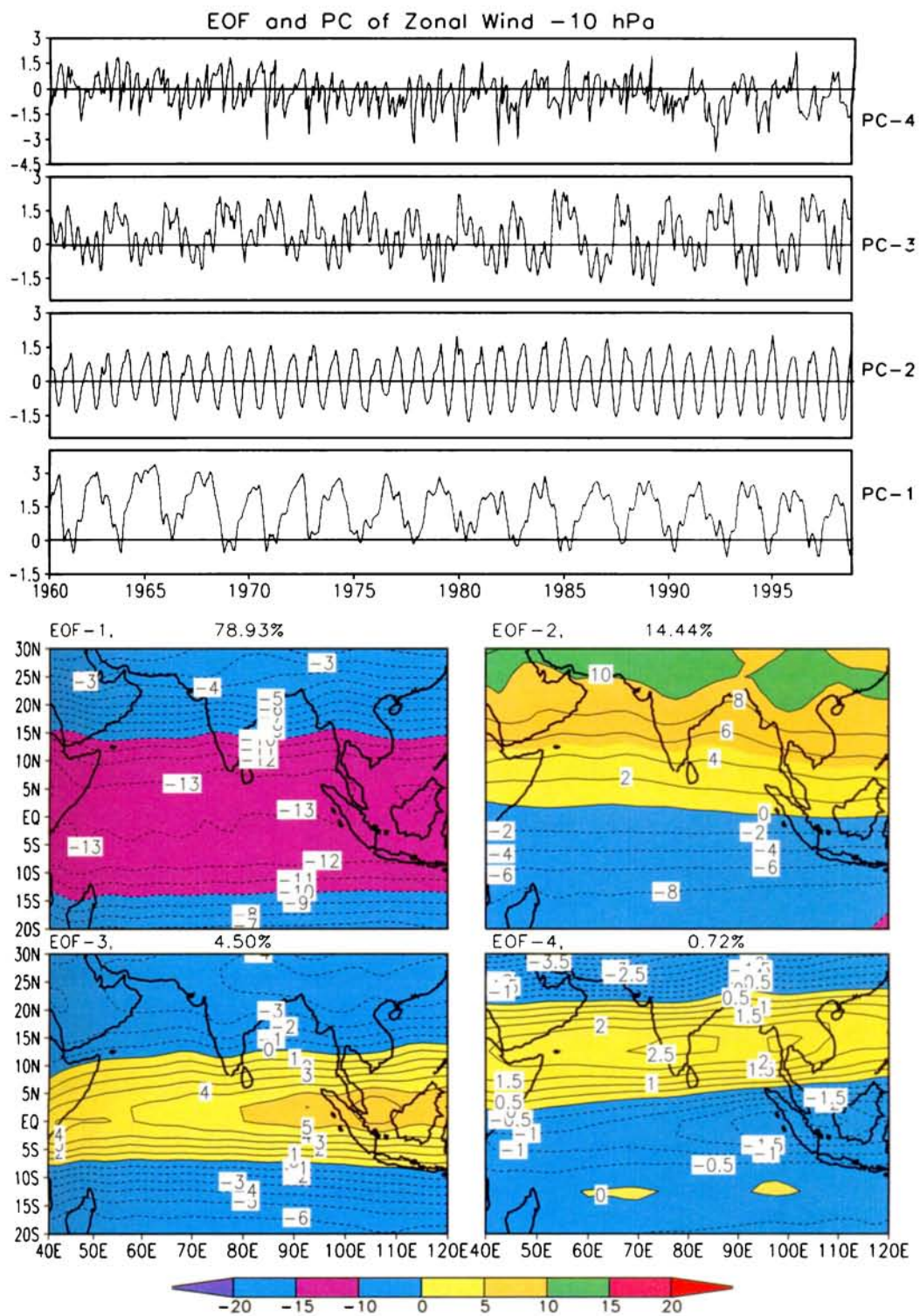
Figure 3.6: EOF patterns and principle components of zonal wind at 10 hPa

Figure 3.7, represents the EOFs and PCs at 20 hPa level with EOF-1, EOF-3 and EOF-4 are exactly similar to the EOF patterns seen at 10 hPa level (figure 3.6). The EOF-1 shows monopole pattern with negative EOF coefficients in the entire Asian monsoon region, representing the QBO mode. The EOF-2 shows a dipole type (annual mode) pattern; however with the negative and positive EOF coefficients reversed from that at 10 hPa level. The percentage contribution to the total variability by QBO mode and annual mode are 10% less at 20 hPa levels. The temporal component of the annual mode at 20 hPa level (PC-2), shows regular pattern throughout the study period, however with some peaks in the amplitude. More work is needed to know the special characteristics during these years with respect to the zonal wind pattern. The EOF-3 shows a tri-pole pattern over the Asian monsoon region. Here the corresponding PC-3 represents the annual mode, which is embedded in the QBO mode. The fourth EOF pattern and corresponding PC4 can be taken as the noise present in the data.

At 30 hPa level (Figure.3.8), the first spatial pattern (EOF-1) shows the qausi-beinnial mode of monopole type with positive coefficients all over the region. It can be noticed that the QBO characteristics in the westerly phase of the QBO at 10 hPa level descends to become almost easterly phase at 30 hPa and the spatial pattern also reversed accordingly. This peculiar feature of the QBO is brought out very clearly in this study. The maximum values of the EOF-1 coefficients are seen on either side of the peninsular India for the QBO mode. So the EOF-1 at levels 30 hPa is entirely different from the levels 10 and 20 hPa. The easterly and westerly phase change of QBO is clearly evident in this pattern (EOF -1) and maximum variability due to QBO mode is seen in the peninsular region of India. The second pattern (EOF-2) shows annual mode in the data and the percentage of variability due to this mode is increases to the lower levels of the atmosphere. The temporal pattern of the annual mode does not show any significant discerning trend.
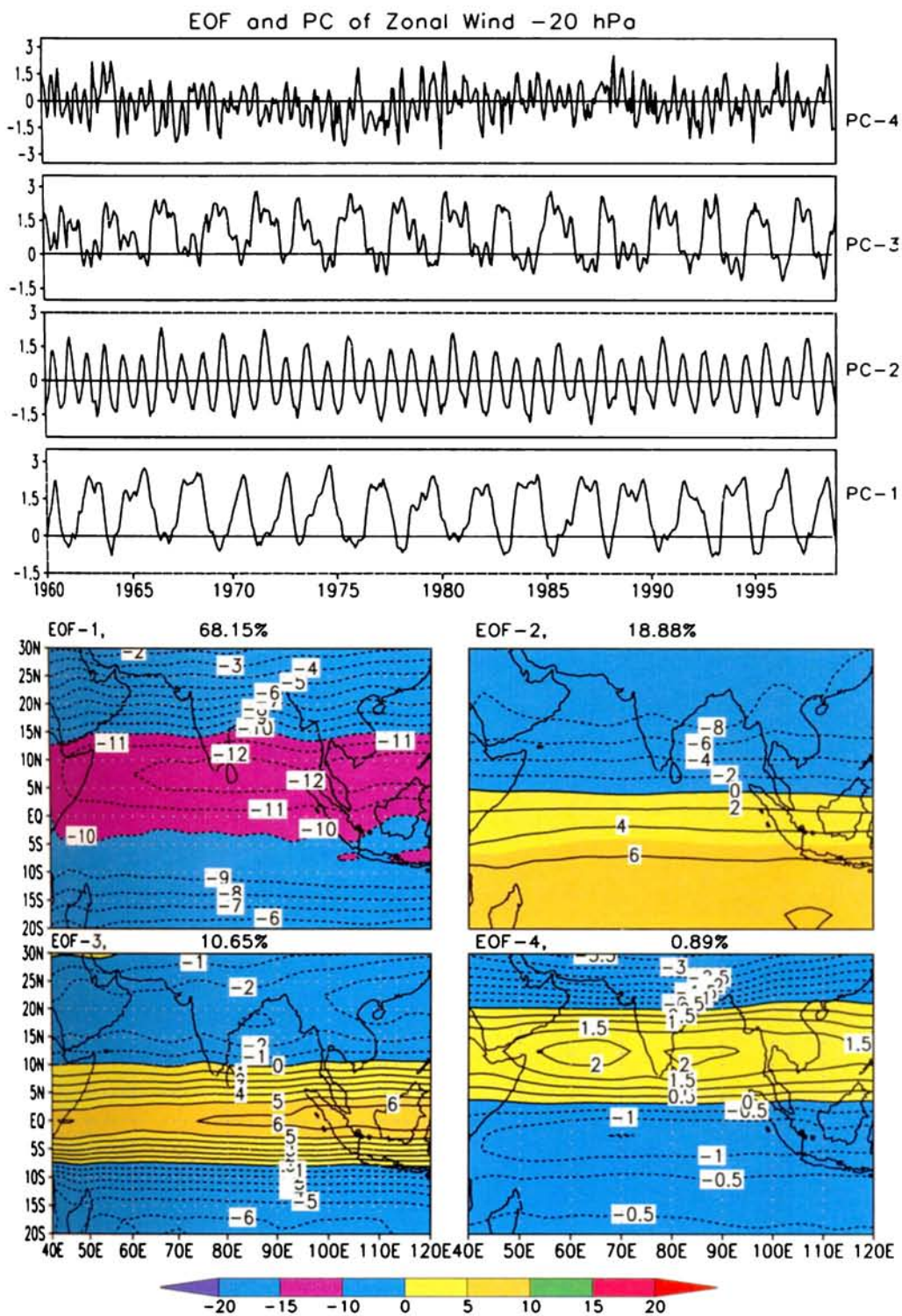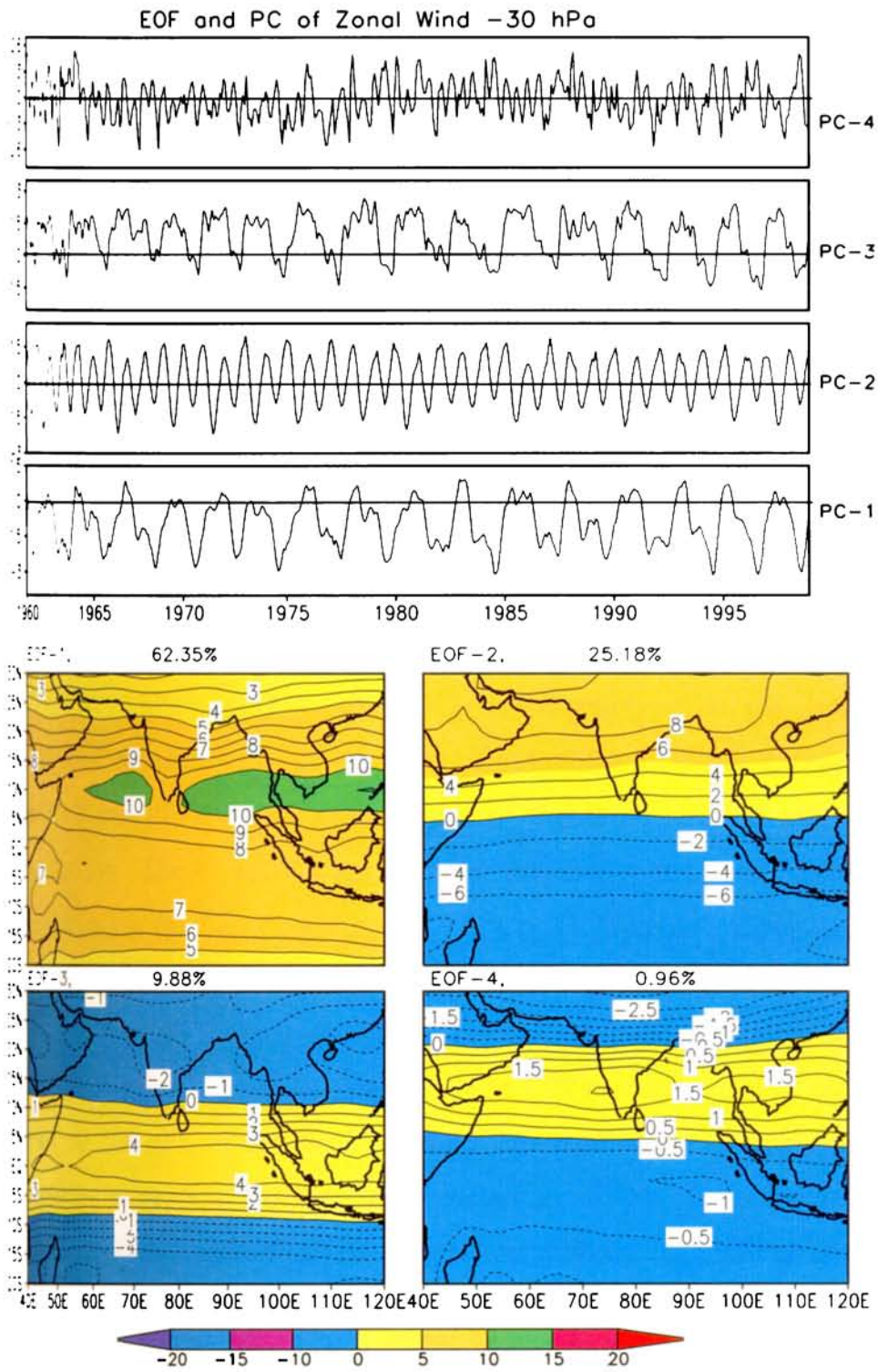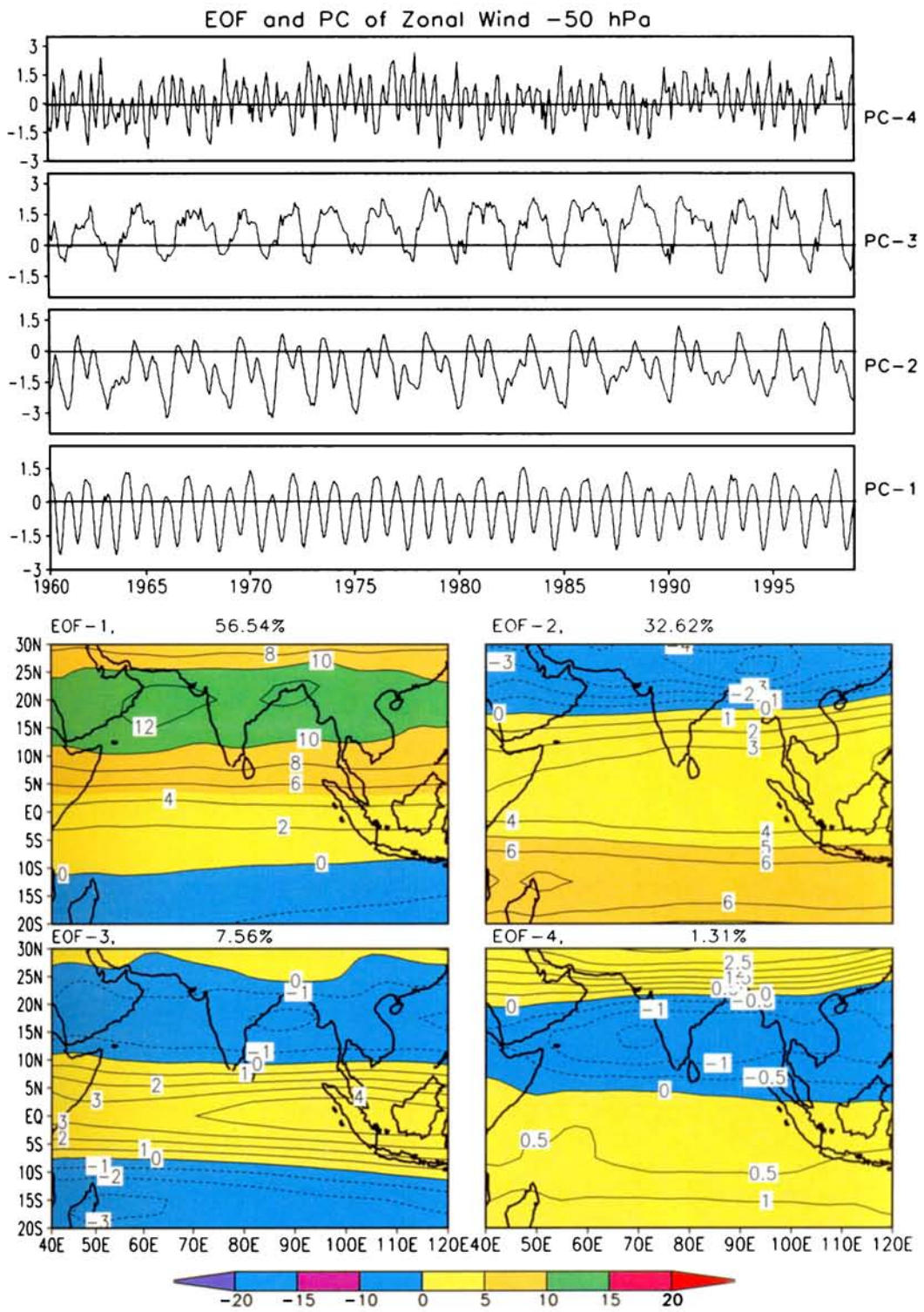
Figure 3.7: EOF patterns and principle components of zonal wind at 20 hPa

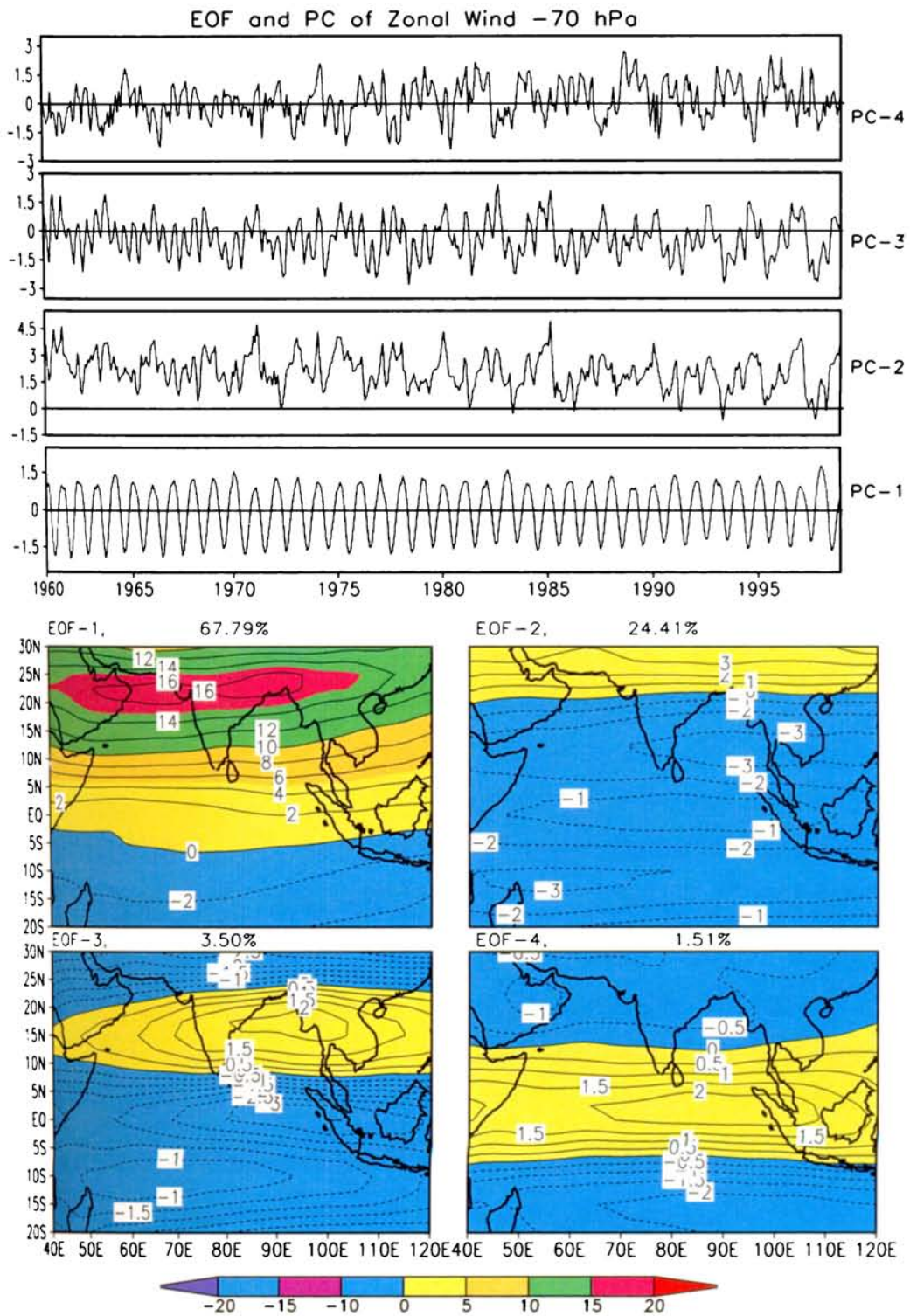Figure 3.8: EOF patterns and principle components of zonal wind at 30 hPa

Figure 3.9 and 3.10; show the EOF pattern and corresponding eigenvector variations with time represented as expansion coefficients (PC) for the levels 50 hPa and 70 hPa respectively. Quasi-biennial oscillation is a zonal wind with the easterly –westerly phase changing with a periodicity of 26-30 months. This mode of variability is most prominent at higher levels and in the lower troposphere; the QBO- mode of variability gives way to the annual mode. This is clearly seen in the spatial pattern (EOF-1) at the 50 hPa level. At this level (figure 3.9), the annual mode (dipole pattern) of EOF1 becomes the dominant variability and the QBO mode and (EOF-2) is seen to be decreasing to the lower levels of the atmosphere. The fact that higher values of EOF-1 are observed in northern parts of India, confirms that the annual variation is more in the northern part of India, which comes here in the maritime influence. The third EOF pattern represent the QBO mode with some perturbations and the percentage of contribution is very less compared to the annual mode at this level.

At 70 hPa level (Fig.3.10), EOF-1 is a dipole type and maximum value of EOF coefficients found in the northern latitudes. The EOF pattern corresponding to PC-2 and PC-3 shows some signal of the QBO, annual and semiannual oscillations. These oscillation (PC-2) together contribute about 24.41% percentages to the total variability at 70 hPa level. Figure 3.11 and 3.12 represent the EOF pattern and corresponding PCs of the upper tropospheric levels (100 hPa, 200 hPa). In the tropospheric levels the dominant variability in the zonal wind (EOF-1), shows the annual mode and QBO mode is almost absent at this level. At 100 hPa, while the annual – mode oscillates between easterlies and westerlies at regular intervals with annual mode variability, at 200 hPa the temporal pattern is entirely of the easterly component. It should be noted that the tropical easterly jet is most prominent at 200 hPa level. The values of EOF coefficients are higher in the northern latitudes from the equator for the tropospheric levels.
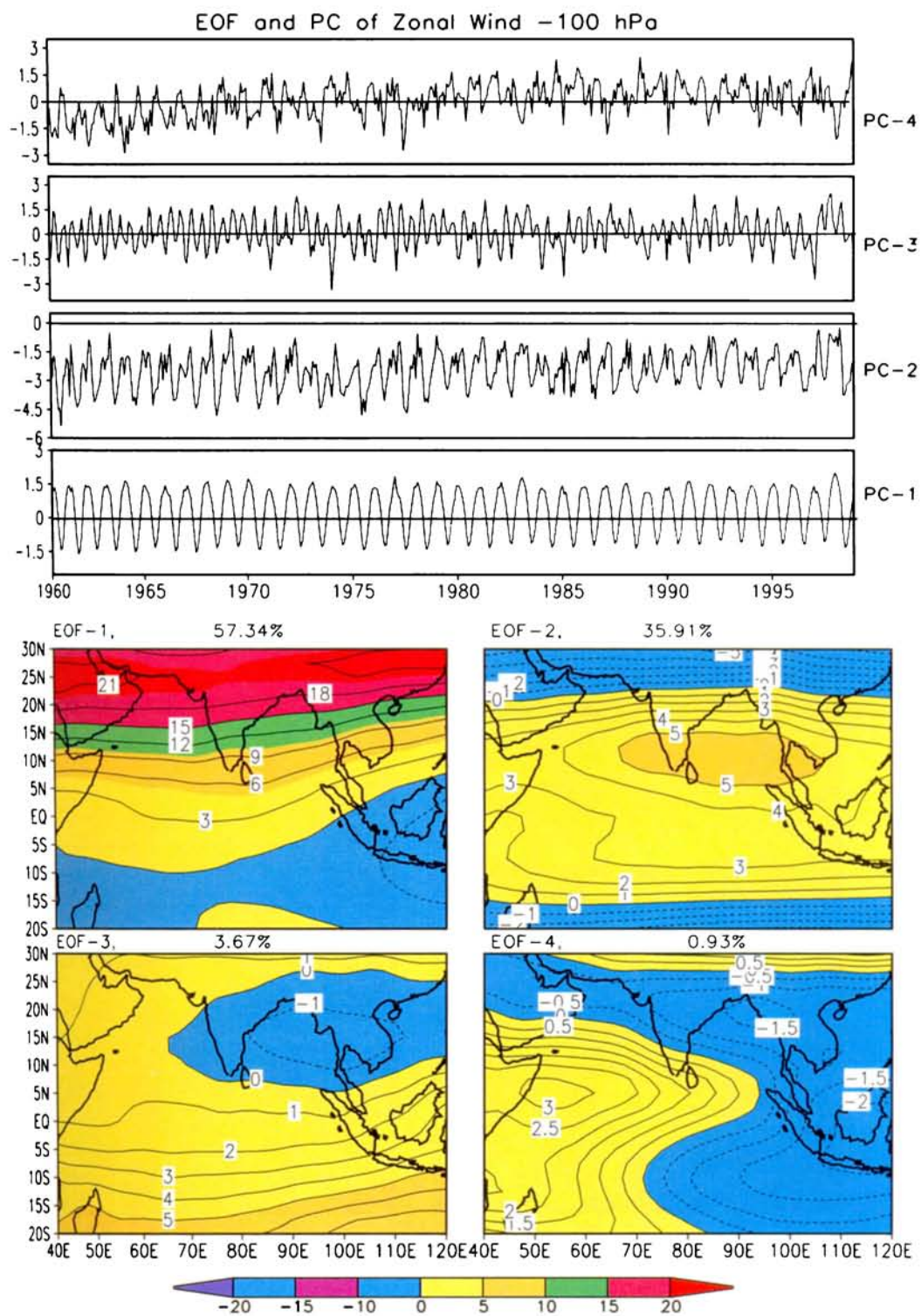
Figure 3.9: EOF patterns and principle components of zonal wind at 50 hPa

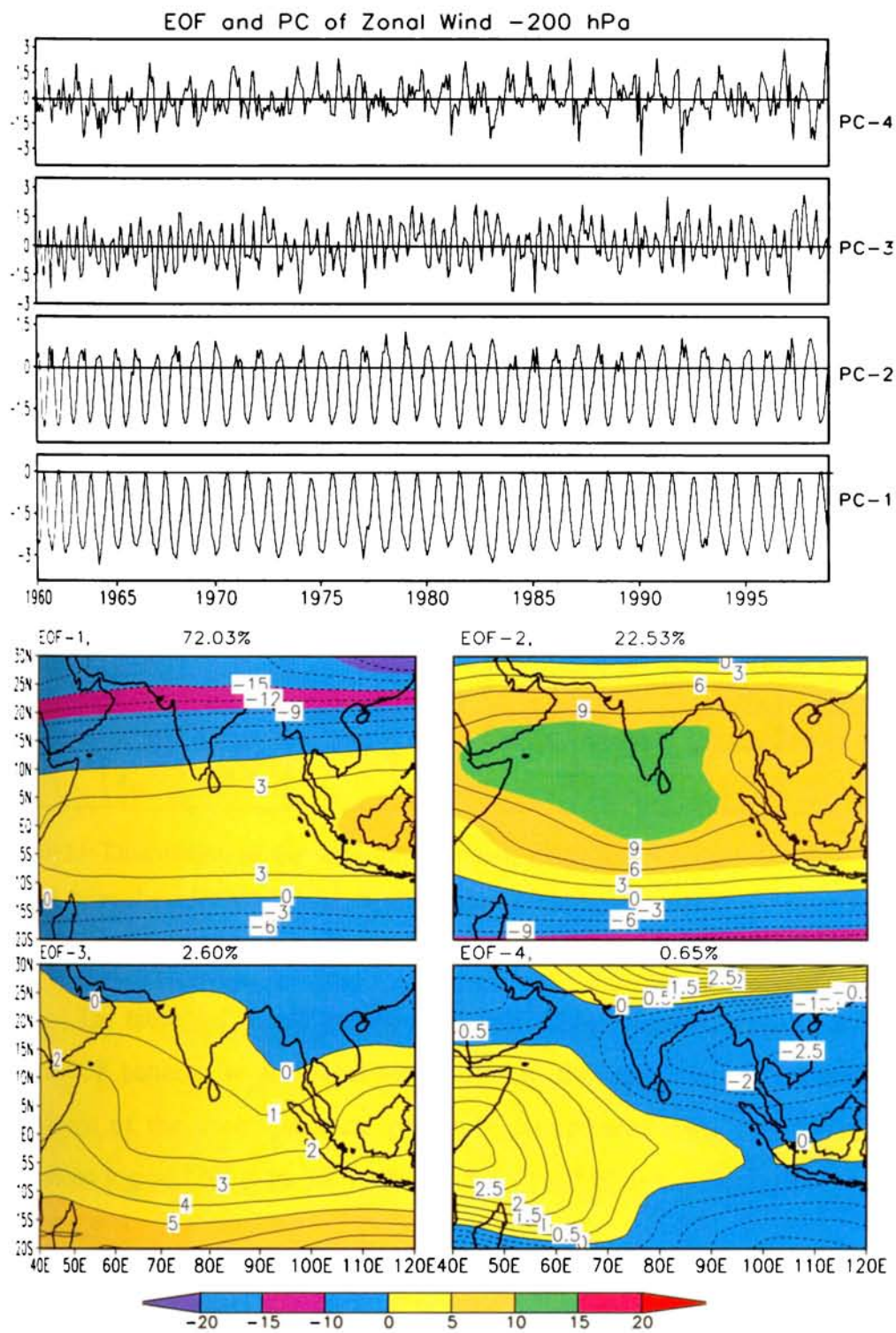Figure 3.10: EOF patterns and principle components of zonal wind at 70 hPa

Figure 3.11: EOF patterns and principle components of zonal wind at 100 hPa

Figure 3.12: EOF patterns and principle components of zonal wind at 200 hPa

Levels (hPa)	Percentage of variability due to each EOF.				Total	Standard Deviation of principle Component			
	EOF-1	EOF-2	EOF-3	EOF-4	EOF	PC-1	PC-2	PC-3	PC-4
10 hPa	78.93 Q	14.44 A	4.50 $Q \& A$	0.72	98.59	265.15	189.50	99.11	41.35
20 hPa	68.15 Q	18.88 A	10.65 $Q \& A$	0.89	98.57	233.66	171.58	97.31	36.99
30 hPa	62.35 Q	25.18 A	9.88 $Q \& A$	0.96	98.37	187.55	161.55	77.10	31.73
50 hPa	56.54 A	32.62 QBO	7.56	1.31	98.03	189.49	112.46	56.50	29.95
70 hPa	67.79 A	24.41 $Q \& S$	3.50	1.51	97.21	226.82	58.47	48.25	33.83
100 hPa	57.34 A	35.91 $A \& S$	3.67	0.93	97.85	284.81	89.33	75.11	38.28
200 hPa	72.03 A	22.53 $A \& S$	2.60	0.65	97.81	220.82	202.94	79.98	40.22

Table 3.1: Contribution of the variability by each EOFs and Standard deviation of PC. Q- Quasi- biennial mode, A- Annual, S- Semi annual Mode of variability present in the zonal wind.

The table 3.1 gives the contribution of the percentage of variability of each EOF patterns to the total variability in the zonal wind and the standard deviation of the corresponding *principle component over the Asian summer monsoon* region (20° S to 30° N & 40° E to 120° E) for different pressure levels of UT/LS.

3.4 Summary

We have analyzed the spatial and temporal variability of zonal wind in the UT/LS region for the period 1960 to 1998 over the Asian monsoon region using the Wavelet transform and EOF methods. Using the wavelet transform, we

found the oscillations present in the zonal wind. The most –prominent mode of temporal variability is the QBO in the stratospheric levels and annual mode in the upper troposphere. The influence of 11-year solar cycle in the zonal wind at stratospheric levels is clearly documented in the study.

We have also studied the spatial and temporal variability of the zonal wind over the Asian summer monsoon region with the help of SVD method of EOF analysis. EOF analysis gives the percentage of contribution due to each mode (eg. quasi- biennial mode, annual mode) to the total variability of the zonal wind both in the spatial and temporal scales. We found that the first EOF pattern up to 30 hPa level contribute maximum to the total variability above 70 % is QBO mode. The second EOF pattern is the annual mode contributing next to the total variability. The influence of QBO mode is more in the equatorial stratosphere and annual mode is away from the equator. The QBO mode shows a monopole and annual mode shows a dipole pattern over the Asian monsoon region. The dipole pattern (annual mode) is changing its negative and positive regions with respect to the pressure levels. In the upper troposphere, the dominant variability is due to the annual mode representing the first EOF pattern and PC-1. Second dominant variability is due to the annual and semiannual oscillations over the region.

The variability of zonal wind (periodicity and amplitude) in the UT/LS region of the tropical atmosphere give more insight into the variability of monsoon due to the QBO and annual oscillation. The above study gives an idea about the percentage of variability due to each mode and its spatial pattern, which helps us to understand the variability of the Asian monsoon. Therefore to understand the monsoon variability, we should have thorough knowledge about the wind pattern over the UT/LS of Asian summer monsoon region.

Chapter 4

A dipole type of Zonal Wind variation in the UT/LS during DRY and WET years of the Indian Summer Monsoon

4.1 Introduction

In this study we have made an attempt to understand the characteristic features of zonal winds in the Upper Troposphere and Lower Stratosphere (UT/LS) region during the south west monsoon season (June to September) over the Indian longitude belt (65° E – 90° E) and its relation to Indian Summer Monsoon Rainfall (ISMR). The lower stratosphere is very much linked dynamically with the upper troposphere, even though characteristics of these regions are different. It is necessary to consider the lower stratosphere along with the troposphere for better understanding of Indian summer monsoon and its variability.

Many studies have been made to relate the changes in the lower stratosphere and upper troposphere with monsoon. A major oscillation in the equatorial stratospheric zonal wind with a period of about 26 months was discovered in the 1960s (*Veryard et al., 1961; Reed, 1965; Lindzen, et al., 1968*). This periodic change of the zonally symmetric easterly and westerly wind regimes became known as Quasi-Biennial Oscillation (QBO). This oscillation occurs simultaneously in both hemispheres and at all longitude regions. An important feature of the oscillation is its downward phase propagation at a speed of about 1km/month (*Holton, 1968; Quiroz, 1981*). Barbara (1986) has recently made an exhaustive study of QBO in the equatorial stratospheric zonal wind. Holton *et al.* (1980) showed strong evidence of QBO modulating the global circulation at 50 hPa.

Mukherjee *et al.* (1985) using short- period data for an equatorial station showed a significant relationship between the phases of the QBO in zonal wind in the lower stratosphere (30 hPa) and the percentage of departure of the summer monsoon rainfall of India. They showed that the strong easterly phase of the QBO was associated with weak Indian monsoon and weak easterly/westerly

phase with strong monsoon. They concluded that 15% of variability in the rainfall over India during the summer monsoon is associated with the phase of the QBO. The interannual variability of the Indian monsoon (June-September) rainfall studied with the zonal wind at 10hPa (30 km) and 30 hPa (24 km) at Balboa for the 28 year period 1958-85 showed that the variations in the zonal wind anomalies at 10 hPa is highly related to the monsoon rainfall. From the above study it was found that zonal wind anomalies at 10 hPa (30 km) lead those at 30 hPa (24 km) by 6 months, providing a longer lead-time for predicting the Indian monsoon rainfall *(Bhalme et al., 1987)*. The link between the stratospheric zonal wind and Indian monsoon was studied by *(Rao et al., 1978; Mukherjee et al., 1979; Thapliyal, 1979)*. The composite of mean tropopause height for good and bad monsoon years showed that all India mean tropopause height is statistically higher in good monsoon years than the bad monsoon years *(Kulkarni et al., 1993)*. *Rajeevan (1993)* studying upper tropospheric circulation and thermal anomalies over the central Asia associated with major drought and floods in India using the upper air data of 21 stations for 22 years (1961-1982) showed that there were significant differences between the anomalies during the drought and flood years. Monthly zonal mean wind anomaly for 10 hPa, 30 hPa, and 50 hPa at Balboa (9° N, 80° W) and the summer rainfall of India for a 29-year period give correlation of 0.57 *(Sikdar et al., 1993)*.

In this chapter we studied the zonal wind anomalies of the upper troposphere and lower stratosphere over the tropical region during the monsoon season (June –September) for the DRY and WET year of Indian summer monsoon.

4.2 Data Used

We have used the monthly data of zonal wind (u), meridional wind (v), vertical wind (w), temperature (T) and relative humidity (R.H) from National Center for Environmental Prediction /National Center for Atmospheric Research

(NCEP/NCAR) Reanalysis (*Kalnay et al., 1996*). This grided binary data has 144 longitude grids 73 latitude grids (2.5 X 2.5 degree latitude/longitude) and 17 pressure levels (1000 hPa, 925 hPa, 850 hPa, 700 hPa, 600 hPa, 500 hPa, 400 hPa, 300 hPa, 250 hPa, 200 hPa, 150 hPa, 100 hPa, 70 hPa, 50 hPa, 30 hPa, 20 hPa, and 10 hPa). This data set spans all the region of the UT/LS covering the whole globe. Relative humidity and vertical component of wind are available from surface to 300 hPa and 100 hPa respectively. We make use of the above monthly data for the period to derive the anomaly data.

Indian Summer Monsoon Rainfall (ISMR) data has been taken from Parthasarathy *et al.* (1994) and updated it upto 1998 from India Meteorological Department. ISMR is the average of 306 fixed raingauge stations from all over India (*Parthasarathy, 1984*). The long-term normal rainfall (R) for the monsoon season (June to September) is 852.4 mm and its standard deviation (S) is 84.5 mm. If the Ri ≥ R+S then the year is WET and Ri ≤ R-S, the corresponding year is DRY, where Ri stands for the rainfall of particular year. Table 4.1 gives the details rainfall in mm, normalized percentage of departure for the monsoon season (June to September) of each year. The DRY and WET years chosen for the study are marked in the table.

4.3 Results and discussion

In this study we examined the characteristics of zonal wind anomalies of the upper troposphere and lower stratosphere over the tropical region during the monsoon season (June – September) for the DRY and WET years of Indian summer monsoon. Also we have examined the vertical behaviour of the Hadley cell variation during the DRY and WET years over the Indian longitude belt 65° E - 90° E).

Year	ISMR (mm)	Normalized Percentage Departure	DRY or WET
1960	839.8	-0.14	
1961	1020.3	1.99	WET
1962	809.8	-0.50	
1963	857.9	0.07	
1964	922.6	0.83	
1965	709.4	-1.69	DRY
1966	739.9	-1.33	
1967	860.1	0.09	
1968	754.6	-1.16	
1969	831.0	-0.25	
1970	939.8	1.03	
1971	886.8	0.41	
1972	652.9	-2.36	DRY
1973	913.4	0.72	
1974	748.1	-1.23	
1975	962.9	1.31	WET
1976	856.8	0.05	
1977	883.2	0.36	
1978	909.3	0.67	
1979	707.8	-1.71	DRY
1980	882.8	0.36	
1981	852.2	0.00	
1982	735.4	-1.38	DRY
1983	955.7	1.22	WET
1984	836.7	-0.19	
1985	759.8	-1.10	
1986	743.0	-1.29	
1987	697.3	-1.84	DRY
1988	961.5	1.29	WET
1989	866.7	0.17	
1990	908.7	0.67	
1991	785.0	-0.78	
1992	785.0	-0.78	
1993	877.0	0.29	
1994	953.0	1.19	WET
1995	827.0	-0.30	
1996	853.0	0.00	
1997	872.0	0.23	
1998	874.0	0.26	

Table 4.1: Indian summer monsoon rainfall (ISMR) from (1960-1998) and their departure from long-term normal of 852.4 mm. in terms of the standard deviation of 84.5 mm. and normalized percentage departure. Five DRY and WET years are shown in the table

4.3.1. Mean conditions of zonal wind in the stratosphere and troposphere

One of the most basic general circulation parameter is zonal wind. This parameter is in approximate thermal wind balance in lower and middle atmosphere. Figure 4.1 (a to d) represents the zonal wind circulation in the troposphere and stratosphere over the Indian longitude belt (65° E - 90° E) from 1960 to 1998.

     a)   December-January-February (Northern Winter)

     b)   March-April-May (Equinox)

     c)   June-July-August (Northern Summer)

     d)   September-October-November (Equinoxes)

In the upper troposphere, near 200 hPa level, there are two well marked westerly wind maxima, are seen in each hemisphere. In the winter hemisphere, the maximum is close to latitude 30°, and in the summer hemisphere, it is close to latitude 45°. During the winter season, the maximum is stronger and more equatorward than during the summer season. This is the Sub-Tropical Jet stream (STJ). Newton *et al.*, (1962) studied the structural characteristics of the subtropical jet and certain lower stratospheric wind systems. Over the equatorial region, winds are generally easterly and these are called trade winds. The zero isopleths separating the subtropical westerly and the equatorial easterlies gives the position of sub-tropical ridgeline. Equatorial tropospheric easterlies are strongest during the northern summer (June-July-August). This is due to the existence of the easterly jet stream over south Asia during the Asian summer monsoon season. Also during the northern summer in the lower layer of the atmosphere from equator to 30° N, we can see the monsoon current extending up to the 400 hPa levels.

64
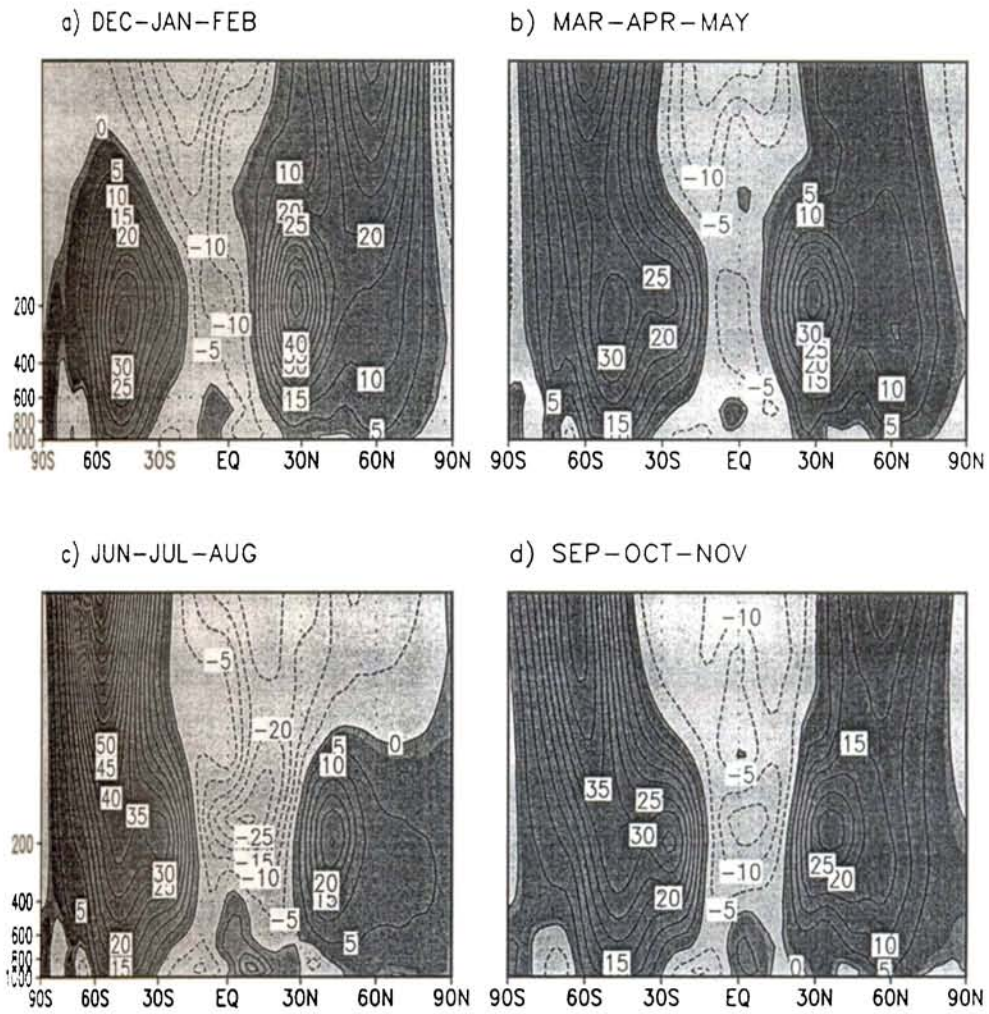
Figure 4.1 Seasonal climatoloy of zonal wind averaged over the
Indian longitude belt (65°E-90°E)

The tropical troposphere easterly and lower stratospheric easterlies appear to form one joint system rather than two separate systems. The tropics have relatively stronger easterlies in the lower stratosphere compared to the troposphere. The stratosphere and mesosphere over the globe are characterized by winter westerly and summer easterlies and maxima occur in the mesosphere over the middle latitude. The middle atmosphere circulation undergoes a strong annual cycle in which the zonal winds in each hemisphere change from westerly to easterly between summer and winter. The interannual variability of the middle atmosphere is large in winter because of the occurrence of the sudden stratospheric warming during which the stratospheric winds reverse temporarily affecting the circulation for several weeks. Circulation of the equatorial stratosphere is dominated by quasi-biennial time scale wind reversal.

4.3.2 Seasonal profiles of zonal wind over the Indian region

Monthly vertical profiles of the zonal wind climatology averaged over the Indian region (65° E - 90° E and 0° - 25° N) shown in figure 4.2. We derived the climatology data from the monthly values of zonal wind from 1960 to 1998. Monthly vertical profiles of zonal wind from 800 hPa to 10 hPa show the seasonal variation of zonal winds. The zonal wind increasing from 700 hPa levels to 200 hPa level then decreasing upto 10 hPa during January and February. During March and April the easterly wind started decreasing at 400 hPa level and westerly wind (4 ms^{-1}) in the lower levels of the troposphere and it turns to easterly at the 150 hPa level in the upper troposphere. Also easterly wind is increasing from 70 hPa to 10 hPa level. During the monsoon period vertical profiles of zonal wind have similar pattern as in the case of pre-monsoons seasons. During the monsoon season the easterly wind increases and reach a core value of -30 ms^{-1} at 150 hPa level and seen only at the time of Asian summer monsoon. This easterly wind is nothing but the appearance of Tropical Easterly Jet streams (TEJ) in the Upper Troposphere and also we can see the monsoon current (westerly) up to 400 hPa level during monsoon season. During
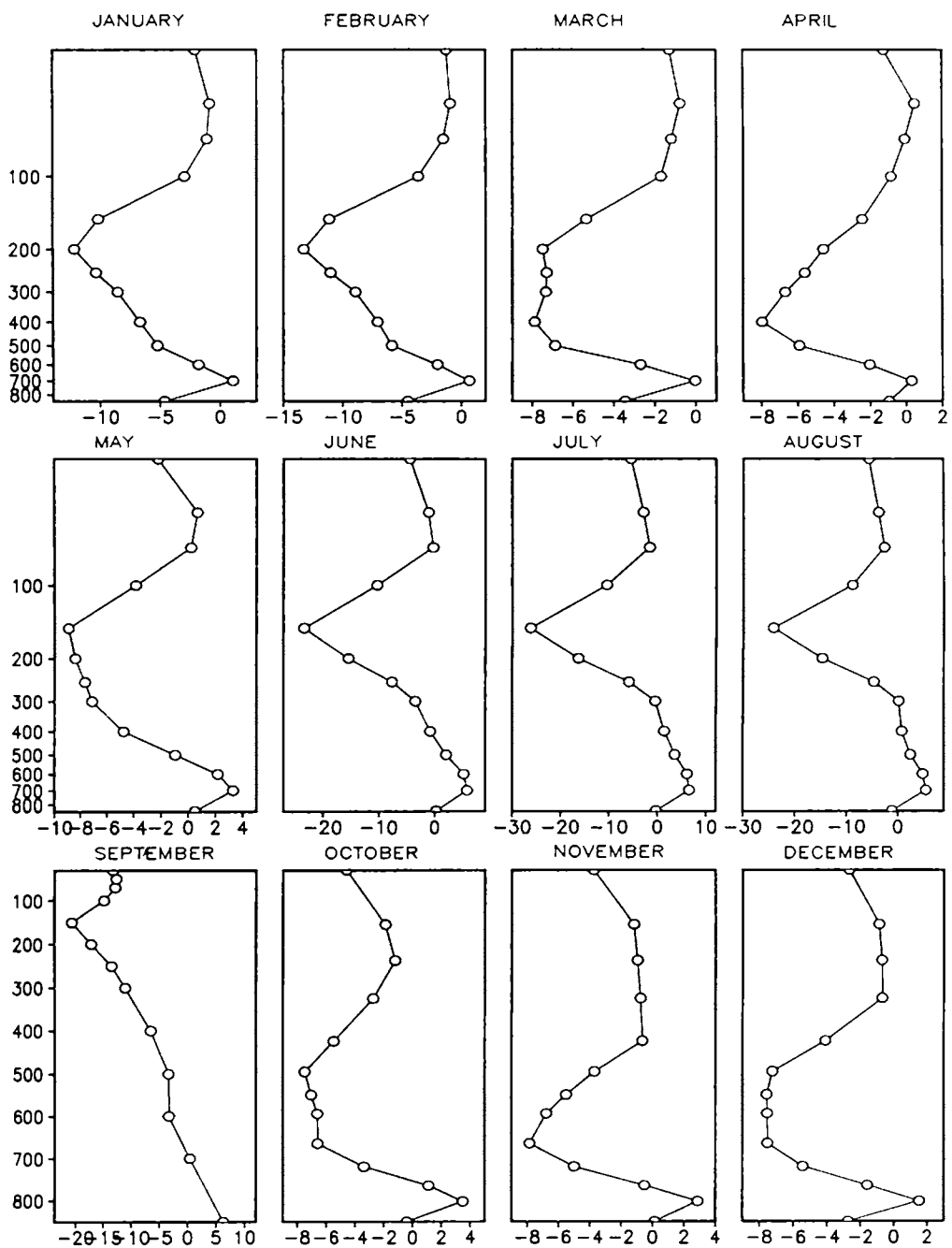
Figure 4.2 : Monthly profiles of zonal wind climatology from 1960 to 1998 averaged over the Indian region (65°E-90°E & 0°-25°N).

the post monsoon period the vertical wind pattern shows the same pattern as in the pre-monsoon.

4.3.3 Circulation in the troposphere and stratosphere

The zonal wind circulation in the stratosphere and troposphere from the surface (1000 hPa) to 10 hPa levels is shown in the figure 4.3. From the figure it is seen that easterly and westerly change of zonal wind for the period 1960- 1998 over the Indian region (0° - 25° N & 65° E- 90° E). Some years the westerly wind extends up to the middle stratosphere (10 hPa) are nothing but the year in which the easterly wind in the stratosphere changes to the westerly phase of the QBO. In some years the westerly winds not extend up to the stratosphere and this year together with easterly wind forms the easterly phase of the QBO in the equatorial lower stratosphere. The El Nino years (1965, 1972, 1982 and 1987) that fall in the easterly phases of QBO, the monsoon rainfall become weak and form drought years. Whereas, the El Nino years (1963, 1969, 1976 and 1991) which coincides with the westerly phases of QBO, the monsoon rainfall were either normal or excess. So the UT/LS circulation and El Nino occurrence coincides with the phases of the QBO may also determine the DRY and WET conditions for Indian summer monsoon rainfall.

Monthly climatology (1960-1998) of vertical cross section of zonal wind pattern over the Indian region is shown in figure 4.4. Here the tropical easterly jet stream starts from the lower levels (500 hPa) of the atmosphere and have a core speed of -30 ms^{-1} at level 150 hPa during the monsoon period. Middle stratosphere (above 30 hPa level) is characterized by the easterly wind for all the season and which is not stronger than the TEJ in the upper troposphere. The appearance of the westerly wind in the lower levels of the atmosphere (up to 400 hPa) during the monsoon period (June to September) and the Low Level Jet (LLJ) with a speed of 10 ms^{-1} embedded in this westerly wind at 850 hPa is another peculiar features of the Asian summer monsoon. On either side of the
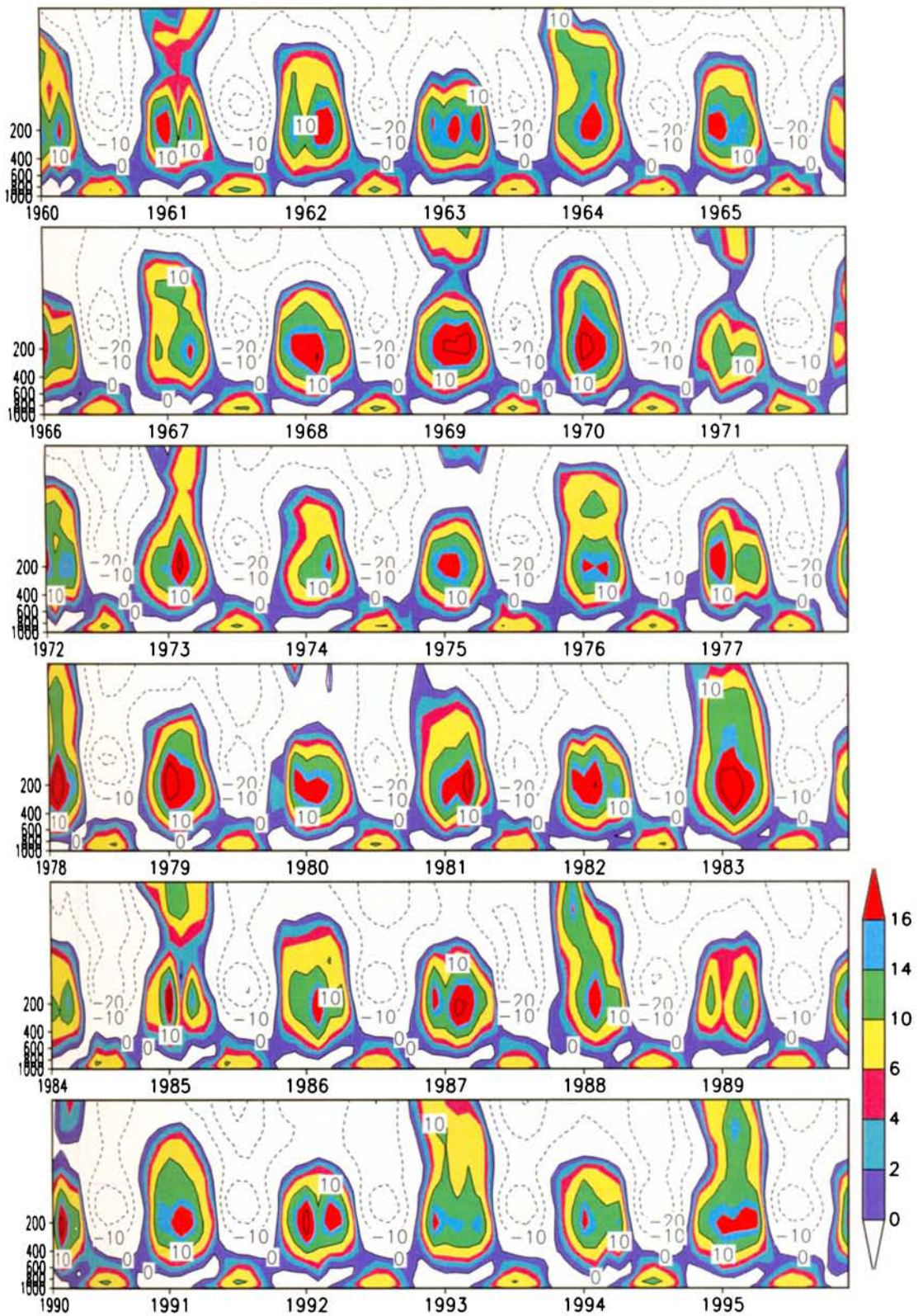
Figure 4.3: Zonal wind (ms⁻¹) circulation in the troposphere and stratosphere over the
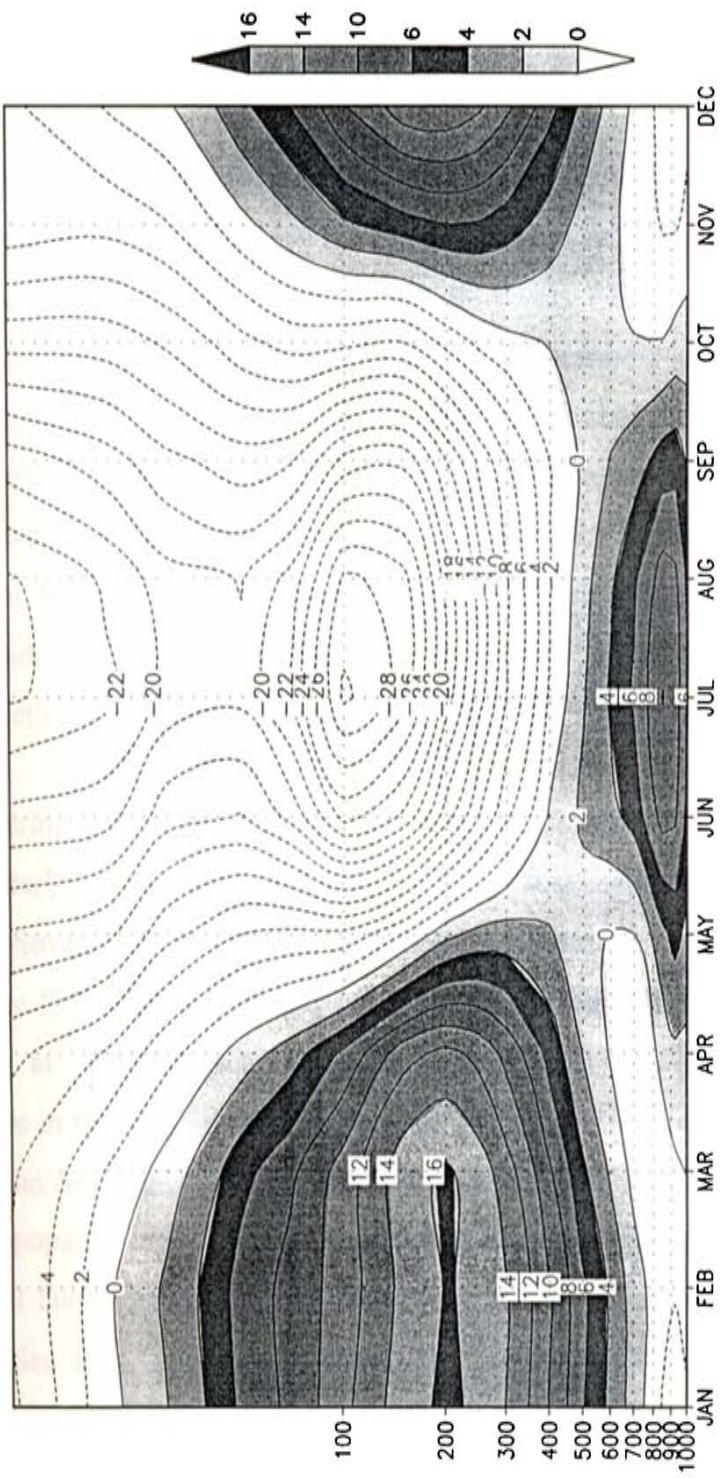Indian region (65°E-90°E & 00°-25°N)

Figure 4.4: Monthly climatology of vertical cross section of zonal wind over the Indian region (65° E - 90° E & 0°-25° N) during 1960-1998.

TEJ westerly winds are seen for other months from 700 hPa to the middle stratospheric levels (about 30 hPa).

4.3.4 Wind anomaly during the DRY and WET years

The wind (anomaly) composites for the DRY (1965, 1972, 1979, 1982, 1987) and WET (1961, 1975, 1983, 1988, 1994) years over the upper troposphere and lower stratosphere (for the levels 70 hPa, 100 hPa and 200 hPa) during the southwest monsoon period (June-September) is depicted in figure 4.5. From figure 4.5 it can be seen that the circulation pattern in the upper troposphere (200 hPa), tropopause level (100 hPa) and lower stratosphere (70 hPa) showed considerable changes during the DRY and WET composites over the Indian subcontinent. In the lower stratosphere easterly wind prevail in the equator side of 8° N in both the DRY and WET years. But beyond 10° N, the wind direction becomes nearly opposite from DRY years to WET years.

During the DRY years westerlies are found in the Arabian Sea area, southwesterly in the subcontinent part and southerlies in the Bay of Bengal region. Strong anticyclonic circulation is observed over the Bay of Bengal during the DRY years. On the other hand, during WET years easterlies/south easterlies at Arabian Sea, north easterlies over the subcontinent part and northerlies in the Bay of Bengal region. Strong anticyclonic activity is noted in the Arabian Sea region during the WET years. The monsoon circulation pattern in the tropopause level (100 hPa) also shows out-of-phase characteristics during WET and DRY years. At 100 hPa level, the wind is westerlies in the entire Arabian Sea area, and southwesterly in the land area. In the Bay of Bengal region, the wind is almost southerly and is cyclonic circulation during the DRY years. In WET years, the wind is northerly beyond 15° N and changes to north easterlies to easterlies towards the equator. Intense cyclonic circulation is found over south Bay of Bengal region.

a1) DRY-70 hPa   a2) WET − 70 hPa

b1) DRY-100 hPa   b2) WET − 100 hPa
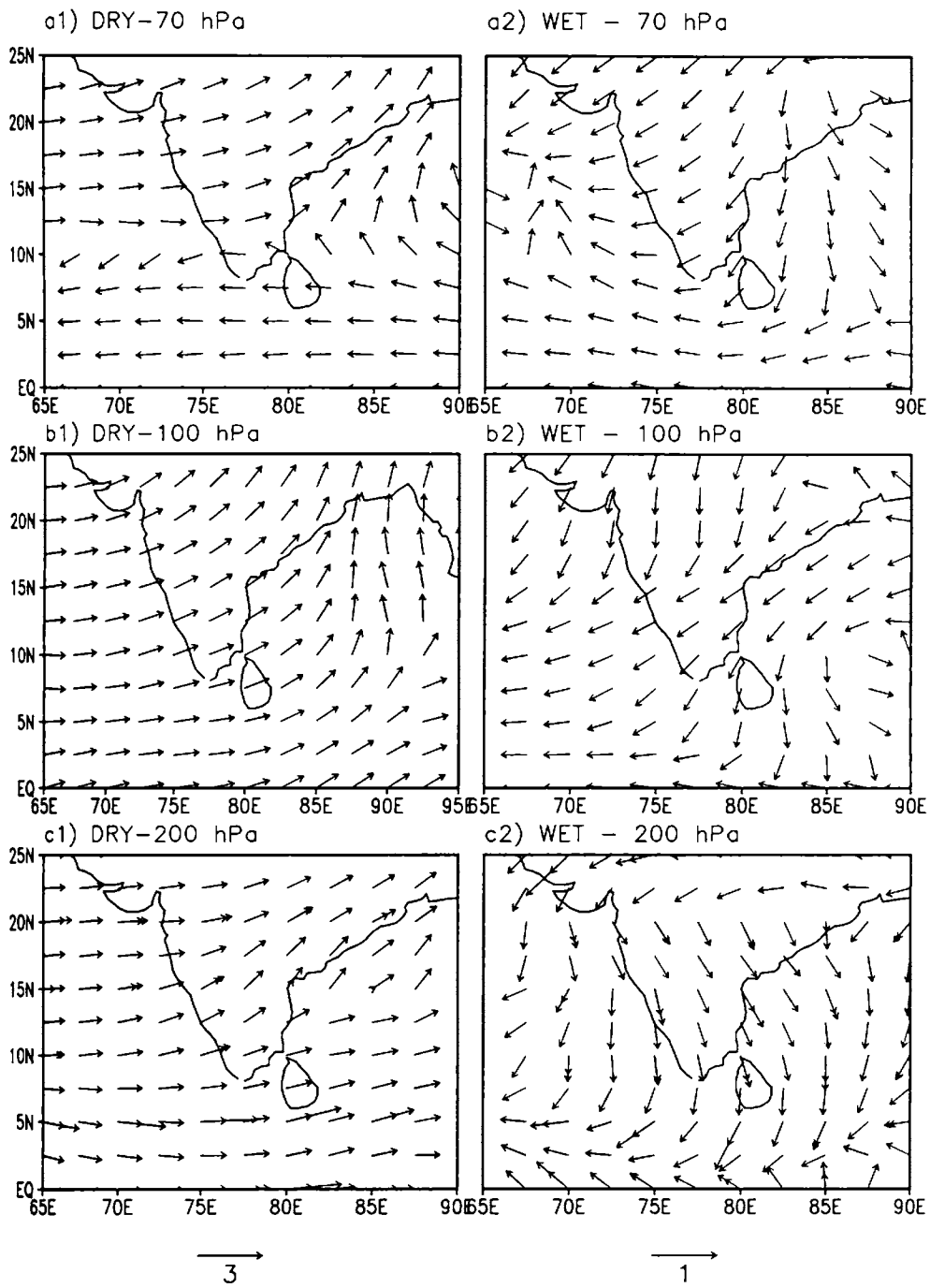
c1) DRY-200 hPa   c2) WET − 200 hPa

Figure 4.5 : Wind anomaly for DRY year composite and WET year composite

In the upper troposphere (200 hPa), the wind is more or less westerlies in the entire monsoon region during DRY composite. On the other hand, northerly predominates during the WET years. At 200 to 100 hPa level, wind must be easterly during the monsoon season due to the appearance of tropical easterly jet (TEJ) stream and it strengthen during the WET years than in DRY years. Therefore, the wind anomaly pattern obtained for DRY years (figure 4.5(b1 & c1) shows the westerly anomalies indicating the weakening of the tropical easterly jet streams. But for the WET years (figure 4.5 (b2 & c2)) the easterly wind anomalies shows the strengthening of TEJ that represents the WET conditions of Indian summer monsoon.

4.3.5 Composite of zonal wind in DRY and WET years

We have considered five DRY years (1965, 1972, 1979, 1982, 1987) and five WET years (1961, 1975, 1983, 1988, 1994) from the period 1960-1998 for the present study. Figure. 4.6 (a & b) represent the composite vertical structure of zonal wind for the WET and DRY years averaged for the Indian region (65° E and 90° E) for the monsoon season (June to September). From the figures we can see that on either side of the equator at 200 hPa altitude (upper troposphere region) there exist westerly maxima around 30° South and 40° North (the Sub-Tropical Jet stream). In the summer months, flows in both Hadley and STJ have weakened; the mean position is further equatorward than the winter position. The southern hemispheric STJ shows the most stable position. This is because the Hadley circulation over the predominantly ocean covered southern hemisphere is more conservative in its geographical behavior than its northern counterpart. The mean position of STJ and the year-to-year variability of the westerly wave crests and troughs are important for determine precipitation pattern in the low latitudes. Kodama (1992, 1993) showed that the South Pacific Convergence Zone (SPCZ) and the South Atlantic Convergence Zone (SACZ) and the associated precipitation zones from along the eastern side of trough in the subtropical jet.
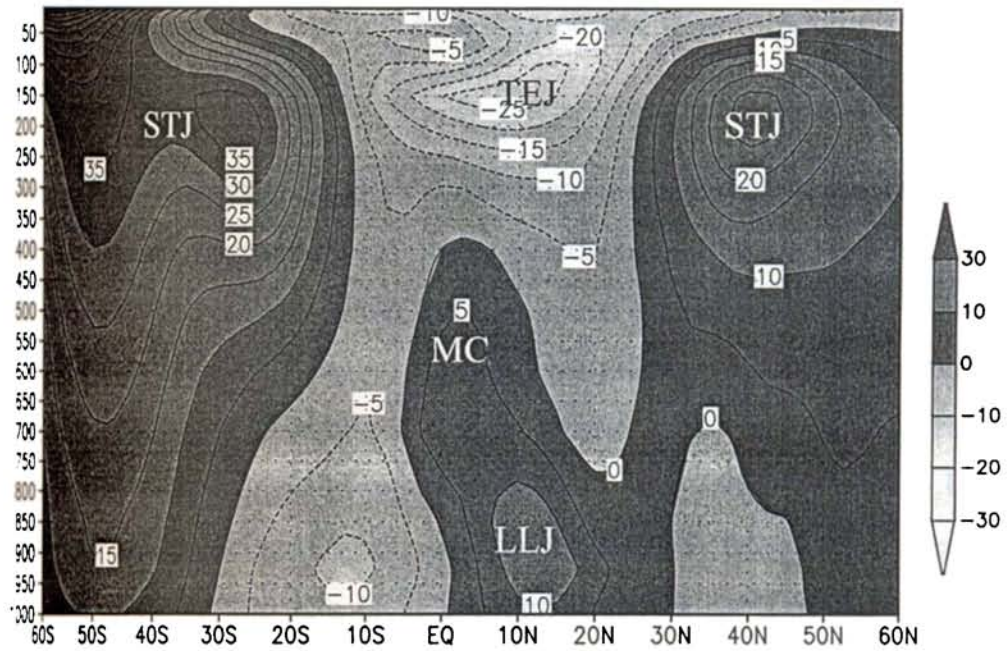
(a) WET YEARS
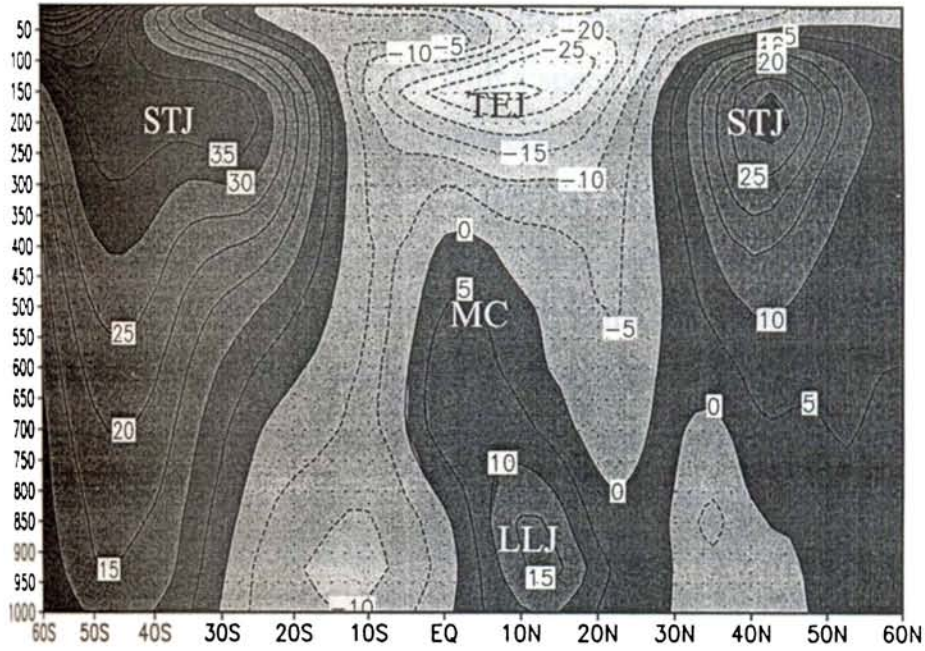
(b) DRY YEARS

Figure 4.6 (a to b) : Vertical variation of zonal wind for the pressure levels 1000 hPa to10 hPa averaged over the Indian longitude belt (65° E-90° E). (a) WET year composite and (b) DRY year composite.

During the Asian summer monsoon a strong easterlies flow of air develops in the upper atmosphere. This upper level easterly wind maximum is identified as the tropical easterly jet (TEJ) with a speed of 28 ms^{-1}. It is located above the Asian summer monsoon current between the equator and latitude 20° N with core between 14 and 16 km (150 hPa and 100 hPa) level centered at 15° N (Koteswaram, 1958). It extends from the China Sea across the Malayan Archeopelago and the Indian Peninsula to Africa. It is maximum developed over the Indian Peninsular region and southeast Arabian Sea overlying the Indian southwest monsoon current. TEJ is found only in the Northern Hemispheric summer (June to September) and it is confined mainly to the Indian Ocean region. The fact that the tropical easterly jet only occurs in the summer season suggests that its development is related to the seasonal cycle of surface heating in the area over which the TEJ lies. As in the case of subtropical jet (STJ), the Tropical Easterly Jet (TEJ) is important for determining rainfall pattern in southern Asia and Africa. At the surface, rainfall has been found to be greatest north of the jet entrance in the southern Asian region and south of the jet exit in the West African region (Hastenrath, 1985).

For the WET composite (figure 4.6 (a)) there is no change in the pattern of wind structure in the troposphere and lower stratosphere. But the magnitudes of the westerly (STJ) and easterly (TEJ) jets are much greater in the WET than the DRY years over the Indian region during the southwest monsoon period. Low Level Jet (LLJ) is also stronger. These results show that the vertical circulation (Hadley cell) is much stronger in the WET than the DRY years. In the lower troposphere to the north of the equator the westerly Monsoon Current (MC) extended up to the 400 hPa level and embedded in the Low Level Jet stream (LLJ) with its center located at 900 hPa level (Joseph and Raman, 1966; Findlater, 1969).

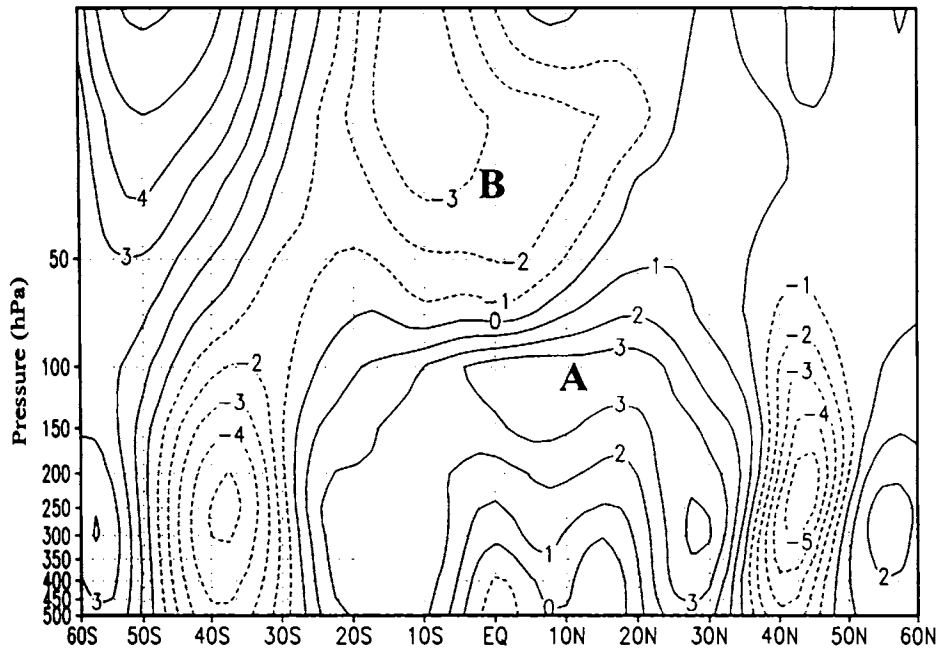### 4.6 A dipole in zonal wind in the UT/LS region

We have observed an interesting phenomenon in the tropical easterly zonal wind in the upper troposphere and lower stratosphere during the southwest monsoon period (June to September) having opposite relation with ISMR (Dipole). In the lower stratosphere above the TEJ winds are easterly but stronger during DRY years than the WET years. This region and TEJ together form a dipole whose one pole is stronger during the DRY years and the other in WET years. We identified two vertical boxes, one in the upper troposphere and another in the lower stratosphere in the latitudinal region 15° S and 15° N of the equator, 200 hPa to 100 hPa in the upper troposphere and 50 hPa to 20 hPa in the lower stratosphere. We call the tropospheric Box as Box A and the lower stratospheric as Box B.

The differences in the composite of zonal wind (DRY-WET) fields and temperature composite (DRY-WET) are shown in Figure 4.7 (a) and (b). The UT/LS dipole AB is clearly seen in zonal winds difference above 200 hPa. From figure 4.7 (b) the dipole is seen clearly here in the north–south temperature gradient from the equator to 50° N latitude. Here the letters C and W shown in the figure represent the COLD and WARM temperature anomaly. Below a point 150 hPa and above it the north-south temperature gradients are opposite in deep layers (lower stratosphere). Thus in DRY years thermal winds (westerly) are such that TEJ is weaker and the winds of the lower stratosphere are strong easterlies (thermal wind is easterly). It is inferred that the tropopause in the region is lower in DRY years than WET years of monsoon and it is supported for the Indian region (*Kulkarni et al., 1993*).

4.7 Relation between UT/LS zonal wind and ISMR

We extracted the zonal wind mean of the two Boxes for the detailed study of the zonal wind in the tropical region occupied by the dipole. Winds in the belt
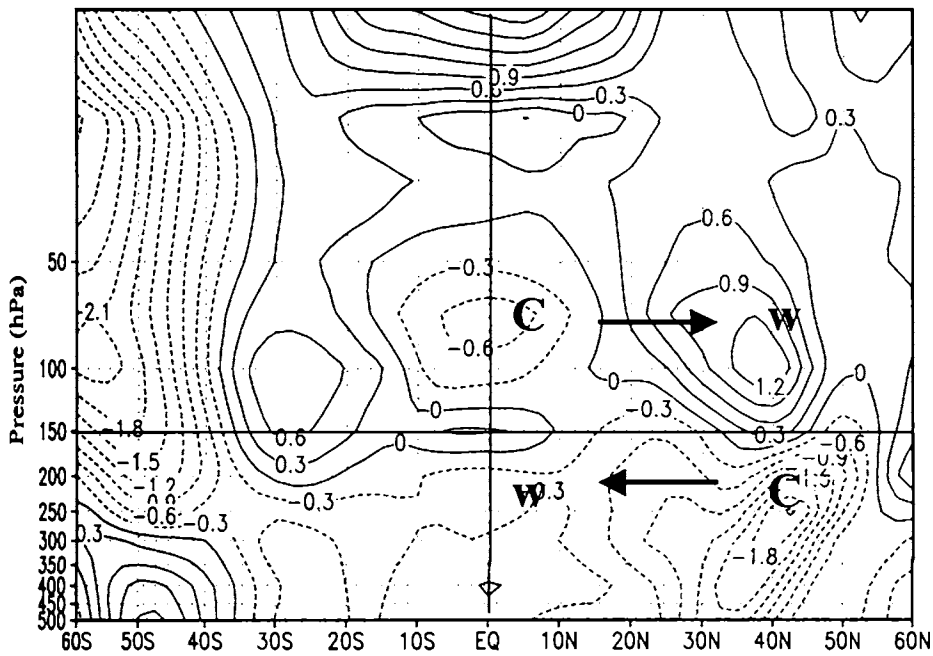
Figure 4. 7 (a to b) : A dipole in the UT/LS over the Indian longitude belt
(65°E -90°E) . a) dipole in zonal wind (DRY-WET) , b) dipole in temperature
(DRY-WET) years of Indian summer monsoon period (June to September)

15°S -15°N were averaged for levels 50 hPa to 20 hPa (Box B) for the months June to September for each year of the period 1960 to 1998. Figure 4.8 (a) & (b) show the averaged zonal wind for the pressure levels 50 hPa to 20 hPa for the longitude region (65° E - 90° E) and for the globe (0° E - 360° E) respectively. There is very little long-term trend in the data. The correlation between this parameter and ISMR is 0.27 for the Indian longitudes and 0.29 for the global using data for the period, 1960-1998. These results are significant at 95% level using Student's t-test. The correlation shows that in the equatorial lower stratosphere DRY (WET) monsoons are accompanied by stronger (weaker) easterly (positive correlation), a result in agreement with Mukherjee (1985).

Data of Box A (upper troposphere, 200 hPa to 100 hPa) shows a prominent increasing trend of zonal wind (decreasing easterlies) in the equatorial region during the southwest monsoon period from 1960 to 1998 (figure 4.9 (a) & (b)). The correlation between the trend-removed values of the zonal wind in Box A and ISMR is -0.32 for the Indian region and - 0.38 for the globe. For the difference between zonal winds (Box B - Box A), which is a measure of the strength of the dipole, the correlation with ISMR is 0.33 for the Indian region and 0.33 for globe. All these correlations are significant at 95% level.

4.3.8 A possible mechanism for the dipole

Kanamitsu and Krishanamurti (1978) have shown that in a DRY monsoon the tropical easterly jet stream over south Asia and also the upper troposphere easterlies over the global tropics are weaker than normal. Such years have colder upper troposphere over sub-tropical latitudes especially over Asia right from the previous winter as shown by several studies (*Rajeevan, 1993*). Accompanying such colder upper troposphere the subtropical westerlies are found to intrude to lower latitudes over south Asia (*Joseph, 1978*). These colder temperatures persist through the monsoon season affecting the north- south temperature gradient that weakens the tropical easterly jet. It is seen that this weakening of

(a)   Box B   (Indian Region)
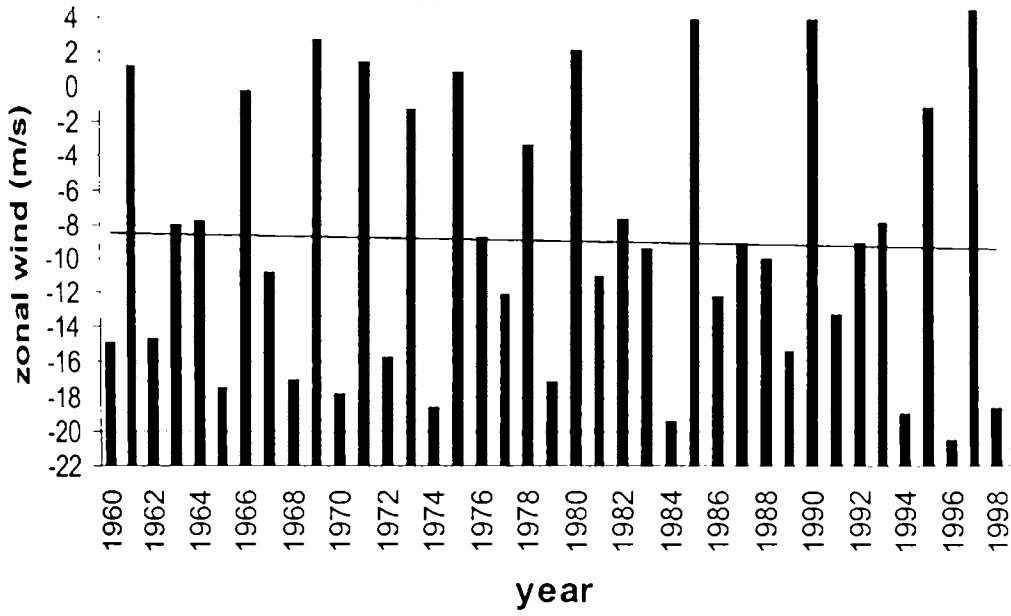
(b)   Box B   (Global Region)
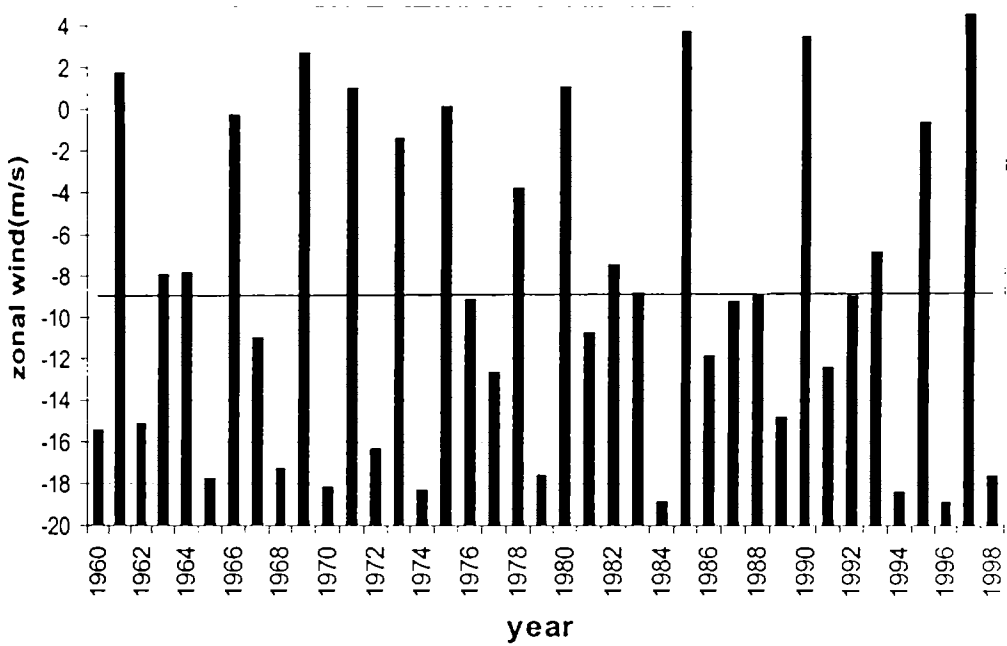
Figure 4.8 (a to b) : Zonal wind in the Box B (lower stratosphere 50 hPa to 20 hPa) averaged over latitude belt (15°S -15°N) for June to September. a) Indian region (65°E-90°E) and b) Global region (0°-360°).
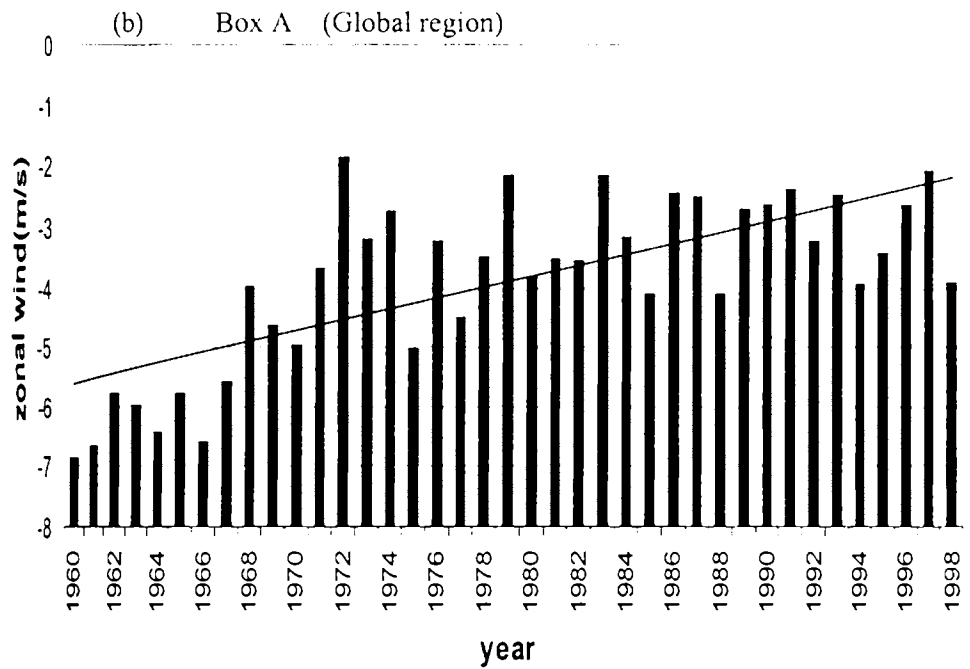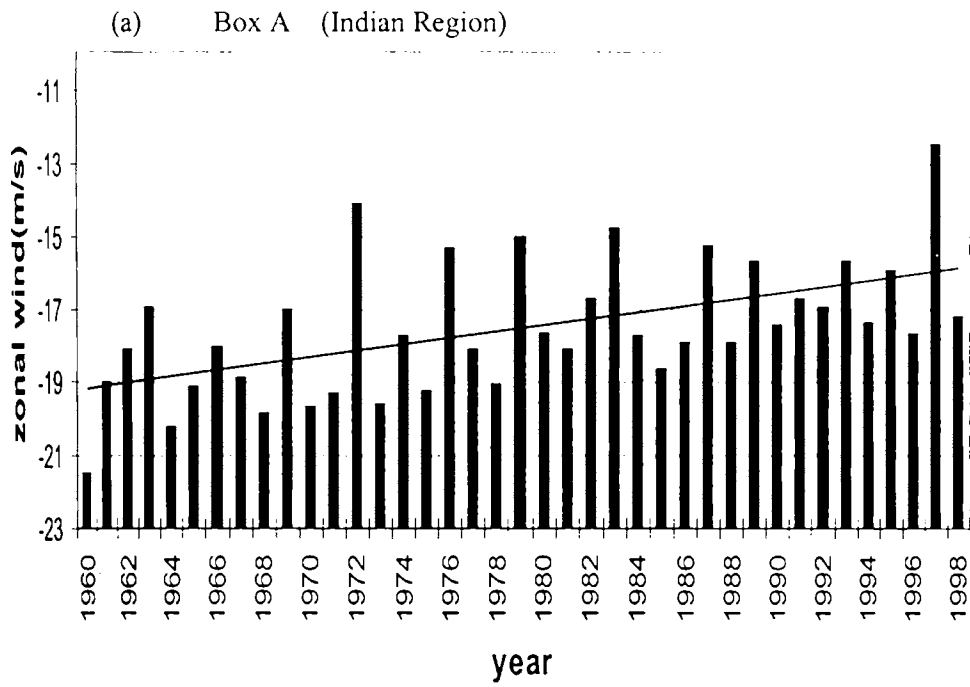
Figure 4.9 (a to b) : Zonal wind in the Box A (upper troposphere – 200 hPa to 100 hPa) averaged over latitude belt (15°S -15°N) for June to September. a) Indian region (65°E-90°E) and b) Global region (0°-360°).

the north-south temperature gradient is a global phenomenon. Available studies show that in the sub-tropics DRY monsoon has lower tropopause height over India (*Kulkarni et al., 1993*). Since the upper tropospheric cooling in DRY years is a global phenomenon, the sub- tropical tropopause globally over Northern Hemisphere may have a lower height in DRY years compared to WET. With a lower height for tropopause in DRY years the lower stratosphere should be warmer, which explains the stronger easterlies there. Thus the dipole in wind fits in very well with the temperature changes.

4.3.9 Hadley circulation anomaly in DRY and WET years of monsoon

The Hadley circulation is a direct thermal circulation, which was postulated by George Hadley in 1735 in his attempt to explain the existence of the easterly trade winds in the tropics. The Hadley cell circulation is composed of a thermally driven rising limb of air in the equatorial zone, a poleward moving flow in the upper atmosphere, a sinking limb in the region of the subtropics and a returning trade wind flow at the surface which converges with its counterpart from the northern or southern hemisphere. The Hadley cells show seasonal variation in their intensity, geographical extends and latitudinal position. Furthermore they are not restricted to their respective hemisphere but display regular cross-equatorial incursion to the opposite hemisphere.

Figure 4.10 (a to d) represent the seasonal behavior of the vertical structure of Hadley cell over the Indian longitude belt (65° E to 90° E) from the 39-year climatology (1960-1998). In the southern hemispheric summer (December-January-February), the strongest ascending motion occurs between 10° and 25° S. In the northern hemisphere, subsidence dominates between the latitudes 10° and 30° N (figure 4.10 (a)). During the Indian summer monsoon period (JJA) over the Indian longitude belt strong ascending motion is centered on latitude 5° N. The contours are representing the magnitude of the wind vector and found the maximum value at 5° N. While low latitudes of the southern
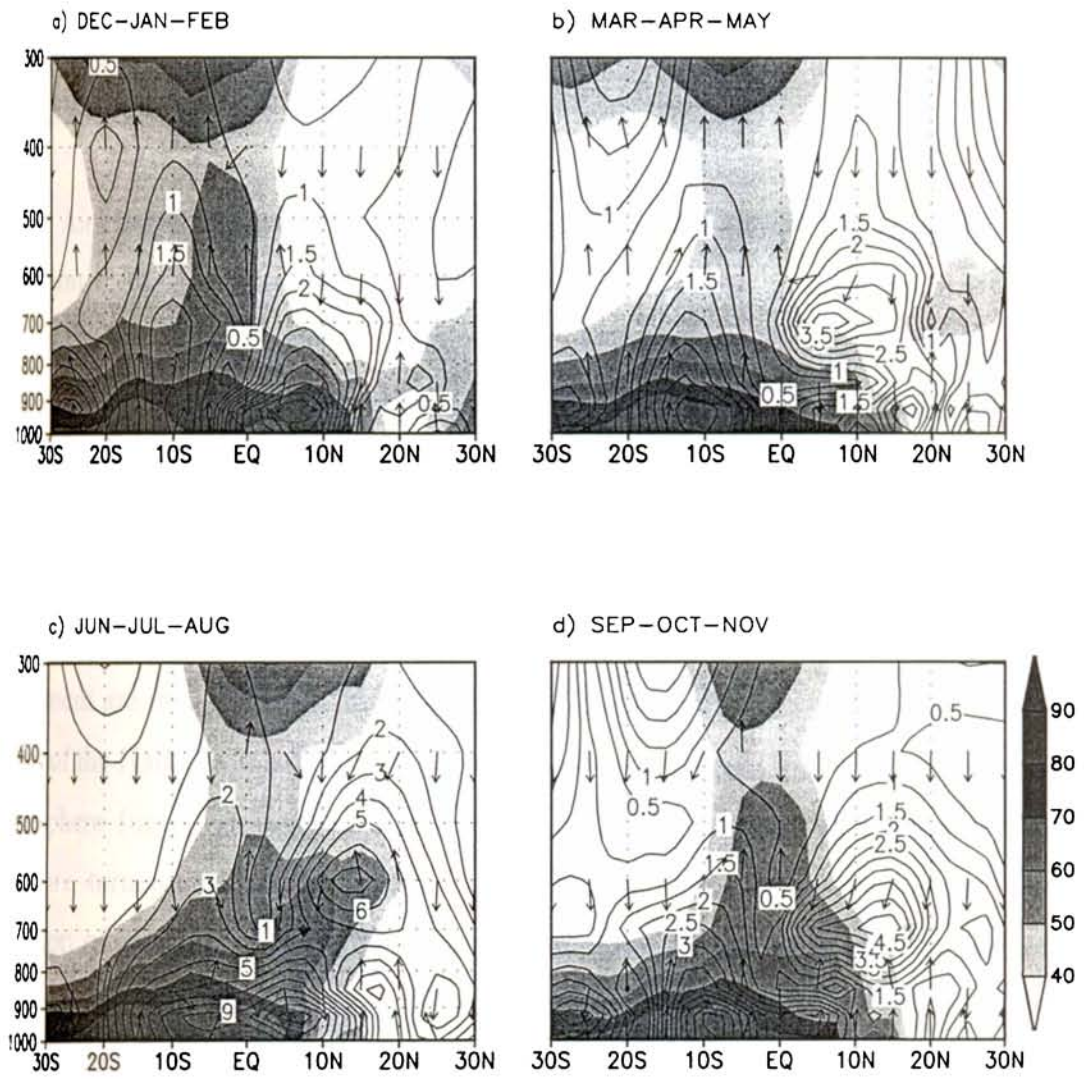
Figure 4.10: Seasonal Hadley circulation over the Indian longitude belt (65°E-90°E). The contour represents the magnitude of wind vector (v and w). The relative humidity is shaded above 40 %.

hemisphere become dominated by sinking motions. These are especially intense around 10° to 15° S (figure 4.10 (c)). In other seasons, March –April – May and September - October – November (figure 4.10 (b) & (d)), the Hadley cell shifts further away from the equator and the air ascending from the equatorial regions. The ascending and the descending motion of air in the Hadley cell are represented with wind vector using the meridional and vertical component of wind velocities.

Air rises in the tropics and the relative humidity (R.H) is high and clouds can form in the tropical region. But where the air sinks (downward arrows) it warms the atmosphere and the relative humidity decreases (non shaded region) and clouds dissolves in the subtropics. The relative humidity above 40% is shaded in the figure 4.10. The relative humidity is high over the northern latitudes during the monsoon period and post monsoon season the relative humidity is decreased over subtropics during the post monsoon season. Hadley circulation carries massive amount of heat and moisture. Such heat and moisture movement are important for maintaining the global energy balance. In the rising limbs of the Hadley cells heat and moisture are carried into the upper parts of the atmosphere (upper troposphere). At about 9-12 km above the earth's surface then are turned polewards in the upper branches of the Hadley cells. The transport of moisture represents an energy transfer, as when moisture condenses latent heat is produce. This represents a large heat from the atmosphere, which is redistributed to higher latitudes by the upper branches of the Hadley cells. Other forms of energy transported by the Hadley circulation are kinetic energy and angular momentum. Therefore the Hadley cell play major role in the UT/LS circulation and stratosphere –troposphere exchange processes and DRY and WET seasons of Indian summer monsoon.

The Hadley circulation pattern (anomaly) for WET and DRY years of Indian summer monsoon period (June - September) for the Indian longitude belt (65° E - 90° E) are represented in figure 4.11 (a & b). The shaded portion
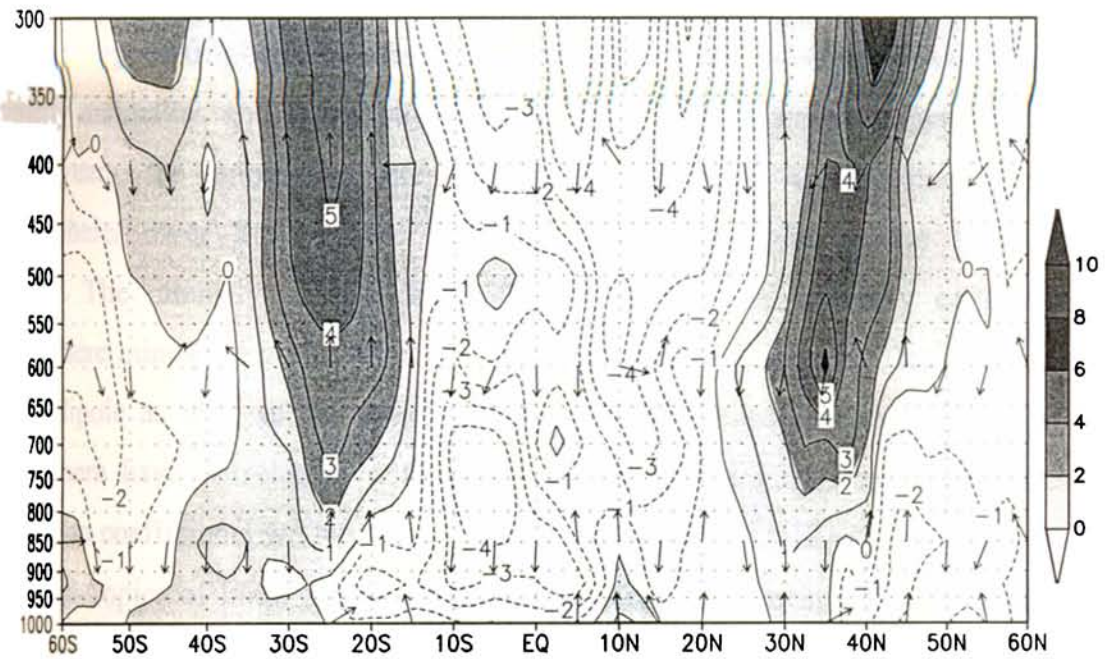
a) WET YEARS (JJAS)
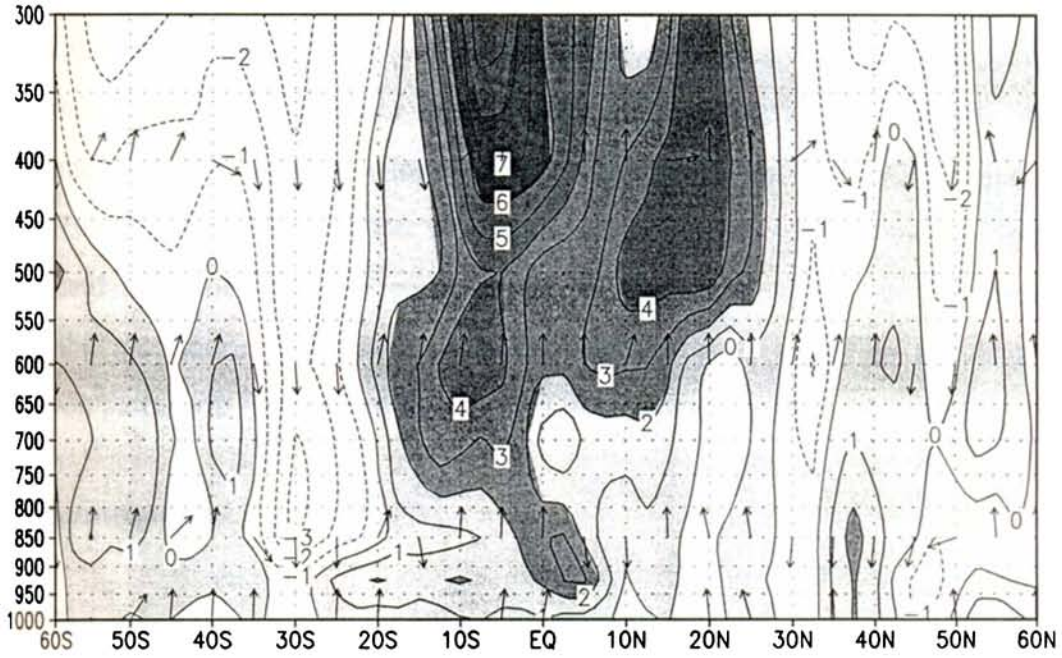
b) DRY YEARS (JJAS)

Figure 4.11 (a to b) : Vertical structure of Hadley circulation anomaly over the Indian longitude belt (65° E–90° E). a) WET year composite b) DRY year composite for June to September. Relative humidity is shaded above 0 % .

represents positive value of R.H (anomaly) and the dashed contour represent the negative anomaly of relative humidity. The up arrows and down arrows shows the rising and sinking motion of air respectively represents with the meridional (v) and vertical wind velocity (w). In the WET composite from the equatorial region there exist a rising motion and the relative humidity (anomaly) is positive (high) and extends to the northern latitudes favorable for the WET monsoon season. But in the case of the DRY year composite shows sinking motion in the tropics and have negative anomaly (low) of relative humidity in the tropics during the monsoon. Therefore a marked difference is noted in the Hadley circulation pattern in the case of WET and DRY years of monsoon.

4.4 Summary

The upper troposphere and lower stratosphere (UT/LS) region over India and over the globe has been studied in relation to the strength of the Indian Summer Monsoon (ISMR), for the period June to September. In the DRY composite upper troposphere winds (tropical easterly jet over South Asia) have westerly anomalies and lower stratospheric winds have easterly anomalies. In WET years the anomalies are opposite. We have named the Upper Troposphere/Lower Stratosphere (UT/LS) anomaly couplet as the 'UT/LS Dipole'. The intensity of the dipole is the zonal wind anomaly of lower stratosphere minus the zonal wind anomaly of upper troposphere. The intensity of the dipole as well as the wind anomalies of upper troposphere and lower stratosphere have correlation with ISMR significant at 95% level. For these correlation coefficients we have used data of 1960-1998. The upper troposphere of the subtropics of India and northern hemisphere is colder in DRY monsoons compared to normal or WET. It is hypothesised that the cold anomaly of DRY years weaken the upper tropospheric easterlies and possibly lower the tropopause, which reverses north-south temperature gradient of the lower stratosphere. This is hypothesised as the cause for the dipole. The mean upper tropospheric zonal wind of the subtropics over Indian longitude (65° E to 90° E)

74

and over the whole globe (0-360°) between latitudes 15° S and 15° N (the lower limb of the dipole) is found to have a long-term trend during the period 1960 to 1998. Over this period the tropical easterlies and the tropical easterly jet stream have weakened from 1960 to 1998. The El-Nino years which coincides with the easterly (westerly) phases of the QBO resulting DRY (Normal/WET) monsoon conditions over the Indian Region. The Hadley cell is stronger in WET years than the DRY years of Indian summer monsoon.

Chapter 5

Temperature Characteristics and its Interannual Variability in Association with Solar Cycle and Asian Summer Monsoon

5.1 Introduction

The temperature at the surface and in the troposphere is determined by radiation and by some representation of the process that determine the vertical advection of heat by fluid motions (normally via a convective schemes). In the stratosphere the thermal state is a balance between the absorbed solar radiations and absorbed and emitted thermal infrared radiation. The middle atmosphere is subjected to very considerable internal forcing by meteorological systems originating in the troposphere, and to external forcing associated with perturbation in the solar output. Observational evidence shows that some component of the middle atmosphere appears to respond to forcing associated with sunspot cycle (*Mohankumar, 1995*). Therefore we need model study to clarify the roles of both troposphere and solar forcing of the middle atmosphere. Many phenomena such as tides and gravity waves, which originate in the lower atmosphere, bear their fruits in the stratosphere. Again spectacular changes in stratospheric temperature are observed to occur in high latitude region and associated stratospheric warming event, which are initiated by upward propagating tropospheric planetary waves (*Matsuno, 1971, Charney et al., 1961; O'Neill et al., 1982*).

Increase in CO_2 and other greenhouse gases should lead to stratospheric cooling, which is considerably greater than the surface warming (*Manabe et al., 1980; Mitchell, 1983*). A summary of stratospheric temperature changes between 1979-80 and 1985-86, as estimated from radiosonde are presented elsewhere (*Labitzke et al.,1986; Angell, 1988*). It is accepted that the global and annual mean thermal profile in the stratosphere represents a balance between solar radiative heating and long wave radiative cooling. Cooling involving the effects of mainly ozone, water vapour, methane, nitrogen oxide, halocarbons and aerosols (*Goody et al., 1989*). The changes in the concentrations of trace gases and aerosols could substantially perturb the radiative balance of the stratosphere and thereby the thermal state. When analyze the satellite data from the

microwave sounding unit (MSU) channel 4 reveals the prominent warming events due to volcanic aerosols in 1982 (El Chichon) and 1991 (Mt. Pinatubo), which are on the order of $1°C$ (*Christy et al., 1994*). For carbondioxide the main 15 μm band is saturated over quite short distance. Hence the upwelling radiation reaching the lower stratosphere originates from the cold upper troposphere. When the CO_2 concentration is increased, the increase in absorbed radiation is quite small and the effect of the increased emission dominates, leading to a cooling at all heights in the stratosphere (*Ramaswami et al., 1996*).

Stratospheric water vapour is an important radiatively active constituent and its rate of change could be subjected to, influence by other physical factors, such as changes in tropospheric water vapour concentration, tropopause temperature and the transport of water vapour across the tropopause. The temperature changes scale approximately linearly with respect to water vapour changes of the magnitude. For a 5% per decade water vapour increase, the general circulation model (GCM) results would suggest a cooling of ~0.2 K / decade.

5.2 Data and methodology

In this chapter we have used the global NCEP/NCAR monthly reanalysis temperature data for the period (1960 to 2002), to study the interannual variability of temperature in the UT/LS of Asian summer monsoon region. This is a global gridded binary data for 17 standard pressure levels from the surface (1000 hPa) to mid stratospheric level (10 hPa) with grid resolution of $2.5°$ x $2.5°$ longitudes and latitudes (*Kalney et al., 1996*). The quality of NCEP/NCAR reanalysis for the temperature is good over the tropical region (*Trenberth et al., 2001*).

To study the solar activity influence on temperature we used the monthly values of 10.7 cm solar radio flux data (1960-2002) obtained from the NOAA website (*ftp://ftp.ngdc.noaa.gov/STP/SOLAR_DATA/SOLAR_RADIO/FLUX*) to study how the temperature is modulated with the 11-year solar cycle. The

monthly rainfall data for the period 1960 –1998 are also used to find the spatial correlation with temperature. A study on the spatial correlation of solar flux with temperature during monsoon period (June to September) from 1960-1998 was also carried out.

The temperature anomaly data computed from the original data set by subtracting the monthly climatology of each month from the corresponding months. Advanced statistical tools such as Wavelet Transform (WT) and Empirical Orthogonal Functional (EOF) are also used to study the temporal and spatial variations of the temperature over the Asian monsoon region. The detailed description of both wavelet transform and EOF analysis is presented in the Appendix I and II respectively. Power spectrum method is used to test the level of significance for the periodicity obtained for temperature using the wavelet analysis.

To determine the temperature trend in the upper troposphere and lower stratosphere we used the principle of least square fit. In the correlative study we found the correlation of monthly value of temperature with solar flux and the temperature with Indian summer monsoon rainfall were also carried out for the Indian region (0°-25° N & 65° E - 90° E). To find the level of significance for the above correlations we used the Student's, 't' test.

5.3 Results and discussion

5.3.1 Climatology of temperature distribution in the UT/LS

Figure 5.1 (a, b, c, and d) shows the longitudinally averaged climatology of temperature for the four seasons for the period 1960-1998 over the Indian longitude belt (65° E to 90° E) with a contour interval of 10° C. The tropopause height is maximum at the tropical region (~ 16-18 km) and height of tropopause is lower at higher latitudes. The height of the mid-latitude tropopause is at level 200 hPa (~ 8-12 km) and that at polar region is at 300 hPa levels (~7-10 km). In
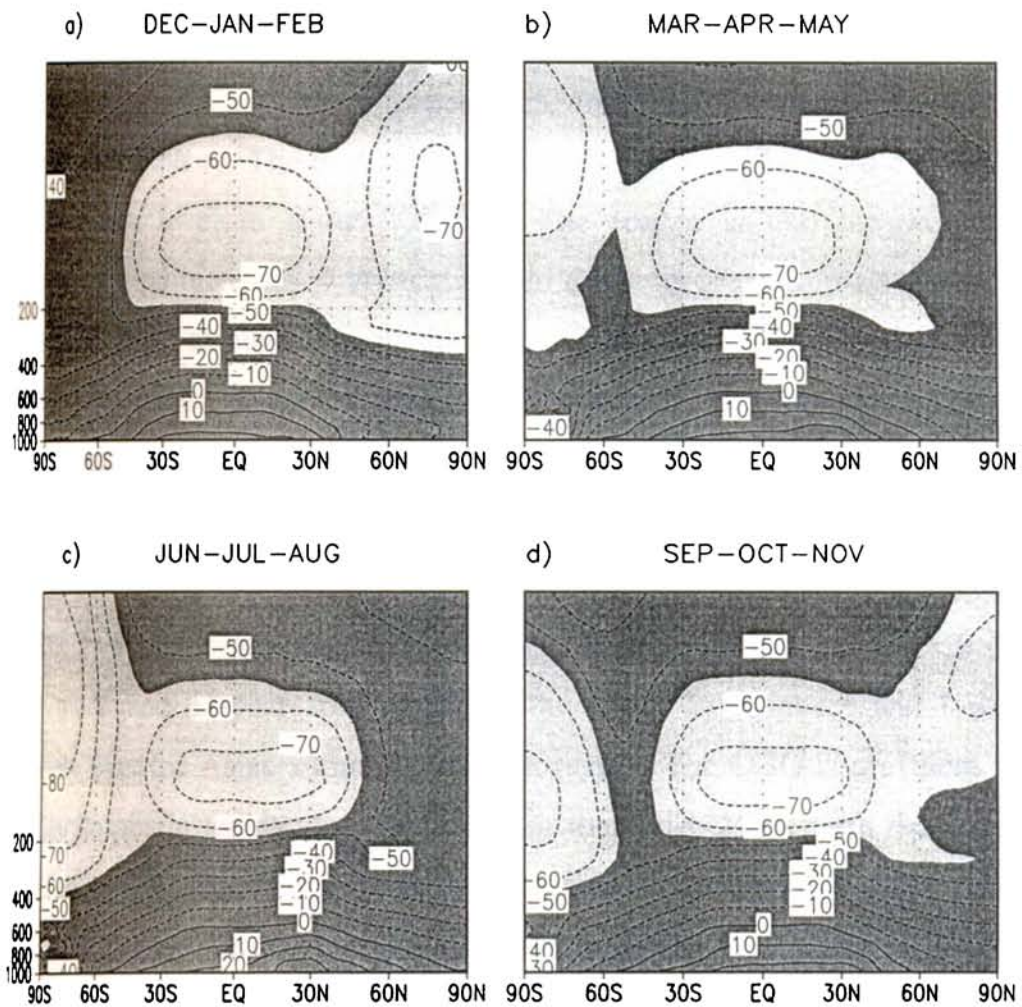
Figure 5.1: Climatology of temperature distribution in the UT/LS region for different season (1960-1998). Contour interval is 10°C.

monsoon season (figure 5.1c) temperature gradient is in the north-south direction and it is reversed during the northeast monsoon season (see figure 5.1a).

In the polar lower stratospheric region a minimum temperature of -90° C reached during the winter hemisphere and a maximum of -40° C in the summer hemisphere. There is a seasonal shift of the latitude of lower tropospheric maximum temperature and upper tropospheric minimum temperature towards the summer hemisphere. The tropical region is warmer than the middle latitude region from sea level to about 200 hPa. The reason is that the westerly component of wind increases with height up to the level of subtropical westerly jet shear (200 hPa), through a geostrophic and thermal wind relationship. And above 200 hPa near the equatorial region there will be lowest temperature due to increase of easterly component of wind.

5.3.2 Interannual variability in temperature

The two major interannual oscillations in temperature are the qausi-beinnial mode and 11-year solar cycle in the upper troposphere and lower stratosphere over the Asian summer monsoon region. The QBO is prevalent in tropical stratospheric temperature, which is in thermal balance with the zonal winds. The global aspects of QBO in stratospheric temperature have been derived from radiosonde observations (*Dunkerton et al., 1985; Labitzke et al., 1988, Angell, 1997*) and satellite derived data sets (*Lait et al., 1989; Randel et al., 1994; Christy et al., 1994*).

Tropical QBO in temperature maximize in the lower stratosphere (~20-27 km) over 10° N-10° S, with amplitude of $\pm$ 2- 4° K. There are two distinct maxima in temperature existing in the lower and upper stratosphere, which are vertically out of phases. There is also evidence for a coupling of the QBO with the lower stratosphere. The polar QBO temperature is out of phases with those in the tropics. Observational evidence for the polar QBO is less significant, than in the tropics or mid-latitude at least partially because of the high level natural

interannual variability in polar vortex structure (*Holton et al., 1980; Lait et al., 1989*).

5.3.2.1 Latitude-time variation of temperature (QBO)

Figure 5.2 and 5.3 represent the latitude - time series of temperature anomaly showing the QBO phases at the stratospheric level 20 hPa and 30 hPa respectively during the period 1960 to 2002. The changing of warm phase and cold phase of temperature anomaly with time can be seen. Here we have averaged the temperature anomaly over the Indian longitude belt (65° E to 90° E) and considered only the northern latitude from equator to 25° N to understand the QBO in temperature over the southwest monsoon region. Warm phases of temperature QBO is maximum ($\leq 4^\circ$ C) in March 1961 and July 1963 during the period of study and is concentrated in the equatorial region below 10° N. The cold phase in temperature QBO is very intense in 1965 with a value greater than -3° C (figure 5.2). There is a qausi-beinnial periodicity in temperature with warm and cold phases are seen at 20 hPa level from 1960 to 1992 and negative anomaly values are also seen from 1993 to 2002. The amplitude of warm and cold phase varies from a maximum value of 4° C to a minimum value -3° C at 20 hPa level and 2° C to -2° C at 30 hPa level over the Indian longitude belt. At 30 hPa level the intensity of the QBO in temperature are not much affected and warm phases are seldom seen from 1993 to 2002 (figure 5.3). There is an abnormal change in temperature (negative anomaly greater than $- 4^\circ$ C) seen in 2000 at 30 hPa level over the Indian longitude belt. The temperature variation in the lower stratosphere will also be a contributing factor in the monsoon variability. Krishnan *et al.* (2003) identified the monsoon in 2000 as the abnormal monsoon by the observational and model simulations. The cold and warm phases of the temperature QBO is extended to the high latitudes and the maximum intensity is concentrated in the equatorial region at the 20 and 30 hPa level.
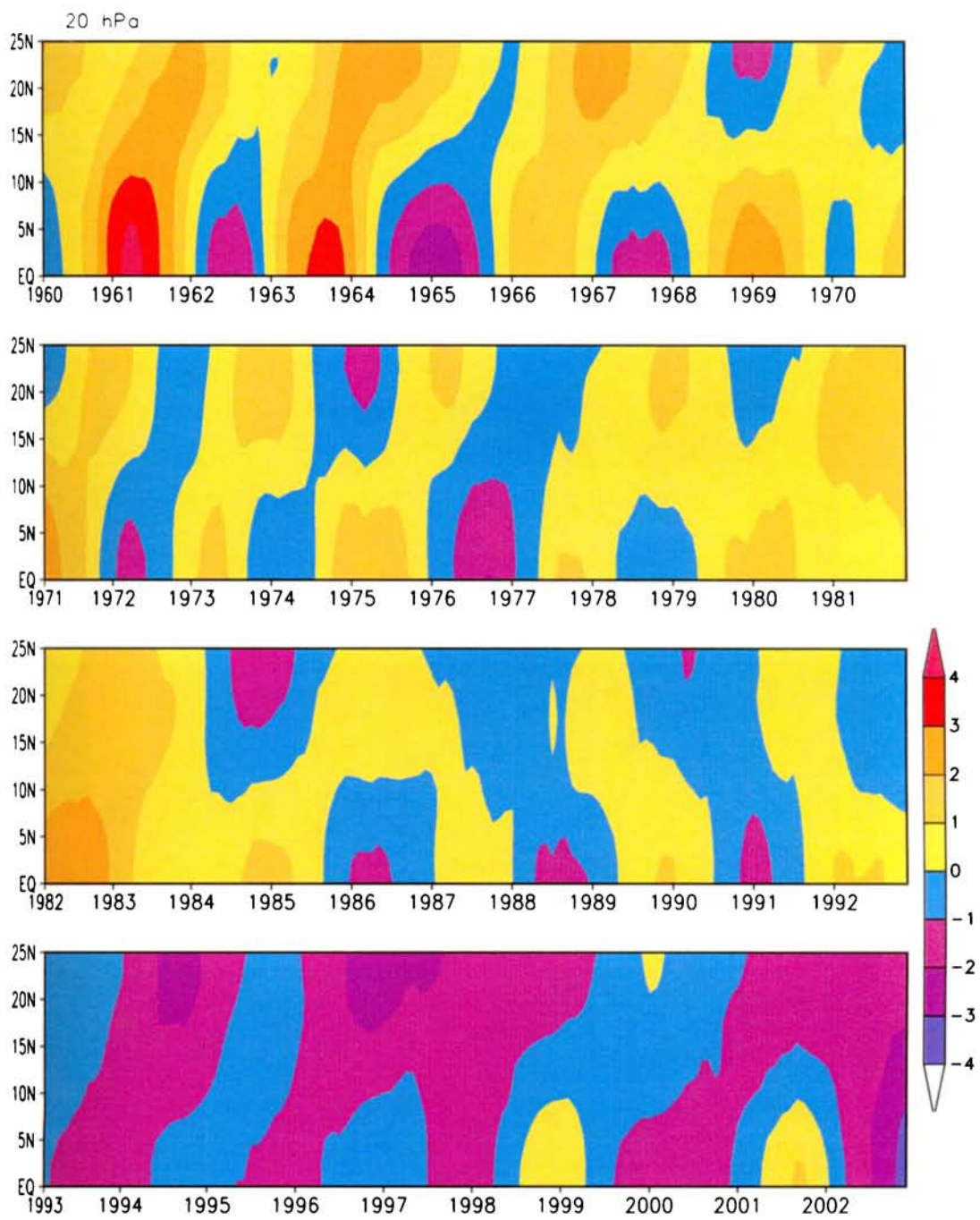
Figure 5.2: Latitude - time variation of temperature anomaly over the Indian longitude belt (65°E-90°E) at 20 hPa level
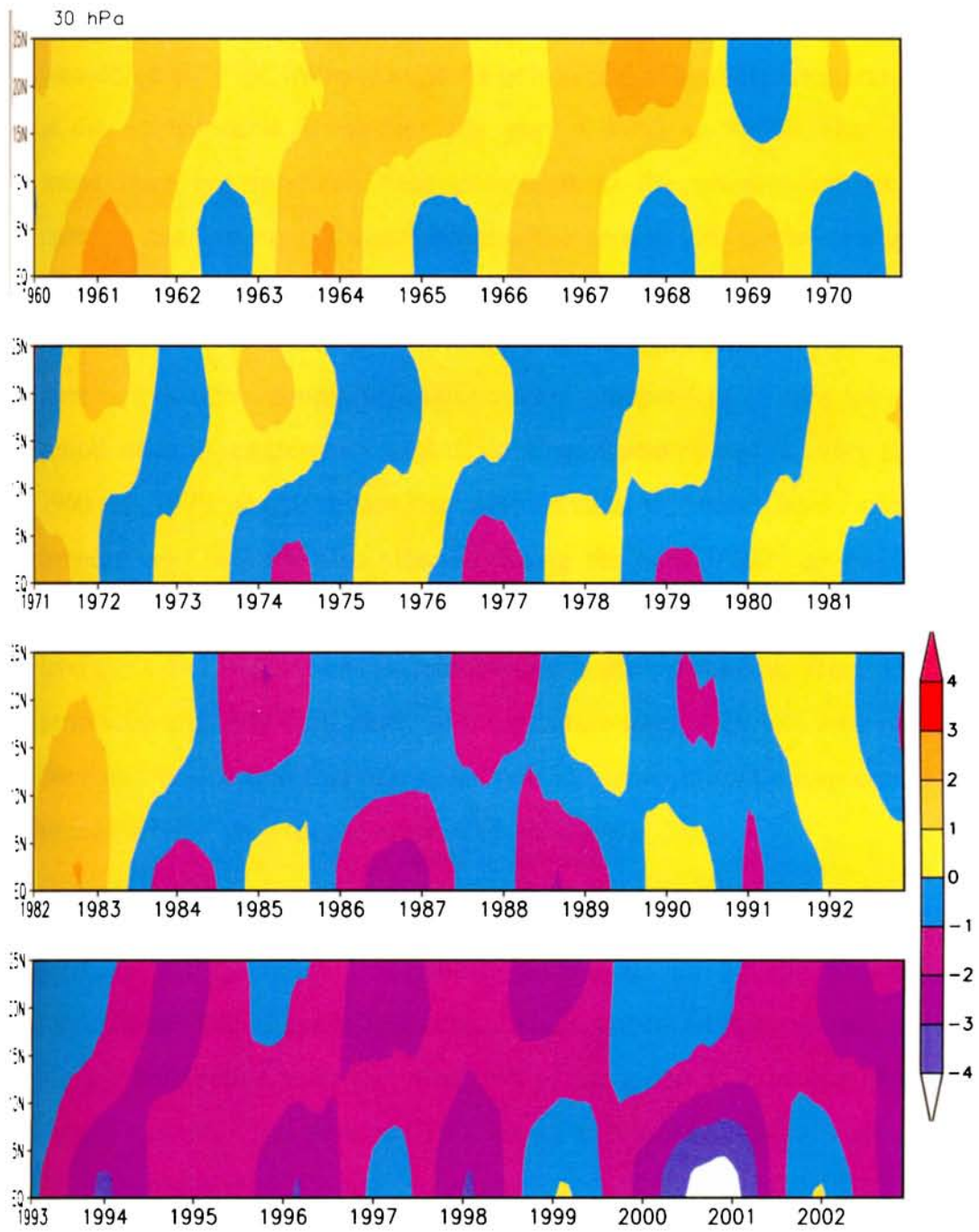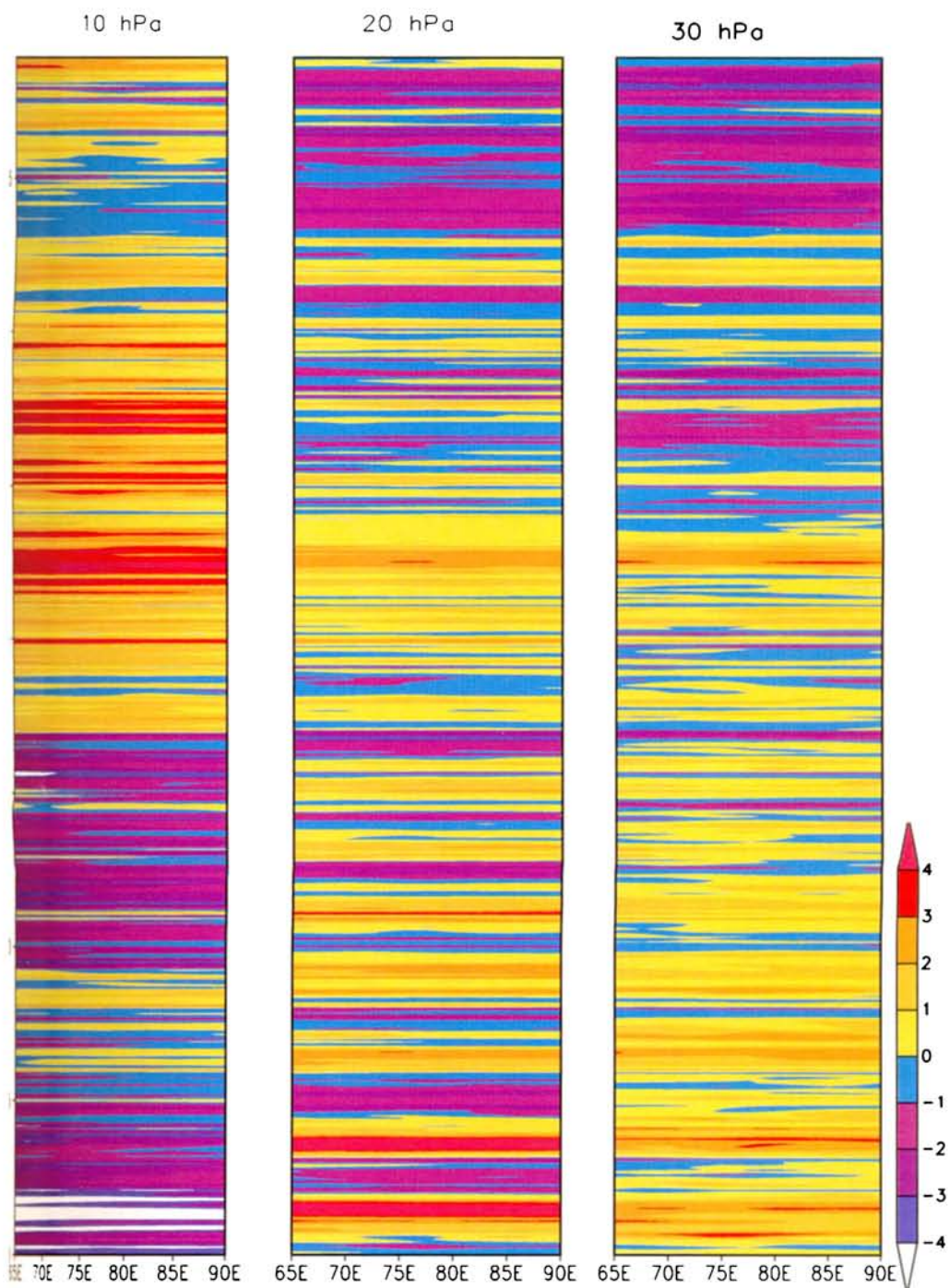
Figure 5.3: Latitude- time variation of temperature anomaly over the Indian longitude belt (65°E-90°E) at 30 hPa level

The longitudinal variation of temperature anomaly averaged over the latitude 0°-15° N for 10 hPa , 20 hPa and 30 hPa is given in figure 5.4. We have considered only the Indian longitude belt to understand the temperature variation at the stratospheric levels for the period 1960 to 1998. The variations in temperature are relatively less compared to the zonal wind variations and therefore the QBO is not that distinct in the case of temperature variations. At 10 hPa there is cooling trend of temperature during the period 1960 to 1977 and after that there is warming over the Indian longitude belt. From 1977 to 1998 there is a positive anomaly in temperature observed at 10 hPa level. The QBO periodicities in temperature with its cold and warm phases are very strong during 1960 to 1979 at 20 hPa. The periodicities of warm and cold phases of temperature QBO are also affected during the period 1977 to 1998. Only cold anomaly in temperature is observed in most of the years at this level. At 30 hPa level the QBO oscillations in temperature is not prominent. From 1993 to 1998 period there is only cold phase of temperature seen at 20 hPa and 30 hPa levels. We could notice that this particular year has some climatic importance with the strong El-Nino year for the century (1997-1998).

This sort of temperature changes with time is not due to the seasonal variation and interannual variability instead it can be due to some climatic fluctuations. The climate fluctuation, which occurs over some part of the globe, has tele-connection with the other part of the globe and thereby changes in the climate systems. The solar activity, changes in ozone concentration, increase in the anthropogenic CFC and increasing effect of the greenhouses gases such as CO_2 may contribute to the disturbance in the radiative balance, thereby changes in the equatorial stratospheric temperature. Hence the temperature variations in the stratospheric levels need further investigations to bring out whether it is due to the climate fluctuations such as El- Nino - southern oscillation, change in ozone concentration, solar activity, etc.

81

Figure 5.4: Longitudinal variation of temperature anomaly (°C) with time over the Indian region averaged over the latitude 00°-15°N for 10 hPa, 20 hPa and 30 hPa

5.3.2.3 Vertical evolution of temperature with time (QBO)

Figure 5.5 represents vertical variation of temperature QBO (the propagation of warm and cold phase) with time in pressure levels (70 hPa to 10 hPa) for the period 1960 to 1998 over the Asian monsoon region .The contour interval is 1° C. The maximum temperature (warm phase) and minimum temperature (cold phase) with QBO periodicity and its downward propagation is very clearly seen over the Indian monsoon region. The westerly phases of the temperature QBO is more prominent during the period 1961-1986. The cold phases of the QBO are prominent during 1986 to 1988 in the stratospheric levels. The stratospheric temperature and its variability depends on many factors such as ozone depletion, carbon dioxide emission and natural hazards like volcanic eruption which may hamper the cold and warm phases of the temperature QBO in some years.

5.3.2.4 Temperature variation over the Indian monsoon region

Figure 5.6 to 5.7 represent temperature variation from 1960-2002 for the different stratospheric and tropospheric levels (10 hPa, 20 hPa, 30 hPa, 50 hPa, 70 hPa, 100-, 150-, and 200- hPa) over the Asian summer monsoon region (65° E -90° E & 0°- 25° N). At 10 hPa level the temperature shows a negative anomaly from 1960 to 1977. From 1977 to 2002 there is a positive anomaly in temperature variation over the Indian summer monsoon region at 10 hPa level. In the stratospheric pressure levels the temperature takes a positive anomaly to negative anomaly variations during the year 1977. So the year 1977 is marked as the reference year for the climatic fluctuations occurs over the monsoon region. Wang (1995) studied the Inter-decadal changes in El Nino onset in the last four decades based on the events, which occur prior and after 1977.

These climatic change prior and after 1977 is evident in the case of temperature variation at the UT/LS of the Indian summer monsoon region. From figure 5.6 and 5.7 the interesting thing we noticed that the temperature variations in the upper troposphere and lower stratosphere show out of phase pattern before

82

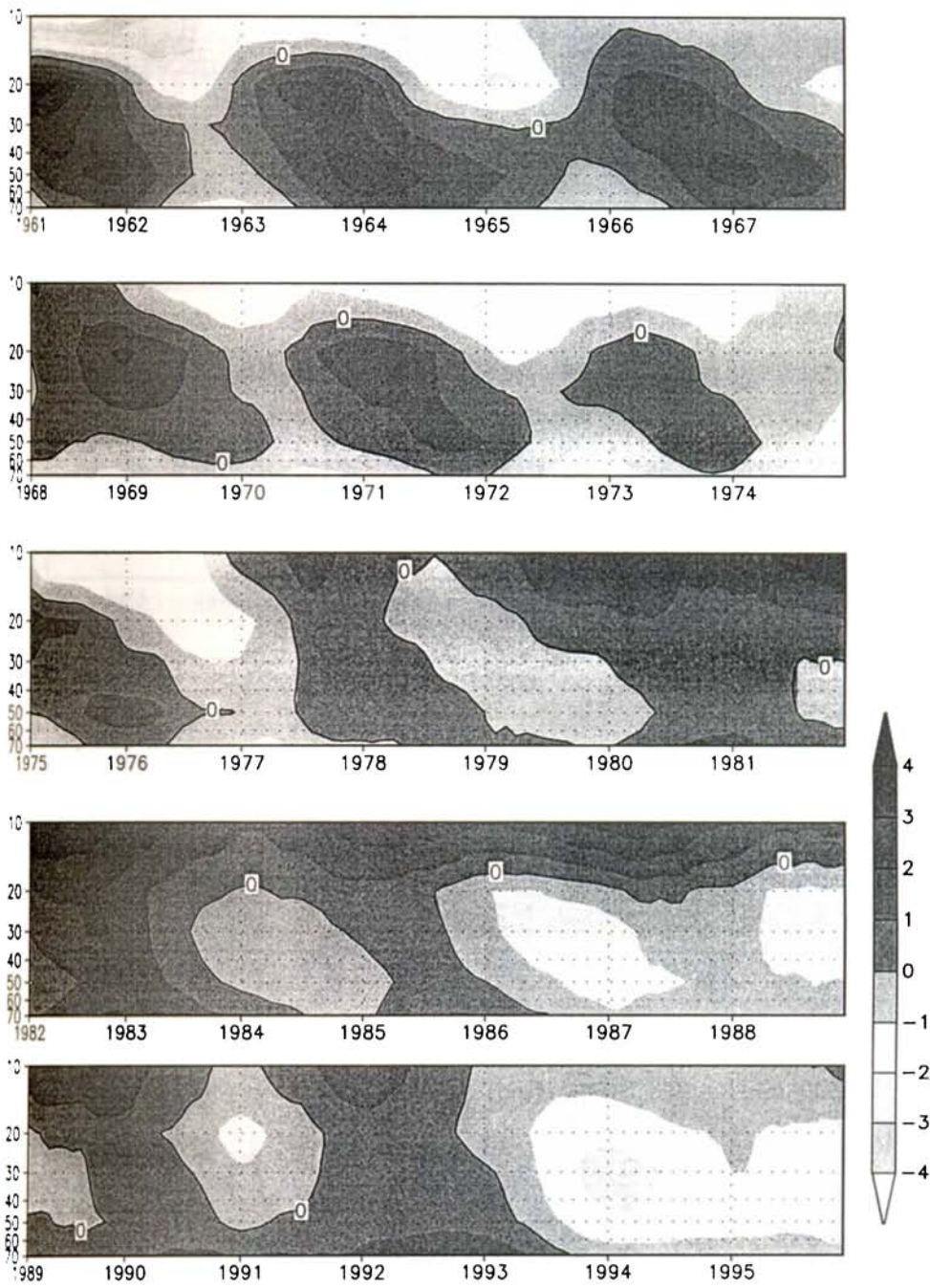Figure 5.5: Vertical structure of temperature of anomaly (QBO) averaged over the region (65°E - 90°E & 0° – 15°N)
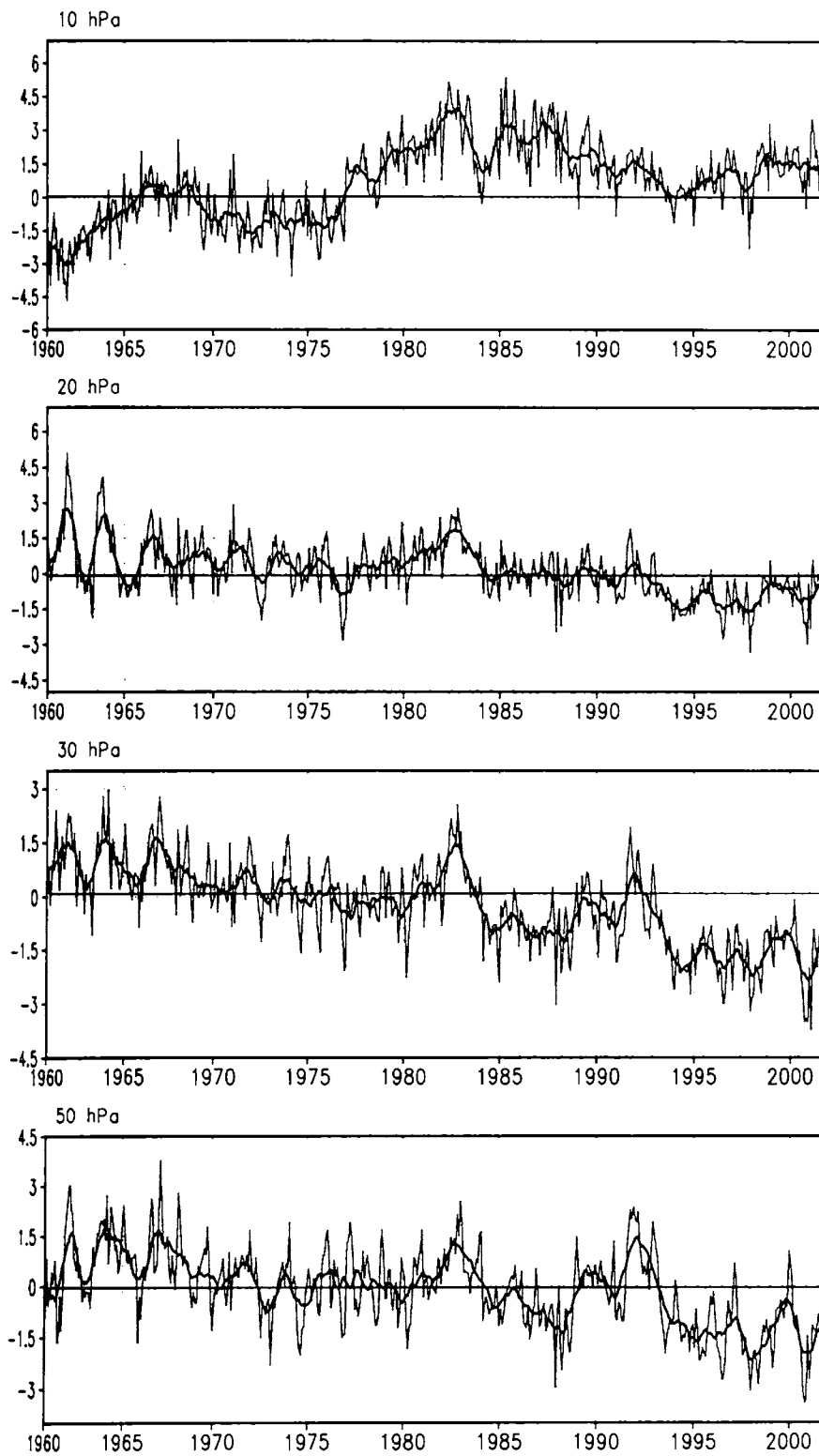
Figure 5.6: Temperature anomaly for the pressure levels (10 hPa, 20 hPa , 30 hPa and 50 hPa) averaged over the region (65°E-90°E & 0°-25°N)
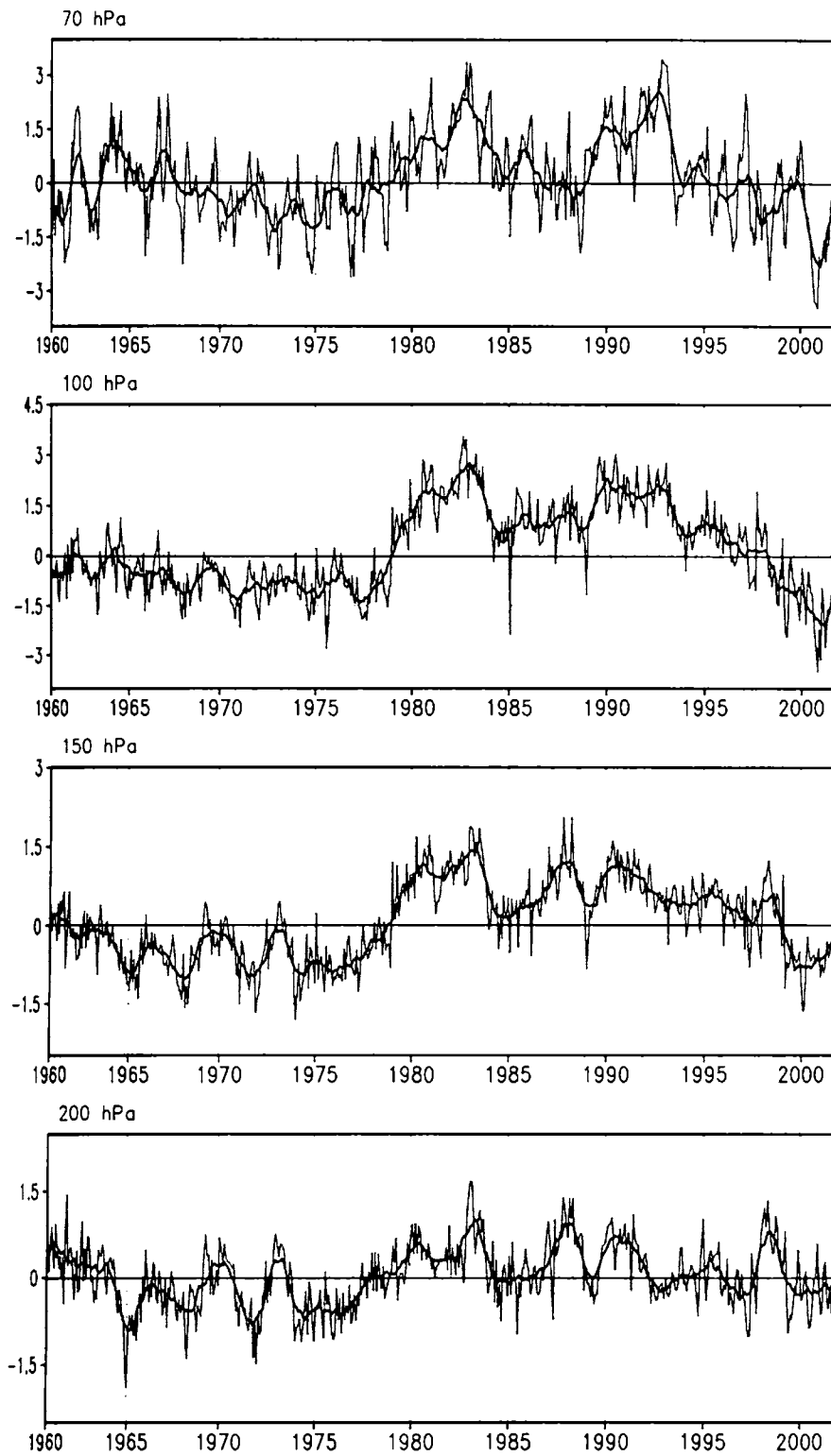
Figure 5.7: Temperature anomaly for the pressure levels (70 hPa, 100 hPa , 150 hPa and 200 hPa) averaged over the region (65°E-90°E & 0°-25°N)

ad after 1977. In the stratospheric levels we observe a temperature variation from positive anomaly prior to 1977 to negative anomaly after 1977. This shows that the stratosphere is in the cooling trend instead of the normal warming conditions in the stratosphere. The reverse effect is noticed in the troposphere temperature variation. Instead of keeping a cooling thermal conditions in the troposphere there is shifting of negative anomaly to positive anomaly prior and after 1977 during the course of study (1960-2001).

5.3.3 Wavelet analysis for the UT/LS temperature

To study the temporal variability of upper tropospheric and lower stratospheric temperature Morlet wavelet method is used. In this method the time series data is split into smaller periodicity waves. We have done the significant test for these oscillations using power spectrum method. The detailed description of different wavelet transform and the method of analysis is illustrated in appendix I.

The temperature data for the period May 1960 to December 2002 (512 monthly values) averaged over the region (65° E - 90° E & 0°-15° N) used for the wavelet analysis. Figure 5. 8 (a, b & c) represent the wavelet spectrum (wavelet coefficients) of temperature for the stratospheric levels (10 hPa, 20 hPa) and tropospheric pressure level 200 hPa respectively for the lower periodicity. The periods in months are represented in the y-axis and the time is represented in x-axis. The dominant mode of oscillation can be seen with variations of positive and negative contours of wavelet coefficients from the wavelet spectrum. The quasi-biennial oscillation is observed in the wavelet spectrum of temperature, at the stratospheric levels with periodicity varying from 26 to 32 months. The amplitude and periodicity of QBO phases are different in the lower stratosphere. Cold phases are very strong during the period May 1960 to July 1977 at 20 hPa level.

Figure 5. 8 (c) shows the wavelet spectrum of temperature for the tropospheric level at 200 hPa with the lower periodicity over the Asian summer
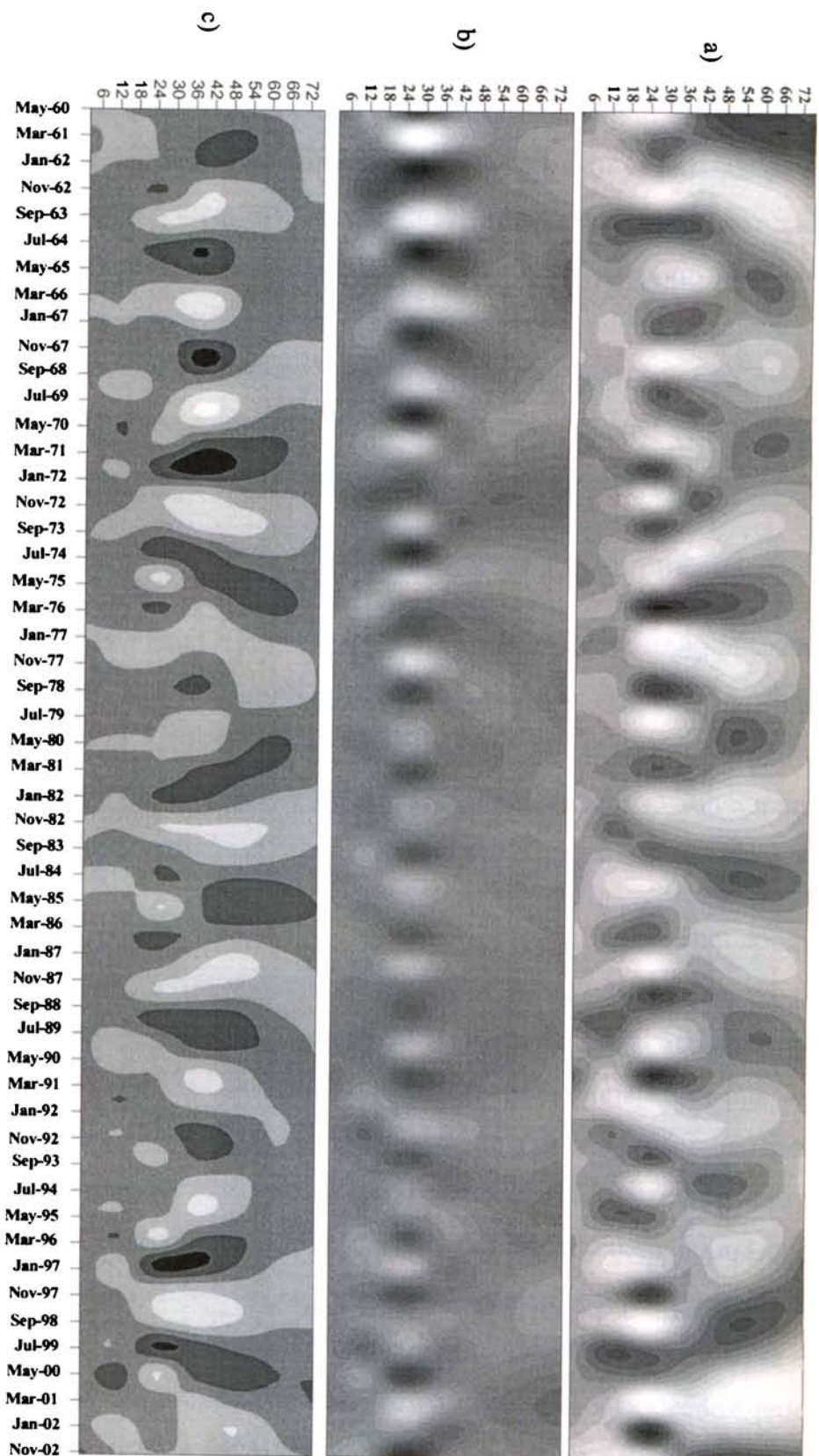
Figure 5.8: Wavelet spectrum of temperature for the shorter periodicity.a) 10 hPa , b) 20 hPa and c) 200 hPa.

monsoon region. The tropospheric temperature exhibits a tropical biennial mode with periodicity ranging from 26 to 34 months (figure 5.8 (a &b)). The QBO in the equatorial tropospheric temperature need further investigation to confirm its periodicity as in the case of zonal wind that does not shows the QBO periodicity at the tropospheric level. Sathiyamoorthy et al. (2000), pointed out the relation of the tropospheric biennial oscillation (TBO) in temperature and monsoon activity. They found that the decadal changes of phase coherence between tropical biennial oscillation (TBO) and quasi-biennial oscillation (QBO) in temperature and correlation between these oscillations suggest that both are different phenomenon. They have also suggested that the strong relation between phases of TBO and the Indian summer monsoon may be due to the atmosphere-ocean-monsoon interaction.

The observed periodicity (QBO) in the stratospheric temperature is verified with the power spectrum analyses. Figure 5.9 (a, b, and c) represent the respective power spectrum for the temperature oscillations obtained from wavelet analysis. Here also we noticed the QBO oscillation with periodicity ~ 26-32 months and these oscillations are significant above 95 % confidence level.

5.4 Solar activity and the UT/LS temperature

The 11-year and 22 -year periods evident in solar activity proxies appear in many climate and paleoclimate records, and some solar and climate time series correlate strongly over multi-decadal and centennial time scales. This statistical relationship suggests a response of the climate system to the changing sun. The 11-year modulation of the UV solar flux is expected through photochemistry to influence stratospheric ozone and therefore stratospheric temperature. A number of investigators have attempted to identify a signature of the 11-year solar cycle in the temperature data sets. Sunspot number is a widely used index of solar activity. Mohankumar (1995) studied the solar activity forcing of the middle atmosphere. The solar proxy used in most studies is the 10.7 cm radio flux, which spans the longest period proxies. Other proxies are the
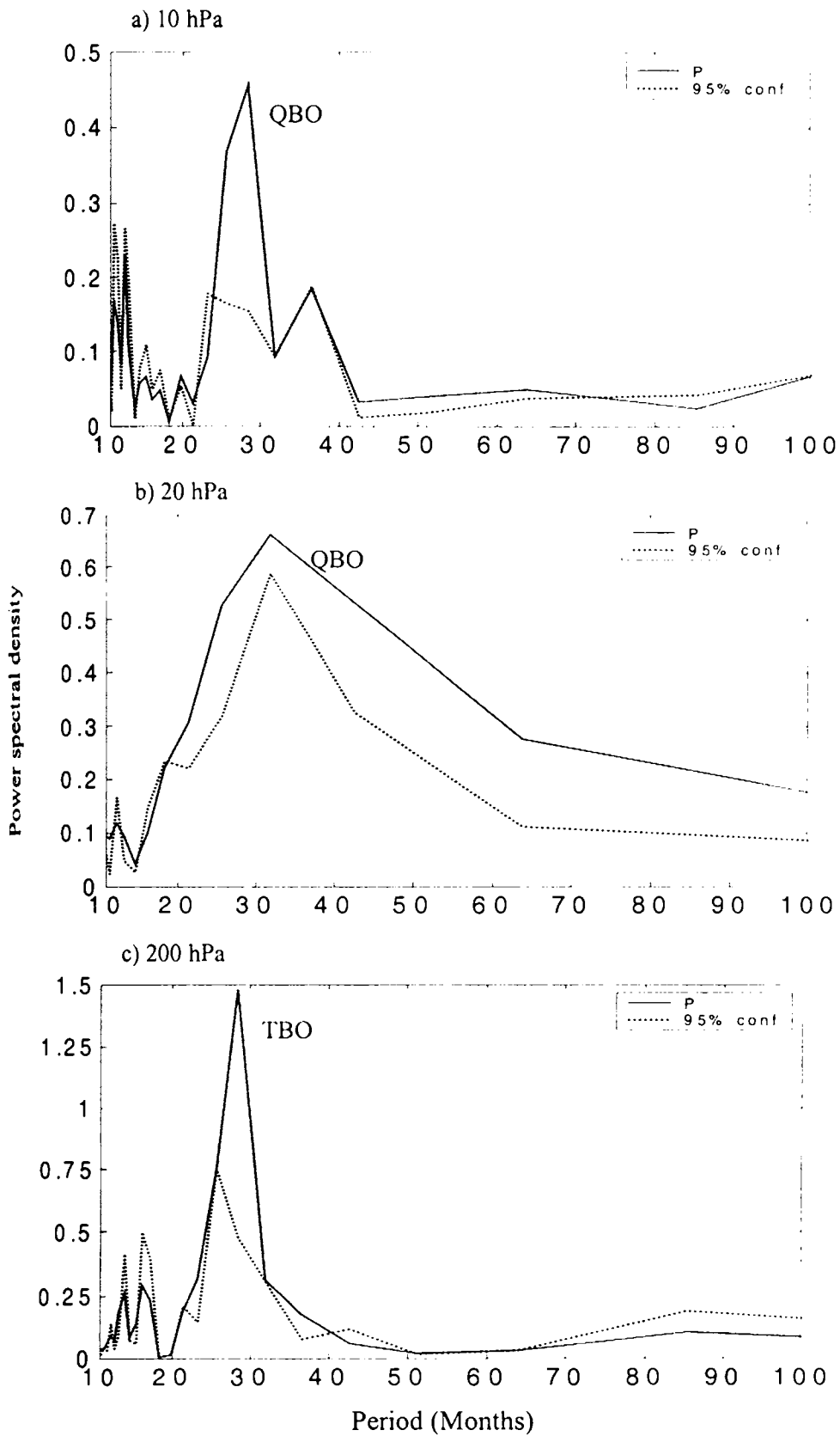
Figure 5.9: Power Spectrum for the temperature anomaly averaged
over the region (0°-15°N & 65°E- 90°E). a) 10 hPa, b) 20 hPa , and
c) 200 hPa.for QBO periodicities

Helium (He), Iodine (I) or UV irradiance. However, several analysis using these different proxies justify the choices of the 10.7 cm solar flux is better for the study of 11-year cycle (*Donnelly et al; 1986, Kechut et al., 1995*). The correlation of reconstructed solar irradiance and Northen Hemisphere (N.H) surface temperature anomalies is 0.86 in the pre –industrial period from 1610 to 1800, implying a predominant solar influence (*Lean, et al., 1998*). It was shown that solar forcing might have contributed about half of the observed 0.55° C surface warming since 1900 and one third of the warming since 1970.

Labitzke and van Loon (1988) showed the evidence of a solar signature in stratospheric temperature when the data are sorted accordingly to the phases of the QBO. There are some studies connecting the QBO and solar cycle and found that the structure of the solar signal in northern summer appears to indicate that the mean meriodional circulation (Hadley and Brewer-Dobson Circulation) also influenced by the solar sunspot cycle (SSC) especially during the east phase of the QBO (*Labitzke, 2003*). The stratospheric temperature and circulation in the northern hemisphere winter for the period 1964-1991 varied interannually on time scales from 2 to 12 years. This interannual variability in temperature showed correlation with solar cycle and is attributed to the QBO and solar cycle (*Dunkerton et al., 1992*). The solar cycle in stratospheric polar temperature rests on a connection to the quasi-biennial oscillation (QBO) of equatorial wind (*Murry et al., 2000*).

There are many studies pointed out that the solar cycles modulate the upper tropospheric and lower stratospheric temperature. Figure 5.10 (a, b, and c) represent the wavelet spectrum of temperature at 10 hPa, 200 hPa levels and the wavelet spectrum of 10.7 cm solar flux respectively for the higher periodicity to study the decadal variability in temperature (solar cycle). The wavelet spectrum of temperature at higher periodicity in the upper tropospheric level (200 hPa) keeps an in-phase relation with the 10.7 cm solar flux. At 10 hPa temperature at high periodicity does not keep an in-phase relation even though it is having an 11 year cycle in the temperature variation. And solar flux and temperature at this

a) Wavelet spectrum of temepratue- 10 hPa

b) Wavelet spectrum of temperature- 200 hPa

c) Wavelet Spectrum of Solar Flux (Anomaly)
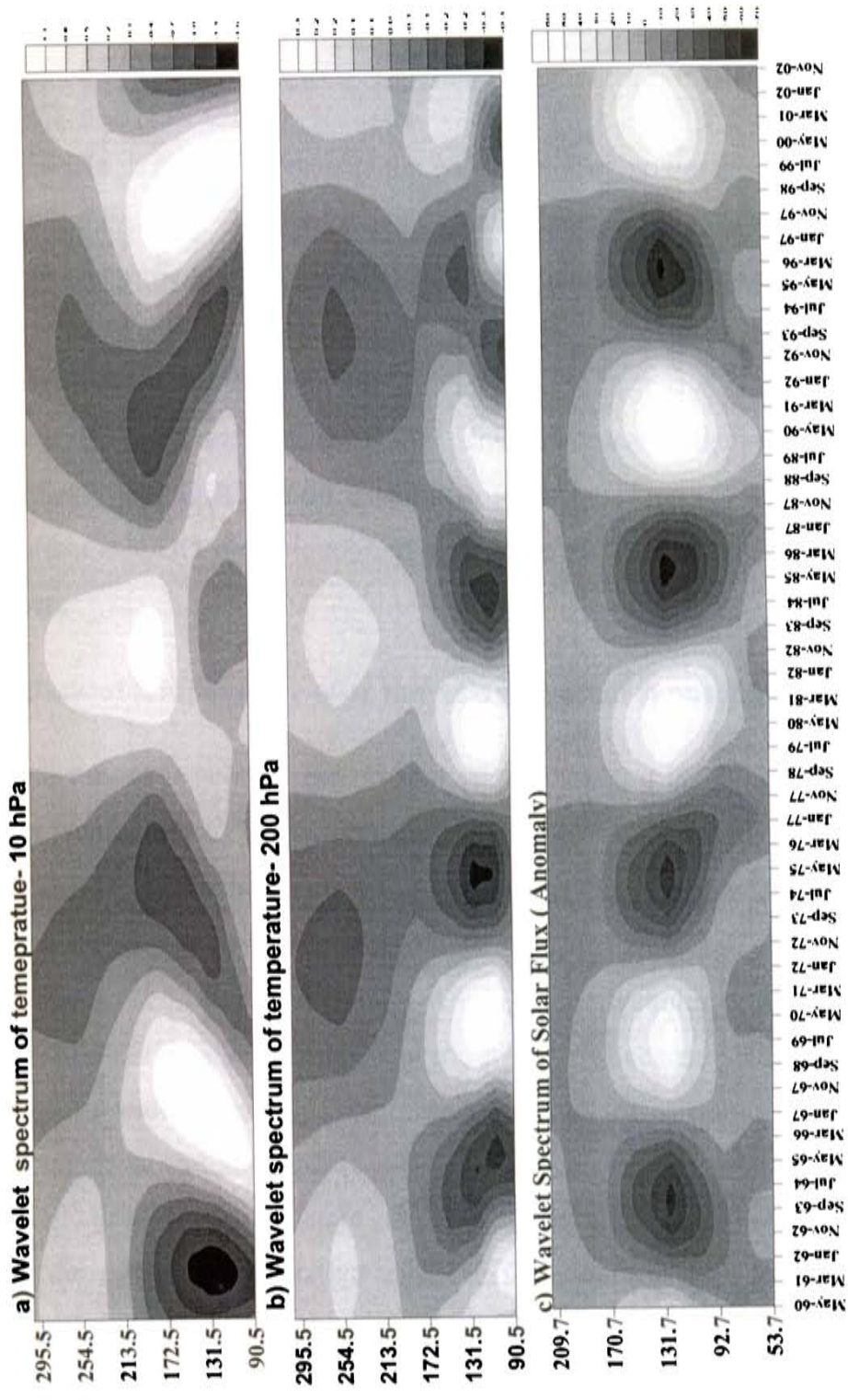
Figure 5.10 : Wavelet spectrum of temperature averaged over the region (65° E-90° E & 0°-15°N). a) for 10 hPa level. b) for 200 hPa level for higher period and c) wavelet spectrum of 10.7 cm solar flux anomaly.

tropospheric level (200 hPa) show a periodicity of 132 months (11-year solar cycle). Also seen a signal of 22-year cycle in temperature with a periodicity (~264 months), which is not significant.

Figure 5.11 (a, b and c) represents the corresponding power spectrum for the temperature and solar flux in which clearly seen the solar cycle in temperature with a significance of above 95 % confidence level. From the above discussion we can say that the temperature in the upper troposphere and lower stratosphere modulates accordingly with the 11-year solar cycle. The power spectral density of both oscillations (QBO and 11- year solar cycle) in temperature indicate that QBO mode is dominant compared to 11- year solar cycle and the effect of QBO mode is more dominant in the stratosphere than the upper troposphere.

5.3.5 EOF analysis of temperature over the Asian summer monsoon region

In climate studies it is important to find out the variability in the climate parameters (eg. temperature) and quantify the same using some standard methods to get an idea about how much it contribute to the total percentage of variability of the climate change. For that purpose several advanced statistical techniques have been used in climate studies. Among these techniques Empirical Orthogonal Function (EOF) analysis stood in the forefront because of its spatial pattern and temporal pattern, which give more details of the variability in the parameter. The layers of the atmosphere are based on the thermal stratification and if any perturbation in thermal state of these layers will affect the UT/LS climate, mainly depend on the radiative balance. Temperature is an important parameter which need detailed study to understand more about monsoon variability and we studied the spatial and temporal variation of temperature over the UT/LS of the Asian monsoon region. For this purpose Singular Value Decomposition (SVD) method of EOF analysis is used to understand the UT/LS temperature at various levels. The detailed theory of SVD EOF techniques and method of analysis are described in Appendix II.

a) Power spectrum of temperature – 10 hPa

11 year solar cycle

b) Power spectrum of temperature – 200 hPa

Power spectral density

11 year solar cycle

c) Power spectrum of 10.7 cm Solar radio flux
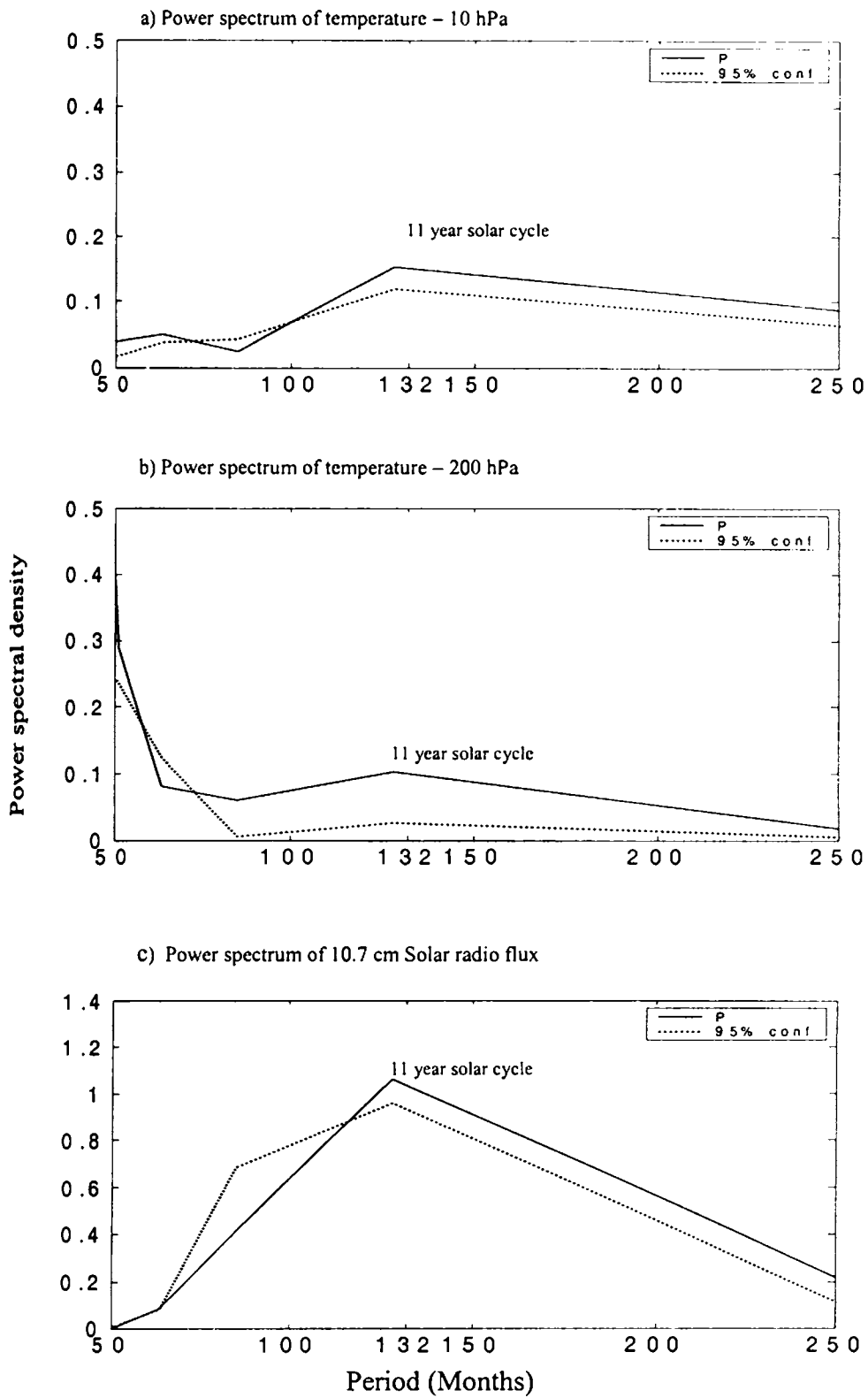
11 year solar cycle

Period (Months)

Figure 5.11: Power spectrum for higher periodicity .a) temperature at 10 hPa , b) temperature at 200 hPa, and c) 10.7 cm solar radio flux.

Figure 5.12 represent the EOF pattern and principal component (PC) of the temperature over the region (40° E - 120° E & 20° S-30° N) at 10 hPa for the period 1960 to 2002. Here we have considered four eigenvalue cases for the EOF analysis and the first eigenvalue itself contribute the maximum percentage of variability in temperature. The EOF coefficients and principle component are normalized with the standard deviations of the corresponding principle component for the better representation. The EOF-1 (higher eigenvalue) represent the dominant percentage of variability and EOF-2 represent the next dominant variability to the total variability in the temperature and so on depending on the decreasing order of eigenvalues. At 10 hPa EOF-1 shows the dominant mode of variability in temperature over the Asian summer monsoon region and it is modulated with solar cycle. The monopole type of spatial pattern with all negative coefficients over the region contributes about 72.98 % to the total variability in the temperature. The corresponding PC-1 represent the principal component which indicate the annual oscillation and semi annual oscillation, which is embedded in the 11-year solar cycle is quite evident from the PC1. Next dominant variability is of quasi-biennial mode, which is represented by EOF-2 and PC-2 respectively. The PC-2 stands for the QBO mode of variability and it contributes 12.68% percentage to the total variability of temperature at this level. EOF-3 contributing less percentage to the total variability may be due to the annual, semi annual cycles in temperature at these levels. And the EOF-4 can be treated as the noises in the data.

Figure 5.13 and 5.14 represent the EOF patterns and corresponding principle components at the level 50-hPa and 150 hPa. Here the EOF-1 and corresponding PC1 represent the QBO mode rather than the solar cycle as we observed at the 10 hPa level of EOF-1 pattern (figure 5.13). Hence the variability in temperature due to the modulation of solar cycle is less evident at the 10 hPa level and QBO mode of variability, which contribute 71.36 % to the total variability in temperature oscillation. Also at 150 hPa levels the influence of solar cycle is greater compared to the stratospheric temperature and EOF1 and
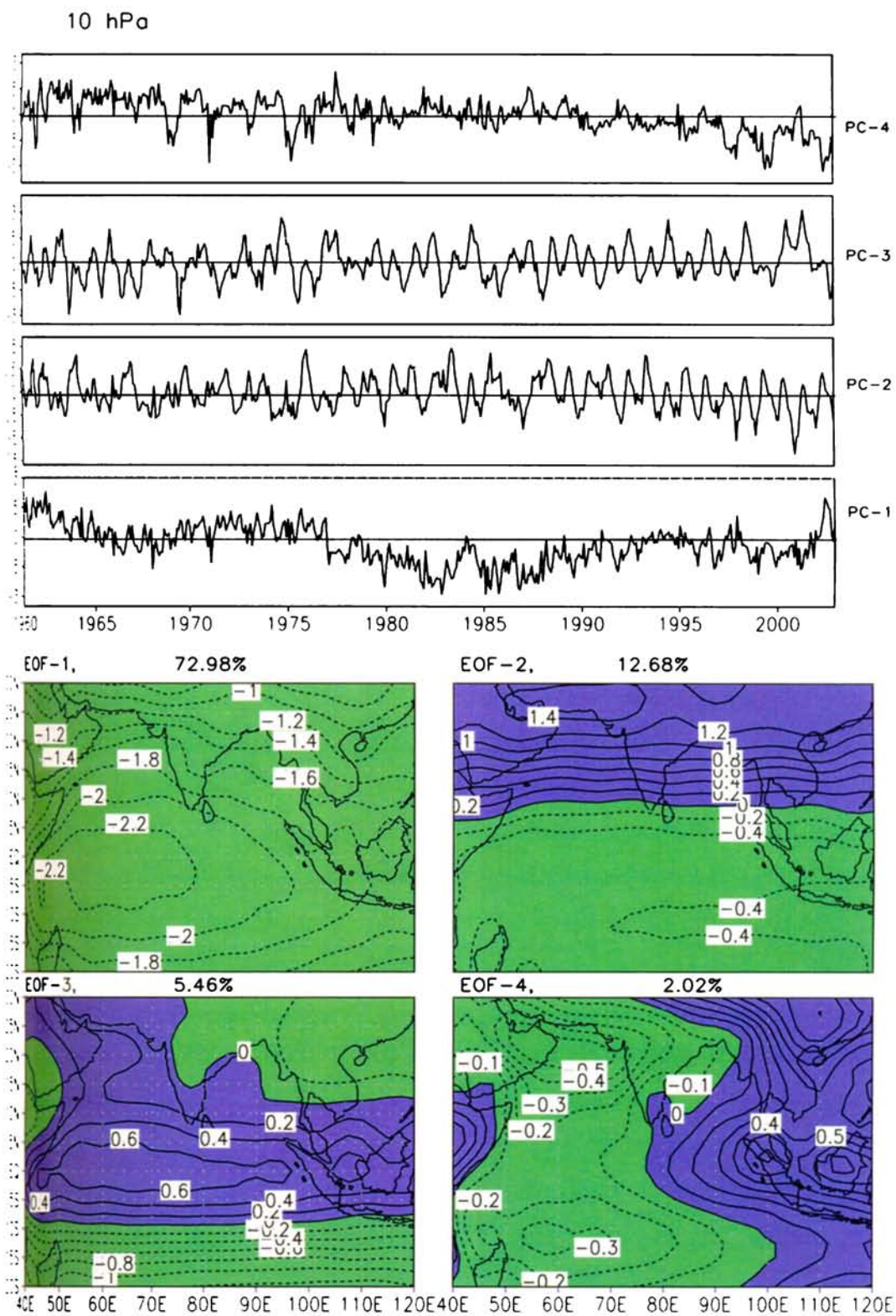
Figure 5.12: EOF pattern and corresponding principle component of temperature anomaly at 10 hPa level
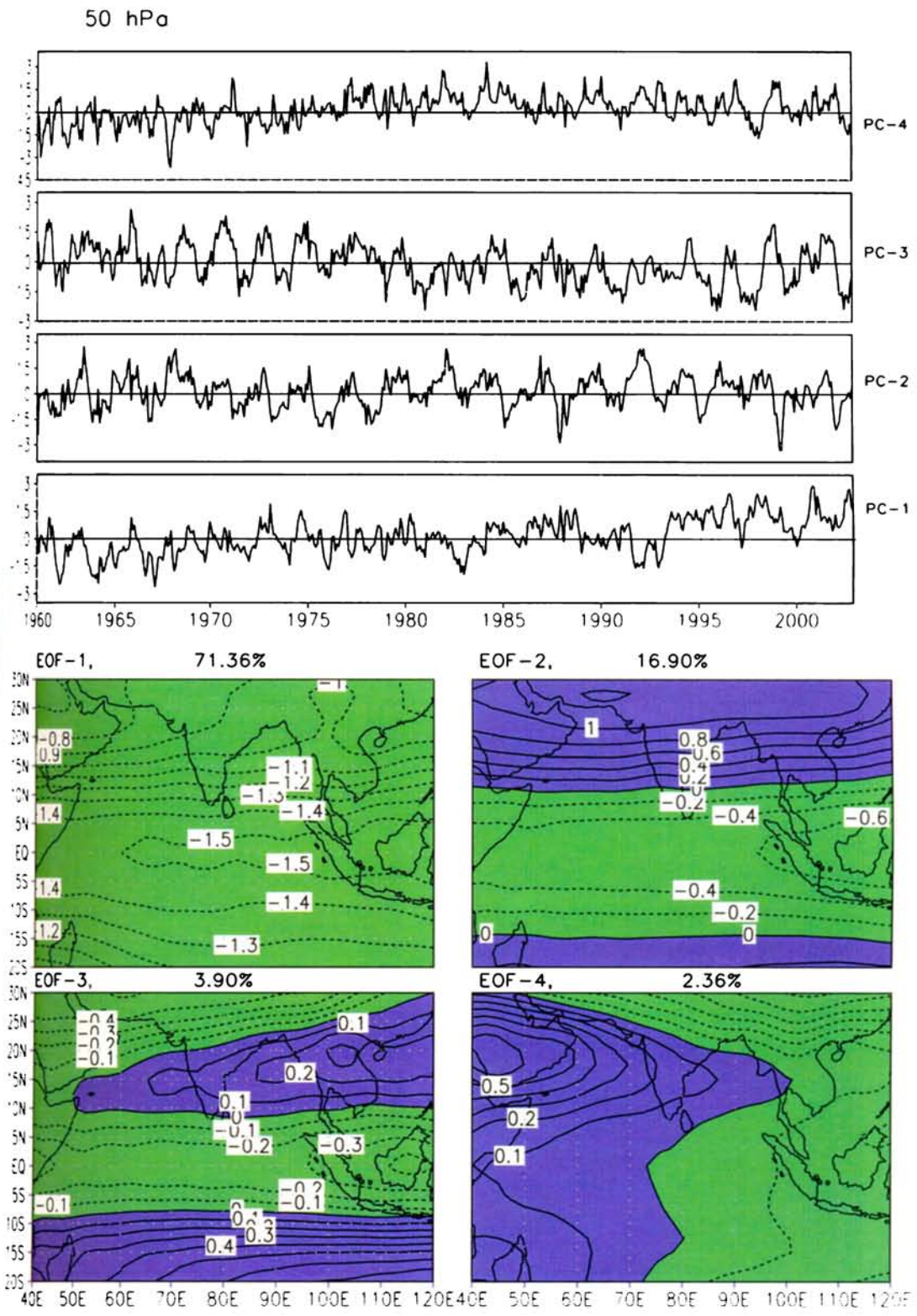
Figure 5.13: EOF pattern and corresponding principle component of temperature anomaly at 50 hPa level
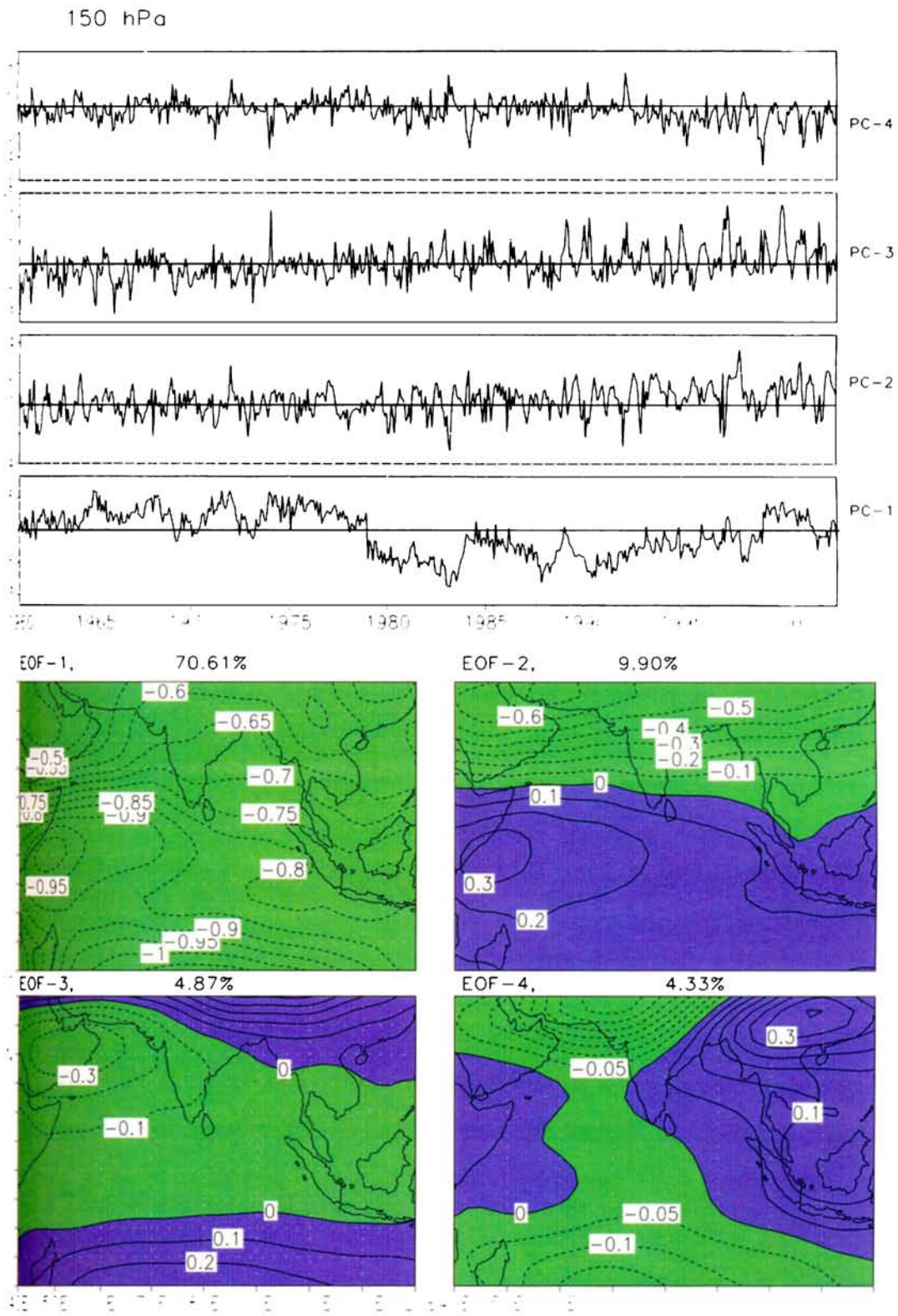
Figure 5.14: EOF pattern and corresponding principle component of temperature anomaly at 150 hPa level

PC-1 shows the same influence of solar cycle which contribute about (70.61%) to the variability in the upper troposphere temperature. The next dominant EOFs and PC representing annual and semi-annual oscillation in the temperature at the tropospheric level. From the above analysis we concluded that QBO mode contribute to the total variability in the lower stratospheric temperature and the 11-year mode in the upper tropospheric temperature variation except at 10 hPa level.

Levels hPa	PERCENTAGE OF VARIABILITY				Total EOF %	STANDARD DEVIATION OF PC			
	EOF-1	EOF-2	EOF-3	EOF-4		PC-1	PC-2	PC-3	PC-4
10 hPa	72.98	12.68	5.46	2.02	93.14 %	44.94	10.71	12.94	7.89
30 hPa	61.67	25.83	3.21	1.38	92.09 %	29.92	19.76	6.98	4.58
50 hPa	71.36	16.90	3.90	2.36	94.52 %	32.58	15.88	7.60	5.89
100 hPa	72.10	9.40	3.89	2.93	88.32 %	34.64	12.53	8.021	6.98
150 hPa	70.61	9.90	4.04	3.19	87.74 %	20.25	7.59	4.87	4.33
200 hPa	53.78	21.15	6.80	3.80	85.53 %	13.99	8.77	4.97	3.58

Table 5.1 Contribution of the variability by each EOFs and standard deviation of PC of temperature anomaly for the UT/LS levels (1960-2002).

Table 5.1 give the summary of the EOF analysis of temperature for other UT/LS levels and the contribution of the percentage of variability of each EOF patterns with standard deviations of the principle components over the Asian summer monsoon region (20° S to 30° N & 40° E to 120° E).

5.3.6 Temperature trend over the Asian summer monsoon region

A comprehensive international scientific assessment of stratospheric temperature changes was undertaken by World Meteorological Organization (WMO, 1990a). The assessment of upper tropospheric and lower stratospheric

88

trend now regarded as a high priority in climate changes research in the detection and attribution of the observed vertical profiles of temperature changes in the Earth Atmosphere (*Hansen et al., 1995; Santer et al., 1996*). An excellent perspective on the evolution in the state of the science of the stratospheric temperature trends is given by the WMO in the yearly ozone assessment report (WMO, 1992, 1995). Temperature changes have also been identified as affecting the microphysical –chemical process occurring in the stratosphere (WMO, 1999). The SPARC formed a Stratospheric Temperature Trends Assessment (STTA) group to focus on the temperature trend analysis. The SPARC stratospheric trend analysis (STTA) found that there is mean cooling trend estimates in the 100 - 50 hPa and 30 hPa region are ~ 0.30 – 0.75° K/ decade and 0.9° K/ decade, respectively (*Ramaswamy et al., 2002*). Ramaswamy *et al.* (2001) and WMO (1999) with regards to the 1979-1992 trends conducted that a cooling trend in the 100-50 hPa regions was confined only at the northern mid latitudes. But there is suggestion that a long period of evaluation yields the tendency for a statically significant cooling even at low latitudes.

Trends and variations in the upper troposphere and lower stratospheric temperatures are an integral part of the changes occurring in the Earth's climate system. The vertical profiles of the annual mean stratospheric temperature changes in the northern middle latitudes over the 1979-1994 period is robust among the different data sets, which is ~ 0.75° K/decade cooling in the ~ 20 to 35 km and increases cooling above ~ 2.5 ° K/decade at 50 km (*Ramaswamy et al., 2001*). In the stratosphere there is a general negative temperature trend on the order of -0.5 to -2° K/dec, which is in agreement with model predictions based on greenhouse gas increase mainly (CO_2) and decrease of solar heating due to ozone depletion (SPARC, 2002). There are number of factors that influences temperature trends in the stratosphere. All three volcanic eruptions aerosols injected into the stratosphere are responsible for the warming in the stratosphere (~15-20 km) centered in the tropics (~30° N-30° S), with a magnitude of 1-2° K (*Angell, 1993; Pollack et al., 1983; Labitzke et al., 1992*).

In this study we have computed the temperature trend over the upper troposphere and lower stratosphere over the Asian monsoon region for three decades namely 1969-1978, 1979-1988 and 1989-1999. We fit a straight line to the temperature data over the Asian monsoon region using the principles of least square method. First we computed the temperature trend at each grid points over the Asian monsoon region and then contoured the trend values for different UT/LS pressure levels for the above decades separately.

Figure 5.15 shows the temperature trend for the decade 1969-1978 over the Asian monsoon region for the UT/LS pressure levels 10-, 20-, 30-, 50-, 70-, 100-, 150-, and 200 hPa, respectively. During this decade there was a positive trend (warm condition) over the monsoon region with very small positive decadal trend with a value of $0.02°$ K/month over the Indian Ocean region. At 20 hPa level there is a cooling trend of the temperature indicating a stratospheric cooling over the Asian monsoon region during this decades. This period there was no complete cooling trend in temperature for all the stratospheric levels. But some regions show the warming trend in the stratosphere during this decade.

Figure 5.16 and 5.17 also represent the temperature trend for the decades 1979 to 1988 and 1989 to 1998. During 1979 to 1988 period at 10 hPa level there is a warming trend and other stratospheric levels shows a complete cooling trend over the monsoon region. For the period 1989 to 1998 shows a cooling trend even at 10-hPa level and cooling trend for all the stratospheric levels, which extends up to the upper tropospheric levels 150 hPa (figure 5.17). From this it is concluded that there is cooling trend in the stratosphere and warming trend in the upper troposphere. The warming trend is concentrated over the Indian Ocean region especially in the upper troposphere.

The cooling trend of temperature indicates the disturbance in the radiative balance of the stratosphere. The main reason for the cooling trend in the stratosphere and warming trend in the troposphere is mainly due to the ozone depletion, man made CFCs, increase in green house gases (eg CO_2, CH4, and
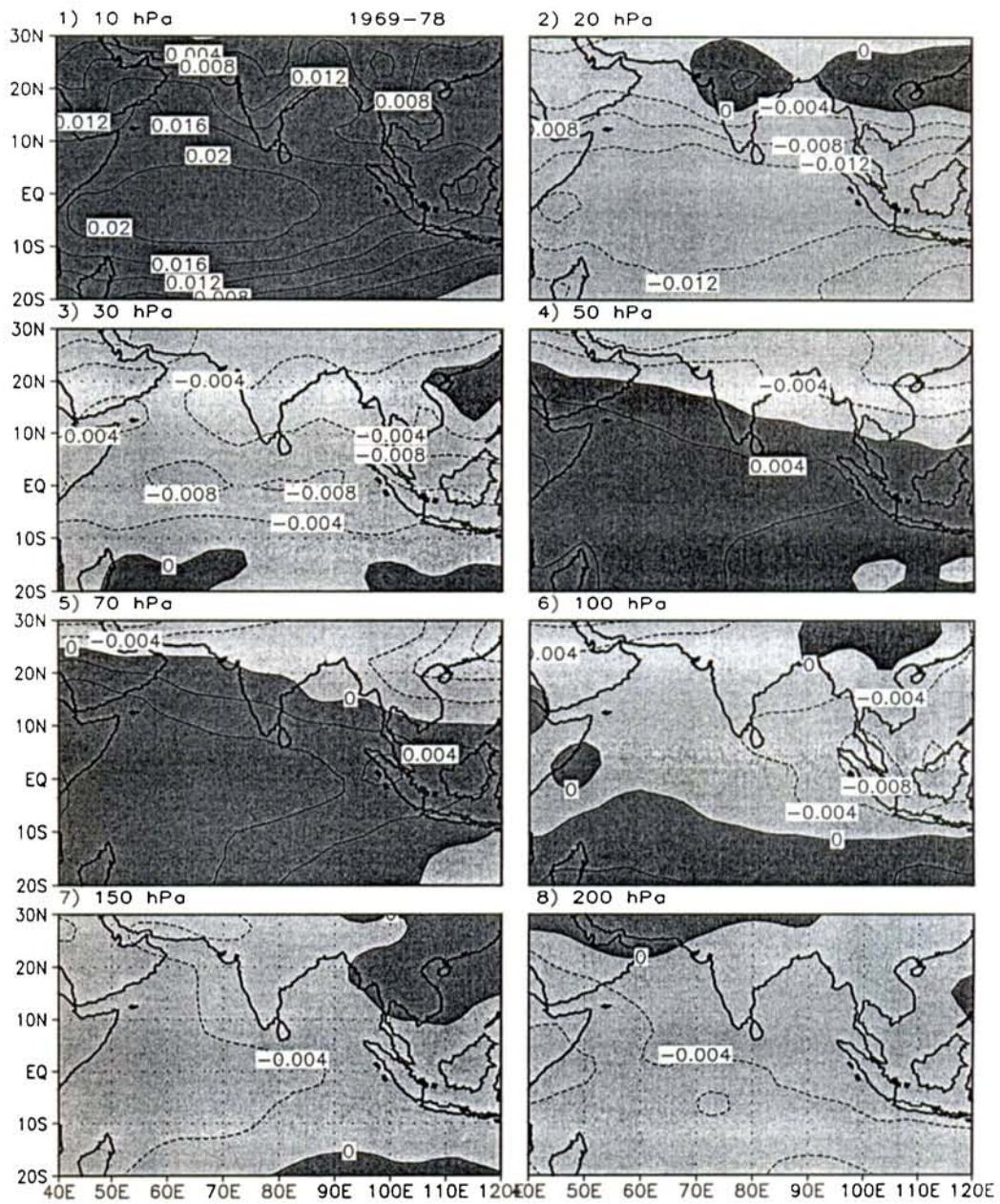
Figure 5.15: Temperature trend for the decade (1969-78). Contour
interval 0.004 ° K/ month.
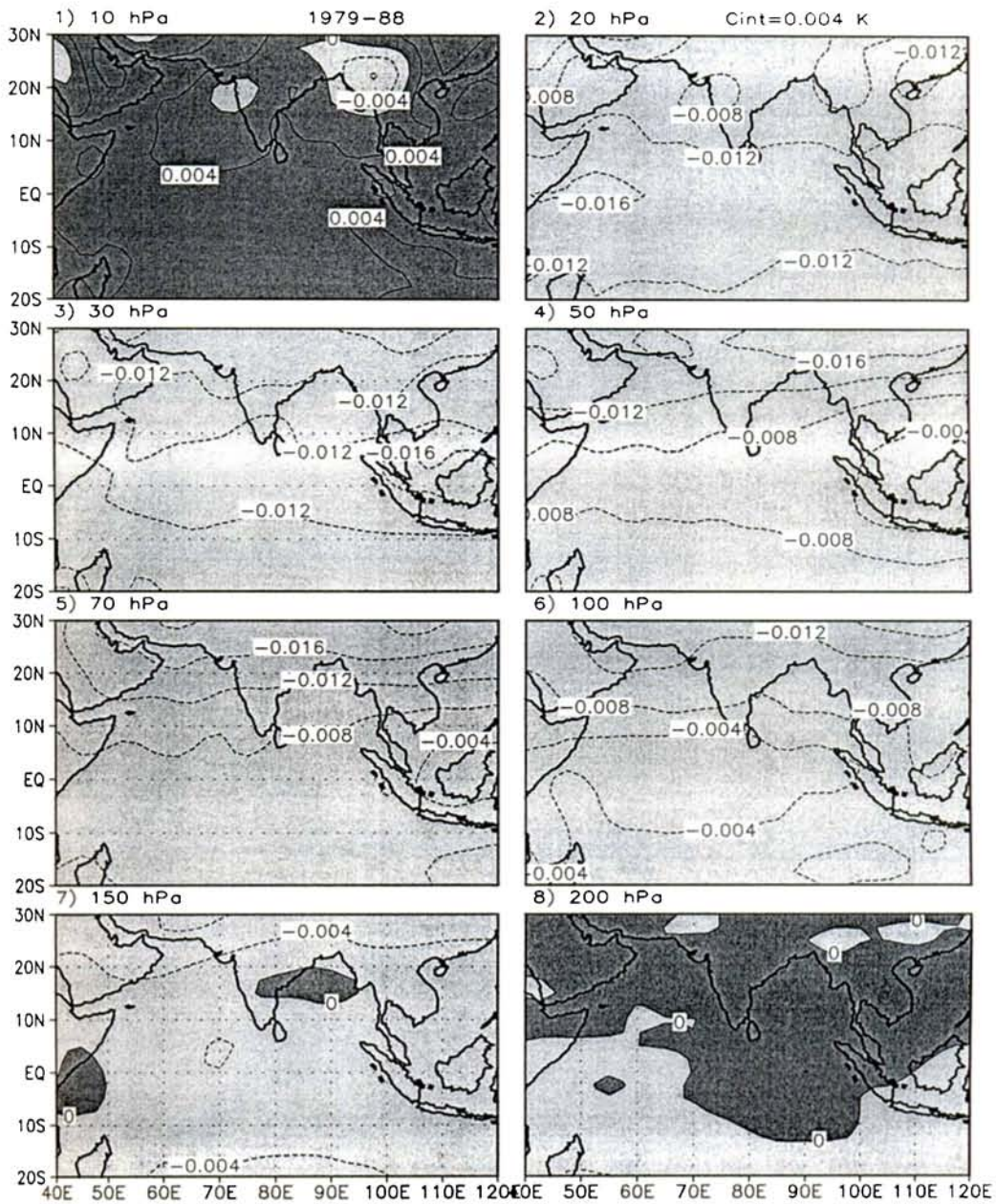
Figure 5.16: Temperature trend for the decade (1979-88). Contour interval 0.004 ° K/ month.
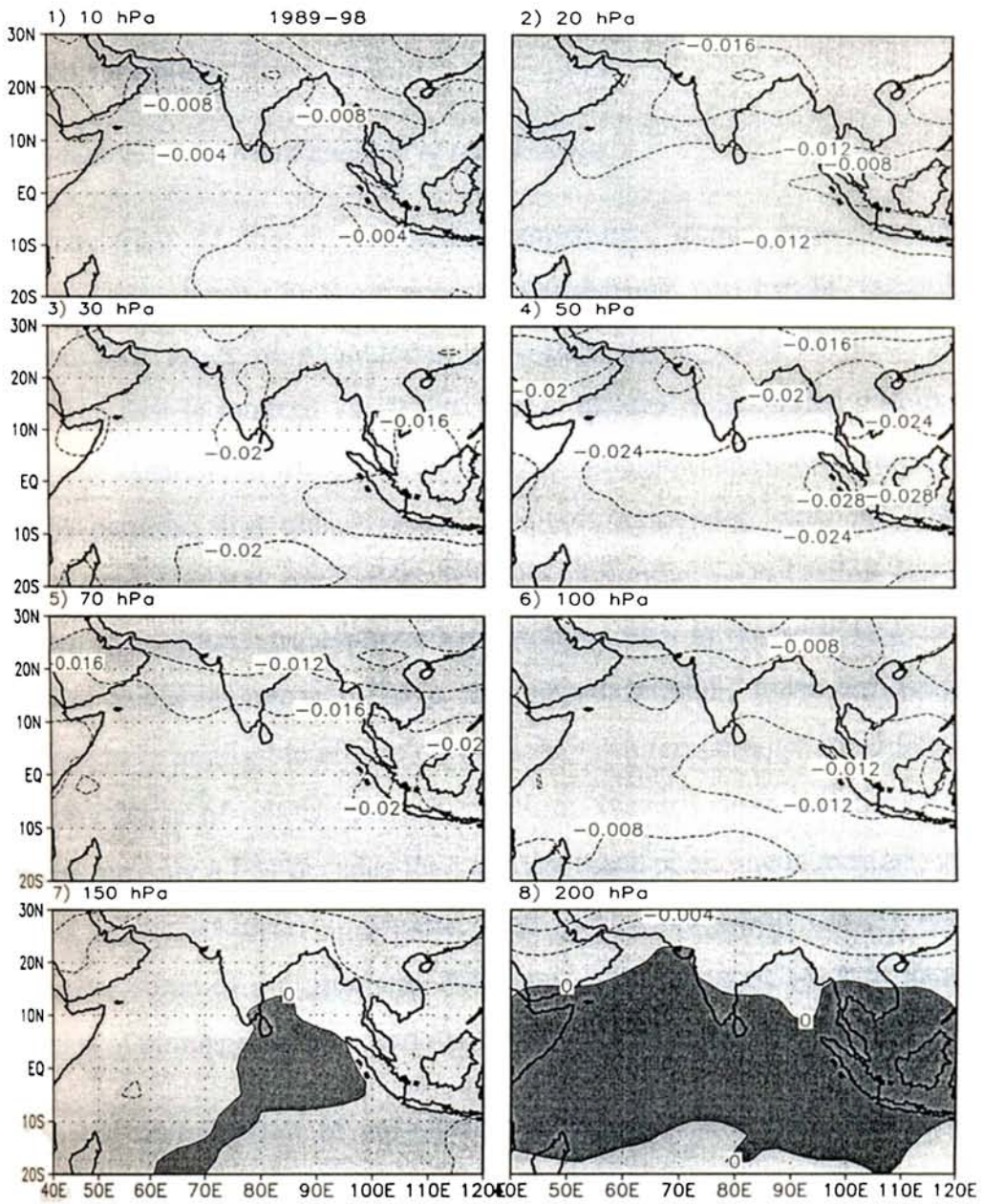
Figure 5.17: Temperature trend for the decade (1989-98). Contour interval 0.004 ° K/ month

H_2O) to the stratosphere and natural hazards such as volcanic eruptions affect the radiative balance between the upper troposphere and lower stratosphere. These changes in the thermal structure of the UT/LS region also certainly contribute to the monsoon variability.

5.3.6.1 Limitations in the trend analysis of temperature

Computation of the stratospheric temperature trends from long-term observation is complicated by the presence of additional, non-trendal variability in the data. Two types of phenomena contribute to the uncertainty in trend estimates. The first is random variability that is internally generated within the atmosphere and that is not trend like in nature. Major sources of such variability include the periodic and quasi- periodic signals associated with the annual cycles, the quasi-biennial oscillation, El Nino – Southern Oscillation and the solar cycles. In addition, stratospheric temperatures vary in response to episodic injections of volcanic aerosols. To a first approximation, these atmospheric phenomenon have negligible effects on the long term temperature trend because they are periodic or of relatively short duration. Nevertheless, because current data records are only a few decades long at most these phenomena may appear to enhance or reduce an underlying trend. Karl *et al.* (*1995*) and Christy *(1995)* have reviewed some of the problems associated with using rediosonde data for the detection of atmospheric temperature trends.

5. 3.7 Spatial distribution of correlation of temperature with solar fluxes and ISMR

The correlation between the sunspot cycle and the zonally averaged annual mean temperature are largest between the low-latitude tropopause and about 25 km, where most of the ozone column resides. This might partly be a direct effect in this layer, because of more absorbed (ozone) and more ultraviolet radiation from the sun. However, it is more likely to be mainly an indirect dynamical consequence of UV absorption by ozone in the middle and upper stratosphere (*van Loon et al.*, 1998). Also find a significant correlation between

the 30 hPa temperature and solar cycle using solar flux and explained that the largest correlation move with the sun from one summer hemisphere to the other (Labitzke, 1994; van Loon et al., 1999).

Figure 5.18 shows the spatial distribution of correlation between temperature and solar flux for the monsoon periods (June to September) at the UT/LS region, specifically over the Indian monsoon region (65° E - 90° E & 0°-25° N) from 1961 to 1990. The temperature shows a positive correlation with solar flux for the stratospheric levels except at 50 hPa where negative correlation values are also seen below 15° N. In the upper stratosphere at 10 hPa shows a high positive correlation and concentrated near the peninsular Indian region and the east and west coast of the Indian region. Other stratospheric levels show a lower less value of correlation with solar flux indicates that the influence of the solar activity has no direct effect in the lower stratospheric temperature. But in the upper tropospheric levels such as 150 hpa and 200 hPa shows a high positive correlative value indicate that the solar flux has got direct influence in the temperature variation in the upper troposphere of the Indian summer monsoon region. The tropopause temperature at 100 hPa shows a high positive correlation with solar flux with a value of 0.54 concentrated in the west coast of the Indian monsoon region. Therefore, the variation of tropopause temperature with solar flux need further study to understand the role of tropopause in controlling the radiative balance between upper troposphere and lower stratosphere in accordance with solar activity.

The spatial distribution of correlation between Indian summer monsoon rainfall and temperature averaged for the period June to September at different pressure levels of the upper troposphere and lower stratosphere are represented in figure 5.19. Indian summer monsoon rainfall (ISMR) is negatively correlated with temperature over the monsoon region at 10 hPa level. Some region of the southwest monsoon shows positive and negative correlations between temperature and the rainfall. In the upper tropospheric levels (150 hPa and 200 hPa) high positive correlation is seen over the Indian monsoon region and higher
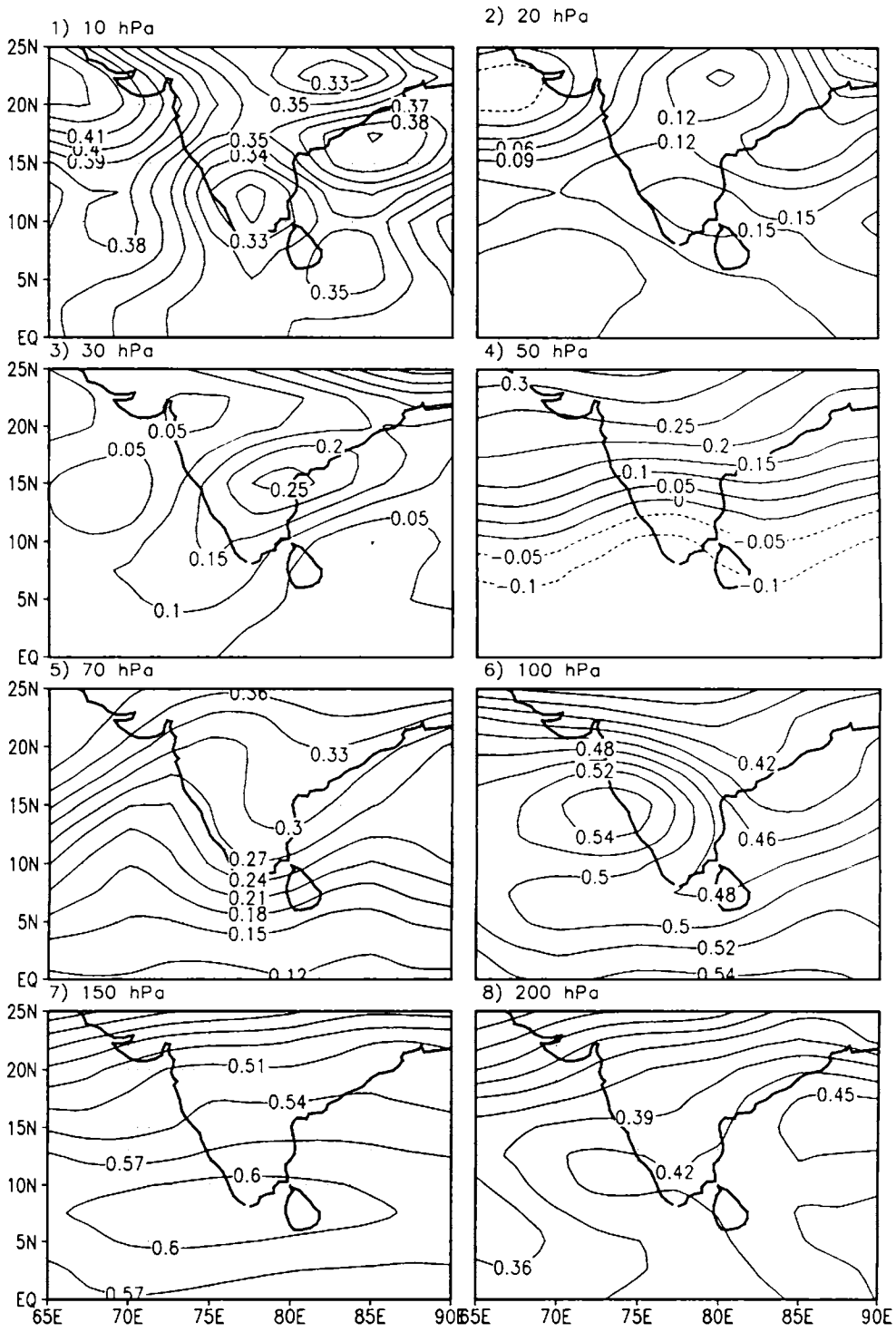
Figure 5.18: Spatial correlation of temperature and 10.7 cm solar flux for June to September (1961 to 1990) for the UT/LS pressure levels.
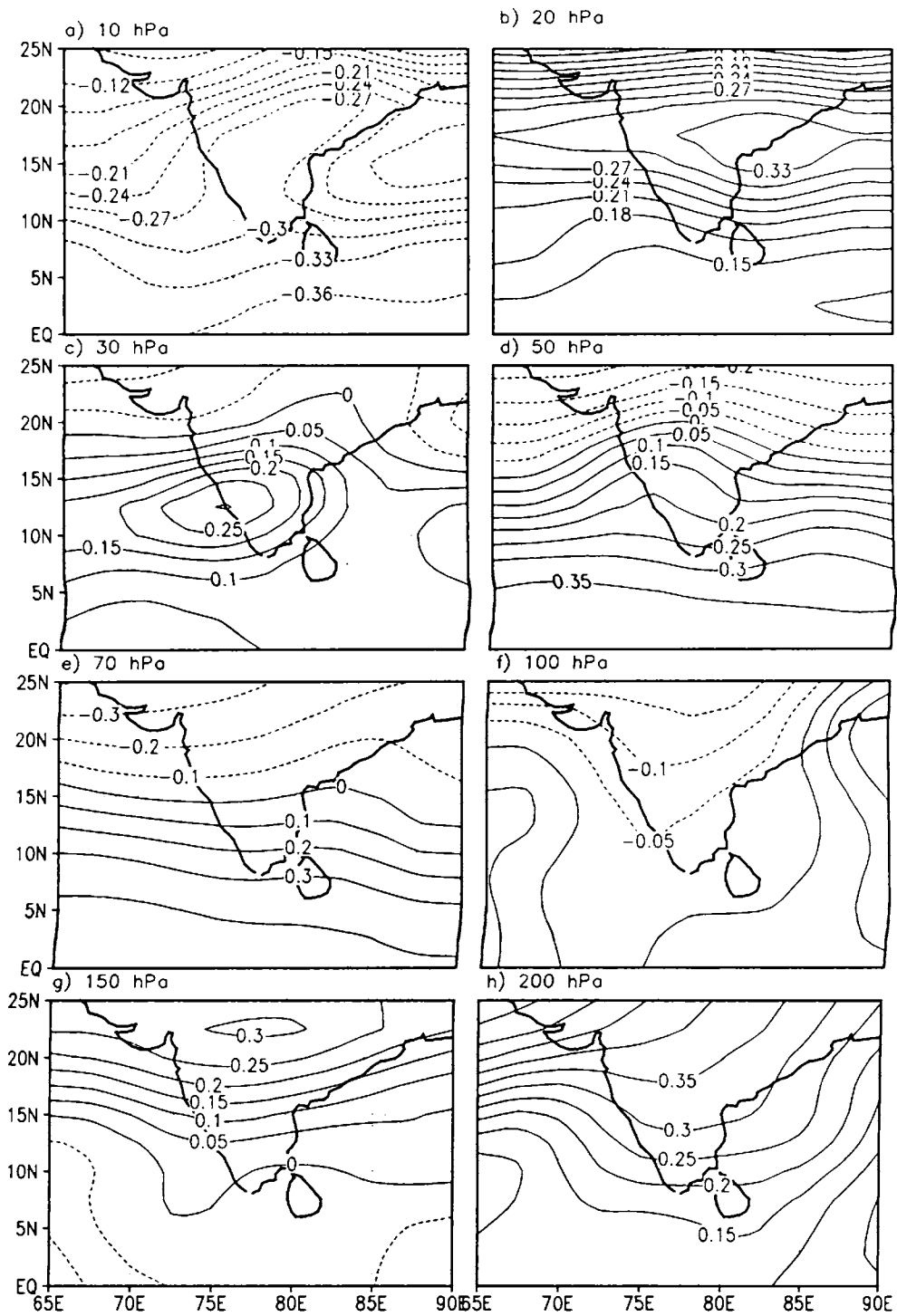
Figure 5.19: Spatial correlation of temperature and Indian summer monsoon rainfall (ISMR) for June to September from 1961 to 1990.

alues are concentrated over the central part of the Indian region. But the temperature in the tropopause level (100 hPa) does not show any significant correlation with ISMR value.
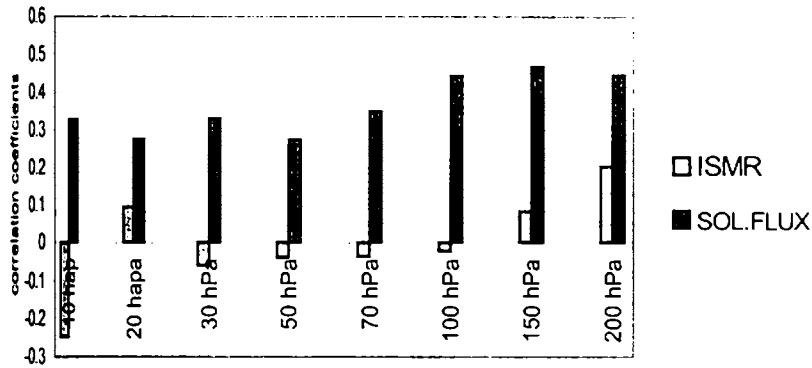
Figure 5.20: Correlation of temperature with 10.7 cm solar radio flux and temperature with ISMR over the region (65° E-95° E & 5° N -25° N) for the period 1960-1998. Solar flux shows a +ve correlation with temperature in the UT/LS

Figure 5. 20 represent correlation of temperature with solar flux and ISMR for the UT/LS levels (10 hPa , 20 hPa 30 hPa, 50 hPa , 70 hPa, 100 hPa , 150 hPa and 200 hPa) averaged over the Indian region (65° E - 95° E & 0° -25° N) during the monsoon period (June to September) from 1960 to 1998. It is noted from the figure that the temperature is positively correlated with solar flux in the UT/LS of Indian summer monsoon region. But the correlation between ISMR and temperature at the stratospheric levels and the upper troposphere temperatures are positive over the monsoon region. We have used the Student's t test to find out the percentage of levels at which the correlations are significant. In stratospheric levels, the correlation with ISMR is not significant. But in tropospheric levels it is significant above 90% level of confidence. The correlation with temperature with solar flux for the UT/LS levels shows a positive correlation over the Indian region and it is significant at 99.5% confidence level in tropospheric levels. The correlations in the stratosphere are significant at 97.5 % confidence level except at 20 hPa and 50 hPa level (95 % significant).

5.4 Summary

Temperature characteristics and its interannual variability in the upper troposphere and lower stratosphere in relation to solar cycle and Asian summer monsoon were studied in this chapter. The advanced statistical tools such as wavelet transform and empirical orthogonal functions were used to explore the interannual variability (both spatial and temporal) in temperature over the UT/LS of Asian summer monsoon region. Computed the temperature trend in the UT/LS pressure levels using the method of principle of least square fit. The spatial correlation of temperature with solar flux and Indian summer monsoon rainfall were also carried out. Some of the results obtained from the above studies are given below.

Two major interannul variability in temperature are the QBO cycle and solar cycle with a periodicity ranging from 26 to 32 and 132 to 136 months respectively over the UT/LS of Asian summer monsoon region. Abrupt variations in the temperature were also noted after and before 1977 in the stratospheric level (10 hPa) and tropospheric levels 150 hPa and 200 hPa during the period 1960 to 2002. This change in temperature may be due to the decadal variability in temperature and other climatic fluctuations. The negative anomaly in temperature during the period 1994 to 1998 at 20 hPa and 30 hPa may be due to effect of El- Nino (1997-98) and the increasing trend of ozone depletion in the stratospheric levels.

In the upper troposphere at 200 hPa level there is a biennial periodicity in the temperature anomaly (TBO) and this will be a separate phenomenon (shows similarity only in the biennial periodicity). The temperature in the UT/LS is modulated by the solar cycle and keeps an in-phase relation with the 10.7 cm solar flux (figure 5.10). We did the EOF analysis of the temperature for the UT/LS pressure levels and found that the major percentage of variability in temperatures is due to QBO mode in the stratosphere and 11- year solar cycle contribute in the upper troposphere.

94

It is noted that there is a cooling trend in the stratosphere and it extends up to the tropopause level during the decade 1989-98, compared to other periods (1969-78 and 1979-88). This may possibly due to the ozone depletion in the stratospheric levels and the increase of CFCs and other green house gases in the atmosphere.

Chapter 6

Variability of Total Ozone over the Indian Subcontinent in Relations to Asian Summer Monsoon

6.1 Introduction

Ozone plays an important role in the global weather and climate even though the total atmospheric composition is less compared to other trace gases. Ozone maintains the thermal structure of the stratosphere, troposphere and the surface. Transport of stratospheric air into the troposphere by the large-scale Brewer–Dobson circulation was once thought to be the primary source of tropospheric ozone (*Junge, 1962*). Presently it is well known that the photochemical ozone formation is a much more important source for tropospheric ozone (*Crutzen, 1974*). Zachariasse *et al.* (2000) made a study of influence of stratosphere-troposphere exchange on tropospheric ozone over the tropical Indian Ocean during the winter monsoon. Stratosphere- Troposphere Exchange by smaller scale processes is believed to play a minor role (*Holton et al., 1995*). Exposure to ozone creates many health problems in human beings such as skin cancer, coughing and breathing difficulties etc. Hence understanding the interannual and seasonal variation, production, depletion and forecasting of ozone is very relevant in the present scenario.

A large component of climate variability in the stratosphere concerns ozone and temperature in the midlatitudes and polar regions. Understanding this variability and its possible link with the troposphere is crucial for delineating anthropogenic ozone loss and climate change. Changes in ozone in the lower stratosphere have a large impact on the surface UV flux. In addition, because of the radiative properties and temperature structure of the atmosphere, changes in ozone have a significant impact on climate when they occur in the Upper Troposphere/Lower Stratosphere (UT/LS) region. Kerr *et al.* (1993) showed that decreased ozone levels have caused increase of ultraviolet radiation at the surface. Stratospheric ozone plays a critical role in the energy budget because it absorbs both solar UV and the terrestrial Infra Red (IR) radiation. Moreover ozone in the tropopause acts as a strong greenhouse gas and increasing ozone trends at these altitudes contribute to climate change.

The destruction of ozone and other trace gases are governed by the complex interaction of dynamical, chemical and radiative process, so it is clear that UT/LS ozone research will require an interdisciplinary approach to tackle outstanding scientific issues. The UT/LS region is very important region of the atmosphere and need to be studied thoroughly in order to understand the climate variability.

The ozone trends, in the UT/LS region will be major topics in the next decades because of the emission of tropospheric ozone precursor are expected to increase largely due to the growth of the population and industrial development. Decreased ozone will allow the harmful UV-B and UV-C radiation which can affect the health of human, animal and plants (*Van der Leun et al., 1995*). The concentration of ozone is greatly influenced by the processes, which take place in the tropics such as photochemistry, rapid convective mixing and widespread biomass burning and growing industrial emission. The photochemical production of ozone is greatest in the tropical lower stratosphere, but this will be transported in to the polar night region by wind motion.

6.1.1 Literature review

Many researchers (*Angell, 1993; Stolarski et al., 1991*) have studied a possible connection between the QBO and interannual variation of ozone. They have showed that an average at the easterly phase of QBO the ozone concentration in the polar latitudes is higher than at the westerly phase and the modeled result of total ozone show the agreement with the observations (*Hess et al., 1995*). According to them the QBO influences the total ozone variations by 1-2%. Interannual to decadal variability of ozone is related to dynamical behavior of the atmosphere. Equatorial total ozone change is normally linked with the phases of QBO winds in the lower stratosphere. This cyclic change in wind direction accounts for approximately 3% of the natural variation in ozone concentration.

The ozone variations in the tropics are manly controlled by QBO in lower stratospheric wind and solar cycle. Analysis of long term records of global satellite data from TOMS have clearly documented characteristics of the global QBO in column ozone (*Bowman, 1989; Lait et al., 1989*). Recently Yang and Tung (1994, 1995) established that the QBO signal in column ozone is strong and statistically significant in the extratropics. Several studies revealed that natural oscillation of the tropical atmosphere also influences ozone in mid-latitudes (*Zerefos et al., 1992; Bowman, 1989; Shiotani, 1992*) and leads to a differing quantity of transport of stratospheric ozone from the tropical source region to mid-latitudes. Bojkov (1987) reported that there exists El-Nino-Southern Oscillation (ENSO) influence in total ozone. There is still some debate whether there is sufficient case to separate the QBO effects from any supposed ENSO effect.

In addition to dynamically induced variations in total ozone, there are sources of ozone variability like 11-year solar cycle. The changes in solar ultraviolet spectral irradiance directly modify the production of ozone in the upper stratosphere (*Brasseur, 1998*) and hence it is reasonable to expect a solar cycle variations in ozone amounts. Analysis of ground based records extending over three to six decades indicate the existence of decadal time scale variations of total ozone that is approximately in phase with the solar cycle (*Angel, 1989; Zerefos et al., 1997*). The global satellite ozone records since 1979 show evidence for decadal oscillations of total ozone with maximum amplitude (~2 %) at low latitudes (*Hood et al., 1992; Hood, 1997*). Solar constant shows a small variation (0.1 %), which is more significant in the ultraviolet spectrum than in the visible. Since ozone is created and destroyed by solar UV radiation, there is some correlation of ozone concentration with 11- year sunspot cycles.

A study by Jadin (1998) established that the interannual and intra-decadal variation of stratospheric angular momentum are closely associated with total ozone anomalies including the development of the ozone hole in the Antarctica. Many have studied the seasonal cycles (*Martin et al., 2000*), trends (*Thomson et*

al., 2000) and inter-annual variability (Ziemke et al., 1999) in tropical ozone. A three-layer neural network model is used for the prediction of daily surface ozone one-hour advance in a tropical station Pune, India (Guhathakurta, 1999). Jain et al. (1998) made a surface study over the metropolitan city Delhi using the Differential absorption LIDAR (DIAL) techniques. A very few studies are available on long-term variations of total ozone over Indian stations (Mani et al., 1973; Tiwari, 1992; Kundu et al., 1993). Chakrabarty et al., (1998) used the ozone data for the period 1957 to 1994 for trend analysis of total column ozone over Indian stations. Detailed analysis of about 30 years total ozone data and associated meteorological process have been carried out in the region where global maps of total ozone shows a minimum value during the northern summer. They concluded that the reason for ozone minima in total ozone over the subtropical belt of the Indian subcontinent might be the result of some unique features of thermal and dynamical process appearing in that region (Hingane, 1990).

6.1.2 Modeling studies of ozone

Over the past two decades, the increasing recognition of the relative impacts of ozone has motivated the development of General Circulation Models (GCM) which extends up to the stratopause and beyond. This allows the investigation of the climate impacts of ozone change, first studied in the GCM context by Fels et al. (1980) as well as interactions between stratospheric cooling caused by CO_2 increases and the ozone problems (Shindell et al., 1998). For the middle atmosphere the main objectives are to produce accurate simulations of the ozone distribution since this is a radioactive gas with important climate consequences. There are several model studies on the trends of ozone in the UT/LS region. Ina et al. (2001) simulated the trend of total ozone on the troposphere and stratosphere using the Action de Recherche Petite Echelle Grande Echelle (ARPEGE) General Circulation Model (GCM). They found that in both hemispheres the lower stratosphere cooled and the polar vortex strengthened significantly during spring/early summer. Some model
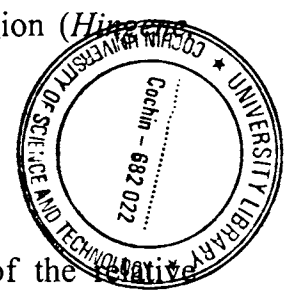
studies revealed that stratospheric ozone is decreasing (*Langematz, 2000; Rosier and Shine, 2000*). The lower stratospheric ozone changes results in over all cooling of the troposphere (*Christiansen, 1999*).

From the above discussion, it is clear that the impact of ozone that plays in the climate change and how it affects the earth atmospheric radiative balance and the circulation in the upper troposphere and lower stratosphere. So in this context the present study of ozone over the Indian stations are quite relevant and it needs further study with more time period data. Here we have studied the interannual variability of ozone over the 12 Indian stations and total ozone variation during the WET and DRY years of Indian summer monsoon.

6.2 Data and methodology

Global ozone monitoring is based on a data quality controlled net work of ground based measurements and controlled observations in order to make best use of the complementary strengths of measurement from ground and space (*Harris et al., 1998*). Ozone absorbs through the entire spectrum, with large absorption in the UV wavelength region (extending from 220 to 240 nm, maximum at 260 nm), a further absorption in the visible from 480 to 800 nm, maximum at 600 nm), and several bands in the Infrared (IR) region. There are two methods of total ozone measurement. One method is from the ground and other method is from the space. In this, we limited our discussion of ozone measurement with satellite from the space. The importance of satellite observation is global coverage, and continuous monitoring on time scales from days to years. Also help us to study the data sparse region of the tropics. Using the TOMS Nimbus 7 version data so many studies of total ozone made by scientist worldwide.

6.2.1 Total ozone mapping spectrometer (TOMS)

TOMS instrument on satellite with sun-synchronous orbit can provide daily maps of total ozone except where the Earth's atmosphere is shaded by

polar night. Total ozone is derived from the differential absorption of scattered sunlight in the ultraviolet region. Ozone is calculated by taking the ratios of two wavelengths (312 nm and 331 nm) where one wavelength is strongly absorbed by ozone while the other is absorbed weakly. TOMS make 35 measurements every 8 seconds, each covering 50-200 km wide on the ground except areas near the poles. These individual measurement vary typically between 100 and 650 Dobson units (DU) and average about 300 DU.

The TOMS data version 7 (Mc Peters *et al.,* 1996) are available as (a) gridded daily, (b) gridded monthly average, (c) GIF images, (d) overpass data and (e) zonal means. We have used the overpass daily ozone data for the 12 Indian stations for the present study. These data are available in the form of CD-ROMS. Also TOMS data is available in Goddard Space Flight Center, (USA) website *(http://toms.gsfc.nasa.gov).* TOMS Nimbus 7 data are available for the period 31 October 1978- 6 May 1993 (~14.5 years).

6.2.2 Validation approach of total ozone

The validation approach of total ozone measured using the TOMS is compared with the total ozone measurement at the ground stations (from Brewer spectrometer). Only stations had homogeneous data coverage for the entire 14.5 years lifetime of TOMS instrument were included for comparison study. A weekly mean was computed from the daily TOMS ground difference at each station. In figure 6.1 the percentage of differences between TOMS and ground based ozone measurements as a function of time is presented (McPeters *et al.,* 1996).

6.2.3 Satellite series that carried the TOMS instruments

6.2.3.1 Nimbus 7 satellite

Provided data for 14.5 years and this instrument had a long lifetime (October 1978 to May 1993), so this time series of total ozone data can be used for the seasonal and of interannual variability study of ozone. Average
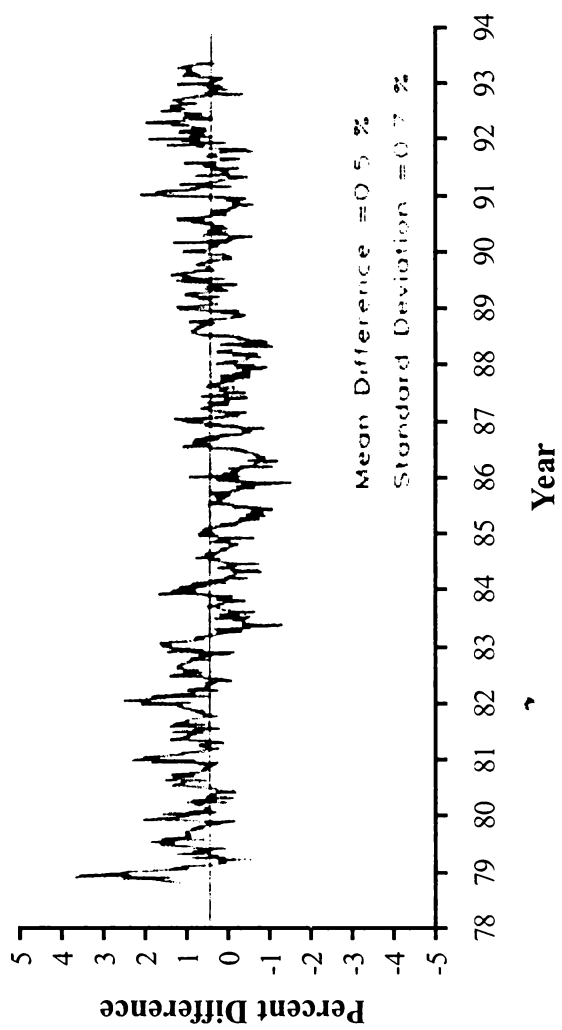
Fig. 6.1 Percent Difference between TOMS and Ground ozone.
Solid line is linear fit trend (After McPeters et al, 1996)

instrumental calibration of long term drift of TOMS Nimbus 7 data is believed to be less than 1% per decade. TOMS data are rather insensitive to changes in tropospheric ozone the orbit was near polar and sun synchronous. Nimbus 7/TOMS measured the amount of backscattered UV radiance in six nanometer wavelength bands (313, 318, 331, 340, 360 and 380 nm).

6.2.3.2 Meteor –3

This satellite was in operation from August 1991 to December 1994. It was not sun-synchronous, its orbit processed from the sunrise terminator to sun set terminator over 106 days, The data from this TOMS is only the orbit of Meteor 3 is close to the near-noon orbit (near–noon equator crossing time).

6.2.3.3 ADEOS (Japanese Satellite)

ADEOS TOMS was launched on August 17, 1996 and provided data until June 29, 1997. Its orbit is higher than EP TOMS, with a spatial resolution similar to Nimbus 7/ TOMS.

6.2.3.4 Earth Probe (EP) TOMS

NASA's Earth Probe satellite was launched on July 2, 1996 to provide supplemented measurements, but was boosted to a higher orbit to replace the failed ADEOS. Earth probe continues to provide near real time data. Its orbit is suns synchronous and lower altitude than the previous TOMS platforms.

6.2.4 Limitations of TOMS version 7 data

Volcanic eruptions, polar stratospheric clouds (PSC), solar eclipse and terrain, etc effect the total ozone measured by TOMS instrument. Problems were noticed after the eruptions of El Chichon in April 1992 and Mt. Pinatubo on June 15, 1991. Gaseous SO_2 emitted from these major eruptions absorbed the bands in 290 nm to 320 nm ranges. Some bands at longer wavelengths coincide with wavelengths used by TOMS to measure total ozone. This produces a false estimation of total ozone measurement by TOMS. This problem is short lived

because the SO_2 is converted rapidly to sulfuric acid aerosols. The contaminated data points were marked with a flags for identification. TOMS measure back-scattered sunlight for total ozone estimation and is not possible when there is no sun. Because of this reason, total ozone data are missing for polar winter season. Another problem is with decrease in incoming solar radiation, which result in decrease in backscattered radiance thereby it affect the ozone measurement.

6.2.5 Stations selected for the study

In this study daily ozone data from the NIMBUS 7 TOMS satellite were used. The period of study is from 1979-1992 and used the overpass daily ozone data for the 12 Indian stations selected as per the availability of data. Figure 6.2 shows the Indian stations selected for the total ozone study on the basis of availability of data. The stations are arranged from low latitudes to high latitude in the figure.

6.2.6 Method of analysis

We have used the monsoon rainfall (June -September) data of 7 stations (Chennai, Hyderabad, Pune, Nagapur, Dum-Dum-Culcutta, Ahemadabad, Delhi) as per the availability of data for the correlative study between total ozone in DRY and WET year Indian summer monsoon conditions. To study the latitudinal variation of total ozone anomaly, we used the daily ozone data from $12.5° S$ to $12.5° N$ with grid intervals $5°$ for the period 1979 to 1992, averaged to monthly in order to study the interannual oscillation (QBO in ozone). We have taken the daily total ozone for 12 different Indian stations (with latitudes varying from low to high) averaged on monthly basis in order to study the characteristic of total ozone variability for the period1979-1992.

6.2.6.1 Morlet wavelet analysis

Morlet wavelet is used in order to understand the interannual variability of the ozone for the 12 stations. We have used the monthly values of total ozone for study and the significance of the oscillation are tested by power spectrum.

103

STATIONS SELECTED

1) Bangalore (12.98N,77.58E)
2) Chennai (13.08N,80.17E)
3) Hyderabad (17.38N,78.47E)
4) Pune (18.53N,73.85E)
5) Bombay (19.12N,72.85E)
6) Nagapur (21.10N,79.05E)
7) Dum dum (22.65N,88.45E)
8) Ahmedabad (23.02N,72.65E)
9) Mount Abu (24.65N,72.70E)
10) Banaras (25.00N,83.00E)
11) Delhi (28.67N,72.22E)
12) Srinagar (34.08N,74.84E)
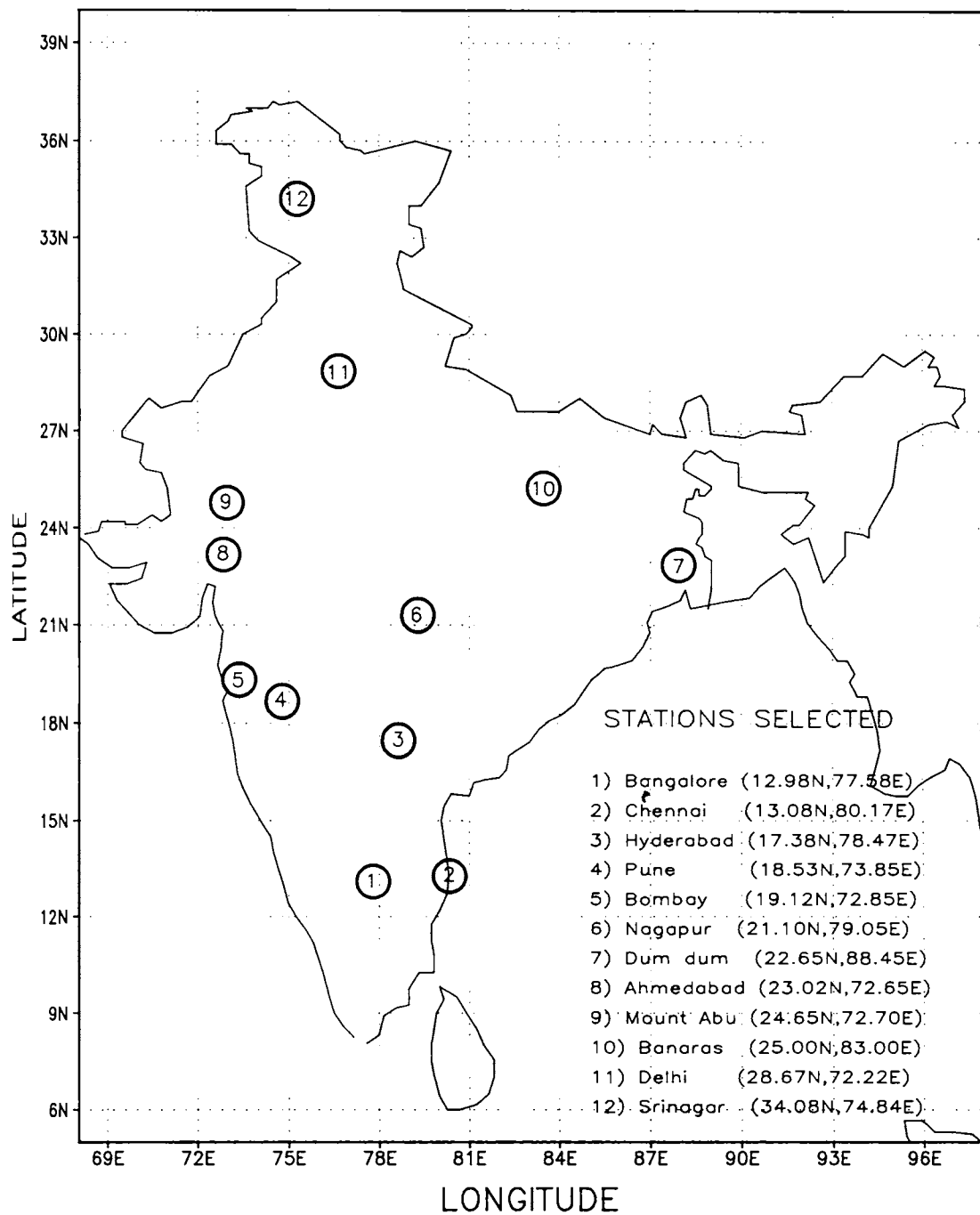
Figure 6.2: Stations selected for the total ozone study

The method of analysis and principle behind the wavelet transforms are discussed in appendix I.

6.2.6.2 Factor analysis

Using the factor analysis we have found the spatial correlation of total ozone between stations selected for the study. Factor analysis is a statistical technique concerned with the reduction of a set of observable variable in terms of a small number of latent factors. The underlying assumptions of a factor analysis is that there exit a number of unobserved latent variable (or factor) that account for the correlation among observed variable, such that if the latent variable are held constant, the partial correlations among observed variables, all become zero.

Factor analysis starts with assumption of an underlying basic model for the data given as

$$\Sigma = \Lambda\Lambda^T + \psi \qquad \qquad ...(6.1)$$

Where Σ is the P x P population correlation matrix, Λ is the P x M matrix of a factor loading relating the common factor f_i to be observed variables X_i (T is the transpose), and ψ is the P x P matrix co-variance of the specific factors Σ_i. The relationship between the common factors, the specific factor and the observations is given by

$$X - \mu = \Lambda F + \Sigma \qquad \qquad ...(6.2)$$

Where the expected value of Σ, F and $X - \mu$ are zero. Each common factor has unit variance and is independent of each other and the common factor and specific factor are mutually independent of each other and the common factor and specific factor are mutually independent. The factor loading are computed from the equation

$$\Lambda = \Gamma\Delta^{-1/2} \qquad \qquad ...(6.3)$$

Where Γ and Δ are the eigenvectors and eigenvalues of the matrix $(R - \psi)$. The element of R is given by

$$r_{ik} = \delta_{ik} \qquad \qquad ...(6.4)$$

Where δ_{ik} is the sample covariance between stations i and k given by

$$\delta_{ik} = \Sigma(X_{ij} - X_i)(X_{kj} - X_k) \qquad \qquad ...(6.5)$$

The 'eigenvalues greater than one' rule has been used to select the number of significant factors (Kaiser-Guttman rule). It sates that the number of factors to be extracted should be equal to the number of factors having an eigen value (variance) greater than 1.0. The rationale for choosing this particular value is that a factor must have variance at least as large as that of a single standardized original variable. The details of the analyzing techniques are taken from Carter and Elsner (1996).

6.3 Results and discussion

6.3.1 Interannual variability of total ozone

The interannual variability in total ozone for the 12 Indian stations has been studied. We have used the monthly total ozone anomaly computed from the daily ozone data for the period January 1979 - December 1992 from the TOMS instrument. Latitudinal variations of total ozone with easterly (minimum ozone anomaly) and westerly (maximum ozone anomaly) phases of QBO for the period January 1979- December 1992 is shown in the figure 6.3. We have taken the latitudinal region from 12.5° S to 12.5° N and the contour interval is 3 DU for the period of study. The variability in the total ozone shows a periodicity ranging 26 to 32 months in the equatorial region. This represents the latitudinal structure of the QBO in total ozone and the change over from maximum to minimum takes places in the equatorial region. Also noted that the easterly phases of ozone QBO is stronger during 1984, 1987, and 1991 and the westerly phases stronger in 1980, 1985 and 1990. Ozone anomaly usually seen maximum during June and
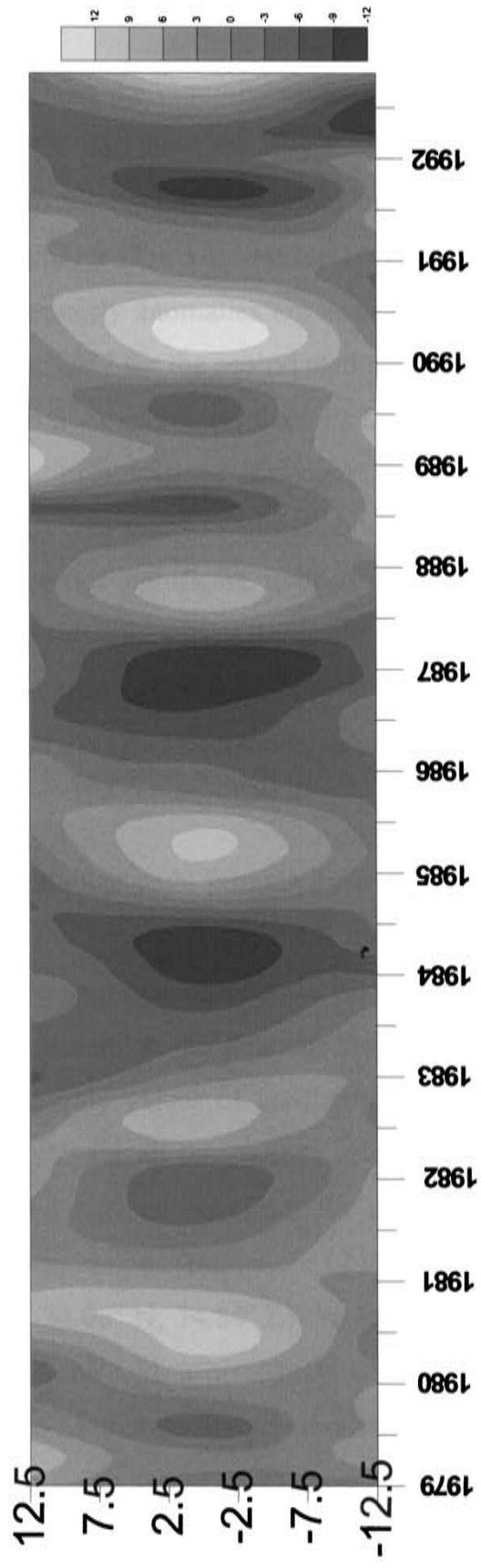
Figure 6.3: Quasi-biennial Oscillation in total ozone over the equatorial region. The contour interval is 3DU

July months and there are variations in the low and high phases of ozone QBO during the period of study 1979-1992.

Figure 6.4 and 6.5 show the monthly variations of total ozone anomaly for the period 1979 to 1992 for the 12 stations selected for the study. The latitudinal influence in the total ozone variation can be seen from the low latitude stations to high latitudes with a low value 15 DU to a high value of 40 DU. Maximum values of easterly anomalies are seen in the total ozone during March 1985, and November 1987 for the central stations. During 1985 and 1986 total ozone anomaly shows a value greater than 40 DU indicate that the ozone variations at the higher latitude stations (Srinagar) do not depends only on latitudinal effect (figure 6.5). The interannual variability in total ozone (QBO) at Bangalore and Srinagar are not significant indicate that there might be some other factor contributing to the total variability in the ozone over these stations. Annual oscillations are also present in the total ozone variation at all the stations (figure is not presented) and the QBO oscillation in total ozone is significant for the central Indian stations.

To understand the smaller scale periodicity in the total ozone for these stations we have adopted the advanced statistical tool such as Morlet wavelet analysis. In this method the data decomposes for all the periodicities including smaller to higher periods present in the data. In the present study we did the wavelet analysis of the monthly values of total ozone anomaly for the period January 1979 to August 1989 for all the stations selected for the study. Figure 6.6 (1 to 12) represent the wavelet spectrum for the twelve Indian stations starting from the low latitude stations (Bangalore 12.98° N, 77.58° E) to the high latitude stations (Srinagar, 34.08° N, 74.84° E). From the wavelet spectrum we got two major oscillations, one with a periodicity of 16 to 18 months and the other is varying from 26 to 28 months (approximately the periodicity of quasi-biennial oscillation). And it is found that over the central Indian stations 16 to 18 months oscillations in the total ozone alternate its periodicity during 1979 to 1992. There is also a well-marked QBO periodicities in the total ozone variation
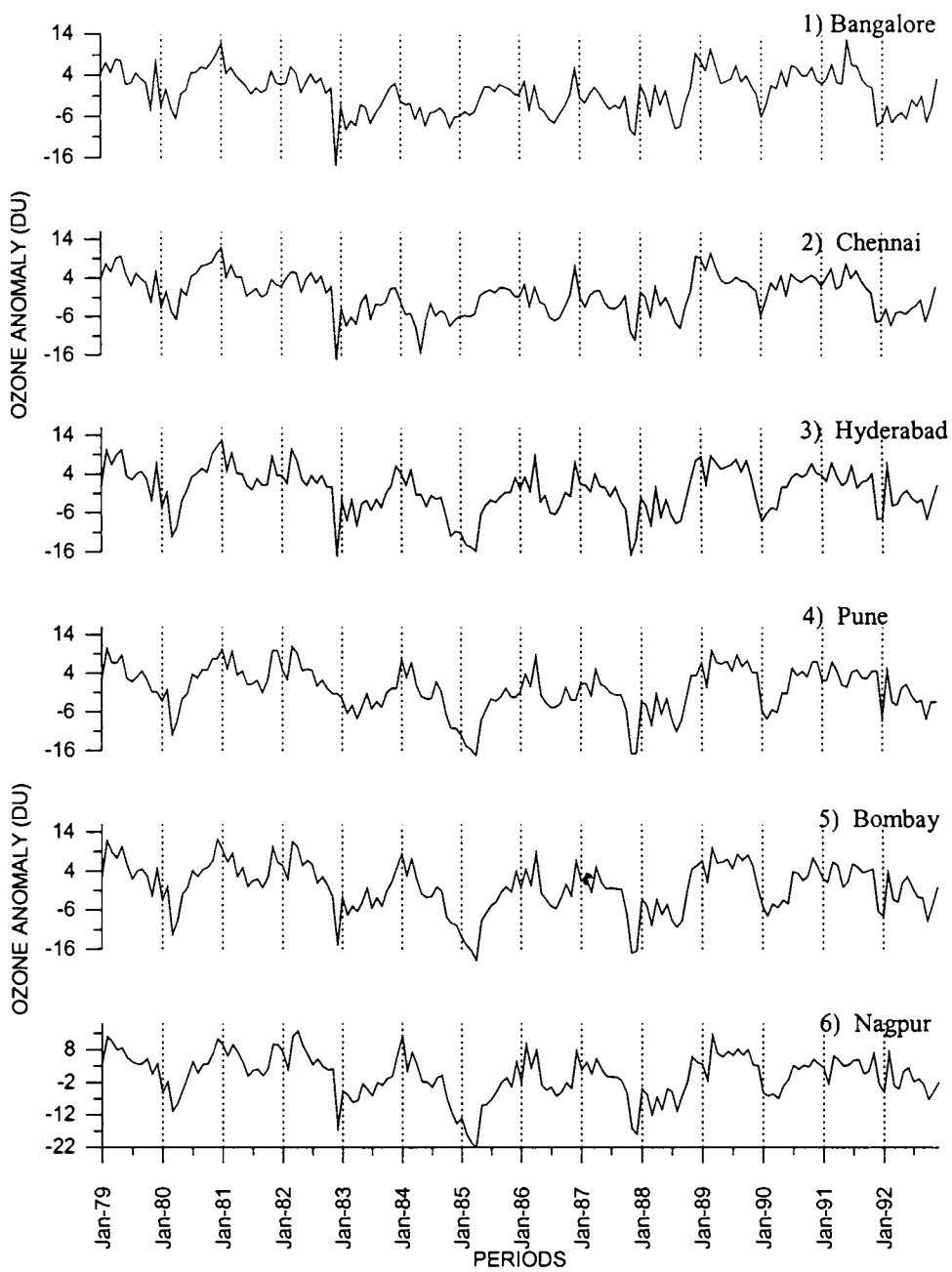
Figure 6.4 : Total ozone (anomaly) variation in Dobson Units over the stations during the period January 1979 to December 1992.
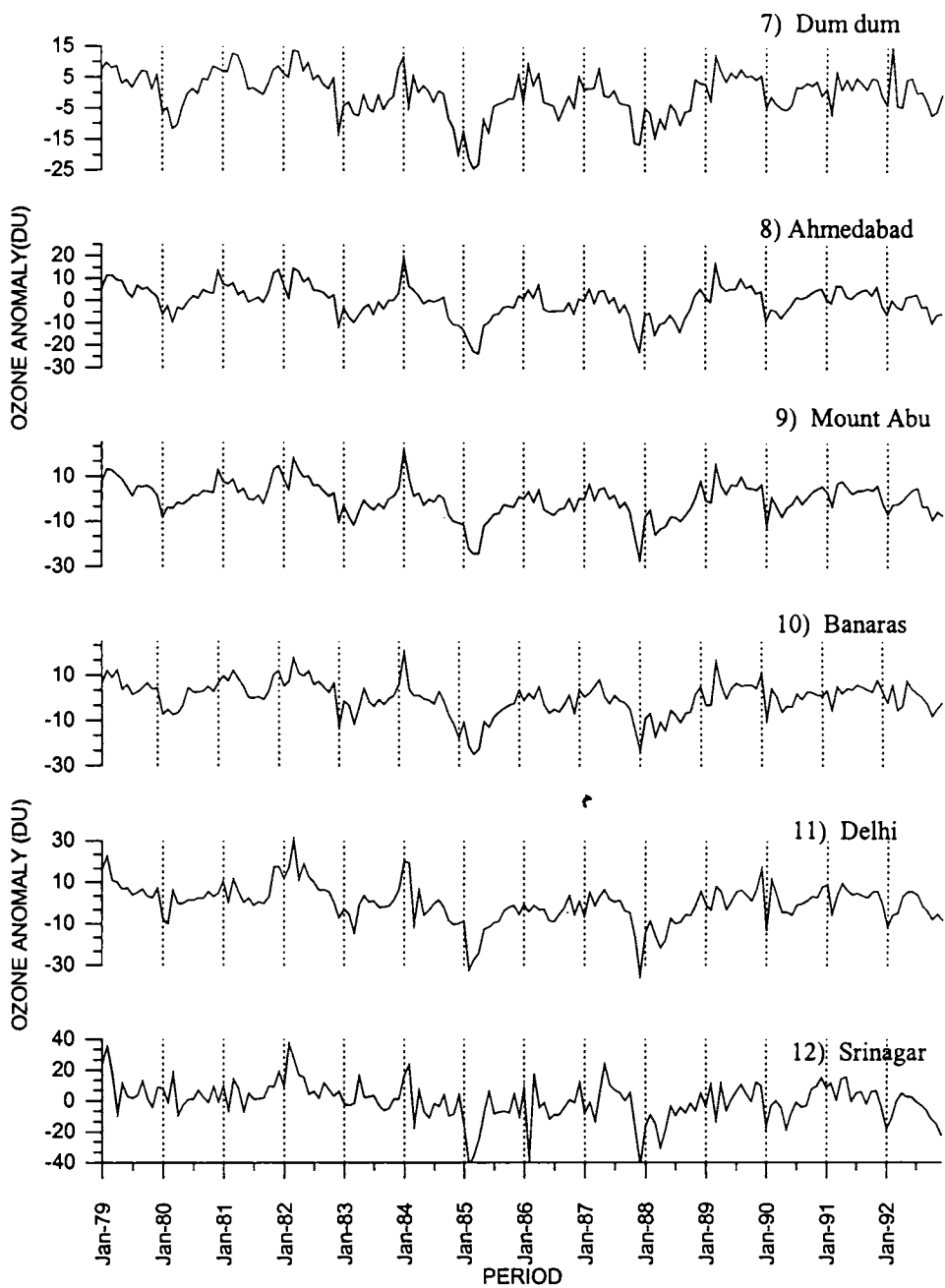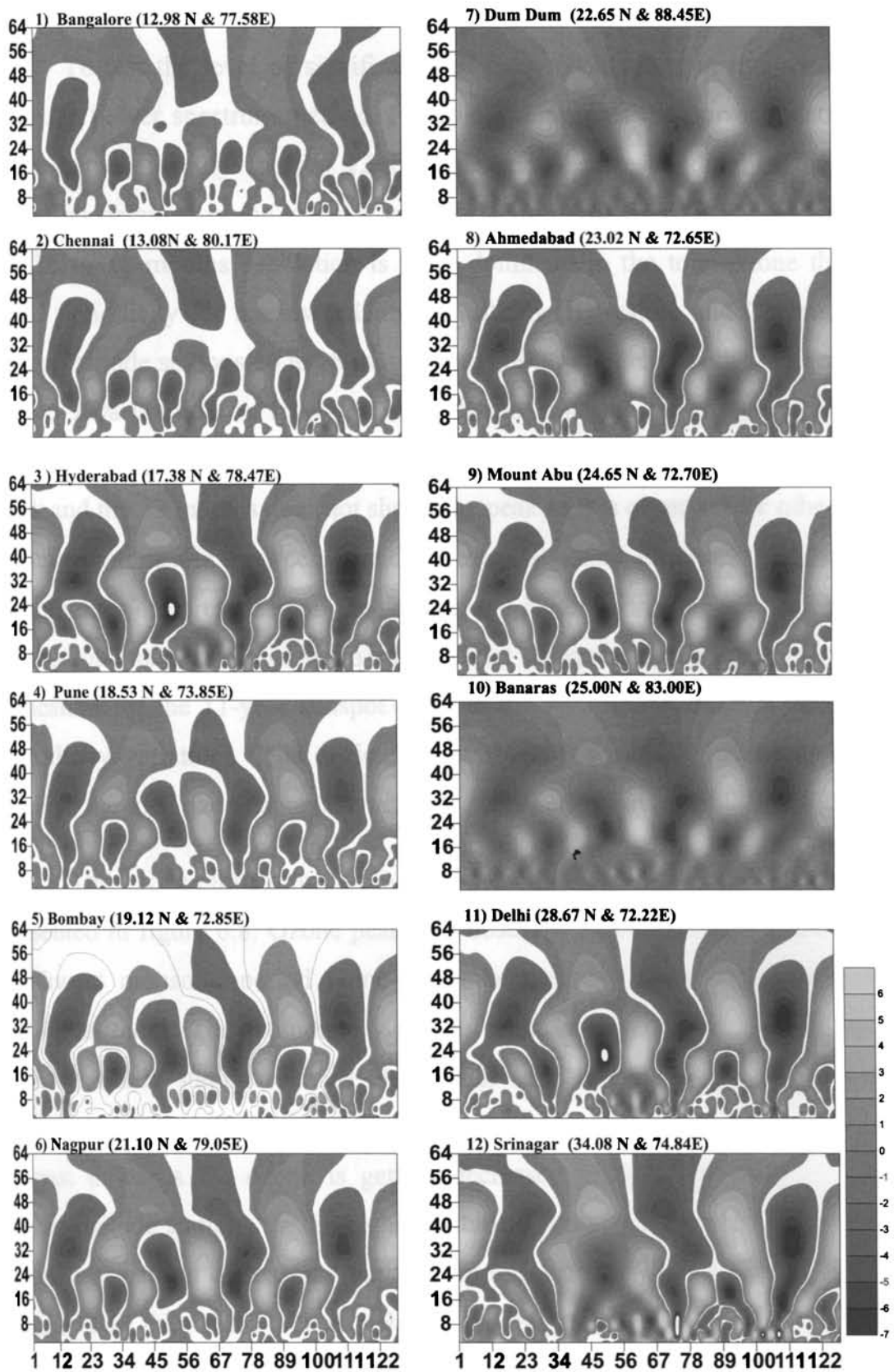
Figure 6.5 : Total ozone (anomaly) variation in Dobson Units over
the stations during the period January 1979 to December 1992.

Figure 6.6: Wavelet spectrum of total ozone for the stations

are seen over the stations. But the power spectral density of 16 to 18 months oscillations is higher than the QBO oscillations over these central stations.

To test the level of significance of these oscillations in total ozone we used the power spectrum method. Figure 6.7 represents the power spectrum of total ozone anomaly for the 12 Indian stations corresponding to the wave spectrum obtained in the wavelet analysis (figure 6.6). Here it is seen that that the 16 to 18 months oscillation is more dominant in the total ozone than the QBO periodicity for the lower latitudes stations (Bangalore and Chennai). For higher latitude stations 16 to 18 months and QBO periodicity both are significant above 95% confidence level. Power spectrum analysis for the extreme north station (Srinagar, 34.08° N, 74.84° E), shows the 16-moths oscillation, produces peak and the 32 months does not shows the peak as it is observed for other lower latitude stations. In between 0 and 12 months period there are smaller scale periodicities are present in all the stations and it can be treated as noises present in the total ozone variation. In the wavelet analysis the spectrum shows an indication for the 11-year sunspot cycle in the total ozone anomaly for higher periodicity variations. It is difficult to establish the presence of 11-year solar cycle in the total ozone anomaly with this short period data set (1979-1992).

The ozone climatology from 1979-1992 (14 years) for the 12 stations are presented in figure 6.8. Ozone peaks are observed at all the stations, during the southwest monsoon period (June-September) except the stations, located at higher latitudes. The latitudinal variation of ozone is very clearly seen in the higher latitude station such as New Delhi and Srinagar. In the low latitude station, total ozone is started increasing from January to August and from August onwards the ozone is getting decreased from all the stations except higher latitude stations. In the higher latitude station (Srinagar) it is noticed that a different pattern of seasonal variation in total ozone and it is increasing from January and then reach a peak value in the month of February to March. This sort of seasonal variation in total ozone is due to latitudinal effect and may be due to the ozone transport from the low latitudes to mid latitudes. All the stations

107
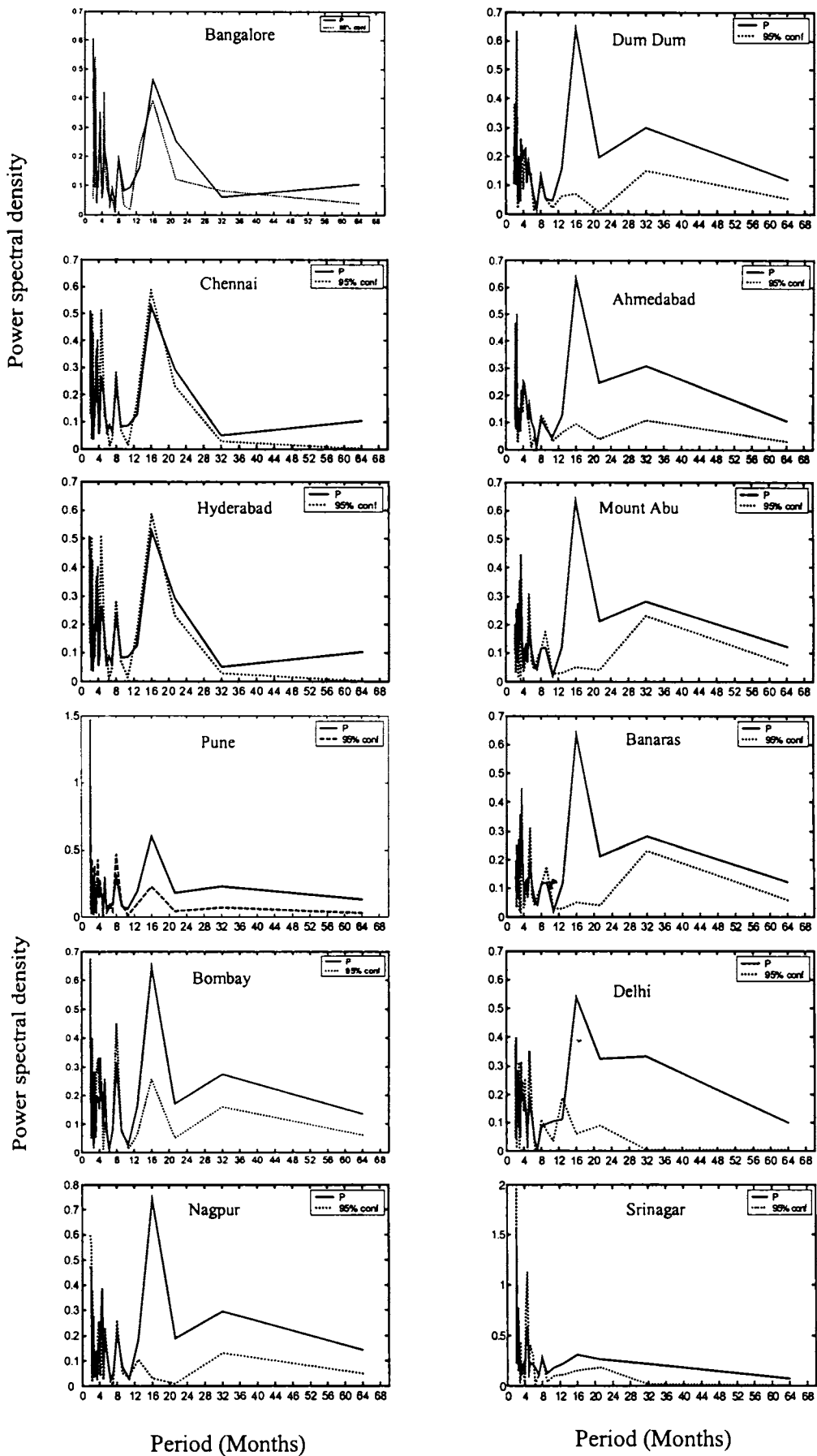
Figure 6.7: Power spectrum analysis of total ozone over the stations. X–axis represent period and Y-axis represent the power spectral density
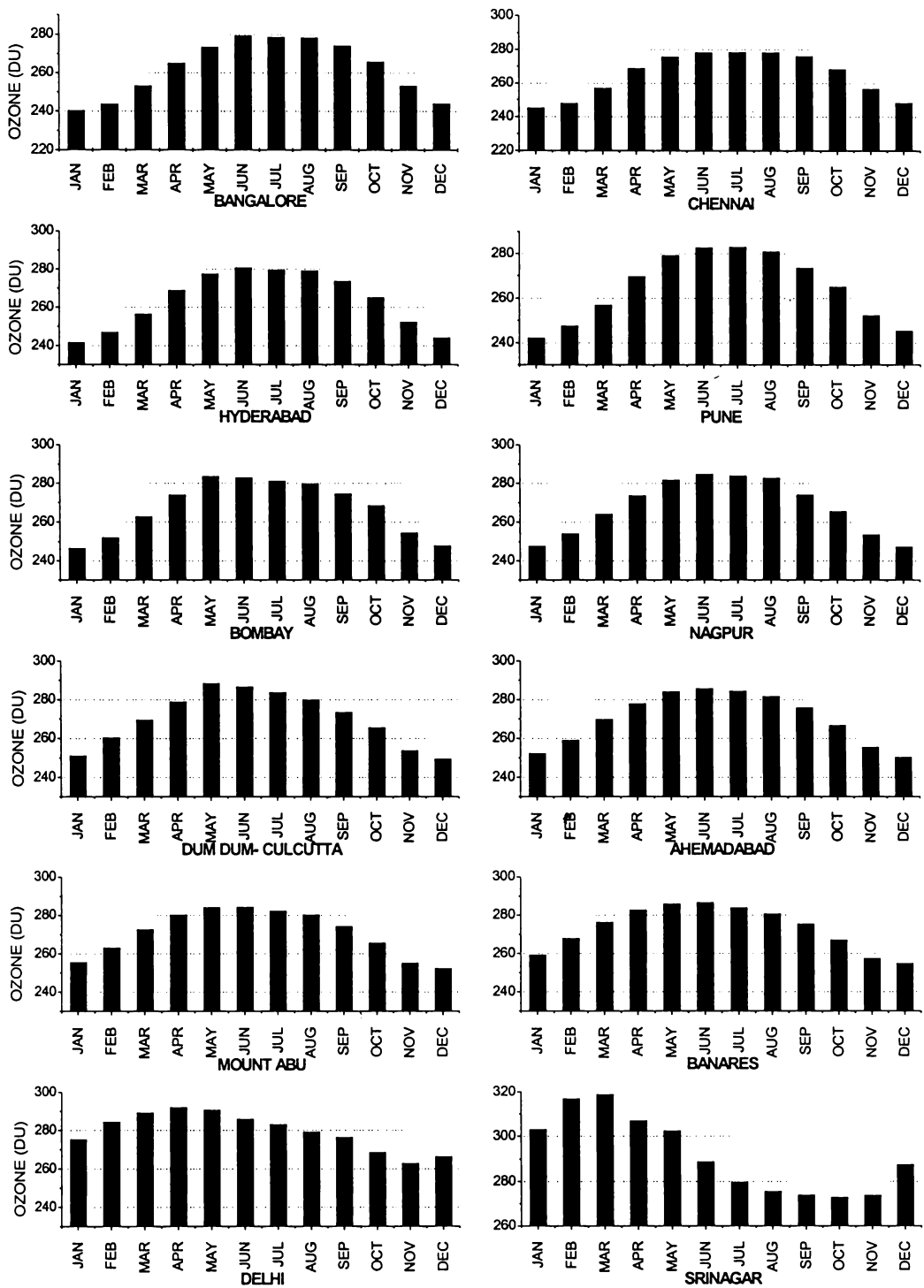
Figure 6.8 : Climatology of total ozone over the Indian stations (1979-1992)

a minimum value of total ozone varies between 250 DU to 270 DU and maximum values between 280 to 300 DU.

6.3.2 Spatial correlations of total ozone

We have used the factor analysis techniques to classify the stations, which has got commonness in total ozone variation during the period 1979-1992. We have used the monthly anomaly value of total ozone for the analysis. The total ozone variation over the Indian stations are grouped into two clusters (Eigen value greater than 1) with the method of factor analysis.

(a)   Group I, stations with Ist factor as the primary loading, i.e., Ist factor greater than IInd factor.

(b)   Group II, stations with IInd factor as the primary loading, i.e., IInd factor greater than Ist factor.

Table 6.1 shows the names of stations with Ist and IInd factor as the primary loading in the total ozone variability study. And it is found that the central stations come under the same nature of variability, mainly due the first factor as the primarily loading and which contribute about 79% to the total variability of the total ozone. Whereas the two high latitude stations (Delhi and Srinagar) and two low latitude stations (Bangalore and Chennai) the primary loading is due the IInd factor indicates a similar type of total ozone variation due to some other features other than the stations with Ist factor as the primary loading.

Table 6.2 represents spatial correlation of total ozone between 12 stations for the period 1979 to 1992. The correlations of total ozone between the central stations (Hyderabad, Pune, Bombay, Nagpur, Dum Dum, Ahemadabad , Mount Abu and Banares) for the period 1979 to 1992 show high correlation values of 0.9 between the above stations. These correlation values are well agreed with the result obtained in the factor analysis. Therefore it shows that the variability in

108

Stations with Ist factor as primary loading	Stations with IInd factor as primary loading
Hyderabad (17.38°N, 78.47°E)	
Pune (18.53°N, 73.85°E)	Bangalore (12.98°N, 77.58°E)
Bombay (19.12°N, 72.85°E)	Chennai (13.08°N, 80.17°E)
Nagpur (21.10°N, 79.05°E)	Delhi (28.67°N, 72.22°E)
Dum- Dum (22.65°N, 88.45°E)	Srinagar (34.08°N, 74.84°E)
Ahmedabad (17.38°N, 78.47°E)	
Mount Abu (24.65°N, 72.70°E)	
Banares (25.00°N, 83.00°E)	

Table 6.1: Stations with Ist factor and IInd factor as the primary loading

Station	BNGR	CHNN	HYDE	PUNE	BMBY	NGPR	DUMM	AHMD	MUNT	BNRS	DELH	SRNR
BNGR	1.00	0.96	0.83	0.7	0.76	0.7	0.63	0.65	0.61	0.59	0.49	0.32
CHNN	0.96	1.00	0.82	0.7	0.75	0.69	0.625	0.64	0.61	0.59	0.51	0.35
HYDE	0.83	0.82	1.00	0.91	0.96	0.93	0.87	0.86	0.81	0.8	0.65	0.46
PUNE	0.70	0.70	0.91	1.00	0.94	0.93	0.88	0.92	0.87	0.84	0.72	0.53
BMBY	0.76	0.75	0.96	0.94	1.00	0.96	0.90	0.93	0.88	0.85	0.72	0.52
NGPR	0.70	0.69	0.93	0.93	0.96	1.00	0.95	0.95	0.92	0.92	0.76	0.52
DUMM	0.63	0.63	0.87	0.87	0.90	0.95	1.00	0.91	0.88	0.93	0.75	0.49
AHMD	0.65	0.64	0.86	0.92	0.93	0.95	0.91	1.00	0.98	0.93	0.83	0.59
MUNT	0.61	0.61	0.81	0.87	0.88	0.92	0.88	0.98	1.00	0.94	0.91	0.66
BNRS	0.59	0.59	0.80	0.84	0.85	0.92	0.93	0.93	0.94	1.00	0.88	0.59
DELH	0.49	0.51	0.65	0.72	0.72	0.76	0.75	0.83	0.91	0.88	1.00	0.8
SRNR	0.32	0.35	0.46	0.53	0.52	0.52	0.49	0.59	0.66	0.59	0.8	1.00

Table 6.2: Spatial correlation of total ozone between stations

total ozone over the stations are also due to the interannual variability such as QBO and solar cycle rather than the latitudinal effect.

6.3.3 Variation of total ozone in DRY and WET years

Another part of the study is to establish some relation with the South West Monsoon Rainfall with variation of total ozone. Figure 6.9 represent the composite of the total ozone at 12 stations plotted with DRY (1979, 1982, 1987) and WET (1983, 1988) year composites. In DRY years ozone composite is greater than the WET year composite. This result is well supported with the total ozone variation at New Guinea and found that maximum ozone episode occur during the DRY season (Jae et al., 1998). Also total ozone variation is latitudinal dependant and its is high as it goes from lower to high latitude stations. Figure 6.10 show the total ozone difference in the DRY minus WET years. Here we have taken ozone for all the months from January to December and made it composite for DRY and WET years for the stations. From the figure 6.10 we can see the spatial distribution of ozone in different stations during the DRY and WET seasons of Indian summer monsoon. Here low value of ozone difference in the low latitude station (Bangalore) and high value is seen in the extreme northern Indian stations, such as Delhi and Srinagar with a maximum of 11.0 DU units of ozone variation. There is a difference of approximately 8 DU of total ozone in the southern and northern Indian stations. Western coastal station of India shows higher values of ozone anomaly compared to the eastern coastal region.

6.3.3.1 Variation of total ozone and ISMR during monsoon period (JJAS)

Figure 6. 11 (a) show the composite of the total ozone variation for the deficient rainfall years (DRY and below normal) (1979, 1982, 1985, 1986, 1987) and WET (1983 and 1988) years ozone during the southwest monsoon period. Here it is noted that the monsoon period, DRY year ozone is much higher than the WET year ozone value. We have tested the variation summer rainfall data of seven station with the monthly ozone data for the (June-September). For this we
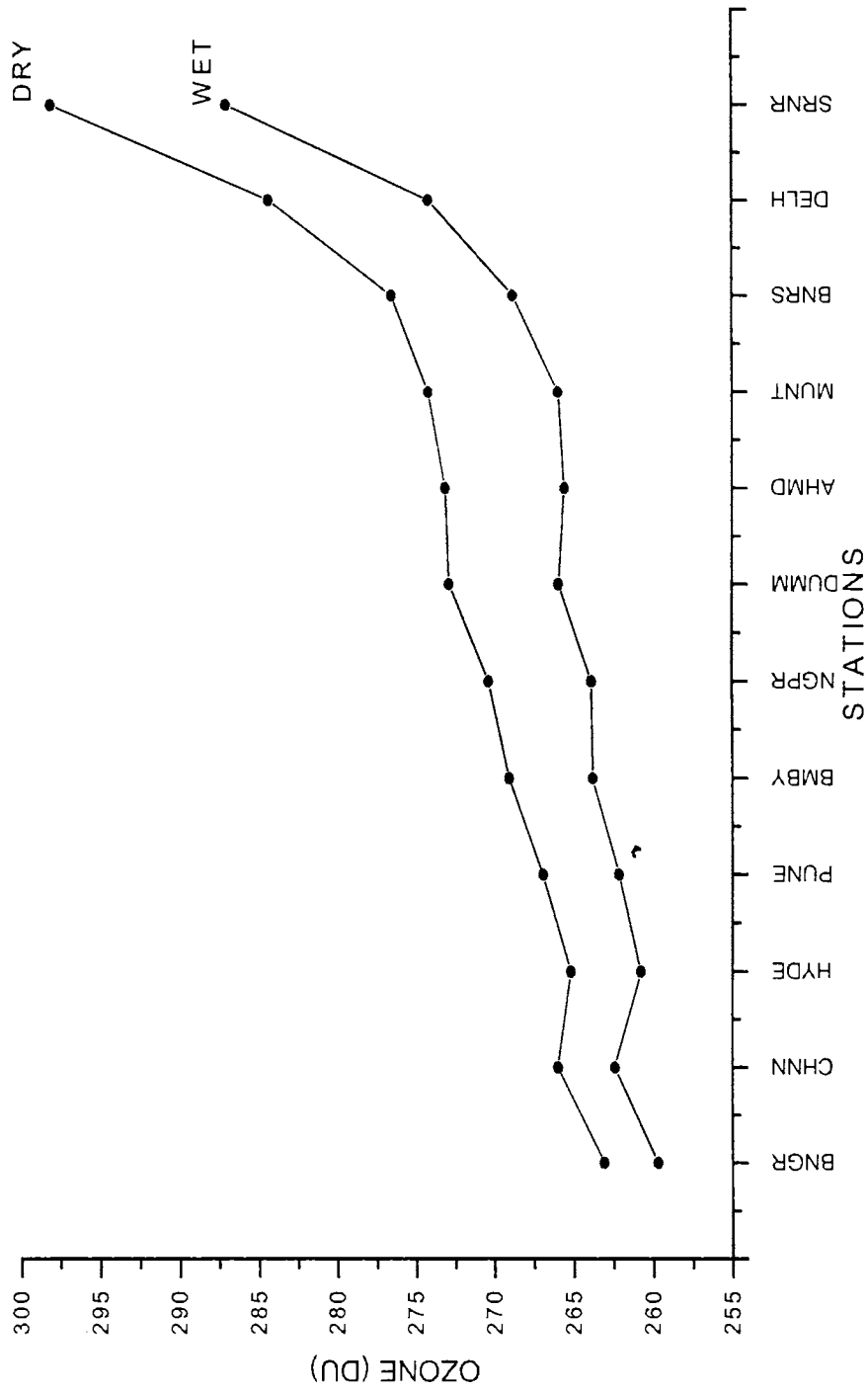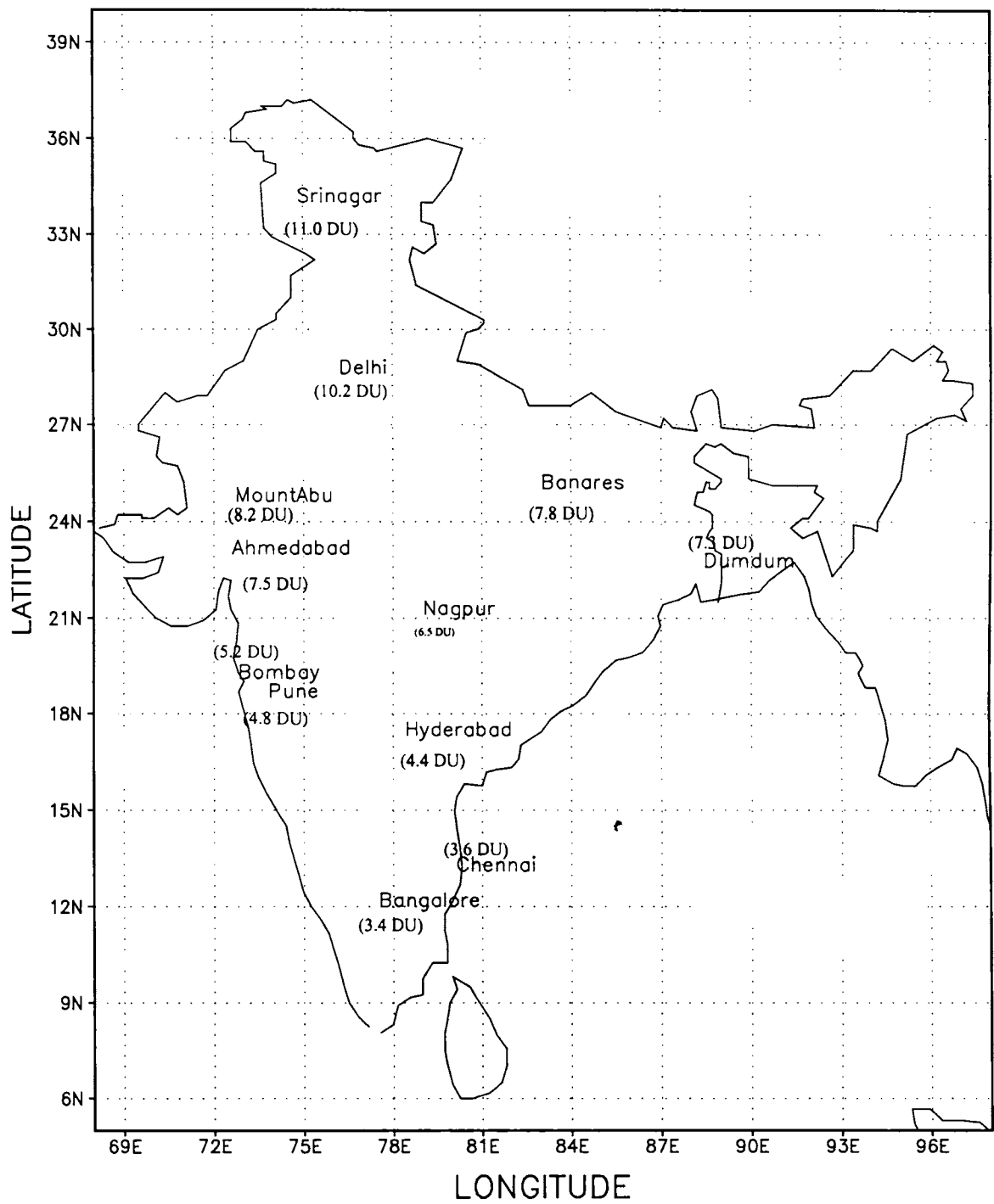
Figure 6.9 : Total ozone variation during DRY and WET years.

Fig 6.10 :Difference of total ozone between DRY and WET years of monsoon
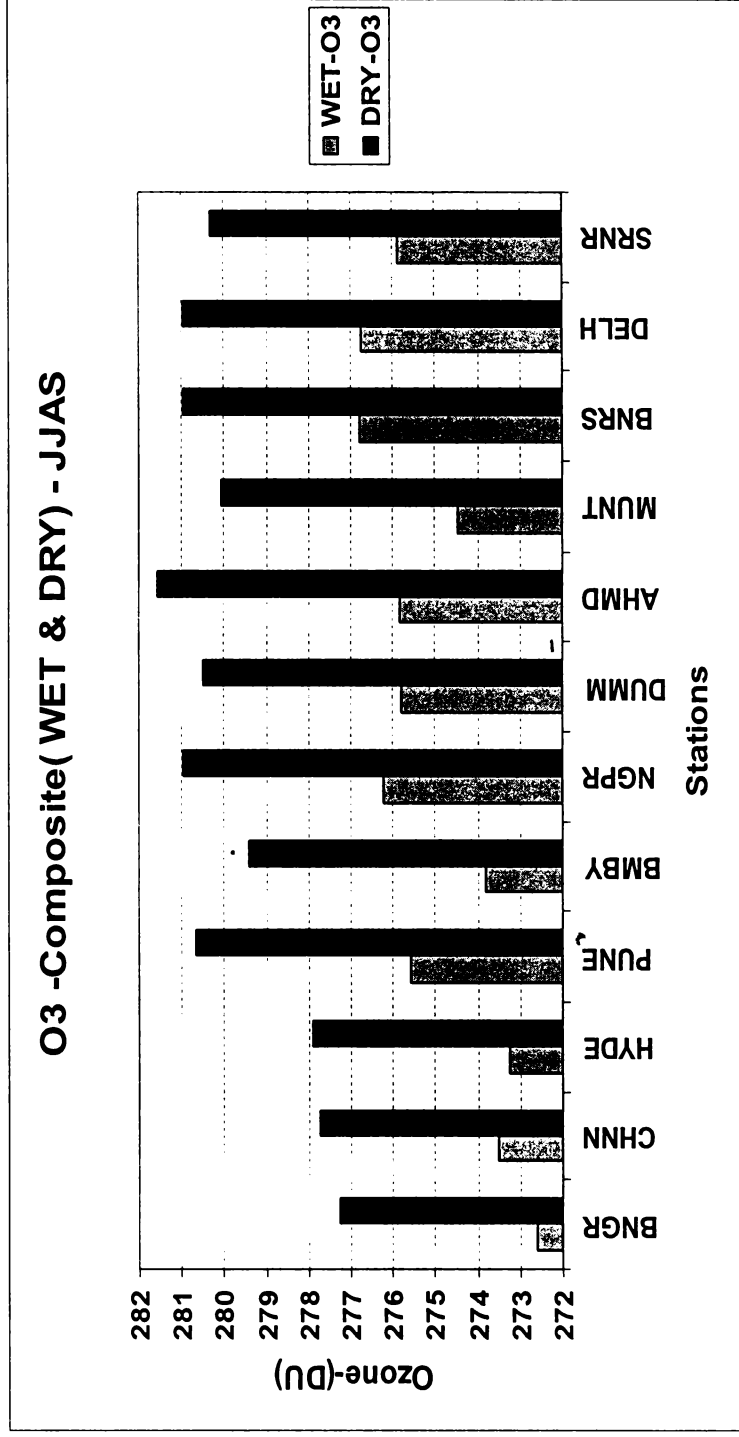
Figure 6.11: Total ozone variation during June to September in DRY and WET years of Indian summer monsoon

have selected the seven stations, Chennai, Hederbad, Pune, Nagpur, Dum Dumm and Ahmedabad and Delhi. The rainfall data for the DRY years and WET years collected and made composite for all the seven stations. Figure 6.12(a) show the rainfall in mm for the DRY and WET years. Figure 6.12 (b) is the ozone value at these stations for the DRY and WET years and found that when the rainfall increases total ozone decreases at these stations and vice- versa.

From the above results we can conclude that in DRY monsoon years total ozone is greater than the WET monsoon years. It is known that the easterly and westerly phases of QBO is linked with the DRY and WET seasons of Indian summer monsoon (*Mukherjee et al., 1985*). The variations of total ozone are linked with the phases of QBO and it is higher during the easterly phases and low values during the westerly phases (Hess *et al.*, 1995) of QBO. The tropopause height is higher during the WET years of Indian summer monsoon than the DRY years (*Kulakarni et al., 1993*). Appenzeller *et al.* (2000) showed that the vertical integrated column of ozone is higher when the tropopause height is low and vice versa. From the above discussions it canbe noted that the variation of total ozone during the DRY and WET years of monsoon are linked with the interannual variability (phases of QBO) of total ozone and also modulated by the height of the tropopause (thermal structure of the upper troposphere and lower stratosphere).

6.3.4 Correlation between total ozone and solar flux

The correlation between total ozone and the sunspot cycle are lowest in the equatorial regions, where ozone is produced, and in the sub polar regions, where the largest amount are found (*Labitzke et al., 1997*). Some researchers   (*Stolarski et al., 1991; Chandra et al., 1999*) have tried to connect the observed interannual anomalies of ozone with solar activity. It was found that the ozone variations caused by the 11-year solar cycle are within the limits of 1-3 %. According to the WMO Ozone Assessment (1995), the global average total

(a)

(b)

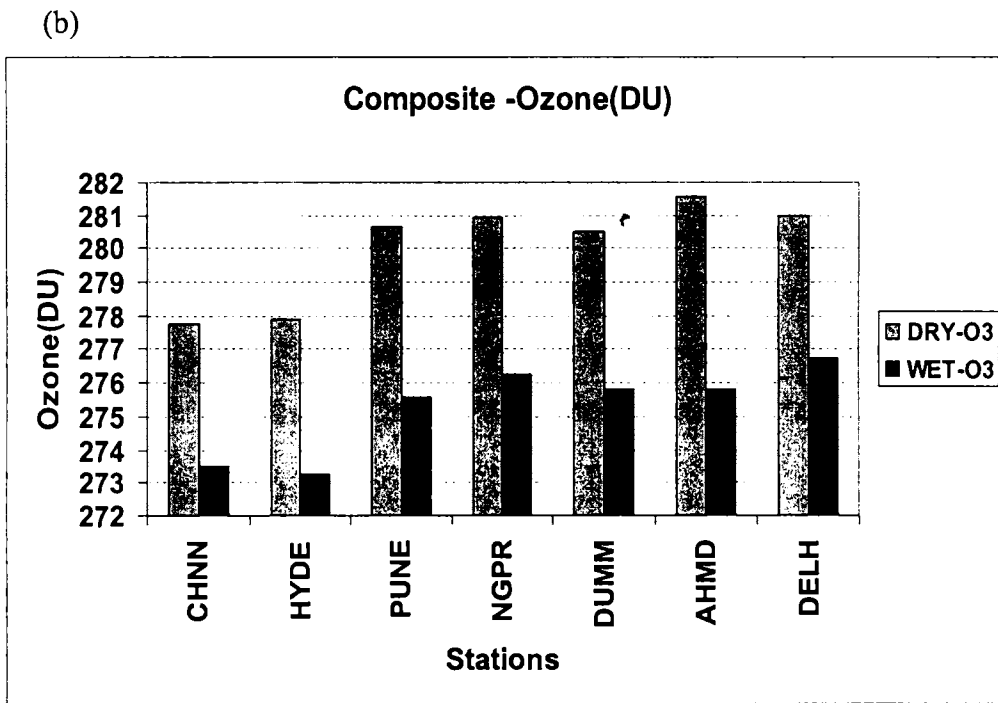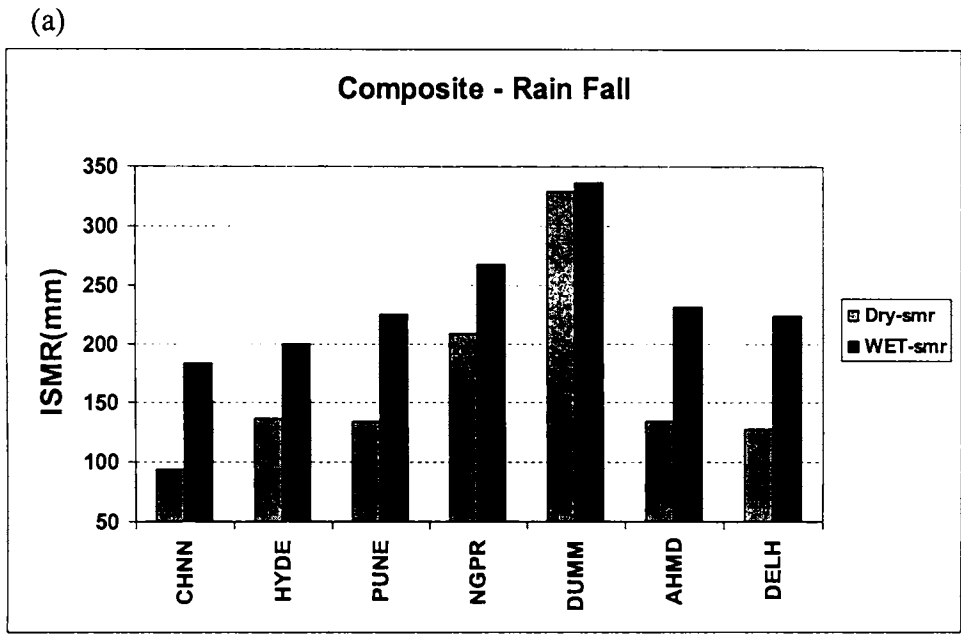*Figure 6.12:* (a) *The rainfall during June to September in DRY and WET years for the stations (Chennai , Hyderabad, Pune, Nagpur, Dum-Dum, Ahmedabad and Delhi).* (b) *Total ozone over the stations during June to September for DRY and WET years of monsoon.*

ozone changes are correlated with solar UV flux variations in the 11-year solar cycle, changing by about 1-5 % from solar maximum to solar minimum.

The correlation value between the solar flux and the total ozone over the stations are marked in the y-axis (figure 6.13). We did the correlations with the monthly values of total ozone for each station with the 10.7 cm solar flux data for the period January 1979 to December 1992. It is found that there is positive correlation between solar flux and total ozone for all the stations and it increases from the low latitude stations to higher latitude stations. We have used the Student's 't' test for testing the level of significance for these correlations. The higher latitude stations such as Srinagar and Delhi shows correlations significant at 99.5 % confident level. Nagpur and Bombay have correlations significant at 95.5 % level and the least correlation is for the Pune station. This results show that the variations in total ozone is influenced by the solar flux only at higher latitude station and the variations of total ozone is less influenced by the solar flux for the lower latitude stations.

6.4 Summary

In this chapter, we have analyzed the total ozone over the 12 Indian stations using the TOMS over pass data. It is found that total ozone is higher in the northern latitude stations and peak value is noted during the southwest monsoon period (June - September). There are two major type of oscillation with periodicity 16-18 months and 26 to 28 months (quasi-biennial oscillation) are found in the total ozone over these stations. These oscillations are significant at above 95 % confidence level and 16 to 18 month oscillation is prominent compared to qausi-beinnial mode. Another part of the study is the variation of ozone during the DRY and WET seasons of Indian summer monsoon and it is found that total ozone is more during the DRY years than WET years. The ozone variation is linked with the phases of QBO in the ozone (Interannual variability) and also depends on the thermal structure of the UT/LS region (height of the tropopause). The correlation of total ozone with solar flux found that, the
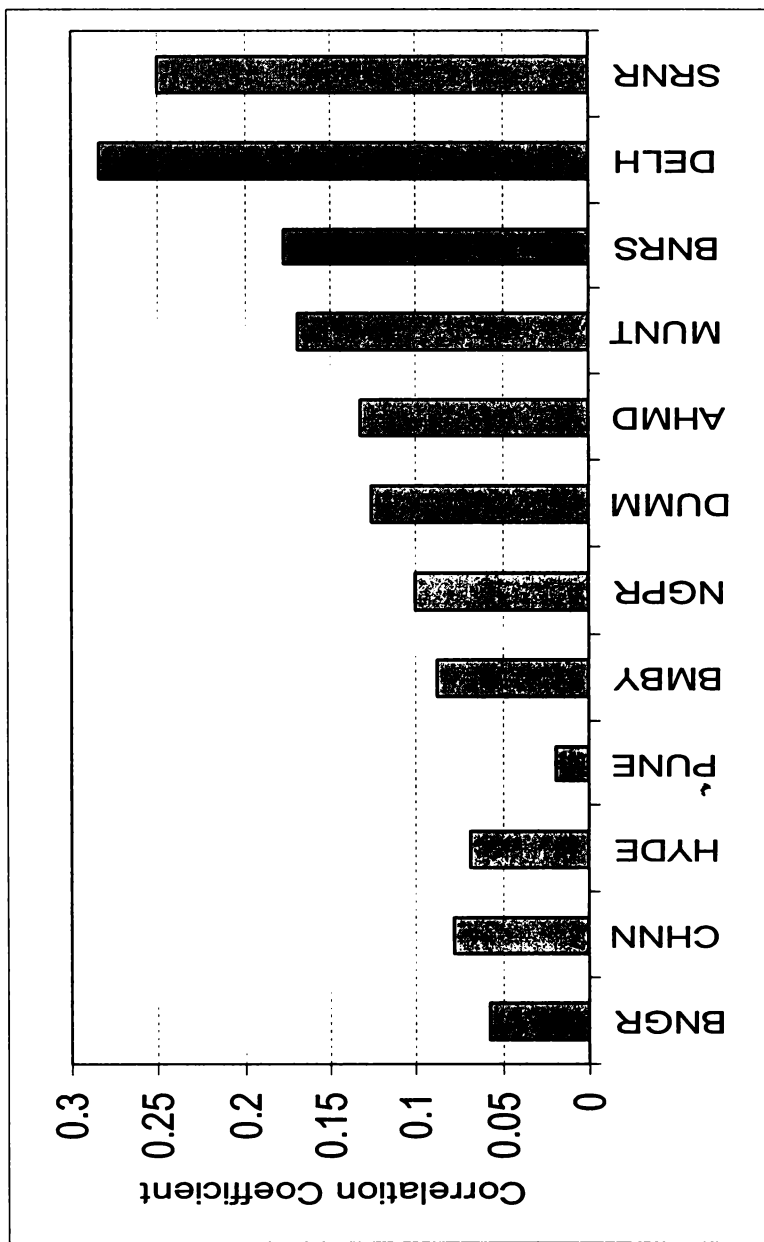
Figure 6.13 : Correlation coefficients between ozone and 10.7 cm solar flux

correlations are significant at 99.5% confidence level for northern latitude stations. Hence the total ozone variations at northern latitude stations are more influenced by the solar activity than at low latitude stations.

Chapter 7

Summary and Conclusions

7.1 Summary and Conclusions

Recently atmospheric research established the role of stratosphere in the climate variability and weather changes. The upper troposphere and lower stratosphere regions are very sensitive to the climate changes compared to other layers of the atmosphere. Even though these two layers have entirely different characteristics , the interaction between them cannot be neglected when we study the climate change. There is exchange of mass, energy and momentum takes place by the process of stratosphere-troposphere interactions. Atmospheric waves originating in the dynamically active troposphere and radiatively strong stratosphere play the major role in the stratosphere-troposphere interaction. The ozone in the stratosphere also play a role in the radiative balance between the earth and atmosphere system and it protect the life on the earth from harmful ultra violet radiations.

In the present study we made an attempt to understand the characteristics of the upper troposphere and lower stratosphere over the Asian summer monsoon region, more specifically over the Indian subcontinet. Mainly we had taken three important atmospheric parameters such as *zonal wind, temperature and ozone* over the UT/LS of the Asian summer monsoon region. We made a detailed study of its interannual variability and characteristics of theses parameters during the Indian summer monsoon period. Monthly values of zonal wind and temperature from the NCEP/NCAR reanalysis for the period 1960 - 2002 are used for the present study. Also the daily overpass total ozone data for the 12 Indian stations (from low latitude to high latitudes) from the TOMS Nimbus 7 satellite for the period 1979 to 1992 (14 years) were also used to understand the total ozone variation over the Indian region. The major outcomes of the present study are presented as follows.

The zonal wind in the upper troposphere and lower stratosphere over the Asian summer monsoon region shows that the major interannual variability in the lower stratospheric zonal wind is QBO with a varying periodicity from 26 to

113

32 months. The amplitude and period of the QBO vary over the Asian summer monsoon region. The approximate duration of easterly and westerly phases of QBO are 14 and 13 months respectively with a QBO periodicity of 27 moths over the Asian summer monsoon region. The phase transition of QBO over the Indian region revealed that the westerly to easterly transition generally occur during the month of May and easterly to westerly transition in January. Also noted that there exist a link between the stratospheric zonal wind variability (QBO phases) and Indian summer monsoon. If QBO phases in the stratosphere is easterly or weak westerly then the respective monsoon is found to be DRY or below Normal. On the other hand, if the phase is westerly or weak easterly the respective Indian summer monsoon is noted as a WET year. This connection of stratospheric QBO phases and Indian summer monsoon gives more insight in to the long-term predictions of Indian summer monsoon rainfall.

Wavelet analysis and EOF methods are the two advanced statistical techniques used in the present study to explore more information of the zonal wind that from the smaller scale to higher scale variability over the Asian summer monsoon region. Both the techniques show that the QBO periodicities are dominant in stratospheric levels. But some years its amplitude and periodicity have greater variations. The above oscillation in the zonal wind is significant above 95% confidence level. The EOF methods give the spatial pattern of the parameter and how it varies over the monsoon region with time. Here also the dominant variability over the summer monsoon region is QBO periodicity, which contributes more than 70% to the total variability in the stratosphere. The spatial pattern of the QBO mode shows a monopole and annual oscillations shows a dipole pattern over the Asian summer monsoon region. The annul oscillation changes it sign between north and south in the alternate levels of the stratosphere. The QBO mode gives way to the annul oscillation at 50 hPa level and contribute above 50 percentage to the total variability in zonal wind. From the analysis it is found that the QBO mode is contributing greater

percentage in the stratospheric levels and annul mode is contributing significantly in the upper tropospheric levels.

A peculiar characteristics of the zonal wind is observed in the DRY and WET years of Indian summer monsoon over the UT/LS of the tropical atmosphere. The zonal wind in the equatorial upper troposphere and lower stratosphere exhibit opposite wind anomalies during the DRY and WET years of Indian summer monsoon period (JJAS). In DRY years, upper troposphere zonal wind (tropical easterly jet over the south Asia) have westerly anomalies and lower stratosphere have easterly anomalies. In WET years, the anomalies are opposite. We named this upper troposphere and lower stratosphere wind systems in the tropical region during the DRY and WET years of Indian summer monsoon season as "UT/LS dipole". The intensity of the dipole is found to be well correlated with the Indian summer monsoon rainfall. Another interesting fact noted is the weakening of the stratospheric easterly and tropical easterly jet during the period of study 1960-1998. It is found that the Hadley circulation during the WET years of Indian summer monsoon is stronger than the DRY years. The wind direction in the UT/LS of DRY and WET years show entirely opposite characteristics.

The interannual variability of temperature for different stratospheric and tropospheric levels over the Asian summer monsoon region have been studied. The 10.7 cm solar radio flux is used to find the modulation of temperature with the 11-year solar cycle. We used the Morlet wavelet and EOF analysis to study the major oscillations present in the temperature and its percentage of contribution to the total variability over the Asian summer monsoon region. The two major oscillations in the temperature are the quasi-biennial oscillation (26-32 months) and 11-year solar cycle (132-136 months) in the UT/LS region. These oscillations are significant at above 95% level of confidence. Abrupt variations in the UT/LS temperature during the period of study prior and after 1977 are noticed. These changes in the temperature may be due to the decadal

variability (11- year solar cycle) and the climate fluctuation, which occur prior and after 1977.

A QBO periodicity in temperature in the upper troposphere is noted at level 200 hPa. It is observed that there exit an 11-year solar cycle in temperature in the UT/LS levels at 200 hPa and 10 hPa. The temperature at 200 hPa shows an in-phase relation with the solar flux and at 10 hPa shows an out- of- phase relation. The QBO mode in the temperature oscillation is greater than the 11-year cycle. The QBO mode contributes more percentage of variability to the stratospheric temperature whereas the 11-year mode contributes more to the tropospheric temperature variability. We computed the temperature trend over the Asian summer monsoon region for three periods (1969-1978, 1979-1988 and 1989-1998). It is found that there is a cooling trend in the stratospheric levels and which extends upto the upper tropospheric levels.

An attempt has been made to understand the total ozone characteristics and its interannual variability over 12 Indian stations spread from south latitudes to north latitudes. It is noticed that total ozone is maximum during the monsoon period (JJAS) for all the stations except the stations (Srinagar and New Delhi) at northern latitudes. There are two significant interannual oscillations present in total ozone over these stations are observed. One is with a periodicity varying from 16-18 months and the other is with a QBO periodicity varying from 26-32 months. Both these oscillations in the total ozone are significant at 95% level of confidence. Another finding is that total ozone is high during DRY years of Indian summer monsoon than the WET years. Using factor analysis we classified these stations into two groups with the same nature of total ozone variability at these stations. All the central Indian stations fall in the first group with a first factor as the primary loading. There are four stations (two northern stations (Srinagar& Delhi) and two southern stations (Chennai and Bangalore) come under the second group with the second factor as the primary loading. This implies that the total ozone variations over these stations are not fully

116

latitudinal depended. The correlation between the total ozone and solar flux shows high correlation for the north Indian station compared to south stations.

7.2 Scope for the future study

In the present study we explored the interannual variability of zonal wind, temperature and total ozone over the UT/LS of Asian monsoon region. It is found that the upper troposphere and lower stratosphere contribute significantly to monsoon variability and climate changes. It is also observed that there exists a link between the stratospheric QBO and Indian summer monsoon. So more research work on these aspects will be needed for a better understanding of the physical mechanism responsible for the stratosphere-troposphere interaction. From the results obtained from the present study, a suitable atmospheric model can be developed to study the stratosphere–troposphere interaction processes. If we understand more about the total ozone variability over the Asian summer monsoon region, it will help us to protect the ozone layer by reducing the increased production of chlorofluorocarbons. The ozone variability is a prime concern now a days because the depletion of ozone in the stratospheric levels lead to the imbalance between earth and atmosphere radiative equilibrium.

References

Ancellet, G., J. Pelan, M. Becekmann, A. Payannis, and G. Megie, Ground-based lidar studies of ozone exchange between the stratosphere and the troposphere, *J. of Geophys. Res.*, **96**, 22 401- 22 421, 1991

Andrews, D. G., J. R., Holton and C. B. Leovy, *Middle Atmospheric Dynamics*, Academic, San Diego, California., **pp 489**, 1987.

Angell, J. K., and J. Korshover, Quasi-biennial variation in temperature, total ozone, tropopause height, *J. Atmos. Sci.*, **21**, 479-492, 1964.

Angell, J. K., Comparison of stratospheric warming following Agung, El Chichon, and Pinatubo Volcanic eruption, *Geophys. Res. Lett.*, **20**, 715-718, 1993.

Angell, J. K., On the relation between atmospheric ozone and sunspot number, *J. Clim.*, **2**, 1404-1416, 1989.

Angell, J. K., Re-examination of the relation between depth of the Antarctic ozone hole, and an equatorial QBO, and SST, 1962-1992, *Geophys. Res. Lett.*, **20**, 1559-1562, 1993.

Angell, J. K., Stratospheric warming due to Agung , El Chichon, and Pinatubo taking into account the quasi-biennial oscillation, *J. Geophy. Res.*, **102**, 9479-9485, 1997.

Angell, J. K., Variation of tends in the tropospheric and stratospheric global temperature 1958-87, *J. Climate.*, **1**, 1296-1313, 1988.

Appenzeller, C. A., Weiss, and J. Staehlin, North Atlantic Oscillation modulates total ozone winter trends, *Geophys. Res. Lett.*, **27**, 1131-1134, 2000.

Appenzeller, C., and J. R. Holton, Tracer lamination in the stratosphere: a global climatology, *J.Geophy. Res.*, **102**, 13, 555-13,569, 1997.

Appu, K.S., K. Sivadasan, and V. Narayanan, The thermal structure of troposphere, stratosphere and mesosphere over equatorial India, *Mausam.*, **31**, 19-30, 1980.

Atticks, M. G., and G. D. Robinson, Some features of the structure of the tropical tropopause, *J. Roy. Meterological Soc.*, **109**, 295-308, 1983.

Baldwin, M., L. J. Gray, T. J. Dunkerton *et al.*, The Quasi-Biennial Oscillation, *Rev. Geophysics.*, **39**, 179-229, 2001.

Baliunas, S., P. Frick, D. Sokoloff, and W. Soon, Time scales and trends in the central England temperature data (1659-1990): A wavelet analysis. *Geophys. Res. Lett.*, **24**, 1351-1354, 1997.

Barbara, N., An update of the observed quasi-biennial oscillation of the stratospheric winds over the tropics, *J. Atmos. Sci.,* **43**, 1873-1880, 1986.

Bethen, S., G. Vaughan and S. J. Reid, A comparison of ozone and thermal tropopause height and the impacts of tropopause definition on quantifying the ozone content of the troposphere, *Q. J. Roy. Meteor. Soc.,* **122**, 924-944, 1996.

Bhalme, H. N., S. S. Rahalkar and A. B. Sikder, Tropical quasi-biennial oscillation of the 10-mb wind and Indian monsoon rainfall- Implications for forecasting, *J. Climate.,* **7**, 345-353, 1987.

Boering, K. A., et al., Stratospheric mean ages and transport rates from observations of carbon dioxide and nitrogen oxide, *Science.,* **274**, 1340-1343, 1996.

Bojkov, R. D., The 1983 and 1985 anomalies in ozone distribution in Perspective, *Mon. Weather. Rev.,* **115**, 2187-2201, 1987.

Booker, J. R., and F. P. Bretherton, The critical layer for internal gravity --waves in a shear flow, *J. Fluid. Mech.,* **27**, 513-539, 1967.

Bowman, K. R., Global patterns of quasi-biennial oscillation in total ozone, *J. Atmos. Sci.,* **46**, 3328-3343, 1989.

Brasseur, G. P., R. A., Cox, D. Hanglustaine, I. Isaksen, J. Lebieveld, D. Lister, R. Sausen, V. Sehumann, A. Wahner and P. Weisen, European Scientific Assessment of the atmospheric effects of aircraft emission, *Atmos. Environ,* **32**, 2329-2418, 1998.

Bretherton, F. P., Momentum transport by gravity waves, *Q. J. R. Meteorol. Soc.,* **95**, 213-243, 1969.

Brewer, A. W., Evidence for a world circulation provided by the measurement of helium and water vapour distribution in the stratosphere, *Q. J. R. Meteorolo. Soc,* **75**, 351-363, 1949.

Browell, E. V., E. F. Danielson, S. Ismail, G. L. Gregory, and S. M. Bleck, Tropopause fold structure determined from airborne and in situ measurements, *J. Geophys. Res.,* **52**, 2112-2120, 1987.

Carter, M. M. and J. B. Elsner, Convective rainfall regions of Puerto Rico, *Int. J. Climatolo.,* **16**, 1033-1043, 1996.

Chakrabarty, D. K., S. K. Peshin, K. V. Pandya and N. C Shah, Long term trend of ozone column over the Indian region, *J. Geophys. Res.,* **103**, 19 245- 19 251, 1998.

Chan, J. C. L., Tropical cyclone activity in the western North pacific in relation to the stratospheric quasi-biennial oscillation, *Mon. Weather. Rev.,* **123**, 2567-2571, 1995.

Chandra, S., J. R. Ziemke, and R.W. Stewart, An 11- year solar cycle in troposphere ozone from TOMS measurements, *Geophys. Res. Lett.,* **26**, 185-188, 1999.

Chapman, S., A theory of upper atmospheric ozone, *Mem.R. Meteorol. Soc.*, **3**, 103-125, 1930.

Charney, J. G., and P. G. Drazin, Propagation of planetary scale disturbance from the lower into the upper atmosphere, *J. Geophys. Res.*, **66**, 83-109, 1961.

Christiansen, B., Radiative forcing and climate sensitivity: The ozone experience, *Q.J. R. Meterol. Soc.*, **125**, 3011-3036, 1999.

Christy, J. R., and S. Drouilhet, Variability in daily, zonal mean lower- stratospheric temperature, *J. of Climate.*, **7**, 106-120, 1994.

Christy, J. R., R. W. Spencer, and R. T. McNider, reducing noise in the daily MSU lower tropospheric temperature data set, *J. Climate.*, **8**, 888-896, 1995.

Chui, C. K., An introduction to wavelets. *Academic Press.*, **266 pp**, 1992.

Clough, S. A., M. J. Iacono, J. -L. Moncet, Line-by-line calculations of atmospheric fluxes and cooling rates: Application to water vapour, *J. Geophys. Res.*, **97**, 15,761, 1992.

Collineau, S., and Y. Brunet, Detection of turbulent coherent motions in a forest canopy. Part1: wavelet analysis. *Bound. Layer Meteo.*, **65**, 357-379, 1993.

Coy, L., The vertical propagation of internal gravity waves in a compressible atmosphere, Ph.D. thesis, University of Washington, **195 pp.**, 1983.

Crutzen P.J., Photochemical reactions initiated by and influencing ozone in unpolluted tropospheric air, *Tellus.*, **26**, 47-57, 1974.

Danielsen, E. F., Stratosphere-Troposphere Exchange based on radioactivity, ozone and potential vorticity, *J. Amos. Sci.*, **25**, 502-518, 1968.

Danielson, E. F., A dehydration mechanism for the stratosphere, *Geophys. Res. Lett.*, **9**, 605-608, 1982.

Donnelly, R. F., H. E. Hinterreger, and D. F. Health, Temporal variation of solar EUV, UV, and 10830 A° radiation, *J. Geophys. Res.*, **191**, 5567-5578, 1986.

Dunkerton, T. J., and M. P. Baldwin, Modes of interannual variability in the stratosphere, *Geophys. Res. Lett.*, **19**, 49-52, 1992.

Dunkerton, T. J., C. –P. F. Hsu and M. P. Baldwin, Distribution of major stratospheric warming in relation to the quasi- biennial oscillation, *Geophys. Res. Lett.* **15**, 136-139, 1988.

Dunkerton, T. J., C.-P. F. Hsu, and M. E. McIntyre, Some Eulerian and Lagrangian diagnostics for a model stratospheric warming, *J. Atmos. Sci.*, **38**, 819-843, 1981.

Dunkerton, T. J., D. C. Fritts, Transient gravity wave-critical layer interaction. Par I: convective adjustment and the mean zonal acceleration, *J. Atmos .Sc.*, **41**, 992-1007, 1984.

Dunkerton, T. J., Eigenfrequencies and horizontal structure of divergent barotropic instability originating in tropical latitudes. *J. Atmos. Sci.*, **47**(11), 1288-1301, 1990.

Dunkerton, T. J., The role of gravity waves in the quasi-biennial oscillation, *J. Geophys. Res.*, **102**, 26,053–26,076, 1997.

Dunkerton, T., and D. P. Delisi, Climatology of the equatorial lower stratosphere: An observational study, *J. Atmos. Sci.*, **42**, 376-396, 1985.

Farge, M., Wavelet transform and their applications to turbulence. *Annu. Rev. Fluid Mech.*, **24**, 395-457, 1992.

Farman, J. C., B. G. Gardiner, and J. D. Shanklin, Large losses of total ozone in Antarctica reveal seasonal; ClO_x/ NO_x interaction, *Nature.*, **315**, 207-210, 1985.

Fels, S. B., J. D. Mahlman , M. D. Schwarzkopf, Perturbation in ozone and carbon dioxide radiative and dynamical response, *J. Atmos. Sci.*, **37**, 2265-2297, 1980.

Ferranti, L., J. M. Slingo, T. N. Palmer and B. J. Hoskins, Relation between interannual and intraseasonal monsoon variability's diagnosed from AMIP integration. *Quart. J. Roy. Met. Soc.*, **123**, 1323-1357, 1997.

Findlater, J. A., Major low-level air current near the Indian Ocean during the northern summer, *Q. J. R. Meteo. Soci.*, **95**, 362-380, 1969.

Fusco, G., Y. Cotroneo, and G.M.R. Manzella, Multivariate Empirical Orthogonal Function Analysis in the Mediterranean sea, *Geophys. Res. Abstracts.*, **5**, 11329, 2003.

Gamage, N., and C. Hagelberg, Detection and analysis of micro fronts and associated coherent events using localized transforms, *J. Atmos. Sci.*, **50**, 750-756, 1993.

Geller, M. A., W. Shen, M. Zhang, and W. -W. Tan, Calculations of the stratospheric quasi-biennial oscillation for time varying wave forcing, *J. Atmos. Sci.*, **54**, 883–894, 1997.

George N. K., J. S. Dian and H. S. Katherine, Validity of the tropical tropopause, *SPARC News. Lett.*, No. **18**, 18-19, 2002.

George, P. A., and V. Narayanan, Circulation pattern in the equatorial stratosphere and its relation with the circulations in the mesosphere and upper troposphere- Part I, *Indian J. Met.Hydrol. Geophys.*, **26**, 4, pp.443-454., 1975.

Goody, R., and Y. Yang, Atmospheric Radiation, *chapt 9. pp. 388-345*, Oxford Univ. Press, New York, 1989.

Goswami, B .N., D. Sengupta and Suresh Kumar, Intraseasonal oscillations and interannual variability of surface winds over the Indian monsoon region, *Proc. Ind. Aca. Sci. (Earth and Planetary Sci.).*, **107**, 45-64, 1998.

Gowariker V., V. Thapliyal, S. M. Kulshrestha, G. S. Mandal, R. Sen Roy, D. R. Sikka, Power regression model for long range forecast of southwest monsoon rainfall over India. *Mausam.*, **42**, 2, 125-129, 1991.

Gray, L. J., and J. A. Pyle, A two-dimensional model of the quasi-biennial oscillation in ozone, *J. Atmos. Sci.*, **46**, 203–220, 1989.

Gray, W. M., Atlantic seasonal hurricane frequency part 1: El nino and 30 mb QBO influences, *Mon. Wea. Rev.*, **112**, 1649-1668, 1984.

Gu, D., and S. G. H. Philander, Secular changes of annual and interanuual variability in the tropics during the past century, *J. Climate.*, **8**, 864-876, 1995.

Guhathakurta. P., A short-term model for surface ozone at Pune: Neural Network approach, *Vayumandal.*, **29**, 355-358, 1999.

Hamilton, K., R. J. Wilson, and R. Hemler, Middle atmosphere simulated with high vertical and horizontal resolution versions of a GCM: Improvement in the cold pole bias and generation of a QBO-like oscillation in the tropics, *J.Atmos. Sci.*, **56**, 3829–3846, 1999.

Hamilton, K., The vertical structure of the quasi-biennial oscillation: Observations and theory, *Atmos. Ocean.*, **19**, 236– 250, 1981.

Hansen, J. E., H. Wilson, M. Sato, R. Ruedy, K. Shah and E. Hansen, Satellite and surface temperature data at odds? *Clim. Change*, **30**, 103-117, 1995

Hardy, D. M., Empirical eigenvector analysis of vector observations, *Geophys. Res. Letters.*, **4**, 319-320, 1977.

Harris, N. R. P., et al., Trends in stratospheric and free tropospheric ozone, *J. Geophys. Res.*, **102**, 1571-1590, 1997.

Harris, N. R., Hudson and C. Philips (Eds), Assessment of trends in the vertical distribution of ozone, stratospheric process and their Role in climate/International Ozone commission global Atmospheric watch (SPARC/IOC/GAW) Report 1, *World Meto. Orag. Ozone Res. and Monit. Proj.*, **Rep 43**, 289pp, Geneva, 1998.

Hastenrath, S., *Climate and Circulation of the Tropics*, D. Reidel, Dordrecht., The Netherlands, 1985.

Hayashi, Y., Spectral analysis of tropical disturbance appearing in a GFDL general circulation model, *J. Atmos.Sci.*, **31**, 180-218, 1974.

Haynes, P. H., and M. E. McIntyre, On the evolution of vorticity and potential vorticity in the presence of diabatic heating and frictional or other forces, *J. Atmos. Sci.*, **44**, 828-841, 1986.

Haynes, P. H., et al., On the 'downward control' of extra-tropical diabatic circulation by eddy induced mean zonal forces. *J. Atmos. Sci.*, **48**, 651-678, 1991.

Hess, P. G., and D. O'Sullivan, A three-dimensional modeling study of the extratropical quasi-biennial oscillation in ozone, *J. Atmos. Sci.*, **52**, 1539 1554, 1995.

Hingane, L. S., Ozone valley in the subtropics, *J. Atmos. Sci.*, **47**, 1814-1816, 1990.

Holton, J. R., A note on the propagation of the biennial oscillation, *J. Atmos. Sci.*, **25**, 519-521, 1968.

Holton, J. R., and H. -C. Tan, The influence of the equatorial quasi-biennial oscillation on the global circulation at 50 mb, *J. Atmos. Sci.*, **73**, 2200-2208, 1980.

Holton, J. R., and R. S. Lindzen, An updated theory for the quasi-biennial cycle of the tropical stratosphere, *J. Atmos.Sci.*, **29**, 1076-1080, 1972.

Holton, J. R., P. H. Haynes, M. E. Mc Intyre, A. R. Douglass, R. B. Hood and L. Pfister, Stratosphere-troposphere exchange, *Rev. Gepohys.*, **33**, 403-449, 1995.

Holton, J. R., The dynamics of sudden stratospheric warming, *Ann. Rev. Earth Planet. Sci.*, **8**, 169-190, 1980.

Holton, J. R., Waves in the equatorial stratosphere generated by the heat sources, *J. Atmos. Sci.*, **29**, 368-375, 1972.

Hood, L. L. and J. P. Mc Cormack, Components of Interannual ozone change based on Nimbus 7 TOMS data, *Geophys. Res. Lett.*, **19**, 2309-2312, 1992.

Hood, L. L., 1997, The solar cycle variation of total ozone: Dynamical forcing in the lower stratosphere, *J. of Geophys. Res.*, **102**, 1355-1370, 1997.

Horel, J. D., A rotated principal component analysis of the interannual variability of the Northern Hemisphere 500 mb height field, *Mon. Wea. Rev.*, **109**, 2080-2092, 1981.

Horel, J. D., Complex principal component analysis: theory and examples, *J. Appl. Meteor.*, **23**, 1660-1673, 1984

Hoskins, B. J., M. E. McIntyre, and A. W. Robertson, On the use and significance of isentropic potential vorticity maps, *Q. J. R. Meteorol. Soc.*, **111**, 877-946, 1985.

Houghton, et al., Intergovernmental Panel on Climate Change, *Radiative Forcing of Climate Change and evaluation of the IPCC IS92 Emission Scenarios*, Cambridge Univ. Press, New York, 1995.

Hudgins, L., C. A. Friche, and M. E. Mayer, Wavelet transforms and atmospheric turbulence, *Phys. Rev. Lett.*, **71**, 3279-3282, 1993.

Ina, T. Kindem and Bo.Christiansen, Tropospheric response to stratospheric ozoneloss, *Geophys. Res. Lett.*, **28**, pp 1547-1550, 2001.

Jadin, E. A., Inter-annual variability of total ozone and stratospheric angular momentum, *Inter. J. of Geomag. And Aero*, **1**, No.2, November 1998.

Jae, H. K., and M. J. Newchurch, Biomass-burning influence on tropospheric ozone over New Guinea and South America, *J. Geophys. Res.*, **103**, 1998.

Jaeger, L., Monthly and aerial pattern of mean global precipitation variation in the global water budget, a. Street-Perrott, M. Beran and R. Ratcliff, Eds., *D. Reidel Publlising Co.*, 129-140, 1983.

Jain, S.L., and B. C. Arya, Surface ozone measurement over New Delhi, Sem. Proceed. "Stratosphere-Troposphere Interactions", Cochin-16, Nov.24-26, 1998.

Johnston, H. S., Reduction of stratospheric ozone by nitrogen oxide catalysts from supersonic transport exhaust, *Science*, **173**, 517-522, 1971.

Jones, A. E., and J. D. Shanklin, Continued decline of total ozone over Halley, Antarctica, Since 1985, *Nature.*, **376**, 409- 411, 1995.

Joseph, P. V., and P. L. Raman, Existence of low-level westerly jet stream over peninsular India during July, *Indian. J. Meteo and Geophy.*, **17**, 407-410, 1966.

Joseph, P. V., Sub-tropical westerlies in relation to large-scale failure of Indian monsoon, *Indian J. Met. Hydrol. Geophys.*, **29**, 412-418, 1978.

Junge, C. E., Global ozone budget and exchange between stratosphere and troposphere, *Tellus.*, **14**, 363-377, 1962.

Kalnay, E. and Co Authors, The NCEP/NCAR 40- year Reanalysis Project, *Bull. Ame. Meteo. Soc.*, **77**, 437-471, 1996.

Kanamitsu, M., and T, N. Krishnamuti, Northern summer tropical circulation during drought and normal rainfall months, *Mon. Wea. Rev.*, **106**, 331-347, 1978.

Karl, T.R., and Co-authors, Critical issues for long-term climate monitoring, *Clim. Change*, **31**, 185-221, 1995.

Keckhut, P., A. Hauchecorne, and M. L., Chanin, Midlatitude long-term variation of the middle atmosphere: Trends and cyclic and episodic changes, *J. Gephys. Res*, **100**, 18 887- 18 897, 1995.

Kerr, J. B. and C. T., McElroy, Evidence for large upward trends of the ultraviolet –B radiation linked to ozone depletion, *Science.*, **262**, 1032-1034, 1993.

Kodama, Y., Large–scale common features of subtropical precipitation zones (the Baiu Front, the south pacific convergence zone, the South Atlantic convergence zone). Part I: Characteristics of the subtropical frontal zones, *J. Met. Soc. Japan.*, **70**, 813-835, 1992.

Kodama, Y., Large–scale common features of subtropical precipitation zones (the Baiu Front, the south pacific convergence zone, the South Atlantic convergence zone) Part II: Conditions for generating the subtropical convergence zones, *J. Met. Soc. Japan.*, **71**, 581-610, 1993.

Koteswaram, P., The easterly jet streams in the tropics, *Tellus.*, **10**, 43-57, 1958.

Krinshnamuti, T. N., E. Astling and M. Kanamitsu, 200 mb wind filed in June and August 1972, Rep. 75-2, Dept. of Meteorology, *Florida State University*, 115 pp., 1975.

Krishnamurti, T. N., and H. N. Bhalme, Oscillations of a monsoon system, Part 1, Observational aspects, *J. Atmos. Sci.*, **33**, 1937-1954, 1976.

Krishnan, R., M. Mujumdar, V. Vaidya, K.V. Remesh, and V Satyan, The abnormal Indian Summer monsoon of 2000, *J. Climate.*, **16**, 1177-1194, 2003.

Kulkarni, J. R., R. K. Verma, On the spatio- temporal variations of the tropopause height over India and the Indian summer monsoon activity, *Adv. In .Atmos. Sci.*, **10**, 481-488, 1993.

Kundu, N. and Jain, M., Total ozone trends over low latitude Indian stations, *Geophys. Res. Lett.*, **20**, 2881-2883, 1993.

Kundu, P. K., and J. S. Allan, Some three dimensional characteristics of low frequency current fluctuations near the Oregon Coast, *J. Phys. Oceanogra.*, **6**, 181-199, 1976.

Kutzbach, J. E., Empirical eigenvectors of sea-level pressure, surface temperature and precipitation complexes over North America, *J. Appl. Meteorol.*, **6**, 791-802, 1967.

Labitke, K., and H. van Loon, Association between the 11 year solar cycle, the QBO, and the atmosphere, Part 1, The troposphere and stratosphere in the northern hemisphere in winter, *J. Atmos. Terr. phys.*, **50**, 197-206, 1988.

Labitzke, K., and H. van Loon, *The Global Range of the Stratospheric Decadal Wave. PartII:The QBO Effect on the Global Stratosphere in the Northern Winter, Tellus, March , 1999 (personal communication).*

Labitzke, K., and H. van Loon, The signal of the 11-year sunspot cycle in the upper troposphere- lower stratosphere, *Space Sci. Res.*, **80**, 393-410, 1997.

Labitzke, K., and M. P. Mc Cormick, Stratospheric temperature increases due to Pinatubo aerosols, *Geophys. Res . Lett.*, 19, 207-210, 1992.

Labitzke, K., B. Naujokat and J. K. Angell, Long term temperature trends in the middle stratosphere of the northern Hemisphere, *Adv. Space. Res.*, **6**, 7-17, 1986.

Labitzke, K., H. van Loon, Connection between the troposphere and stratosphere on a decadal scale. -- *Tellus* **46A**, 275-286, 1994.

Labitzke, K., On the Signal of the 11-Year Sunspot Cycle in the Stratosphere and its modulation by the Quasi-Biennial Oscillation (QBO), *J.Atmos. Sci.*, 2003 (personal communication),)

Lait, L. R., M. R. Schoeberl, and P. A. Newman, Quasi-biennial modulation of the Antarctic ozone depletion, *J. Geophys. Res.*, **94**, 11559-11571, 1989.

Lamarque, J., and P. G. Hess, Cross-tropopause mass exchange and potential vorticity budget in a simulated tropopause folding, *J. Atmos. Sci.*, **51**, 2246-2269, 1994.

Langemmatz, U., an estimation of the impact of observed ozone losses on stratospheric temperature, *Geophys. Res. Lett*, **27**, 2077-2028, 2000.

Lau, K. M., and P. H. Chan, Intrannual and intraseasonal variations of tropical convection: A possible link between the 40-50 day oscillation and ENSO? *J. Atmos. Sci.*, **44**, 506-521, 1988.

Lean, J., and D. Rind, Climate forcing by changing solar radiation, *J. of Climate*, **11**, 3069-3094, 1998.

Legler, D. M., Empirical orthogonal Function Analysis of Wind vectors over the Tropical Pacific Region, *Bull.Am.Meteorol.Soc.*, **64(3)**, 234-241, 1983.

Leun, V. J., X. Tang, and M. Tevini, Environmental effects of ozone depletion; 1994 Assessment, *Ambio.*, **14**, 138, 1995.

Lindzen, R. S., and J. R. Holton, A Theory of the Quasi-Biennial Oscillation, *J. Atmos. Sci.*, **25**, 1095-1107, 1968.

Lindzen, R. S., On the development of the theory of the QBO, *Bull.Ame. Met.Soc.*, **68**, 329-337, 1987.

Ling, X. –D., and J. London, The quasi-biennial oscillation of ozone in the tropical middle stratosphere: A one-dimensional model, *J. Atmos. Sci.*, **43**, 3122-3136, 1986.

Liu, P. C., Wavelet Spectrum analysis and ocean wind waves. *Wavelets in Geophysics*, 4, E. *Foufoula and P.Kumar*, Eds., 151-166, 1994.

Lorenz, E. N., Empirical Orthogonal Functions and Statistical Weather Prediction, Scientific Report 1, Statistical Forecasting Project, *Mass. Inst. Tech., Cambridge.*, Mass. (Defense Doc. Center No. 110268), **49 pp**, 1956.

Ludwig, F. L., and G. Byrd, A very efficient method for deriving mass consistent flow fields from wind observations in rough terrain, *Atmos. Environ.*, **14**, 585-587, 1980.

Lumley, J. L., *Coherent Structures in Turbulence, Transition and Turbulence (R. E. Meyer, edi).*, Academic Press, New York, 215-242, 1981.

Manabe, S., and R. J. Stonffer, Sensitivity of a global climate model to an increase of CO_2 concentration in the atmosphere, *J. Geophys. Res.*, **85**, 5529-5554, 1980.

Mani, A., and C. R. Sreedharan, Studies of variations in the vertical ozone profiles over India, *Pure and Apllied. Geophys.*, **108**, 1180-1191, 1973.

Marko, J. R., and D. B. Fissel, Empirical linkage between Arctic Sea ice extents and Northern Hemisphere mid-latitude column ozone levels, *Geophys. Res. Lett.*, **20**, 73-40, 1993.

Martin, R.V., Jacob, D. J. Logan, J. A., Ziemko, J.R., and Washington, R., Detection of lightening influence on tropical tropospheric ozone, *Geophys. Res. Lett.*, **27**, 1639-1642, 2000.

Maruyama, T., Large-scale disturbances in the equatorial lower stratosphere, *J. Meteoro. Soc. Japan*, **45**, 391-408, 1967.

Maruyama, T., The quasi-biennial oscillation (QBO) and equatorial waves - a historical review. *Paper in Meteo. & Geophys.*, 48, 1-17, 1997.

Matsuno, T., A dynamical model of the stratospheric sudden warming, *J. Atmos. Sci.*, **28**, 1479-1494, 1971.

Mc Intyre, M. E., How well do we understand the dynamics of stratospheric warming? *J. Meteor. Soc. Japan*, **60**, 37-65, 1982.

Mc Peters, R. D., and G. C. Labour, An assessment of accuracy of 14.5 years of Nimbus 7 TOMS version & Ozone data by comparison with the Dobson network, *Geophys. Res. lett.*, **23**, 3695-3698, 1996.

Meyers, S. D., B. G. Kelly, and J. J. O'Brien, An introduction to wavelet analysis in oceanography and meteorology: with application to the dispersion of Yanai waves, *Mon. Wea. Rev.*, **121**, 2858-2866, 1993.

Mitchell, J. F. B., the seasonal response of general circulation model to change in CO_2 and sea surface temperature, *Quart. J. Roy. Metero. Soc.*, **109**, 113-152, 1983.

Mohankumar, K., Effects of solar activity and stratospheric QBO in tropical monsoon rainfall, *J. Geomag. Geoelctr.*, **48**, 343-352, 1996.

Mohankumar, K., Solar activity forcing of the middle atmosphere, *Ann. Geophys.*, **13**, 879-885, 1995.

Morlet, J., Sampling theory and wave propagation, Issues in Acoustics signals/Image Processing and Recognition, *Vol.1, NATO ASI Series, C.H. Chen, Ed., Springer-Verlag.*, **1**, 233-261, 1983.

Mukehrjee B. K., K. Indira, R. S. Reddy, Bh.V. Ramana Murty, Quasi-biennial oscillation in stratospheric zonal wind and Indian summer monsoon. *Mon. Wea. Rev.*, **113**, 8, 1421-1424, 1985.

Mukherjee B. K., R. S. Reddy, Bh.V. Ramanamurty, High-level warming, winds and Indian summer monsoon. *Mon. Wea. Rev.*, **107**, 1581-1588, 1979.

Murakami, T., Atmospheric response to heat sources during July, UHMET 74-04, Dept. of meteorology, *University of Hawaii*, 50 pp., 1974.

Murry, S., and C. Patrick, connection between the solar cycle and the QBO: The missing Link, *J. Climate.*, **13**, 2652-2662, 2000.

Narasimha, R. D., R. Sikka and A. Prabhu, The monsoon trough boundary layer, *Indian. Acd. of Science*, pp 422, 1997.

Naujokat, B., An update of the observed quasi-biennial oscillation of the stratospheric winds over the tropics, *J. Atmos. Sci.*, **43**, 1873-1877, 1986.

Neuendorfer, A.C., Ozone monitoring with TIROS-N operational vertical sounders, *J. Geophys. Res.*, **101**, 18, 807-18, 828, 1996.

Newton, C. W., and A.V. Persson, Structural characteristics of the subtropical jet stream and certain lower stratospheric wind systems, *Tellus*, **14**, 221-241, 1962.

O'Neill, A., and C. E. Youngblut, Stratospheric warming: diagnosed using the transformed Eulerain- mean equations and the effect of the mean state on wave propagation. *J. Atmos. Sci.*, **39**, 1370-1386, 1982.

O'Sullivan, D., Interaction of extratropical Rossby waves with westerly quasi-biennial oscillation winds, *J. Geophys. Res.*, **102**, 19,461-19,469, 1997.

Ortland, D. A., Rossby wave propagation into the tropical stratosphere observed by the High Resolution Doppler Imager, *Geophys. Res. Lett.*, **24**, 1999-2002, 1997.

Parthasarathy, B., A. A. Munot, and D. R. Kothawale, All- India monthly, and seasonal rainfall series: 1871-1993, *Theor. Appli. Climatol.*, **49**, 217-224, 1994.

Parthasarathy, B., Some aspects of large- scale fluctuations in the summer monsoon rainfall over India during 1871 to 1978. Ph. D. Thesis, University of Poona, Pune, 370pp, 1984.

Pawson, S., and M. Fiorino, A comparison of reanalysis in the tropical stratosphere. Part1: thermal structure and the annual cycle, *Climate Dyn.*, **14**, 631-644, 1998a.

Pawson, S., and M. Fiorino, A comparison of reanalysis in the tropical stratosphere. Part 2: the quasi-biennial oscillation, *Climate. Dyn.*, **14**, 645-658, 1998b.

Pawson, S., and M. Fiorino, A comparison of reanalysis in the tropical stratosphere Part 3: inclusion of the pre-satellite data era, *Climate Dyn.*, **15**, 241-250, 1999.

Pawson, S., K. Labitzke, R. Lenschow, B. Naujokat, B. Rajewski, M. Wiesner, and R. -C. Wohlfart, Climatology of the Northern Hemisphere stratosphere derived from Berlin analyses, part 1, Monthly means, technical report, Ser. A, 7(3)., Freie Univ. Berlin, 1993.

Penner, et al., Intergovernmental Panel on Climate Change, *Aviation and the Global Atmosphere*, Cambridge Univ. Press, New York, 1999.

Pepler, S. J., G. Vaughan and D. A. Cooper, Detection of turbulence around jet streams using a VHF radar, *Q. J. R. Meteorol. Soc.*, **124**, 447-462, 1998.

Pollack, J., and T. Ackerman, Possible effects of the El Chichan cloud on the variation budget of the northern tropics, *Geophys. Res. Lett.*, **10**, 1057-1060, 1983.

Quiroz, R. S., Period modulation of the stratospheric quasi-biennial oscillation, *Mon. Wea. Rev.*, **109**, 665-674, 1981.

128

Rajeevan, M., Upper tropospheric circulation and thermal anomalies over central Asia associated with major drought and flood in India, *Current Sciences.*, 64(4), 244-247, 1993.

Ramage C. S., *Monsoon Meteorology*, Academic Press, New York, 1971.

Ramaswamy, V., and Co- Authors, An update of stratospheric temperature trends, *SPARC. News Lett*, 18, 7-9, 2002.

Ramaswamy, V., and Co authors., Stratospheric temperature trends: observation and model simulations, *J. Geophys. Res.*, 39, 71-122, 2001.

Ramaswamy, V., M. D. Schwarzkopf, and W. Randel, Finger print of ozone depletion in the spatial and temporal pattern of recent lower-stratospheric cooling, *Nature.*, 382, 616-618, 1996.

Ramaswamy, V., M. D. Schwerzkoff, and K. P. Shine, Radiative forcing of climate from halocarbons induced global stratospheric ozone loss, *Nature.*, 355, 810-812, 1992.

Randel, W.J., and J. B. Cobb, Coherent variations of monthly mean total ozone and lower stratospheric temperature, *J. Geophys. Res.*, 99, 5433-5447, 1994.

Rao, R. K. S., and N. T. Lakhole, quasi-biennial oscillation and summer southwest monsoon, *Ind. J. Met. Hydrol. Geophys.*, 29, 142, 403-411., 1978.

Rao, R. K. S., and N. T. Lakhole, quasi-biennial oscillation and summer southwest monsoon, *Ind. J. Met. Hydrol. Geophys.*, 29, 142, 403-411, 1978.

Rasmusson, E. M., P. A, Arkin, W. Y. Chen, and J. B. Jalickee, Biennial variation in surface temperature over the United States as revealed by Singular decomposition, *Mon. Weath. Rev.*, 109, 181-192, 1981

Reed, R. G., W. J. Campbell, L. A. Rasmussen and D. G. Rogers, Evidence of downward propagating annual wind reversal in the equatorial stratosphere. *J. Geophys. Res.*, 66, 813-818, 1961.

Reed, R. J., A tentative model of the 26-month oscillation in tropical latitudes, *Q.J.R. Meteoro. Soc.*, 90, 441-466, 1964.

Reed, R. J., The quasi-biennial Oscillation of the atmosphere between 30 and 50 km over Accention Island, *J. Atmos. Sci.*, 22, 331-333, 1965.

Reid, G. C, and K. S., Gage, Interannual variations in the height of the tropical tropopause, *J. Geophys. Res.*, 90, 5629-5635, 1985.

Reid, G. C., and K. S. Garge, On the annual variation in height of the tropical tropopause, *J. Atmos. Sci.*, 38, 1928-1938, 1981.

Reid, G. C., Seasonal and interannual temperature varations in the tropical stratosphere, *J. Geophys. Res.*, 99, 18 923-18 932, 1994.

Reiter, E. R., M. E. Glaner, and J. D. Mahlman, The role of the tropopause in stratosphere- troposphere exchange processes, *Pure. Appl. Geophys.*, **75**, 185-218, 1969.

Rosier, S. M., and K. P. Shine, The effect of two decades of ozone change on the stratospheric temperature as indicated by a general circulation model, *Geophys. Res. lett.*, **27**, 2617-2620, 2000.

Santer, B. D., and co Authors, A search for human influence on the thermal structure of the atmosphere, *Nature.*, **382**, 39-46, 1996.

Sasi, M. N., and K. Sengupta, Annual and semi-annual oscillations in the temperature and zonal winds over Thumba' *VSSC Technical Note .*, 47:038:80, 1980.

Sathyamoorthy, V., K. Mohankumar, Charectersitics of tropospheric biennial oscillation and its possible assocaition with the stratospheric QBO, *Geophys. Res Lett.*, **27**, 5, 669-672, 2000.

Schmidt, V., and A. Khedim, In situ measurements of carbon dioxide in the winter Arctic vortex and mid latitudes: An indicator of the age of stratospheric air, *Geophys. Res. Lett.*, **18**, 763-766, 1991.

Schoeberl, M. R., Stratospheric warming: Observations and theory, *Rev. Geophys. Space. Phys.*, **16**, 521-538, 1978.

Seidel, D. J., R. J. Ross and J. K. Angell, Climatological characteristics of the tropical tropopause as reveled by radiosondes, *J. Geophys. Res.*, **106**, 7857-7878, 2001.

Shapiro, M. A., Further evidence of the mesoscale and turbulent structure of the upper level jet stream frontal zone systems, *Mon. Wea. Rev.*, **106**, 1100-1111, 1978.

Shapiro, M. A., Turbulent mixing within the tropopause folds as a mechanism for the exchange of chemical constituents between the stratosphere and the troposphere, *J. Atmos. Sci.*, **37**, 994-1004, 1980.

Shindell, D. J., D. Rind, and P. Lonergan, Increased polar stratospheric ozone loses and delayed eventual recovery owing to increasing green house gas concentrations, *Nature.*, **392**, 589-592, 1998.

Shiotani, M., Annual, quasi-biennial and El-nino-Southern oscillation(ENSO) time scale variation in equatorial total ozone. *J. Geophys.Res.*, **97**,7625-7633, 1992.

Shukla, J., and D. A. Polino, The Southern Oscillation and long range forecasting of the summer monsoon rainfall over India. *Mon. Wea. Rev.*, **111**, 1830-1837, 1983.

Sikder, et al., Tropical stratospheric circulation and monsoon rainfall, advances in atmospheric features, Beijing, China, 10(3), 379-385, 1993.

Sikka, D. R., and S. Gadgil, On the maximum cloud zone and the ITCZ over India longitude during the southwest monsoon, *Mon. Weather. Rev.*, **108**, 1840-1853, 1980.

130

Sinha, A., J. E. Harries, Water vapour and greenhouse trapping - the role of far-infrared absorption. *Geophys. Res. Lett.*, 22, no.16, 2147-2150, 1995.

SPARC Seminar on " Trends in the upper atmosphere" held at Kuhlingshorn, Germany, May 13-16, 2002.

SPARC Tropopause workshop, held at Bad Tolz, Germany, *SPARC Newsletter*, 17, 17-21, 2001.

Staehelin, J., N. R. P. Harris, C. Appenzeller, and J. Eberhard, Ozone trends: A review, *Rev. Geophys.*, 39, 231-290, 2001.

Stolarski, R.S., P., Bloomfield, R. D., Mc Peters, and J. R., Herman, Total ozone trends deduced from Nimbus 7 TOMS data, *Geophys. Res. Lett.*, 18, 1015, 1991.

Stolarski, R.S., R. Bojkov, L., Bishop, C., Zerefos, J., Staehelm, and J. Zawodny, Measurement trends in stratospheric ozone, *Science*, 256, 342-349, 1992.

Takahashi, M., Simulation of the stratospheric quasi-biennial oscillation using a general circulation model, *Geophys. Res.Lett.*, 23, 661-664, 1996.

Tanaka, H., and N. Yoshizawa, Quasi-biennial oscillation and its analog under the assumption of waves self-acceleration, *J. Atmos.Sci.*, 42, 2350-2359, 1985.

Tang, X., S. Madronich, T. Washington, and D. Calamari, Changes in tropospheric composition and air quality, *J. Photochem. Photobiol.*, B, 46, 83-95, 1998.

Thapliyal, V., Stratosphere circulation in relation to summer monsoon over India, *Proc. Sympos On Hydrological aspects of Droughts*, IIT, New Delhi, 3-7, December, pp347, 1979.

Thompson, A.M. and R. D. Hudson, Tropical tropospheric ozone (TTO) maps from Nimbus7 and Earth Probe TOMS by the modified residual Method,: Evaluation with soades, ENSO signal and trends from Atlantic regional time series, *J. Geophys. Res.*, 105, 26961-26975, 2000.

Tiwari, V. S., Ozone variations over tropics: Treads reveled from Dobson measurements over Indian stations, *Mausam*, 43, 65-70, 1992.

Toumi, R., S. Bekki, and K. S. Law, Indirect influence of zone depletion on climate forcing by clouds, *Nature*, 372, 348-351, 1994.

Trenberth, K. E., D. P. Stepaniak, and J. M. Caron, The global monsoon as seen through the divergent atmospheric circulation, *J. Climate*, 13, 3969-3993, 2000.

Trenberth, K. E., D. P. Stepaniak, and J. W. Hurrell, Quality of Reanalysis in the tropics, *J. Climate*, 14, 1499-1510, 2001.

Uchino et al., Essential characteristics of the Antarctic spring ozone decline: update to 1998, *Geophys. Res. Lett.*, 26, 1377-1380, 1999.

Untch, A., Simulation of the quasi-biennial oscillation with the ECMWF model, in *Research Activities in the Atmosphericand Oceanic Modelling*, pp. 6.26-6.27, *World Meteorol. Organ.*, Geneva, 1998.

van der Leun, J., X. Tang, and M. Tevini, Environmental effects of ozone depletion: 1994. *Assessment. Ambio.*, 14, 38, 1995.

van Loon, H., and K. Labitzke, The global range of the stratospheric decadal wave, Part I: Its association with the sunspot cycle in summer and in the annual mean, and with the troposphere. *J. Climate.*, 11, 1529-1537, 1998.

van Loon, H., and K. Labitzke, The 10-12 year atmospheric oscillation. *Meteorl. Zeitschr.*, N.F., 3, 259-266, 1999.

Veryard, R. G., and R. A. Ebdon, Fluctuations in tropical stratospheric winds, *Meteo Mag.*, 90, 125-143, 1961.

von Storch, H. and F. W. Zwiers, *Statistical analysis in climate research.*, Cambridge University Press, Cambridge, 484 pp, 1999

Wallace, J. M., and J. R. Holton, A diagnostic numerical model of the quasi-biennial oscillation, *J. Atmos. Sci.*, 25, 280-292, 1968.

Wallace, J. M., and V. E. Kousky, Observational evidence of Kelvin waves in the tropical stratosphere, *J. Atmos. Sci.*, 25, 900-907, 1968a.

Wallace, J. M., C. Smith and C. S, Bretherton, Singular Value Decomposition of winter time sea surface temperature and 500 mb height anomalies, *J. Climate.*, 5, 561-576, 1992.

Wang, B., and Y. Wang, Temporal structure of the southern oscillation as revealed by waveform and wavelet analysis, *J. Climate*, 9, 1586-1598, 1996.

Wang, B., Inter-decadal Changes in El Nino Onset in the Last Four Decades. *J. Climate.* 8, 267-285, 1995.

Weng, H., and K. -M. Lau. Wavelets, period doubling, and time-frequency localization with application to organization of convection over the tropical western Pacific. *J. Atmos. Sci.*, 51, 2523-2541, 1994.

Wilks, D. S., *Statistical methods in the atmospheric sciences. an introduction.* Academic Press, 467 pp, 1995.

Wirth, V., and J. Egger. Diagnosing extratropical synoptic-scale stratosphere-troposphere exchange: a case study. *Quart. J. Roy. Met. Soc.*, 125, pp. 635-655, 1999.

Wirth, V., Comments on "A New Formulation of the Exchange of Mass and Trace Constituents between the Stratosphere and Troposphere". *J. Atmos. Sci.*, 52, 2491-2493, 1995.

Wirth, V., Cyclone-Anticyclone Asymmetry Concerning the Height of the Thermal and the Dynamical Tropopause. *J. Atmos. Sci.*, **58**, 26-37, 2001.

WMO (World Metrological Organization), " Meteorology- a three -dimensional Science. *WMO Bull.*, October, 134-138, 1957.

World Meteorological Organization, Report of the international ozone trends panel: 1988, Global Ozone Res. and Monit. Proj. *Rep.18*, Chap.6., pp 443-458, Geneva, 1990a

World Meteorological Organization, *Scientific Assessment of Ozone Depletion:* 1998, Rep. 44, *Global Ozone Res. and Monit. Proj.*, Geneva 1999.

World Meteorological Organization, Scientific Assessment of Ozone Depletion: 1994, Rep. 37, *Global ozone Res. and Monit. Proj.* Geneva., 1995.

World Meteorological Organization, Scientific assessment of stratospheric ozone: 1994, Global *Ozone Res. and Monit. Proj.*, Rep 37, Chapter 8, pp 8.1-8. 26, Geneva, 1995.

World Meteorological Organization, Scientific assessment of stratospheric ozone: 1998, *Global Ozone Res. and Monit. Proj.*, Rep 44, 546pp, Geneva, 1999.

World Meteorological Organization, Scientific assessment of stratospheric ozone: 1991, *Global Ozone Res. and Monit. Pro.*, Rep 25, Chapter 2 and 7, pp 2.1-2.33 and 7.1-7.28, Geneva, 1992.

Yanai, M., and T. Maruyama, Stratospheric wave disturbances propagating over the equatorial Pacific, *J. Meorolo.Soci., Jpn.*, **44**, 291-294, 1966.

Yang, H., and K. K. Tung, Statistical significance and pattern of extra-tropical QBO in column ozone, *J. Geophys Res.*, **21**, 2235-2238, 1994.

Yang, H., and K.K. Tung, On the phase propagation of extra-tropical quasi-biennial oscillation in observation data, *J.Geophys.Res.*, **100**, 9091-9100, 1995.

Yasunari, T., Impact of Indian monsoon on the coupled atmosphere/ocean system in the tropical pacific, *Met. Atmos. Phys.*, **44**, 29-41, 1990.

Yasunari, T., The Monsoon year- A new concept of the climatic year in the Tropics, *Bull. Ame. Met. Soc.*, **72**, 1131-1138, 1991.

Zachariasse, M., P. F. J. Van Velthoven, H. G. J. Smit, J. Lelieveld, T.K. Mandal and H. Kelder, Influence of stratosphere-troposphere exchange on tropical ozone over the tropical Indian ocean during the winter monsoon, *J. Geophys. Res.*, **105**, 15,403-15,416, 2000.

Zerefos, C. S., A. P., Bais, I. C. Ziomas, and R. D. Bojkov, On the relation and Elnino-Southern Oscillation in the revised Dobson total ozone records, *J. Geophys. Res.*, **97**, 10,135-10,144, 1992.

Zerefos, C. S., K. Tourpali, B. R., Bojkov, and D. S., Balis, Solar activity –total column ozone relationship: Observations and model studies with heterogeneous chemistry, *J. Geophys. Res*, **102**, 1561-1569, 1997.

Zhou, X. L., Tropical cold point tropopause characteristics derived from NCMWF reanalysis and soundings, *J. Climate*.,**14**, 1823-1838, 2001.

Ziemke, J. R., S. Chandra, P. K. Bhartia, Seasonal and interannual variabilites in tropical tropospheric ozone, *J.Geophys. Res*., **104**, 21245-21442, 1999.